

**MAINE YANKEE MARINE SAMPLING STUDY
FINAL REPORT**

**Report to the
Maine Yankee Atomic Power Company**



**MAINE YANKEE MARINE SAMPLING STUDY
FINAL REPORT**

**Report to the
Maine Yankee Atomic Power Company**

C.T. Hess, Ph.D.

University of Maine

G. P. Bernhardt, Ph.D.

University of Maine

J. H. Churchill, M.S.

Woods Hole Oceanographic Institute

M. Bowen, M.S.

Normandeau Associates

V. Guiseppe, B.S., D. Breton, M.S., T. Gould, M.S., P. Smitherman

University of Maine

February 2005

Table of Contents

	Page
1. EXECUTIVE SUMMARY.....	1
1.1 CHARACTERIZATION OF RADIONUCLIDES IN THE BACK RIVER AND INTERTIDAL ZONE AROUND THE FORMER MAINE YANKEE NUCLEAR POWER PLANT SITE.....	1
2. PURPOSE OF THE MARINE SAMPLING STUDY	3
3. FIELD SAMPLING	4
3.1 SEDIMENT SAMPLING	4
3.1.1 Phase I	4
3.1.1.1 Intertidal Surface	11
3.1.1.2 Intertidal Subsurface.....	11
3.1.1.3 Subtidal Surface.....	11
3.1.1.4 Subtidal Subsurface	12
3.1.2 Phase II	12
3.1.2.1 Intertidal Surface and Subsurface.....	12
3.1.2.2 Subtidal Surface and Subsurface	12
3.1.3 Hard to Detect.....	12
3.2 GAMMA SCAN OF INTERTIDAL ZONE	12
3.3 BIOTA SAMPLE COLLECTION	13
3.4 QUALITY CONTROL	14
3.4.1 Sample Tracking and Custody	14
3.4.2 Sample Storage and Transfer	14
3.5 LABORATORY ANALYSIS.....	14
3.5.1 Gamma Screening.....	14
3.5.2 Lead-210 and Cs-137 Dating.....	15
3.5.3 Hard to Detects	15
3.5.4 Quality Control	15
3.5.5 Sample Disposal	15
3.5.6 Safety	15
3.5.7 Quality Assurance.....	16
3.5.8 Background Measurements.....	16
4. NUMERICAL MODELING OF FLOWS AND RADIONUCLIDE TRANSPORT IN THE SHEEPSCOT RIVER ESTUARINE SYSTEM	17
4.1 INTRODUCTION	17
4.2 HYDRODYNAMIC MODELING	17
4.2.1 Model Description	17
4.2.2 Model Grid Generation	18
4.2.3 Model Results	19
4.2.4 Field Evaluation of the Model	30
4.3 MODELING OF RADIONUCLIDE TRANSPORT.....	38
4.3.1 Model History and Description.....	38
4.3.2 Model Results	39
4.3 MODELING SUMMARY	47

Maine Yankee Marine Sampling Study

5	GAMMA SCAN RESULTS	49
5.1	SEDIMENT CORES	49
5.2	LEAD-210 CORE RESULTS	51
5.3	SURFICIAL SEDIMENTS	51
5.4	BIOTA GAMMA SCAN	52
5.5	HARD TO DETECT NUCLIDES.....	53
5.6	ERROR DISCUSSION OF GAMMA SCANS	53
6.	HOT PARTICLE SEARCH RESULTS	102
7	MARINE SAMPLE DOSIMETRY	106
7.1	MARINE SAMPLING DOSE ASSESSMENT	106
7.1.1	Purpose of the Dose Assessment Document.....	106
7.1.2	Inputs and Data Sources.....	106
7.1.3	Current Maine Yankee Intertidal Zone Uses	107
7.1.3.1	Offsite Dose Calculation Manual (ODCM).....	107
7.1.3.2	Bailey Cove Mudflats Occupancy	107
7.1.3.3	Worm Digging	108
7.1.3.4	Clam Harvesting.....	108
7.1.3.5	Swimming	108
7.1.3.6	Fishing	108
7.1.4	Potential Future Uses of the Intertidal Zone	109
7.1.4.1	Seaweed Growing and Harvesting	109
7.1.4.2	Flooding for Lobster Pound or Fish Farming.....	110
7.1.4.3	Land Reclamation Gardening.....	110
7.1.5	Identification of Scenarios and Pathways/Dose Assessment Framework.....	110
7.1.5.1	Commercial Worm/Clam Digger and Fish/Shell Fish Ingestor	110
7.1.5.2	Seaweed Cultivator, Eater and Fertilizer User	111
7.1.5.3	Land Reclamation Farmer	112
7.1.6	Identification of Flora & Fauna Dose Contributors and Bioaccumulators	112
7.2	DOSIMETRY RESULTS.....	113
8	CONCLUSIONS	116
8.1	SUMMARY.....	116
8.2	KEY FINDINGS	116
9	QUALITY ASSURANCE.....	118
10	PROJECT ORGANIZATION.....	119
11.	REFERENCES CITED	120

APPENDIX A

List of Figures

	Page
Figure 3-1. Project location and background locations.....	5
Figure 3-2. Project locus map and farfield sampling locations.....	6
Figure 3-3. Phase 1 station locations	7
Figure 3-4. Phase 2 station locations around Little Oak and Foxbird Island.....	8
Figure 3-5. Phase 2 station locations north and South of Little Oak and Foxbird Islands.....	9
Figure 4-1. The final version of the grid used for the hydrodynamic and radionuclide models.....	20
Figure 4-2a. Same as Figure 4-1 except showing the model grid over plain land and water fields. Indicated is the boundary junction at which the offshore forcing, in the form of a tidal elevation series, is applied. Also indicated is the Sasanoa River, which is a principal opening to the modeled system not accounted for by the grid.....	21
Figure 4-2b. The section of the model grid with the highest resolution.	22
Figure 4-3a. The volume transport over a flood tide through selected model channels. The transports show the splitting of the incoming tidal flow near the southern end of Westport Island and a minimum of tidal flow at the tidal node, where two opposing streams meet, a few km south of the diffuser location.	24
Figure 4-3b. A smaller scale view of the flood tide volume transport in the vicinity of the Maine Yankee facility.	25
Figure 4-3c. An even smaller scale view of the flood tide volume transport in the vicinity of the Maine Yankee facility.	25
Figure 4-4a. The RMS value of volume transport within channels encircling Westport Island. These RMS transports show a minimum of tidal energy at the tidal node off the western shore of Westport Island.....	26
Figure 4-4b. A smaller scale view of the RMS value of volume transport more clearly showing the minimum of tidal energy at the tidal node. Note that this is roughly 1 km south of the diffuser location.	27
Figure 4-5. Magnitudes of tidal excursions at selected model channels.....	28
Figure 4-6. An ensemble of the positions of particles released from the location of the diffuser into a modeled flow field forced with a boundary elevation series representative of a spring tide.	29
Figure 4-7. An ensemble of the positions of particles released from the location of the Bailey Cove discharge into a modeled flow field forced with a boundary elevation series representative of a spring tide.	29
Figure 4-8. A view of the model grid in the areas of Bailey Cove and Back River. Indicated is the location of a conductivity-temperature-depth (CTD) recorder set out over two tidal cycles during July 7-8, 2004 as well as the model channel (# 281) that encompassed the CTD location.	31
Figure 4-9. Time series of modeled water depth and water velocity in channel 281 (Figure 4-8). The series give evidence of a flood-dominated tidal asymmetry in Bailey	

Cove. This is marked by a brief flood tide with a strong incoming flow and a long ebb tide with a relatively weak outgoing flow. 31

Figure 4-10. A view of the type of drifter used in the field studies of July 7-8, 2004. The unit at the top of the drifter's central cylinder (covered in tape) is a tracking device outfitted with a GPS receiver and a satellite transmitter. 33

Figure 4-11. The top panels show the positions of drifter released during the ebb tide of July 7, 2004. The bottom panels show the positions of particles released into the model flow field at the same time and location as the first drifter position in the panel above. The particle positions encompass the same time period as the drifter tracks shown above. 34

Figure 4-12. The top panels show the positions of drifter released during the ebb tide of July 8, 2004. The bottom panels show the positions of particles released into the model flow field at the same time and location as the first drifter position in the panel above. The particle positions encompass the same time period as the drifter tracks shown above. 35

Figure 4-13. The sensor depth (i.e., water level) of the CTD deployed in Bailey Cove (at the location indicated in Figure 4-8). Indicated are the times of rising and falling water between the highest water level and a water level 0.5 m above the minimum sensor depth. These show a tidal asymmetry in which the rate of rising water of the flood tide exceeds the rate of falling water on the ebb tide. 37

Figure 4-14. The modeled water level of channel 281 in Bailey Cove (Figure 4-8) during the time of the CTD measurements of water level shown in Figure 4-13. As in Figure 4-13, the times of rising and falling water between the highest water level and a water level 0.5 m above the minimum level are indicated. These show a tidal asymmetry of a degree nearly matching that indicated by the measurement of Figure 4-13. 37

Figure 4-15. Time series of the quarterly amounts of ^{60}Co and ^{137}Cs released from the Maine Yankee facility. Time periods of the Bailey Cove, diffuser and Little Oak Island discharges are indicated on the bar above time series lines. The circled values show the amounts of radionuclides released in the simulations of discharges from the Bailey Cove outflow and the diffuser. 40

Figure 4-16a. Modeled concentrations of ^{137}Cs and ^{60}Co in bottom sediments. These were derived from simulations of radionuclide release from the Bailey Cove discharge (depicted by the black diamond) during flood tide conditions. Note that these are volume concentrations in units of pCi l^{-1} . They may be converted to mass concentrations in units of pCi kg^{-1} by dividing by the density of surficial sediment, typically 1.8 kg l^{-1} 42

Figure 4-16b. A smaller scale view of the modeled concentrations of ^{137}Cs and ^{60}Co of Figure 4-16a. 42

Figure 4-17a. Modeled concentrations of ^{137}Cs and ^{60}Co in bottom sediments. These were derived from simulations of radionuclide release from the diffuser (depicted by the black diamond) during flood tide conditions. 43

Figure 4-17b. A smaller scale view of the modeled concentrations of ^{137}Cs and ^{60}Co of Figure 4-17a. 43

Figure 4-18a. Modeled concentrations of ^{137}Cs and ^{60}Co in bottom sediments as derived from simulations of radionuclide release from the Bailey Cove discharge (depicted by

Maine Yankee Marine Sampling Study

the black diamond) during flood tide conditions. These are the same concentration fields shown in Figure 4-16, except with the effects of radioactive decay accounted for.....	44
Figure 4-18b. A smaller scale view of the modeled concentrations of ^{137}Cs and ^{60}Co of Figure 4-18a.	44
Figure 4-19a. Modeled concentrations of ^{137}Cs and ^{60}Co in bottom sediments as derived from simulations of radionuclide release from diffuser (depicted by the black diamond) during flood tide conditions. These are the same concentration fields shown in Figure 4-17, except with the effects of radioactive decay accounted for.	45
Figure 4-19b. A smaller scale view of the modeled concentrations of ^{137}Cs and ^{60}Co of Figure 4-19a.	45
Figure 4-20. Modeled concentrations of ^{137}Cs and ^{60}Co in bottom sediments. These were derived from simulations of radionuclide release from the Little Oak Island Outfall (depicted by the black diamond) during flood tide conditions.	46
Figure 5-1. 6-9 July 2004 Station Locations	54
Figure 5-2. 6-9 July 2004 Station Locations - Close to Plant	55
Figure 5-3. 2-5 Aug 2004 Station Locations	56
Figure 5-4. 2-5 Aug 2004 Station Locations - Close to Plant	57
Figure 5-5. Station Sasanoa core: ^{60}Co and ^{137}Cs vs. depth	58
Figure 5-6. Station Pottle Cove core: ^{60}Co and ^{137}Cs vs. depth.....	58
Figure 5-7. Station Long Creek core: ^{60}Co and ^{137}Cs vs. depth	59
Figure 5-8. Station Barry Cove core: ^{60}Co and ^{137}Cs vs. depth.....	59
Figure 5-9. Station Wiscasset core: ^{60}Co and ^{137}Cs vs. depth	60
Figure 5-10. Station Eddy core: ^{60}Co and ^{137}Cs vs. depth	60
Figure 5-11. Station Chewonki Camp core: ^{60}Co and ^{137}Cs vs. depth	61
Figure 5-12. Station 2 core: ^{60}Co and ^{137}Cs vs. depth.....	61
Figure 5-13. Station 8-1 core: ^{60}Co and ^{137}Cs vs. depth	62
Figure 5-14. Station 25 core: ^{60}Co and ^{137}Cs vs. depth.....	62
Figure 5-15. Station 34, Diffuser, core: ^{60}Co and ^{137}Cs vs. depth.....	63
Figure 5-16. Station 38, Westport Island, core: ^{60}Co and ^{137}Cs vs. depth.....	63
Figure 5-17. Station 44, Eaton Farm Point, core: ^{60}Co and ^{137}Cs vs. depth.....	64
Figure 5-18. Station 50, Pottle Cove, core: ^{60}Co and ^{137}Cs vs. depth	64
Figure 5-19. Station 59, South Oak Island, core: ^{60}Co and ^{137}Cs vs. depth	65
Figure 5-20. Station 60, South Oak Island, core: ^{60}Co and ^{137}Cs vs. depth	65
Figure 5-21. Station 61, Westport Island, core: ^{60}Co and ^{137}Cs vs. depth.....	66
Figure 5-22. Station 62, Westport Island, core: ^{60}Co and ^{137}Cs vs. depth.....	66
Figure 5-23. Station 63, Long Ledge, core: ^{60}Co and ^{137}Cs vs. depth.....	67

Maine Yankee Marine Sampling Study

Figure 5-24. Station 64, Long Ledge, core: ^{60}Co and ^{137}Cs vs. depth.....	67
Figure 5-25. Station 65, Bluff Head, core: ^{60}Co and ^{137}Cs vs. depth	68
Figure 5-26. Station 66-1 core: ^{60}Co and ^{137}Cs vs. depth	68
Figure 5-27. Station 67, Cushman Cove, core: ^{60}Co and ^{137}Cs vs. depth	69
Figure 5-28. Station 68, Foxbird Island, core: ^{60}Co and ^{137}Cs vs. depth.....	69
Figure 5-29. Station 73, Bailey Cove Outfall, core: ^{60}Co and ^{137}Cs vs. depth.....	70
Figure 5-30. Station 74, Bailey Cove Outfall, core: ^{60}Co and ^{137}Cs vs. depth.....	70
Figure 5-31. Station 77, Upper Bailey Cove, core: ^{60}Co and ^{137}Cs vs. depth	71
Figure 5-32. Station 85, South Bailey Cove, core: ^{60}Co and ^{137}Cs vs. depth.....	71
Figure 5-33. Station 99, North Bailey Cove, core: ^{60}Co and ^{137}Cs vs. depth.....	72
Figure 5-34. Station 101, Eaton Farm Bailey Cove, core: ^{60}Co and ^{137}Cs vs. depth	72
Figure 5-35. Station 105, Top of Bailey Cove, core: ^{60}Co and ^{137}Cs vs. depth	73
Figure 5-36. Station 108, Bailey Point West, core: ^{60}Co and ^{137}Cs vs. depth.....	73
Figure 5-37. Station 113, South Foxbird Island, core: ^{60}Co and ^{137}Cs vs. depth	74
Figure 5-38. Station 117 core: ^{60}Co and ^{137}Cs vs. depth.....	74
Figure 5-39. Station 118, Little Oak Island, core: ^{60}Co and ^{137}Cs vs. depth.....	75
Figure 5-40. Station 134 core: ^{60}Co and ^{137}Cs vs. depth.....	75
Figure 5-41. Station 143, Youngs Point, core: ^{60}Co and ^{137}Cs vs. depth	76
Figure 5-42. Station 144, Oak Island Murphy Corner, core: ^{60}Co and ^{137}Cs vs. depth	76
Figure 5-43. Station 145, Oak Island Murphy Corner, core: ^{60}Co and ^{137}Cs vs. depth	77
Figure 5-44. Station 146, Darling Center, core: ^{60}Co and ^{137}Cs vs. depth	77
Figure 5-45. Station 147 core: ^{60}Co and ^{137}Cs vs. depth.....	78
Figure 5-46. Station 148 (Darling Center) core: ^{60}Co and ^{137}Cs vs. depth.....	78
Figure 5-47. Station 149 (Sasanoa) core: ^{60}Co and ^{137}Cs vs. depth.....	79
Figure 5-48. Station 144 core: ^{210}Pb vs. depth.....	79
Figure 5-49. ^{60}Co Concentrations at 6 in. (pCi/kg).....	80
Figure 5-50. ^{137}Cs Concentrations at 6 in. (pCi/kg).....	81
Figure 5-51. ^{60}Co Average Core Concentrations (pCi/kg).....	82
Figure 5-52. ^{137}Cs Average Core Concentrations (pCi/kg).....	83
Figure 5-53. ^{60}Co Surficial Concentrations (pCi/kg).....	84
Figure 5-54. ^{137}Cs Surficial Concentrations (pCi/kg).....	85
Figure 5-55. ^{60}Co Surficial Isocuric Concentrations (pCi/kg) - Close to Plant	86
Figure 5-56. ^{137}Cs Surficial Isocuric Concentrations (pCi/kg) - Close to Plant.....	87
Figure 6-1. Hot Particle Scan, 7 July 2004.....	103
Figure 6-2. Hot Particle Scan, 2 August 2004.....	103

Maine Yankee Marine Sampling Study

Figure 6-3. Hot Particle Scan, 18 August 2004..... 104
Figure 6-4. Hot Particle Scan Map..... 105

List of Tables

	Page
Table 3-1. Number of Sediment Samples Collected for Maine Yankee in Phase 1	10
Table 3-2. Number of Sediment Samples Collected for Maine Yankee in Phase 2	10
Table 3-3. Species Selected For Biota Sampling	13
Table 4-1. According to model simulations, the percent of the total radionuclide released from the indicated location that is absorbed in the bottom sediment. The values were computed from simulations using velocities representative of spring tide conditions.....	47
Table 5-1. Sediment gamma scan results	88
Table 5-2. Summary of ¹³⁷ Cs peaks observed in cores.	98
Table 5-3. Total ⁶⁰ Co and ¹³⁷ Cs activity contained in cores.....	99
Table 5-4. Biota gamma scan results.....	100
Table 5-5. Comparison with Pre- and Post-operational study	101
Table 5-6. Results of the Hard to Detect Nuclides.....	101
Table 7-1. Calculated Doses Using Average Concentrations of Gamma Emitters.....	114
Table 7-2. Calculated Doses Using Peak Concentrations of Gamma Emitters	115

List of Appendix Figures

	Page
Appendix Figure A-1. Project locus map (1978).	A-3
Appendix Figure A-2. Channel network used for Montsweag Bay and Bailey Cove modeling. (Source: Churchill et al. 1980; Hess et al. 1983).....	A-3
Appendix Figure A-3. Actual contours for ⁶⁰ Co measured on September 18, 1974 during licensed releases.	A-4
Appendix Figure A-4. Actual contours for ⁶⁰ Co measured on June 12, 1975 during licensed releases.....	A-5
Appendix Figure A-5. Actual contours for measured ¹³⁷ Cs after Maine Yankee diffuser was in place (Hess et al. 1978).	A-6
Appendix Figure A-6. Sample of currents at slack high tide (1978).	A-7
Appendix Figure A-7. Estimated ¹³⁷ Cs concentrations 4.38 hours after a release beginning at high tide (1978).	A-7
Appendix Figure A-8. Estimated ¹³⁷ Cs concentrations 4.38 hours after a release beginning at mid-ebb tide (1978).....	A-8
Appendix Figure A-9. Estimated ¹³⁷ Cs concentrations 17.5 hours after a release beginning at high tide (1978).	A-8
Appendix Figure A-10. Estimated ⁵⁸ Co concentrations 17.5 hours after a release beginning at mid-ebb tide (1978).....	A-9
Appendix Figure A-11. Simulated contours for ¹³⁷ Cs concentrations 17.5 hours after a release beginning at high tide (Hess et al. 1978).	A-9
Appendix Figure A-12. Simulated contours for ⁵⁸ Co 17.5 hours after a release beginning at high tide (1978).	A-10
Appendix Figure A-13. Actual contours for ⁵⁸ Co measured after 17.5 hours beginning at high tide (1978).....	A-11

List of Appendix Tables

	Page
Appendix Table A-1. Pre-operational Laboratory Soil & Sediment Gamma Ray Analysis	A-12
Appendix Table A-2. Post-operational Laboratory Soil & Sediment Gamma Ray Analysisi	A-13

1. EXECUTIVE SUMMARY

1.1 CHARACTERIZATION OF RADIONUCLIDES IN THE BACK RIVER AND INTERTIDAL ZONE AROUND THE FORMER MAINE YANKEE NUCLEAR POWER PLANT SITE.

As a result of the closure and decommissioning of the Maine Yankee Nuclear Power Plant, and the 1999 Federal Energy Regulatory Commission (FERC) settlement, Maine Yankee agreed with Raymond Shadis, Executive Director of Friends of the Coast (FOTC), to fund and conduct an environmental field survey of marine sediments in the Back River. The purpose of the study was to determine how licensed liquid radioactive effluent discharges from Maine Yankee are distributed in the environment. In the 2001 License Termination Plan (LTP) settlement, Maine Yankee further agreed to conduct a similar study in the intertidal zone surrounding selected portions of Maine Yankee property. By separate agreement, the State of Maine, subject to approval of FOTC, specified various aspects of the sampling program.

Researchers from the University of Maine, the Woods Hole Oceanographic Institute, and Normandeau Associates performed the study. The majority of samples were taken during the summer of 2004 after the final discharge of the plant's spent fuel pool. This report characterizes radionuclides in the marine environment around Maine Yankee and describes the methodologies used in the study. Four sets of sampling were accomplished to complete this study. The results of each type of sampling are provided and are compared with a model of radionuclide distribution from licensed discharges. Additionally, the results are compared to previous work done in the area both pre and post plant operation. The results are also used to calculate an incremental intertidal zone dose, which is compared to the limiting "resident farmer dose calculations in the License Termination Plan for Bailey Point post-decommissioning." Maine Yankee operated from 1972-1996. Plant decommissioning is scheduled to be complete in late spring of 2005.

This sampling effort included a search for areas high in nuclear radiation (hot particle search), samples from the surface of the tidal region, core samples from the tidal region, and samples of biota including seaweed, lobsters, mussels, and fish. The results are discussed in this order. In all, about 600 samples from 147 locations were collected and analyzed. To ensure that the sampling effort was as comprehensive and efficient as possible, a model was used to determine the best locations. The results of this effort are summarized here.

Before any sample collection, a model of the bay was developed to determine the effect of tidal influences on releases of radioisotopes. The model takes into account the action of the tides, the flow of water, and the discharges from various points. The work was necessary due to the changes made over time to the plant. In particular, three different discharge points were used as well as the removal of a causeway over the lifetime of the plant. A theoretical model was developed to determine the location of the hottest zones for radioisotopes. This model was tested using floats to validate the results. The predictions of the model became the points for the first sampling effort. After measuring this first set and refining the model, a second sampling effort was accomplished based on the results of the first set. In this manner, a coordinated study was possible.

The first results to discuss involve the search for localized areas high in radiation. To accomplish this goal, an instrument which measures radiation exposure called a High Pressure Ion

Maine Yankee Marine Sampling Study

Chamber (HPIC) was used. The HPIC was placed on a sled and dragged across the mud flats at low tide. Three sets of measurements were taken. These sets were placed so that the HPIC system would pass close to the discharge points. If a single measurement of three times background was found, the HPIC would signal the researchers that a hot spot was found. No such measurement was found. In fact, the exposure seen away from shore was, in general, less than the background seen on shore. We feel this is due to the mixing of the sediment due to the action of tides and the turnover of sediment due to digging (clam or worm digging).

The next set of results involves the analysis of the samples taken from the surface of the intertidal zone. These samples were analyzed for certain radioisotopes associated with nuclear fission including ¹³⁷Cs and ⁶⁰Co. As expected, these were the predominate radioisotopes seen. The results were compared to measurements taken earlier. In general, the values seen are lower than before the plant was brought on line. We feel that the reason the values are so low is due to a mixing within the tidal flat, lowering the amount of radiation seen on the surface. The distribution of the Cesium and Cobalt is also consistent with the history of discharges. The Cobalt is highest near the recently used diffuser. Since Cobalt has a relatively short half-life, we expected to see very low levels at locations where discharges were stopped and highest where discharges were done more recently. Cesium, with a longer half-life, should be higher at locations that had more discharges. Overall the greatest concentration of plant derived radionuclides is in Bailey Cove and the area of the diffuser. Bailey Cove was the original plant discharge location prior to installation of the diffuser. The distribution is consistent with these assumptions.

As well as surface samples, cores were also taken, sectioned, and counted. The results show that the overall radiation is low. An individual core was sectioned and counted to determine how far into the soil the highest level of radiation exists. Most radiation was found below the surface, which is consistent with results from surface samples. Again, the data indicates that a mixing of the soil is occurring so that radioisotopes are distributed and do not remain localized.

In comparison, naturally occurring radionuclides such as ⁴⁰K are found at higher levels in the marine environment than either Cesium or Cobalt. The average naturally occurring Potassium concentration was about 10 pCi/g, which results in an exposure rate of approximately 8 mrem/yr. The average Cesium or Cobalt concentration was about 0.073 pCi/g or 0.019 pCi/g which results in an exposure rate approximately 0.17 mrem/yr or 0.13 mrem/yr, respectively using NRC approved soil screening values.

Last, several biota samples were taken and analyzed. These samples included lobsters, clams, mussels, seaweed and fish. The samples were crushed and analyzed for the same radioisotopes as above. For the shellfish, the shells were counted separately from the meat. Additionally, these samples were sent to another laboratory to search for radioisotopes, such as Beta emitters and Plutonium, which are difficult to measure (hard to detects). The results show that all levels are very low, including the hard to detect values.

As a final calculation, the results of the above samples were used to calculate the average and peak doses that an individual would receive if they stood on the tidal flat went swimming, went fishing, harvested seaweed, or ingested the biota. The results range between 3 mrem/yr for land reclamation to 2.6×10^{-3} mrem/yr for swimming. Such exposures are a small fraction of normal exposures received naturally through a year. The low exposures are indicative of the low values seen in the data sets.

2. PURPOSE OF THE MARINE SAMPLING STUDY

In accordance with agreements with the Friends of the Coast and the State of Maine, Maine Yankee established a contract with the University of Maine, Wood's Hole Oceanographic Institute and Normandeau Associates to conduct a radiological sampling and analysis study of the marine environment surrounding the Maine Yankee site. The purpose of this study is to:

1. Develop an isotopic (isocuric) picture of how licensed discharges are spatially distributed and accumulated in the environment.
2. Develop information which will be used to educate the public and enhance public confidence in the decommissioning process. This information includes:
 - a. A report of measured radiological concentrations in marine sediment and selected marine biota in the environs surrounding the Maine Yankee site concentrations in Bailey Cove performed by a third-party-contractor..
 - b. A dose assessment of these measured radiological concentrations

3. FIELD SAMPLING

The first sampling survey, Phase 1, entailed acquiring sediment samples over a broad region, including farfield locations and focusing on those areas identified by the numerical modeling as potential regions of sediment and radionuclide accumulation (Figures 3-1, 3-2, 3-3). During this phase, we conducted an intertidal search for particularly radioactive, “hot”, particles, and acquired samples of flora and fauna. This was followed by the more intensive Phase 2 survey with concentrated sampling in those areas identified to be of particular interest on the basis of the results of the first survey, and further guided by additional modeling (Figures 3-4, 3-5). We collected 398 sediment samples as part of this later survey. To ensure that the samples collected by these surveys were counted in a timely fashion, sufficient to guide the ensuing surveys, we employed three gamma counting devices available at the University of Maine, Orono.

Field sampling was conducted in both intertidal and subtidal areas, each with its own protocol. Surface and subsurface (core) marine sediment samples were collected in each area. Numbers of samples are listed in Table 3-1. These include a four-way split for 10% of the samples, which was accomplished by collecting four duplicate samples and delivering one set of duplicates to Maine Yankee, one set to the State of Maine, and one set to Friends of the Coast. Additional sediment samples were collected at the request of Friends of the Coast in farfield locations including Pottle Cove near Wiscasset Harbor, the “Eddy”, Robin Hood Cove, and the Sasanoa River (Station 149) (Figure 3-2). Background sediment samples were collected in Taunton Bay, Clarks Cove at the Darling Center (Station 148) in Damariscotta Bay (Figure 3-1).

The Phase 1 survey was conducted July 6, 7 and 8, 2004. Phase 2 was conducted on August 2-5 and September 16-17, 2004. In accordance with our overall project plan, we designed the Phase 1 survey on the basis of modeling results and the findings of previous studies. This design is described in the next section. The Phase 2 survey was designed based on the Phase 1 results and additional modeling.

All field sampling was conducted in an environmentally conscientious manner. Access was either at public boat launches or by foot along pathways used by harvesters. Only abundant organisms were collected. Every effort was made to minimize disturbance to the marine environment during sampling.

3.1 SEDIMENT SAMPLING

3.1.1 Phase 1

The locations of the Phase 1 sediment sampling sites (Figure 3-3) were based on hydrodynamic modeling (Section 4.0) of the estuarine system that includes the Maine Yankee discharge, and on the results of previous measurements of radionuclide concentration in the area near the discharge. This tests how well the model predicts the location of nuclides in sediment. The initial modeling results revealed that the Maine Yankee discharge is located roughly a kilometer north of a tidal node. As a result, tidal currents in the area of the discharge are relatively weak and tidal excursions are small (on the order of 500 m). Tracking of particles released from the discharge location into the model flow field indicates that material released from the discharge should not be expected to travel very far over the course of a tide, even for spring tide conditions with maximum

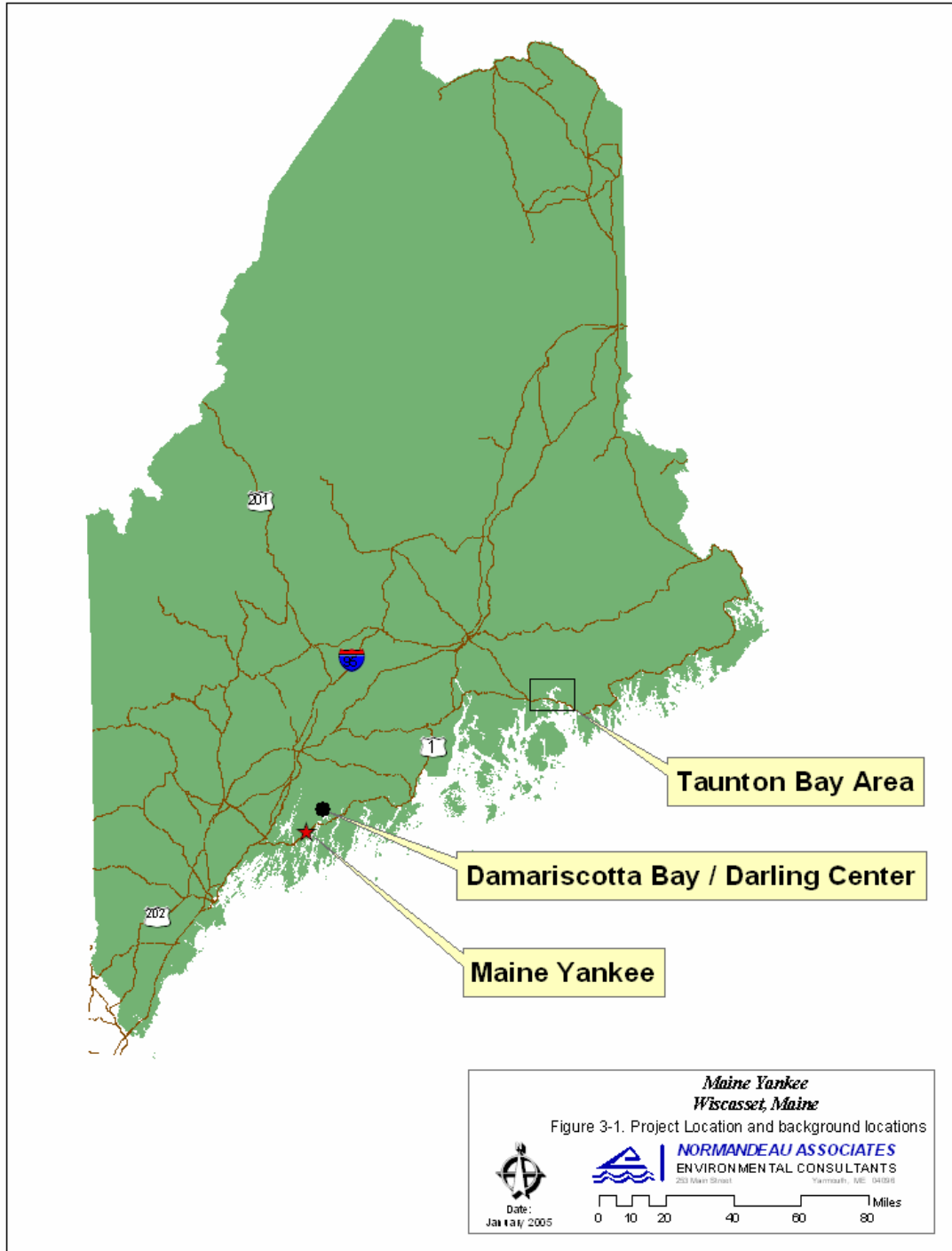


Figure 3-1. Project location and background locations.

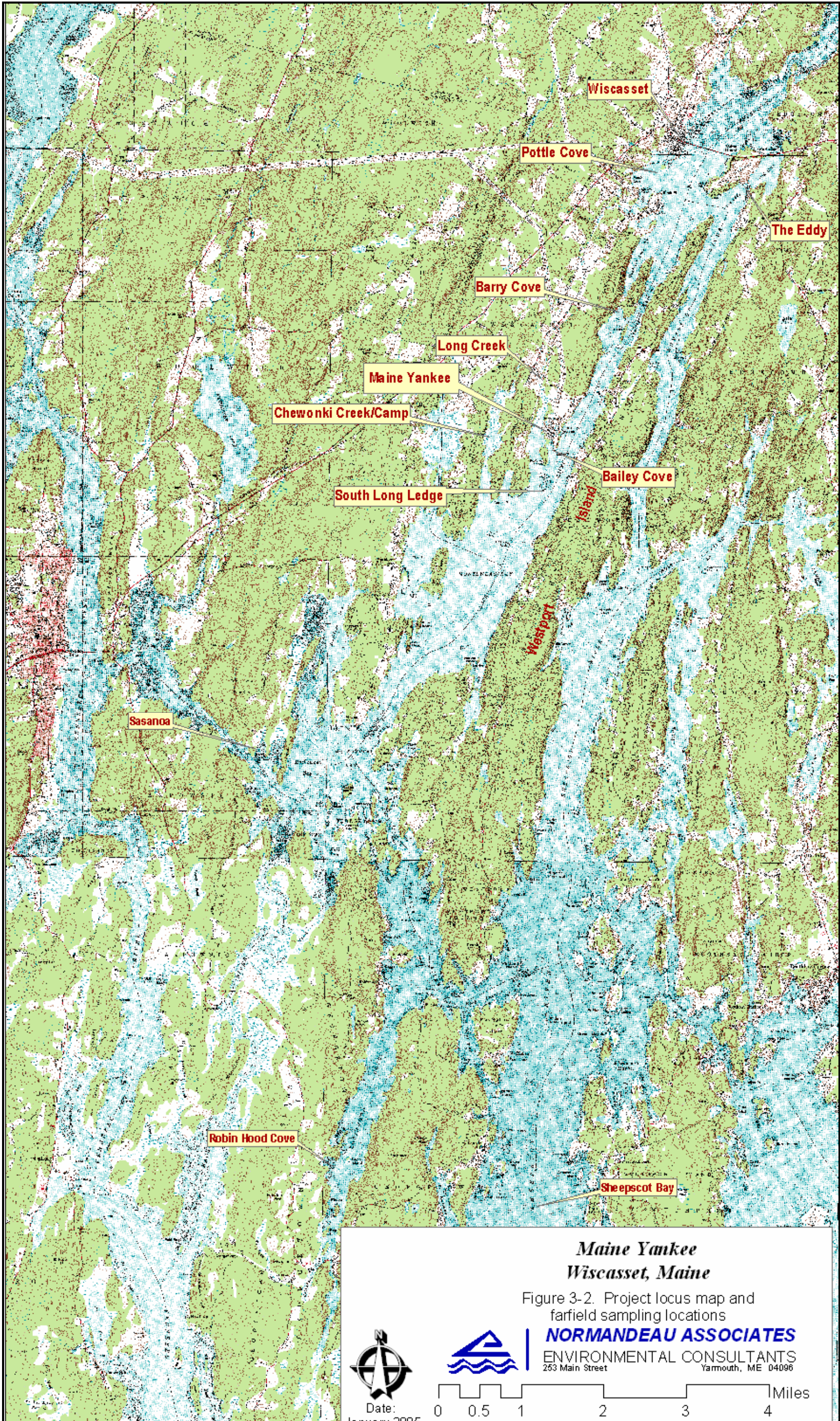


Figure 3-2. Project locus map and farfield sampling locations.

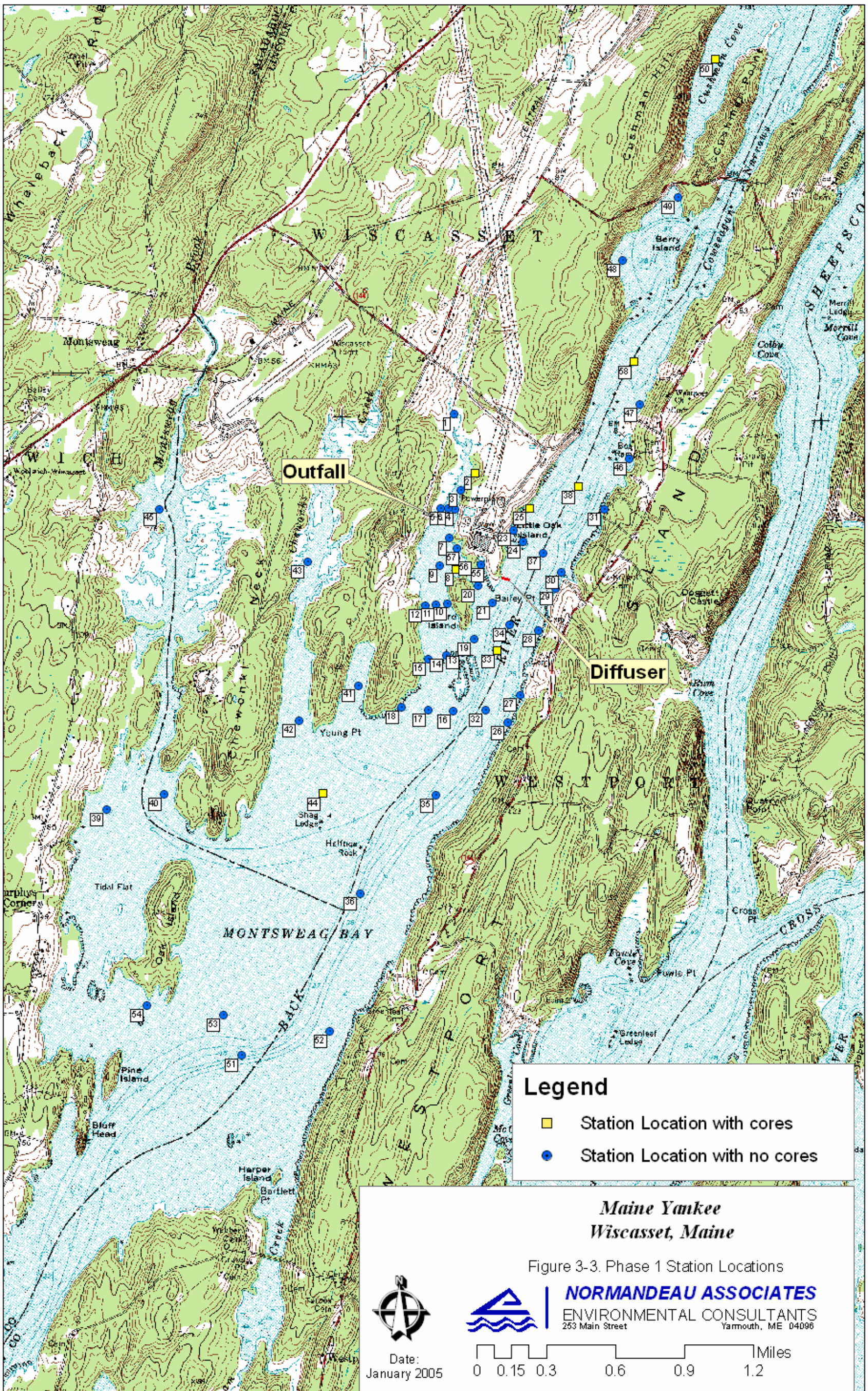


Figure 3-3. Phase 1 station locations

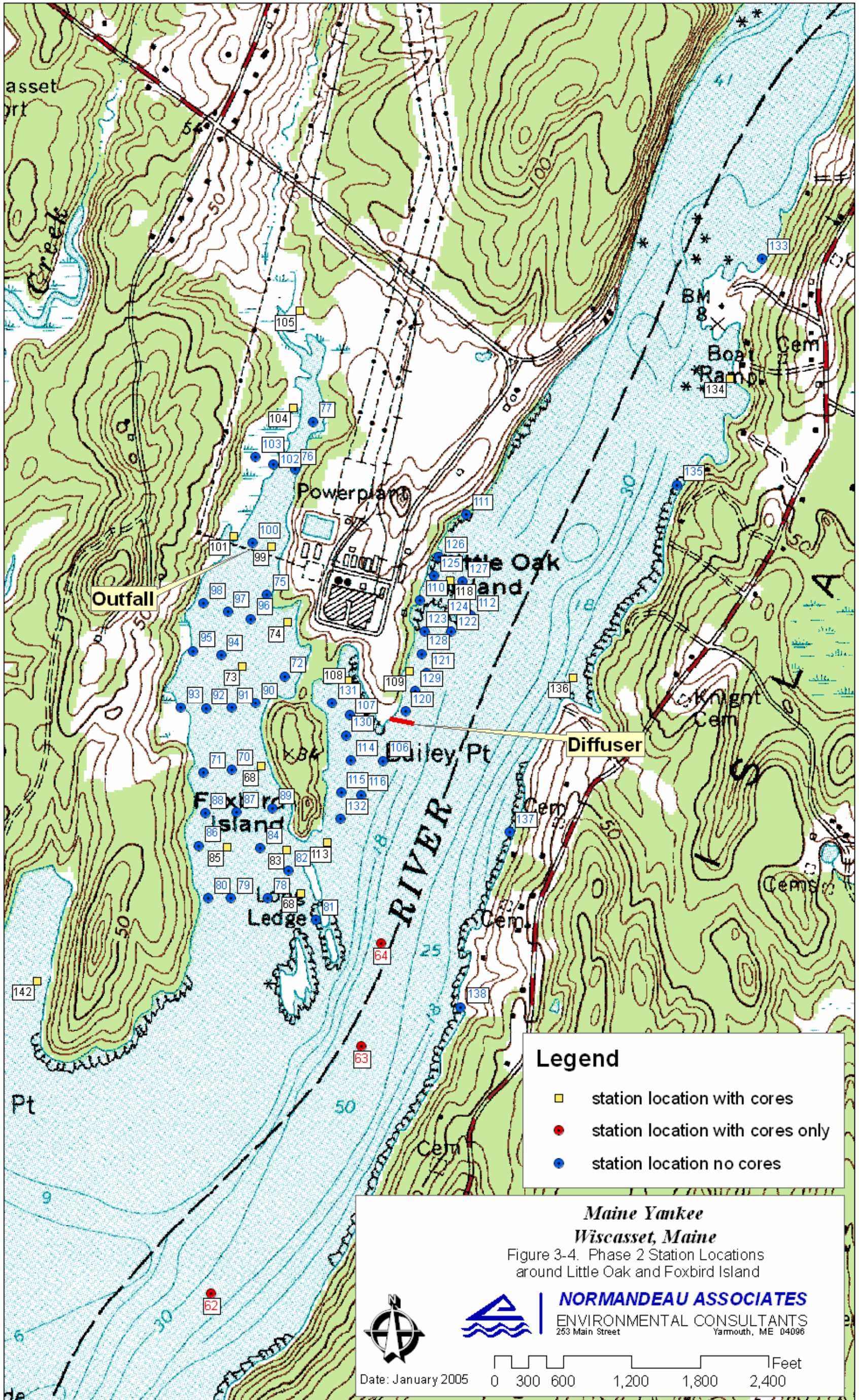


Figure 3-4. Phase 2 station locations around Little Oak and Foxbird Island.

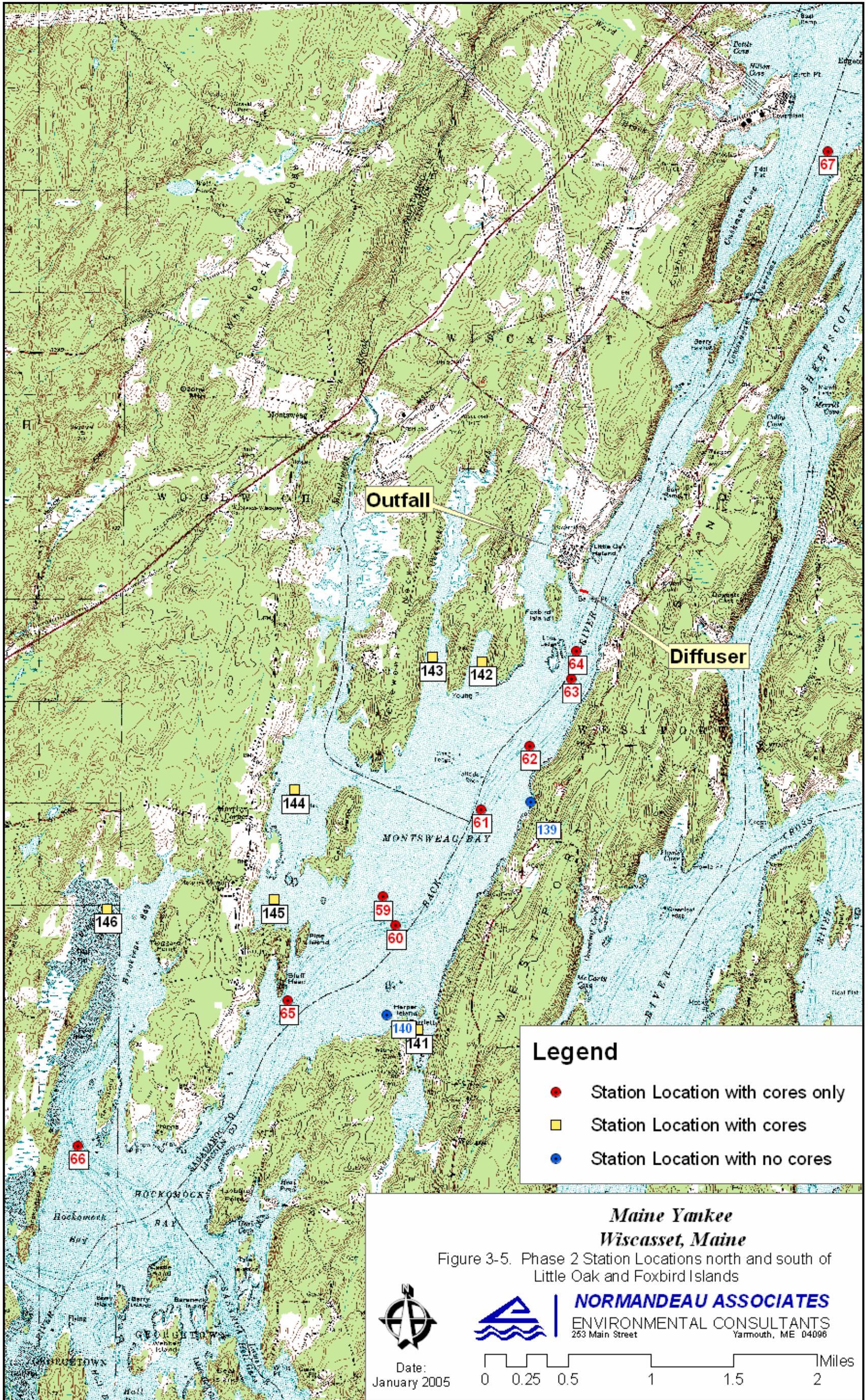


Figure 3-5. Phase 2 station locations north and South of Little Oak and Foxbird Islands.

Maine Yankee Marine Sampling Study

riverine inflow. The model results also indicate a northward bias in the transport of material released from the diffuser, due to the asymmetry of the tidal flow moving northward of the tidal node.

These results are consistent with the findings of previous radionuclide surveys conducted in the region. In particular, the study conducted in 1978 found that radionuclide (^{137}Cs and ^{58}Co)

Table 3-1. Number of Sediment Samples Collected for Maine Yankee in Phase 1

Sample Location	Sample Type	Regular	Duplicate	Total
Intertidal	surface	50	12	62
	core	5	6	11
Subtidal	surface	8	3	11
	core	2*	3	5
Additional cores		4		4
Farfield (Taunton & Darling Ctr)		2		2
Total		74	24	95
Total Phase 1 samples collected for counting			73	surface
			192	core slices

*One core not collected due to unsuitable substrate

Table 3-2. Number of Sediment Samples Collected for Maine Yankee in Phase 2

Sample location	Sample Type	Actual	Duplicate	Total
Intertidal	surface	75	18	93
	core	18	6	24
subtidal	surface	0	0	0
	core	9	3	12
				0
Total stations		102	27	129
Total samples collected for analysis (including all core slices)				398

concentrations in Back River were above background over a relatively small region, extending roughly 1-2 km from the diffuser, and that this region was biased (extended further from the diffuser) to the north of the diffuser (Hess et al., 1983). This survey also found significant radionuclide concentrations in the sediments of Bailey Cove, likely due to a combination of accumulation from early discharges into Bailey Cove and from the later diffuser discharges. Given the weak tidal energy of this area, we expected much of the radionuclide containing sediment of Bailey Cove to remain within the Cove.

Based on the initial hydrodynamic results, we focused much of our Phase 1 sampling in the area of Bailey Cove and in the region of Back River near the diffuser location (Figure 3-3). In hopes of determining the horizon of detectable radionuclide concentrations, we also set sampling locations

further south (into Montsweag Bay), further north in Back River (into Cushman Cove), and into tributary regions of Chewonki Creek and Montsweag Brook. We have identified 5 locations at which core samples were acquired, and later sectioned and analyzed. Analysis of a core sample acquired in February 2004 near the plant intake has shown highest radionuclide concentration at 6 cm depth. For this reason, we acquired core samples from at least 10 additional sites to be set aside for possible analysis, depending on the results of the core samples from the 5 sites designated for analysis.

Details of the sampling collection method follow.

3.1.1.1 Intertidal Surface

Intertidal sediment samples were collected on foot at low tide. Staff made collections in areas accessible from the shore by traversing the area on foot using existing pathways. Collections in areas that were inaccessible by foot (such as Back River and around Little Oak Island) were made by deploying staff at Little Oak Island via boat. Field staff first marked sampling locations for that tide cycle using a wire stake marked with the station number. Staff navigated to the approximate station location using the map and visual cues, and then marked the sampling site. One staff member recorded GPS coordinates as well as reference areas so that the exact location of the sample sites was known. The surficial sediment samples were collected at pre-established locations by removing the top centimeter of sediment from an approximately 32 X 32 cm square with a trowel and depositing the sample in a pre-labeled polyethylene jar, with internal and external labeling. Each marker stake was removed and brought back to the office when the sample had been collected. Samples were kept cool until transport to the laboratory.

3.1.1.2 Intertidal Subsurface

Intertidal subsurface sediment samples were collected in the same manner as intertidal surface samples but using a different device. A four-inch diameter pre-labeled Plexiglas core was deployed by hand to a depth of 12 inches (or refusal) in areas selected for subsurface sampling. The core was capped at both ends, then placed in a pre-labeled plastic bag and stored upright. Samples were kept cool until transport to the laboratory. The core was inspected visually both after sample collection and prior to slicing to ensure that the integrity of the core had been maintained. Samples were discarded if it is determined that the integrity had not been maintained. Each core was sliced using a core slicer into one-inch samples. One-inch layers were extruded from the end of the core and captured with a bucket, then placed into a pre-labeled container. Excessive water in the sediment sample was drained if necessary to maintain the integrity of the sediment.

3.1.1.3 Subtidal Surface

Subtidal sediment samples were collected from a boat using a 0.04 m² Young-Van Veen grab. The locations of the subtidal samples are shown in Figure 3-1. The boat captain occupied the approximate location of each station using a navigational chart, fathometer, and GPS. The location was adjusted if necessary to ensure that samples can be safely collected and consist of soft substrate. Each grab was deployed and retrieved; surface sediment (< 1 cm depth) was removed from the grab and placed in a pre-labeled polyethylene jar, with internal and external labeling. The GPS coordinates were checked, the boat was relocated if necessary, and the Van Veen grab was redeployed. This process continued until sufficient sediment was collected. Samples were kept cool until transport to the laboratory.

3.1.1.4 Subtidal Subsurface

Subtidal subsurface sediment samples were collected using a gravity corer. The approximate locations of the subtidal samples are shown in Figure 3-3. The boat captain occupied the approximate location of each station using a navigational chart, fathometer, and GPS. Each core was deployed and one-inch layers of the sediment were retrieved, placed in a pre-labeled polyethylene jar, with internal and external labeling. Samples were kept cool until transport to the laboratory.

3.1.2 Phase II

The results of Phase I revealed concentrations of radionuclides at depth. The project team recommended that some of the surface samples be replaced with core samples. With Maine Yankee's approval, the samples listed in Table 3-2 and shown in Figures 3-4 and 3-5 were collected.

3.1.2.1 Intertidal Surface and Subsurface

This protocol was the same as for Phase I except that a hand held Magellan GPS was used to record sample locations.

3.1.2.2 Subtidal Surface and Subsurface

This protocol was the same as for Phase I.

3.1.3 Hard to Detect

Hard to detect samples were selected from the highest gamma scan samples for measurement of the hard-to detect nuclides. These were sent out to Duke Framatome ANP

3.2 GAMMA SCAN OF INTERTIDAL ZONE

An in situ gamma scan was conducted after the first phase of sampling was completed. The goal was to ascertain if there are any "hot particles" (defined as >100,000 cpm) in the intertidal areas. The initial survey, in addition to information from previous studies, helped focus this effort on most likely areas of deposition. The effort concentrated on the shoreline adjacent to Maine Yankee. Field staff traversed a 2-m strip encompassing roughly 207 m of shoreline in Bailey Cove and a 1-m strip encompassing roughly 1260 m of shoreline in Back River, resulting in 1674 square meters in total. Areas around the intake, forebay, and diffuser discharge are the most important.

Hot particle measurements were done by the high-pressure ion chamber, capable of measuring microrems/hour, and a three inch by three inch sodium iodide detector and laptop PC with a pulse height analyzer board mounted on a kayak-sled for transport over the wet sediment. The sensitivity of the system allows detection of a one microcurie source at one meter distance, and 0.03 microcuries is detected at 30 cm. Test of the sensitivity has been done by calculation and by actual measurements on land with buried test sources of ^{60}Co , and ^{137}Cs . This sled also had a portable GPS unit to measure position as a function of radioactivity. The sled was moved over the intertidal zone areas for direct measurement of hot particles. If a hot particle had been discovered, we would have flagged the area with a survey stake and recorded its location with GPS, then contacted Maine Yankee. Work would have continued unless an unsafe level is discovered (defined as three times the background level).

3.3 BIOTA SAMPLE COLLECTION

Five species were initially selected for dose pathway estimation based on their likely anticipated contribution to dose pathways as well as anticipated seasonal availability and abundance, based on a review of available literature (Larson, P.F. 1975; Larson, P.F. and Doggett, L 1991; Larson, P.F., Doggett, L. and A.C. Johnson. 1983; Maine Yankee 1978, 1994, 2002). The pathways to be investigated included direct exposure through harvesting activities (algae, soft-shell clam) and direct exposure through consumption (soft-shell clam, lobster, winter flounder) as shown in Table 3-3. These species give highest priority to sessile species (which are subject to continuous input), harvested species, and highest bioaccumulators (those higher in the trophic level that are consumed by humans). Preliminarily, we assumed these to be seaweed (*Ascophyllum nodosum* or *Fucus* spp.), soft-shell clams (*Mya arenaria*), blue mussels (*Mytilus edulis*), lobster (*Homarus americanus*), and winter flounder (*Pleuronectes americanus*). Clam and blood worms were also considered for dose pathway estimation but, since soft-shell clams have two possible pathways (contact and ingestion), they were thought to be a better choice.

Table 3-3. Species Selected For Biota Sampling

Pathway	Primary species	Organism type	Alternative
Direct contact through collection Consumption Fertilizer Use	Rockweed	Algae	none
Direct contact through collection Consumption Fertilizer Use of Shell	Blue Mussel	filter feeding bivalve	consider periwinkles (<i>Littorina</i> spp.) as possible substitute even though not a filter feeder
Direct contact through collection, human Consumption Fertilizer Use of Shell	Soft-shell clam	deposit feeding bivalve	none
Human consumption	Winter flounder	demersal fish	smooth flounder
Human consumption	Lobsters	demersal feeding crustacean	rock crab

Biotic samples of commercially-harvested species (soft-shell clams, and lobster) were obtained directly from harvesters in Bailey Cove (clams) and the Back River (lobsters). Blue mussels and algae were collected at Little Oak Island. Fish (winter flounder and hake) were collected by otter trawl in Back River near Maine Yankee. At least 2.3 kg (five pounds) of lobster and fish were collected; at least 2000 grams of seaweed (4.4 lb.) Clams and mussels were shucked and the edible tissue was macerated in a food processor, with sufficient sample to provide 910 g (2 lb) of wet weight tissue material. Shells were counted as separate samples. Sufficient material was collected in 10% of the samples (determined randomly in advance of sampling) to allow them to be split four ways. Lobster meat was restricted to tail and claw meat, the most commonly consumed tissue. The lobster hepatopancreas (tomalley) is known to accumulate organic contaminants, but there is no evidence that radionuclides would be selectively accumulated in any organ of the lobster. All samples were kept cool until returned to the laboratory where they were frozen in doubled plastic bags with proper indelible internal identification sandwiched between the two bags. As finfish were not of sufficient size to fillet, they were frozen whole. Biota for background measurements were collected the Darling Center in Damariscotta and in South Portland.

3.4 QUALITY CONTROL

Samples have been archived until delivery of this final report. Cross contamination was prevented using individual sample collection devices or by washing with water to remove sediment particles between sample collections.

3.4.1 Sample Tracking and Custody

Tracking and custody of samples in the field was the responsibility of the Normandeau's Field Operations Manager. To ensure proper handling and identification of samples, they were labeled and packaged for shipment as they were collected in the field, or immediately upon returning to the field laboratory. Forms and containers specific to the task were used to ease handling and assure safety of the samples. Appropriate sections of each form were completed in the field and in each subsequent step of the process.

Sample control was accomplished by assigning unique numbers to each sample collected. These numbers were obtained from Normandeau's Quality Assurance Department. In preparation for a collecting trip, a Field Card/Sample Submittal Form(s) was completed for each set of samples taken: Following the sampling event, the field cards were checked to insure that they were completely and correctly filled out. The samples were checked to insure that sample labels were properly filled out with correct sample control numbers are attached Originals of the sample submittal forms were reviewed and put into a fire proof vault at Normandeau-Yarmouth for the Senior Field Biologist's or designee's review. Copies of the original field cards were sent with the samples to the appropriate laboratory.(in this case University of Maine, Maine Yankee, State of Maine, or Friends of the Coast).

3.4.2 Sample Storage and Transfer

Sediment samples were kept cool and transferred as soon as feasible to the University of Maine Department of Physics and Astronomy (or, in the case of duplicates, Maine Yankee, State of Maine, or Friends of the Coast), for gamma scans. Biotic samples were frozen, then sent to University of Maine or, in the case of duplicates, Maine Yankee, State of Maine, or Friends of the Coast . Chain of custody was implemented with documentation and labeling of containers in advance and following the handling to the end of the measurement. Copies of the chain of custody forms accompanied all samples, with the original retained at Normandeau-Yarmouth.

3.5 LABORATORY ANALYSIS

3.5.1 Gamma Screening

The surficial samples and core samples were gamma scanned at the Environmental Radiation Laboratory at the University Department of Physics and Astronomy. Gamma ray counting was done with three Canberra high purity Ge detectors and three 1000 kg low background lead shields. Data were collected using Ace computer boards, and Trump software from Ortec and Gamma Track by Nucleus. The Physics Department's detectors have been intercalibrated with the U.S.EPA National Exposure Research Lab in Las Vegas Nevada for Gammas in Water. Count times varied from four hours to 24 hours depending upon the concentration of radionuclides and interest in a particular sample. Chain of custody was preserved for all samples with labels and documentation in bound notebooks. Gamma ray spectra were analyzed using custom software which has been tailored to very low level counts (much less than Compton background, such as the expected counts at the bottom of the cores).

Isocuric plots were generated from the gamma scan results for the appropriate nuclides found in the samples. In those instances where it is possible, new samples were compared to archived data and samples from previous studies. This step enabled a quantitative before and after comparison of radionuclides levels in the sediments.

Detected hot particles in samples would have been tested by portable counter shielded if the dose on surface exceeded 1mr/h using lead or other sediment samples. However, no hot particles were detected.

3.5.2 Lead-210 and Cs-137 Dating

^{210}Pb and ^{137}Cs quantitative counting of samples was done, although dating can be done using raw counts/sec kg in a Canberra high purity Ge well counter in a 2600 pound tin and copper graded lead shield.

3.5.3 Hard to Detects

Hard to detect radionuclides were measured in an external laboratory (Duke Framatome ANP) including $^{238/239}\text{Pu}$, ^{63}Ni , ^{55}Fe , and ^{90}Sr . These had required minimum detectable concentration of 1, 20, 5, 5 pCi/g respectively. The samples were selected from the highest gamma ray analysis samples. When the highest gamma sample could not be determined (lower than detectable), diffuser samples near Bailey Cove were used.

3.5.4 Quality Control

Samples were measured in a standard geometry, a one liter wide mouth high-density polyethylene Nalgene bottles. This geometry was calibrated utilizing U.S. EPA liquid gamma ray standards from the EPA national exposure research laboratory RADQA program in Las Vegas, Nevada. The initial counting of sediment samples and biota were done wet to speed up the measurements. Detection capabilities conformed to the lower limits of detection specified by the Maine Yankee Atomic Power Company Off-site Dose Calculation Manual Table 2.4. The radionuclides ^{58}Co and ^{60}Co have a MDA specification of 130 pCi/kg concentration for fish and invertebrates and ^{134}Cs and ^{137}Cs have 130 and 150 pCi/kg. The standardization of our geometry used for Ge detector's involved the use of several standards including ^{133}Ba , ^{137}Cs , ^{60}Co , and ^{226}Ra . Larger Marinelli geometries are also available.

3.5.5. Sample Disposal

All samples taken will be archived until delivery of report and acceptance by Maine Yankee and disposed of by subcontractor in accordance with applicable regulations. University of Maine has a general license for radionuclides, including waste disposal capability.

3.5.6 Safety

Personnel had radiation safety training and were film badged for work which may have a hot particle nearby. Portable radiation detection meters were taken in the field for sampling. Health and safety training was included in previous documents submitted with the proposal.

3.5.7 Quality Assurance

Samples were collected under the Normandean QA plan, were counted under the University of Maine QA plan, and modeled under the Churchill quality assurance modeling plan. Framatome was responsible for its QA plan.

3.5.8 Background Measurements

Sediment background samples were taken from Taunton Bay, Clark Cove, and Damariscotta Bay (Station 148), and Sheepscot Bay. Background biota samples were collected from South Portland and Damariscotta Bay. Every effort was made to collect all of the same species collected at Maine Yankee. These samples determined background values of nuclides.

4. NUMERICAL MODELING OF FLOWS AND RADIONUCLIDE TRANSPORT IN THE SHEEPCOT RIVER ESTUARINE SYSTEM

4.1 INTRODUCTION

The modeling component of our project served two primary purposes. One was to examine the flow dynamics of the Sheepscot River estuarine system, which received cooling water and discharged radionuclides from the Maine Yankee nuclear power facility. The second was to study the transport of radionuclides through the estuarine system and the incorporation of these radionuclides into bottom sediments. Modeling results were used in both the planning and data interpretation phases of our project. In planning the project's sediment surveys, model results were used to set geographic bounds for the sample locations. In interpreting the radionuclide concentrations obtained from the surveys, we used the model results to assess the extent to which sediment-bound radionuclides may have been transported after their initial incorporation into the bottom sediment.

Our modeling package consisted of two coupled numerical routines. One was a hydrodynamic model that simulated the flows in Sheepscot River estuary for a given set of tidal conditions. The second was a modified "water quality model". This used the time varying flow field of the hydrodynamic model to simulate the transport of discharged radionuclides and estimate the pattern of radionuclide incorporation into the bottom sediment of the Sheepscot estuarine system.

The modeling effort was carried out in phases. The first phase entailed constructing model grids, of increasing levels of complexity, and conducting numerical integrity tests of the hydrodynamic model. In the second phase, we focused on the dynamics of the Sheepscot River estuarine system. The model results were employed to examine aspects of the dynamics expected to impact the transport of radionuclides discharged from the Maine Yankee facility. As part of this phase, we also carried out a field evaluation of the model. This entailed releasing drifters at various tidal phases near the diffuser location, as well as monitoring the water level in Bailey Cove over two tidal cycles. In our third, and final, modeling phase, we used the water quality model to simulate the movement of plant-discharged radionuclides throughout the estuary and the initial incorporation of these radionuclides into bottom sediments. Among the products produced by the model were geographic plots of radionuclide concentrations in bottom sediments resulting from large historical releases. These were used in the interpretation of the results our sediment radiological surveys.

In the remainder of this section we offer brief descriptions of the hydrodynamic and water quality models, and discuss the findings from these models in some detail. We also describe the model evaluation field study carried out in early July 2004.

4.2 HYDRODYNAMIC MODELING

4.2.1 Model Description

Simulation of flows within the Sheepscot River estuarine system was done using the hydrodynamic model DYNHYD. This numerical model has a history of application in estuarine studies dating from the 1970's (Feigner and Harris, 1970). It has been used to simulate flows near the Maine Yankee power plant in previous studies reported by Churchill *et al.* (1980) and Hess *et al.* (1983).

A principal simplifying assumption of the model is that velocities and water properties are vertically uniform. Simulation of flows within an estuary is carried out by numerically integrating the equations of continuity and motion, expressed in a finite difference form, using a Runge-Kutta technique. This calculation is done within the framework of a grid that segments the volume of an estuary into a series of channels and connecting junctions. The channels are assumed to be flat bottomed and of rectangular cross-section. Properties assigned to each channel are length, width and a “Manning” friction coefficient. Throughout a tidal cycle, the channel length and width remain constant, while the channel cross-sectional area and hydraulic radius (depth of water) vary with the changing water level. Model output includes time series of vertically averaged velocities and hydraulic radii for each channel. The mean water level of each junction, relative to a horizontal datum, is also output by the program.

Application of DYNHYD to the waters near the Maine Yankee facility required modification of the program to allow for drying of channels. This modification and other details of the program’s operation are described by Churchill *et al.* (1980) and Hess *et al.* (1983).

In generating the model results to be shown in ensuing sections, we forced the model flow through two mechanisms: changes in tidal elevation at the boundary of the model grid, and inflow and outflow at specified model junctions. To account for the impact of the power plant’s operation, a steady inflow was specified at a junction coincident with the cooling water intake and a steady outflow was specified at one of the discharge locations: the outflow into Bailey Cove and the diffuser in the Back River. For runs aimed at modeling flows during the decommissioning period after the plant shutdown, a steady outflow was specified at the location of the waste water discharge near Little Oak Island. The influx of freshwater to the Sheepscot River estuary was accounted for in some runs by specifying an influx at a model grid’s northern most (most inshore) junction.

In specifying the changes of tidal elevation at the seaward boundary of the model domain, we made use of the *Eastcoast* 2001 data base of tidal constituents recently developed for the U.S. Army Corps of Engineers and described by Mukai *et al.* (2001). This data base allows a user to compute the tidal elevation for a given time window and at any given location within a domain that includes western North Atlantic. It was derived in the manner described by Westerink *et al.* (1994) by applying the hydrodynamic model ADCIRC (Luettich *et al.*, 1992) to a domain comprised of the western North Atlantic, the Gulf of Mexico and the Caribbean Sea. Using the *Eastcoast* 2001 data base and a Fortran routine supplied by Dr. Richard Luettich of the University of North Carolina, we specified tidal elevation series at the location of the model grid’s southern most junction for a number of different time periods.

We should emphasize that by today’s standards, DYNHYD is relatively crude. The most advanced of the current generation of estuarine models typically represent velocities and water properties as 3-dimensional fields and have highly refined methods for determination of bottom friction. The principal advantages of DYNHYD over this class of models are in its ease of implementation, speed of operation and numerical stability. As will be shown below, DYNHYD provided a useful, albeit imperfect, view of the dynamics of the Sheepscot River estuarine system.

4.2.2 Model Grid Generation

Hydrodynamics of waters near the Maine Yankee power plant have been modeled in three previous studies; two with the use of DYNHYD (Churchill *et al.*, 1980 and Hess *et al.*, 1983) and the third with the use of finite element numerical model (Law, 1979). In all of these studies, only a small

portion of the Sheepscot River estuarine system was included in the simulation. In no study did the model domain extend beyond the diffuser location by more than 6 km to the south or 3 km to the north. Although useful, the previous model results offered little insight into the workings of the entire estuarine system and how the larger scale system dynamics may have impacted the movement of radionuclides discharged from the power plant. For this reason, we chose to extend the model domain of this study over the entire Sheepscot River estuarine system.

Generation of the model grid was accomplished using routines executed in MATLAB programming environment. The procedure was carried out in a number of steps with the user working with the cursor on an electronic chart of Sheepscot River estuary. In the first step, the user specified the center location of each of the grid's junctions (by "left clicking" at the desired cursor location). In the second step, the user connected the junctions with channels. Marking of channel edges and specification of junction depths (relative to mean low water) were accomplished in subsequent steps. The final step entailed specifying junction area. For a particular junction, this could be set equal to the half the sum of the channels entering the junction or to the area of a polygon whose edges were specified by the user (again, by left clicking on desired vertex locations). Routines were also written for editing a particular grid, allowing for deletion or insertion of channels and junctions. Throughout the course of our study, the grid was expanded in steps, with detail added in areas deemed likely to receive plant discharged radionuclides based on results from the soon to be replaced model grid.

The final grid (Figures 4-1 and 4-2) consists of 301 channels and 228 junctions. It is highly resolved in areas considered likely to receive discharged radionuclides in high concentration. This includes Bailey Cove and a portion of the Back River and Montsweag Bay extending roughly 2 km north and 1 km south of the diffuser location. The skewing of this area of high grid resolution relative to the diffuser is consequence of the system dynamics, which will be discussed in the next section. While the grid encompasses most of the closed channels and embayments of the Sheepscot River estuarine system, it does not extend into the adjacent Kennebec River, which is connected to the Sheepscot River estuary by the Sasanoa River (Figure 4-2). The Kennebec-Androscoggin River system is highly complicated and could not have been adequately modeled within the time frame of our project.

4.2.3 Model Results

As noted above, the model was forced by changes in tidal elevation applied at the most seaward boundary (identified in Figure 4-2). Spring, neap and intermediate tidal conditions were simulated. An examination of the model results has revealed two important phenomena that had not been identified by previous studies, but which are expected to have a significant impact on the transport and redistribution of radionuclides discharged from the Maine Yankee facility. One is a tidal node located a short distance south of the diffuser location, and the other is an asymmetry of the tidal flow within Bailey Cove. In this section we examine the details of these phenomena as revealed by the model results.

From a simple examination of nautical charts, an astute navigator or a reasonably alert student of hydrodynamics, would infer the likelihood of a tidal node somewhere in the Sheepscot River estuarine system. Such an observer would note that the deepest channels of the system encircle the system's largest island, Westport Island (Figures 4-1 and 4-2). He or she may then imagine the path of a tidal crest entering the system from the Sheepscot River mouth. At the southern

Sheepscot Model Grid

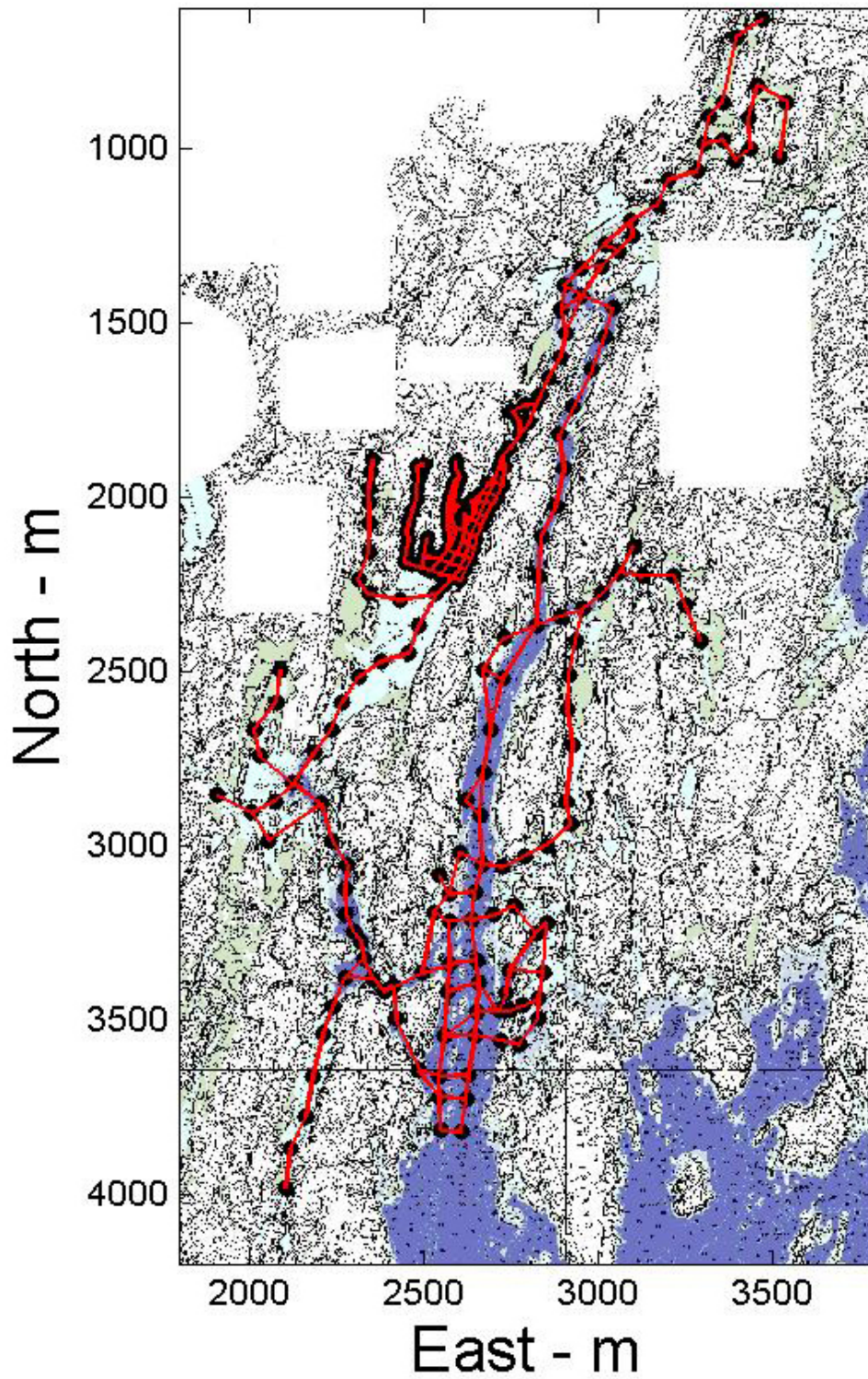


Figure 4-1. The final version of the grid used for the hydrodynamic and radionuclide models.

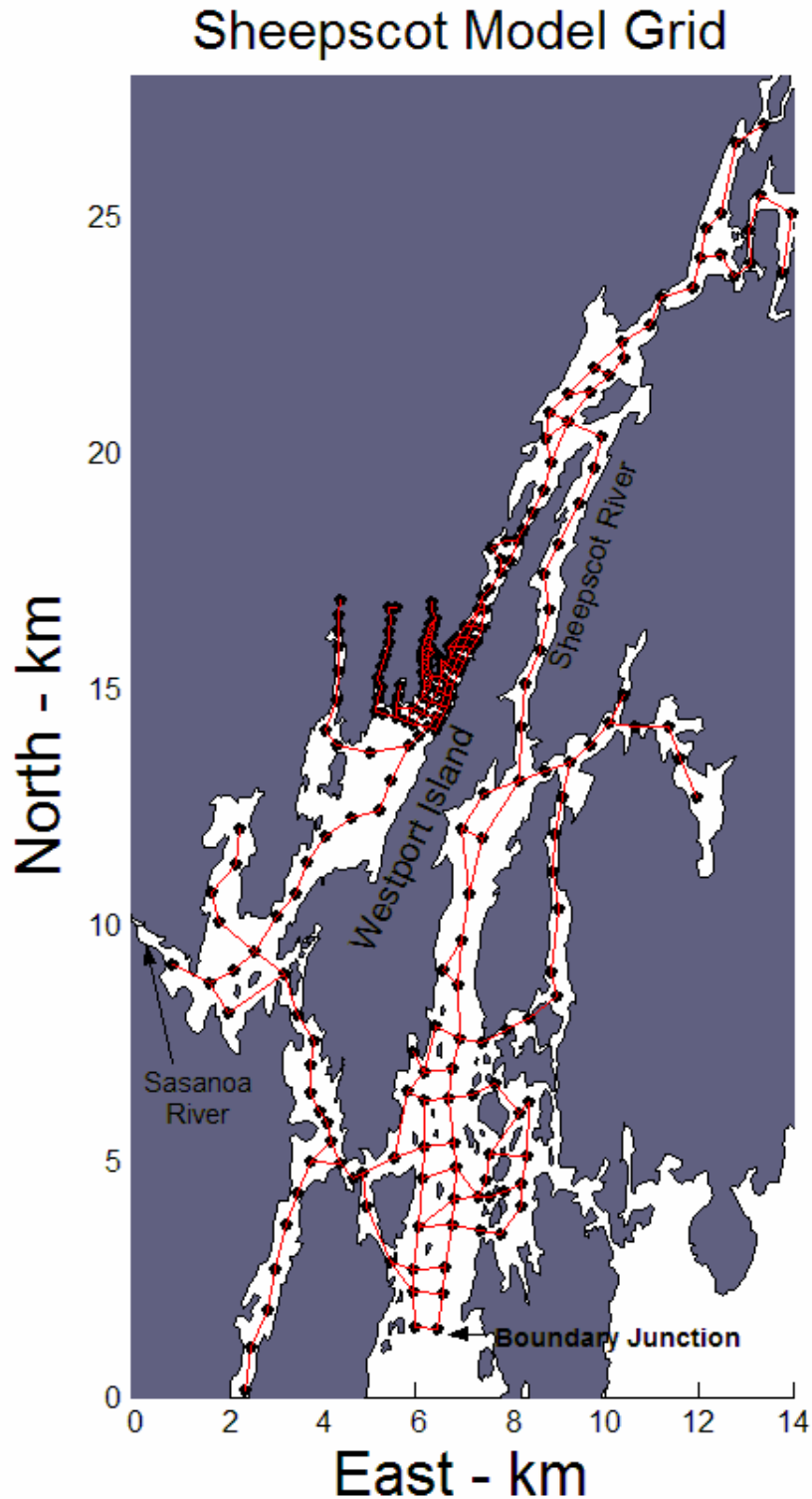


Figure 4-2a. Same as Figure 4-1 except showing the model grid over plain land and water fields. Indicated is the boundary junction at which the offshore forcing, in the form of a tidal elevation series, is applied. Also indicated is the Sasanoa River, which is a principal opening to the modeled system not accounted for by the grid.

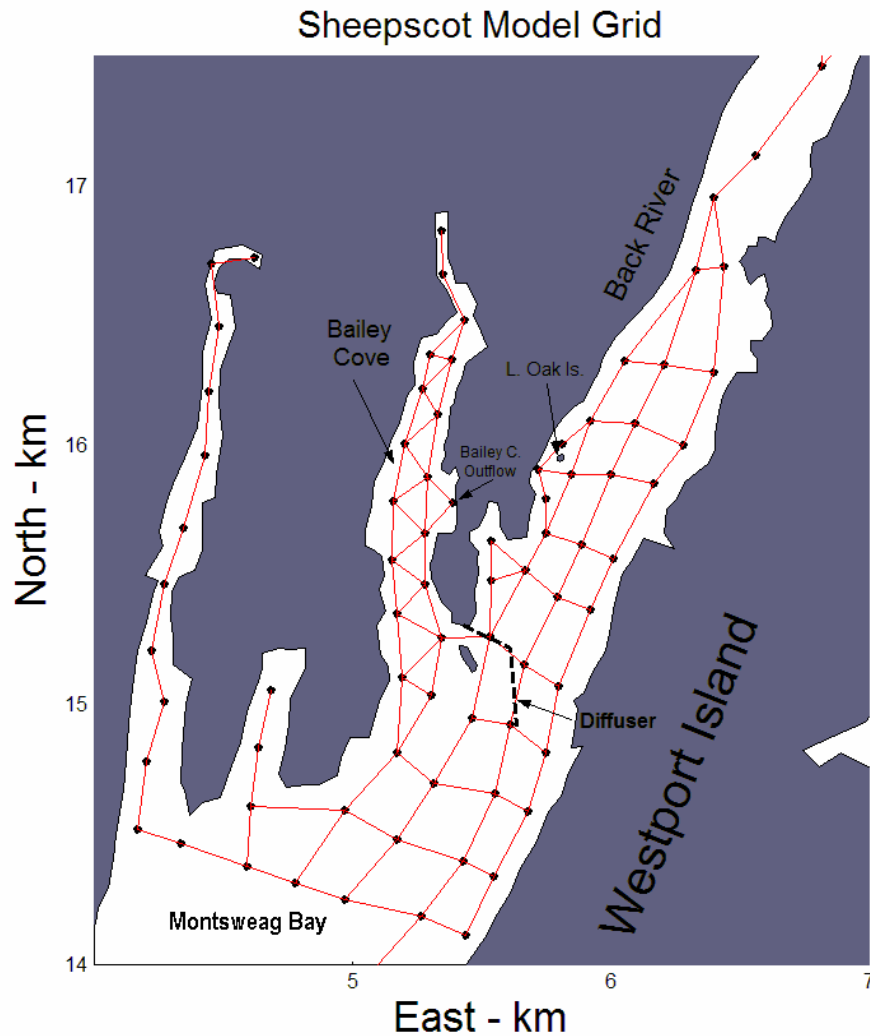


Figure 4-2b. The section of the model grid with the highest resolution.

end of Westport Island, the path this crest would be expected to split into two alternate routes: one moving northward through the Sheepscot River along the eastern shore of Westport Island and the other traveling northward through the series of bays and rivers that abut the western shore of Westport Island. Somewhere along the island, the two crests would recombine to form a tidal node. Our perceptive observer would predict that tidal velocities would be particularly weak at the location of the node. The reasoning would be that the tidal velocities are forced principally by gradients of the tidal elevation, which tend to be largest in the along-channel direction. The elevation of the two tidal waves meeting at the node should be roughly equal, giving a small (or nearly zero) elevation gradient at the node.

To examine the manner in which the tide propagates through the channels ringing Westport Island, we computed the total volume transported by the incoming tide flow through the model channels surrounding the island. This was determined as

$$T = \int_{t_0}^{t_0+t_1} V(t) dt$$

where t is time and $V(t)$ is the channel volume transport defined as

$$V(t) = D(t)v(t)W$$

where $D(t)$ is the time varying water depth in the channel, $v(t)$ is the modeled channel velocity and W is the channel width. The integral for the volume transported, T , is carried out over the period of the incoming tide (from t_0 to t_0+t_1). A plot of flood-tide transport in selected channels (Figures 4-3a,b,c) shows the splitting and recombining of the transport in the channels abutting Westport Island. The principal schism occurs at the southern end of Westport Island where the incoming transport divides into two main streams. One heads into the estuarine region to the west of the island, while the other, larger, stream moves up the main channel of the Sheepscot to the east of the island. At the northern tip of the island, this latter stream splits again with one branch moving southward along the western shore of Westport Island. This branch continues past the location of the diffuser discharge. It then meets the northward moving stream it had parted with at the southern end of Westport Island. According to the model, this point where the flood tide streams encounter one another is roughly 1 km south of the diffuser.

To examine the effect of the splitting of tidal flows around Westport Island on tidal energy, we computed of root mean square (RMS) value of volume transport through the model channels over the course of a tidal cycle. This was computed according to

$$RMS(V) = \sqrt{\frac{1}{t_2} \int_{t_0}^{t_0+t_2} V^2(t) dt}$$

where $RMS(V)$ is the root mean square of the volume transport in the channel over the course of a tidal cycle that extends from t_0 to t_0+t_2 . This quantity (hereafter, RMS tidal transport) is proportional to the square root of tidal energy in a model channel. According to the model, the RMS tidal transport varies over two orders of magnitude in the channels surrounding Westport Island (Figures 4-4a,b). It exhibits a very deep minimum in the area of the tidal node, roughly 1 km to the south of the diffuser. At the diffuser location, the RMS tidal transport is only slightly greater than its minimum and is dwarfed by the RMS tidal transport on the other side of Westport Island, by more than an order of magnitude.

One may question why the flood tide stream that initially moves up the main channel of the Sheepscot manages to cover so much more distance than its weaker brother stream before reaching their collision point. It's because this faster stream passes through a much deeper part of the system than its slower counterpart. The phase velocity of the tidal wave is proportional to the square root of channel depth, and so the location of the point where the model tidal waves meet, and produce the tidal energy minimum, is determined by the depths of the model channels. Accurately predicting this location in the model is principally dependent on properly specifying the main channel depths on either side of Westport Island.

As would be expected, the tidal excursions (the distances a particle moves from low to high tide, or vice-versa) are very small in the area of the tidal node and tend to increase dramatically moving away from the node. Here we show tidal excursions computed for neap-tide conditions

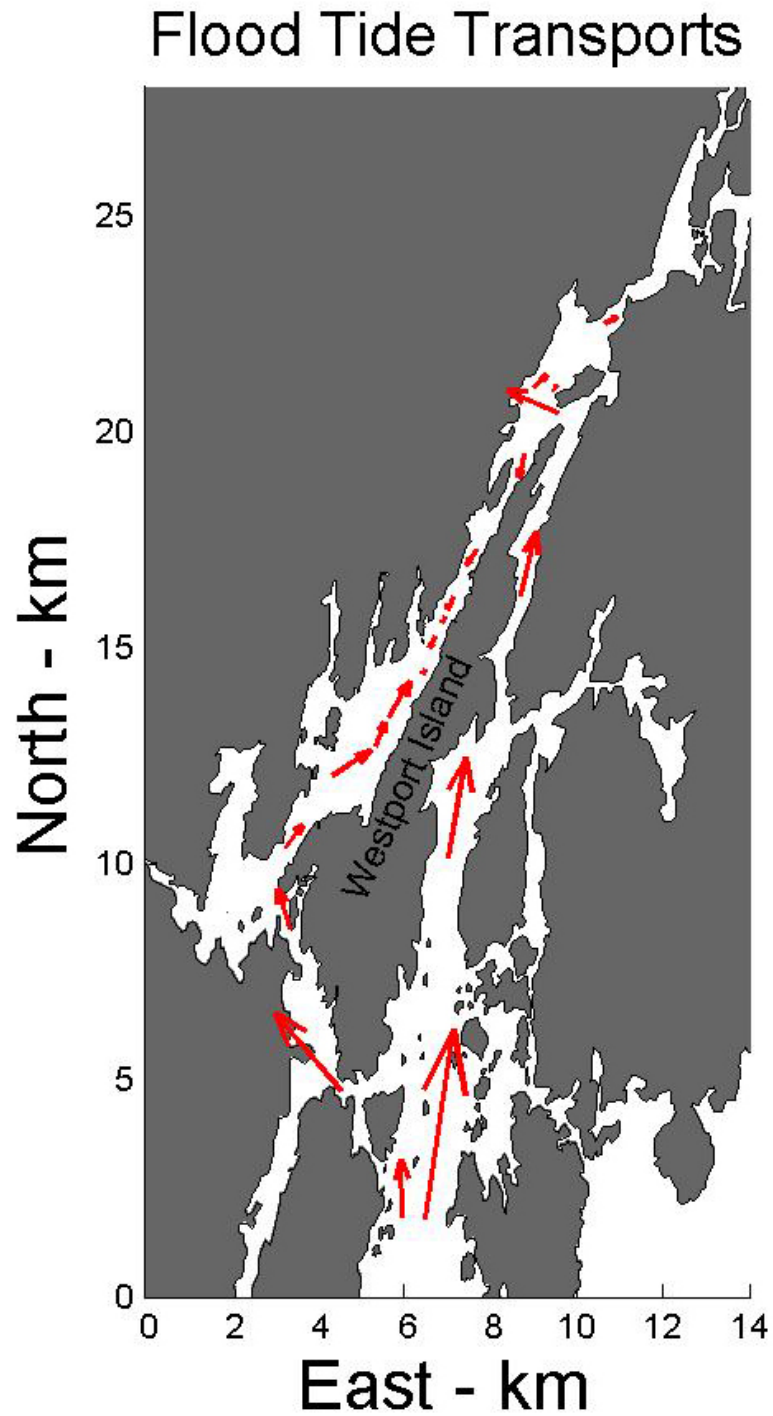


Figure 4-3a. The volume transport over a flood tide through selected model channels. The transports show the splitting of the incoming tidal flow near the southern end of Westport Island and a minimum of tidal flow at the tidal node, where two opposing streams meet, a few km south of the diffuser location.

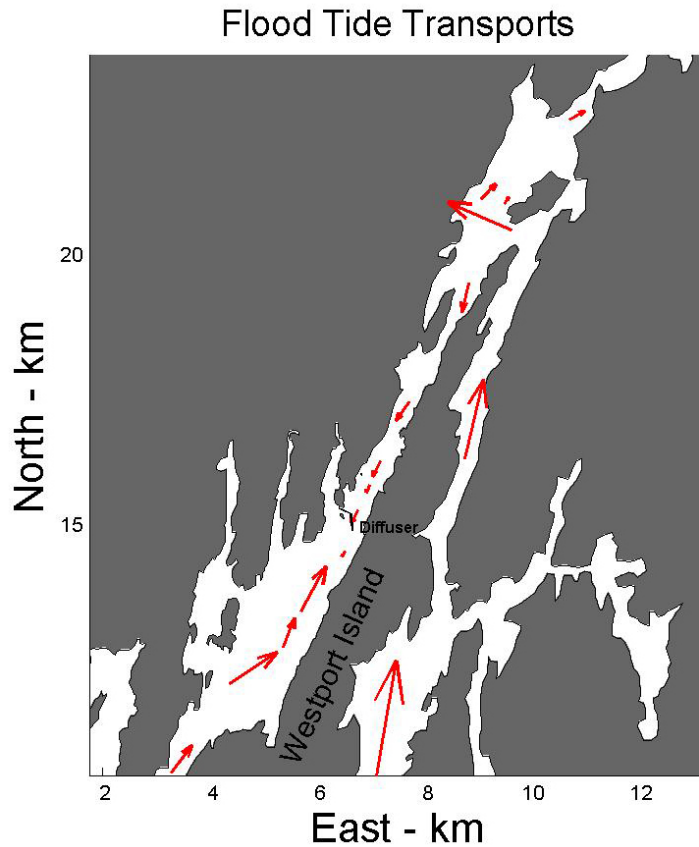


Figure 4-3b. A smaller scale view of the flood tide volume transport in the vicinity of the Maine Yankee facility.

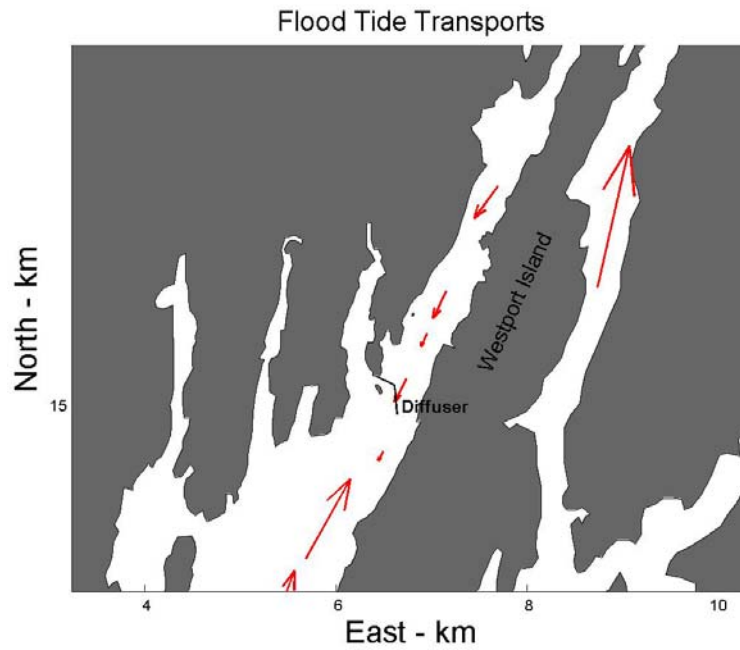


Figure 4-3c. An even smaller scale view of the flood tide volume transport in the vicinity of the Maine Yankee facility.

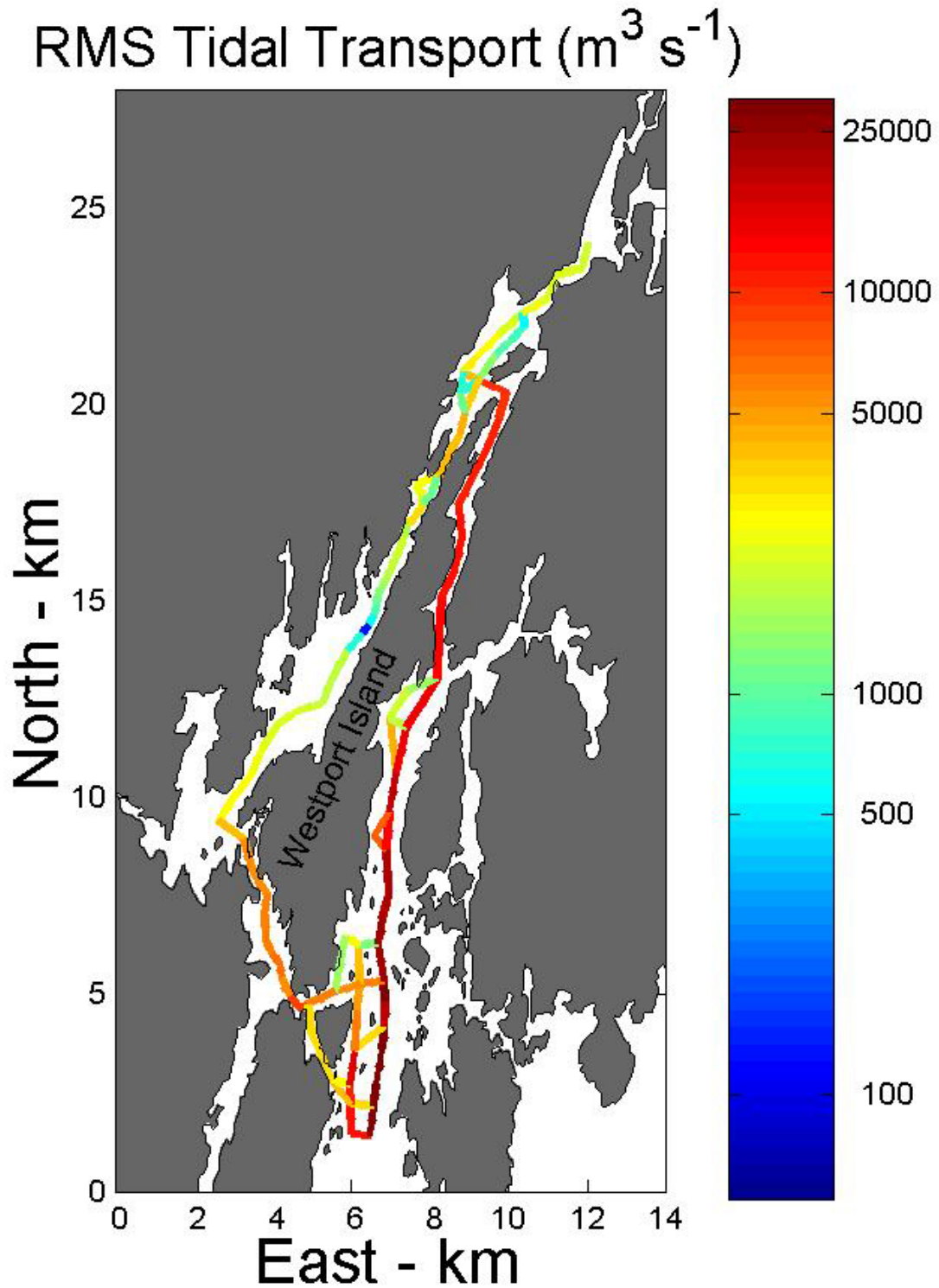


Figure 4-4a. The RMS value of volume transport within channels encircling Westport Island. These RMS transports show a minimum of tidal energy at the tidal node off the western shore of Westport Island.

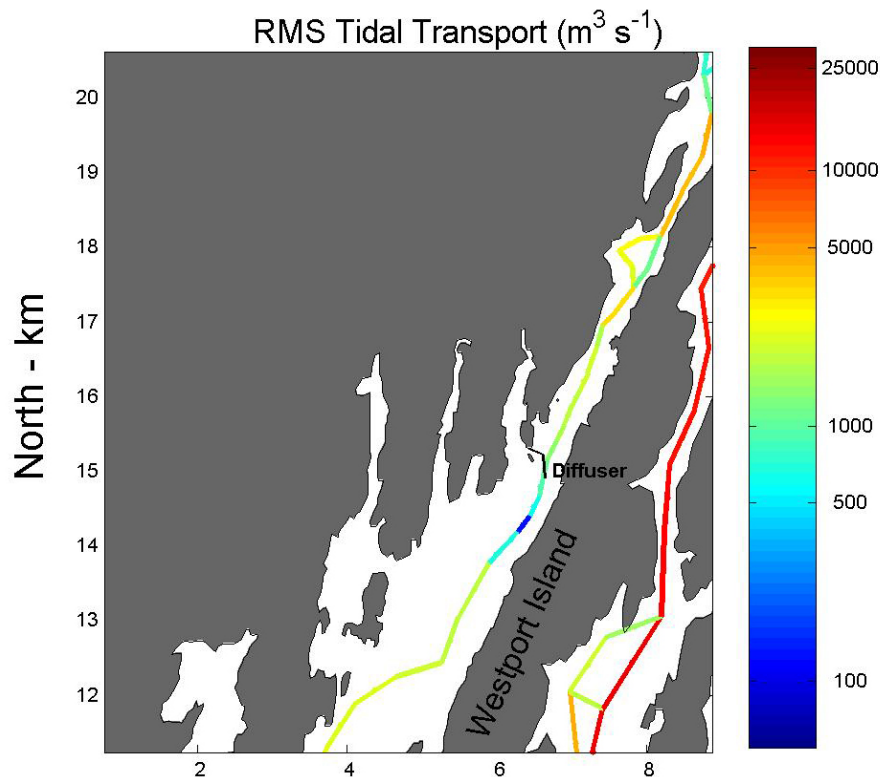


Figure 4-4b. A smaller scale view of the RMS value of volume transport more clearly showing the minimum of tidal energy at the tidal node. Note that this is roughly 1 km south of the diffuser location.

(Figure 4-5). Near the diffuser, these neap tide excursions are of order 1.5 km. Only 1.2 km to the north of the diffuser, the excursions are substantially larger, of order 3.4 km.

The tidal node acts as something of a barrier to the north-south movement of material within the estuary. In particular, it may be viewed as an obstruction to the southward movement of material released from the diffuser. On an outgoing tide, material released from the diffuser is carried to the north. On an incoming tide, the movement of material discharged from the diffuser is somewhat more complicated, with some portion of the material being carried into Bailey Cove and some other portion being transported southward within the main navigation channel. However, this southward transport tends to stall at the tidal node.

To study the impact of the tidal node on the transport of material released at the diffuser, and discharged from the old Bailey Cove outflow, we conducted a number of particle tracking experiments using the modeled velocity fields. The basic approach was to release an ensemble of particles from the location of the diffuser, or the Bailey Cove outflow, and track these using the modeled velocity field over a specified period. The tracking routine was relatively simple. It was assumed that particles followed the modeled flow perfectly (i.e. they did not experience any diffusive “kicks”) and were confined to the model channels. Their path was thus explicitly defined at all times except when they encountered a junction where the flow could carry them into two or more channels. In such a case, the channel that a particle would enter was chosen through a modified Monte Carlo scheme in which the probability of entering a channel was prorated based on the transports of all the

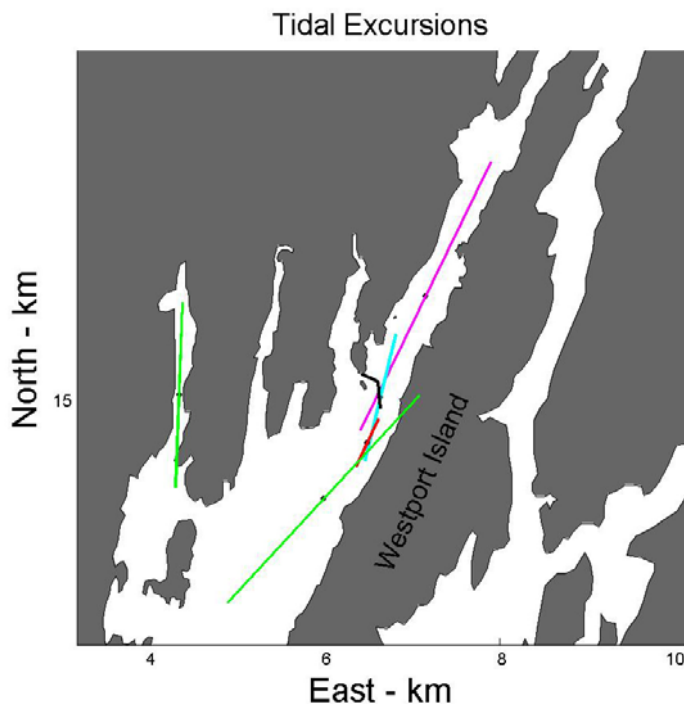


Figure 4-5. Magnitudes of tidal excursions at selected model channels.

possible channels of entry. That is, the greater the transport of a channel, relative to companion channels meeting at the junction, the higher its probability of receiving particles entering the junction.

To define the scope over which the tide carried material released from a discharge location, we followed a procedure in which an ensemble of particles (typically 100 particles) was set out from the discharge location at some given time and then tracked for a full tidal cycle of 12.5 hours. This procedure of releasing a group of particles was repeated at regular time intervals (typically every 0.5 hours) through a full tidal cycle. The full collection of particle positions, from all the releases, gave the estimated region over which the tide may be expected to carry material set out from the given discharge location. Plots of these collections of particle locations were used in designating the scope of our sediment collection surveys and in choosing areas of high station density.

Here we show two examples of particle positions determined from the above procedure, one with the release point at the diffuser and the other with the release point at the Bailey Cove outflow (Figures 4-6 and 4-7). Both were determined using a flow field representative of spring tide conditions. The collection of particle positions released from the diffuser reflects the impact of the tidal node in that they are skewed to the north of the diffuser. The furthest extent of these particles is roughly 2.5 km to the north of the diffuser but no more than 1 km to the south of the diffuser. It is noteworthy that a number of the particles set out from the diffuser extend well into Bailey Cove. Not surprisingly, the collection of particles released from the Bailey Cove discharge fill up the cove. In the Back River, this ensemble of particle positions also reflects the influence of the tidal node, extending further to the north of their point of entry into the river than to the south.

We must caution against viewing the tidal node indicated by the model as an impermeable barrier. As will be shown in the results of Section 4.3.2, the modeled flow fields can carry material released from the diffuser to the south of the node. There also are a number of mechanisms not

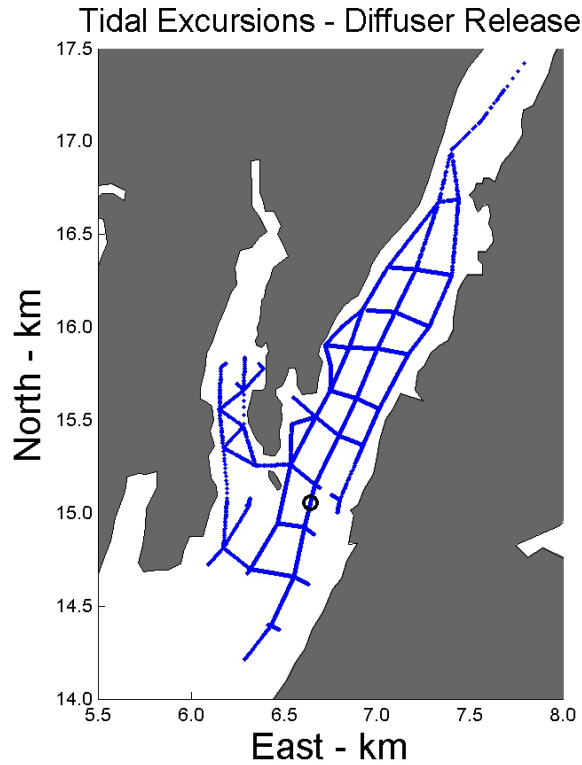


Figure 4-6. An ensemble of the positions of particles released from the location of the diffuser into a modeled flow field forced with a boundary elevation series representative of a spring tide.

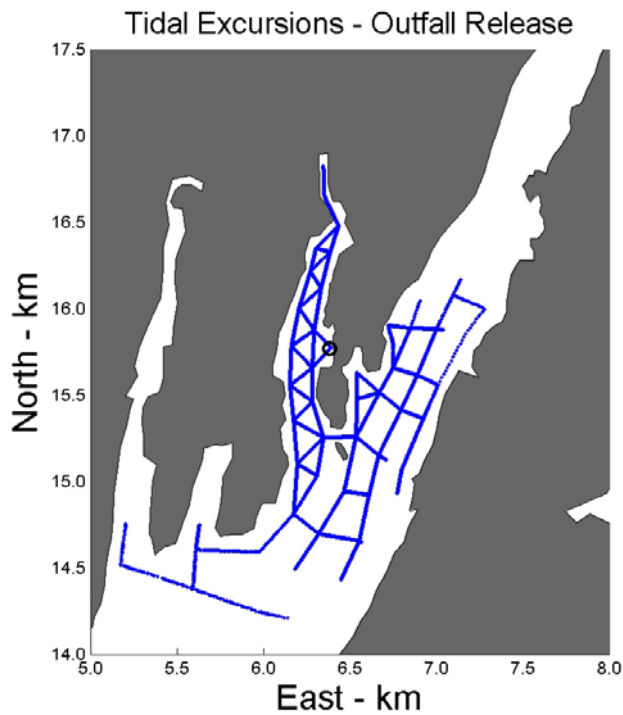


Figure 4-7. An ensemble of the positions of particles released from the location of the Bailey Cove discharge into a modeled flow field forced with a boundary elevation series representative of a spring tide.

accounted for in the model which may result in the transport of material across the node. Wind forcing of near-surface flow is one obvious candidate. Another is gravitational circulation associated with density differences within the estuary (which are ignored by DYNHYD). Nevertheless, the tidal node indicated by the model is an actual element of the Back River and Montsweag Bay flow field known to many who frequent the river (Don Hudson, Chewonki Foundation, personal communication). It is a feature that will clearly have a significant impact on the transport of material entering the river.

As noted above, the other important flow feature revealed by the model results was an asymmetry in the properties of the tide within Bailey Cove. Tidal asymmetries, marked by a significant difference in the length of the flood versus the ebb tide, have been recognized in a number of embayments (Boon and Bryne, 1981; Aubrey and Speer, 1985; Speer and Aubrey, 1985; Lincoln and Fitzgerald, 1988; Ranasinghe and Pattiaratchi, 2000). They have been attributed to the generation of short period “overtides” within the embayments (Speer and Aubrey 1985; DiLorenzo, 1988; van de Kreeke, 1988).

The model results show a “flood-dominant” tidal asymmetry in Bailey Cove. This is characterized by a short period flood tide with strong incoming flows and a longer period ebb tide with relatively weak outgoing flows. According to the model results, the degree of asymmetry depends principally on tidal range and position in Bailey Cove. It tends to increase with increasing tidal range and with increasing distance into the cove (going to the head of the cove). Here we show the signature of the tidal asymmetry revealed by the flows and water levels determined for spring tide conditions in a model channel (channel 281) located roughly 150 m NE of the old Bailey Cove discharge (Figures 4-8 and 4-9). Notably, under these tidal conditions, the modeled flood tide exhibits a maximum of velocity of 32 cm/s whereas the ebb tide flow peaks at only 14 cm/s. A flow pattern such as this would tend to lead to particle accumulation within the cove. This would occur because of a tendency for particle resuspension on the strong incoming flood tide and for particle settling on the weaker outgoing tide. As discussed in an ensuing section, particle accumulation in Bailey Cove is indicated by vertical profiles of radionuclides in bottom sediment samples acquired in this project and in previous projects.

4.2.4 Field Evaluation of the Model

In this report we have focused on the tidal node and the tidal asymmetry revealed by the model because these features are likely to have had a significant effect on the transport of radionuclides released into the Sheepscot estuarine system and on the retention of these radionuclides within the system. As noted above, the tidal node acts as something of a semi-permeable barrier to the southward transport of material released from the Maine Yankee facility into the estuary. As also noted above, the tidal asymmetry in Bailey Cove would tend to favor particle accumulation in the cove and possibly lead to the burial of radionuclides absorbed by sediments in the cove. These factors were taken into account when designing our sediment surveys. Based on the simulated particle trajectories produced with the model results (e.g., Figures 4-6 and 4-7), we biased our sample collection sites to the north of the Back River diffuser location. In view of the indication of tidal conditions favorable for particle accumulation in Bailey Cove, our sample plan called for a relatively large number of core samples to be collected from the cove.

Our reliance on the model results in the survey design makes the question of model reliability, especially in regard to the above mentioned features, especially important. Unfortunately,

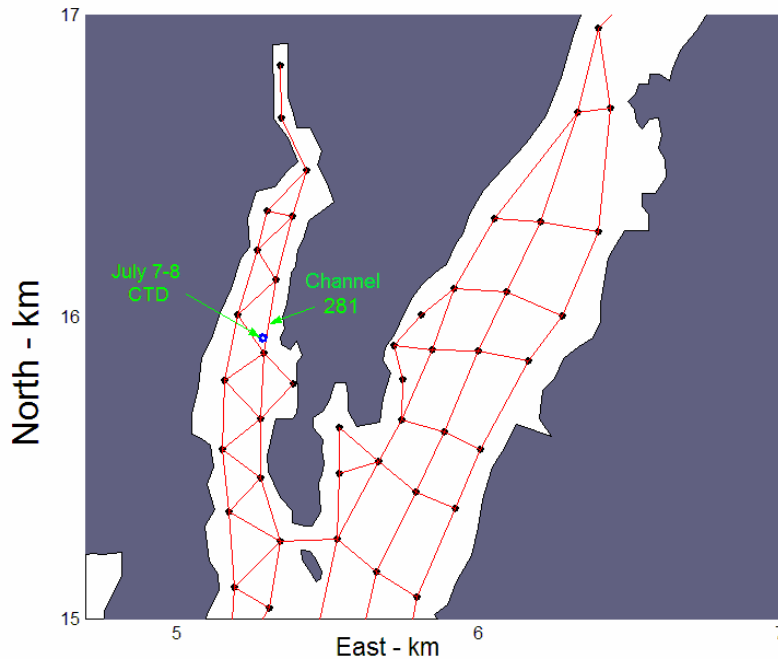


Figure 4-8. A view of the model grid in the areas of Bailey Cove and Back River. Indicated is the location of a conductivity-temperature-depth (CTD) recorder set out over two tidal cycles during July 7-8, 2004 as well as the model channel (# 281) that encompassed the CTD location.

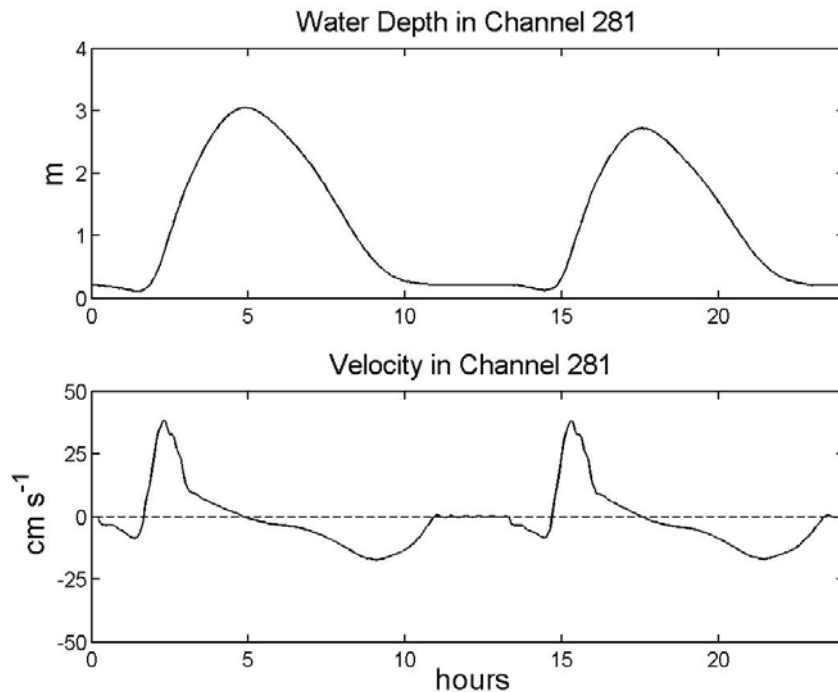


Figure 4-9. Time series of modeled water depth and water velocity in channel 281 (Figure 4-8). The series give evidence of a flood-dominated tidal asymmetry in Bailey Cove. This is marked by a brief flood tide with a strong incoming flow and a long ebb tide with a relatively weak outgoing flow.

the limited time period and financial resources of our project did not allow for an extensive field evaluation of the model. Nevertheless, we were able to devote two days (July 7-8) to acquiring field measurements to compare with the model results. The measurements were directed at addressing two critical questions regarding the model's performance. These were: how well does the model represent the actual movement of material in the region near the Back River diffuser; and is the tidal asymmetry indicated in Bailey Cove an actual feature, or simply a model artifact?

To address the first question, we released drifters near the location of the diffuser and tracked these over a number of hours. The drifters we employed were "Davis-style" surface trackers, designed to follow flow in the surface 1.3 m of the water column (Davis, 1985). They were purchased from the Gulf of Maine Lobster Foundation by contractor J. Churchill for use on another project and were effectively on loan for this study.

Each drifter consisted of central ballasted cylinder and four "sails", which radiated from the cylinder and provided drag (Figure 4-10). The sails were suspended between four fiberglass rods that extended through cylinder. Affixed to the cylinder top was an electronics package manufactured by the Axonn Corporation, which included a GPS receiver and a satellite transmitter. The drifters were kept afloat by buoyant rings attached to the ends of the upper rods. In the water, each drifter was nearly fully submerged with only a small portion of the cylinder and the masthead electronics package above water.

Drifter tracking was accomplished via the drifter's masthead electronics unit. This obtained GPS fixes of the drifter's position and regularly transmitted these to satellites. The positions were available on the website of the tracking company, AeroAstro, in nearly real time. We had preprogrammed the masthead electronic units used in our study to transmit updated positions every 15 minutes, the smallest update time interval allowed by AeroAstro. However, the actual times between positions received through the AeroAstro system were often much longer, many exceeding 30 min.

A drifter was set out near the diffuser location and subsequently tracked four times, twice on July 7 and twice on July 8. All drifter releases occurred on the outgoing tide. In agreement with the flow pattern indicated by the model, the drifters initially traveled to the north (top panels of Figure 4-11 and 4-12). All drifters also experienced a reversal of motion with the tide change.

To generate modeled particle trajectories for comparison with the drifter tracks, we ran the model to simulate flows over the period of July 6-9, 2004. The model was forced only by the changes in tidal elevation at the seaward boundary, which were determined with the program ADCIRC as described in Section 4.2.1.

For comparison with the drifter trajectories, a total of 100 particles were set out into the model flow field at the time and location of each drifter release. Using the method described in Section 4.2.3, the trajectories of these particles were simulated over a period corresponding to the time of the drifter tracking. The resulting ensemble of modeled particle trajectories compare rather favorably with the drifter trajectories with regard to the direction of movement and time of tidal reversal (Figures 4-11 and 4-12). However, the overall extent of the modeled particles northward movement was generally 30-50 % of the northward extent of the drifters.



Figure 4-10. A view of the type of drifter used in the field studies of July 7-8, 2004. The unit at the top of the drifter's central cylinder (covered in tape) is a tracking device outfitted with a GPS receiver and a satellite transmitter.

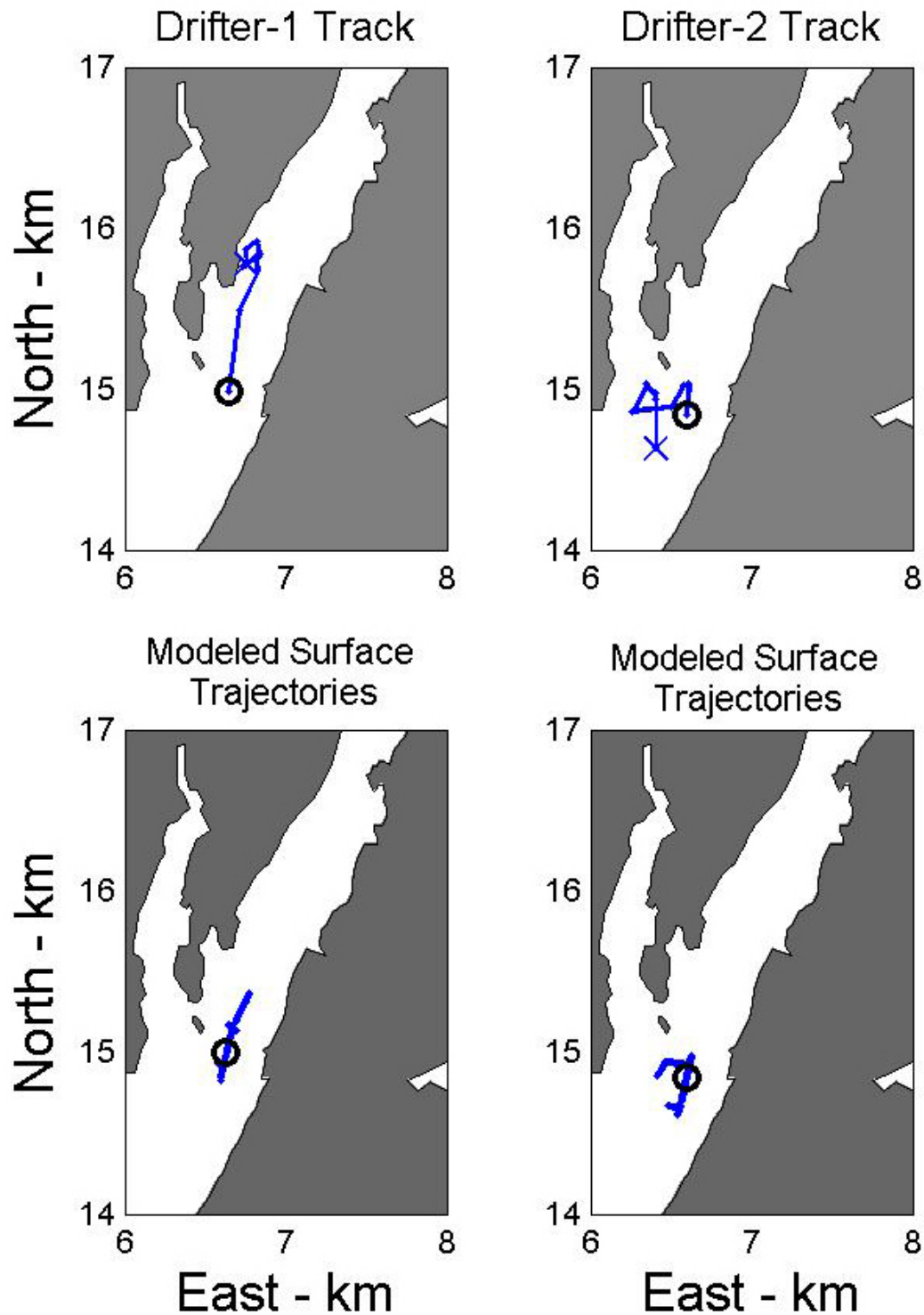


Figure 4-11. The top panels show the positions of drifter released during the ebb tide of July 7, 2004. The bottom panels show the positions of particles released into the model flow field at the same time and location as the first drifter position in the panel above. The particle positions encompass the same time period as the drifter tracks shown above.

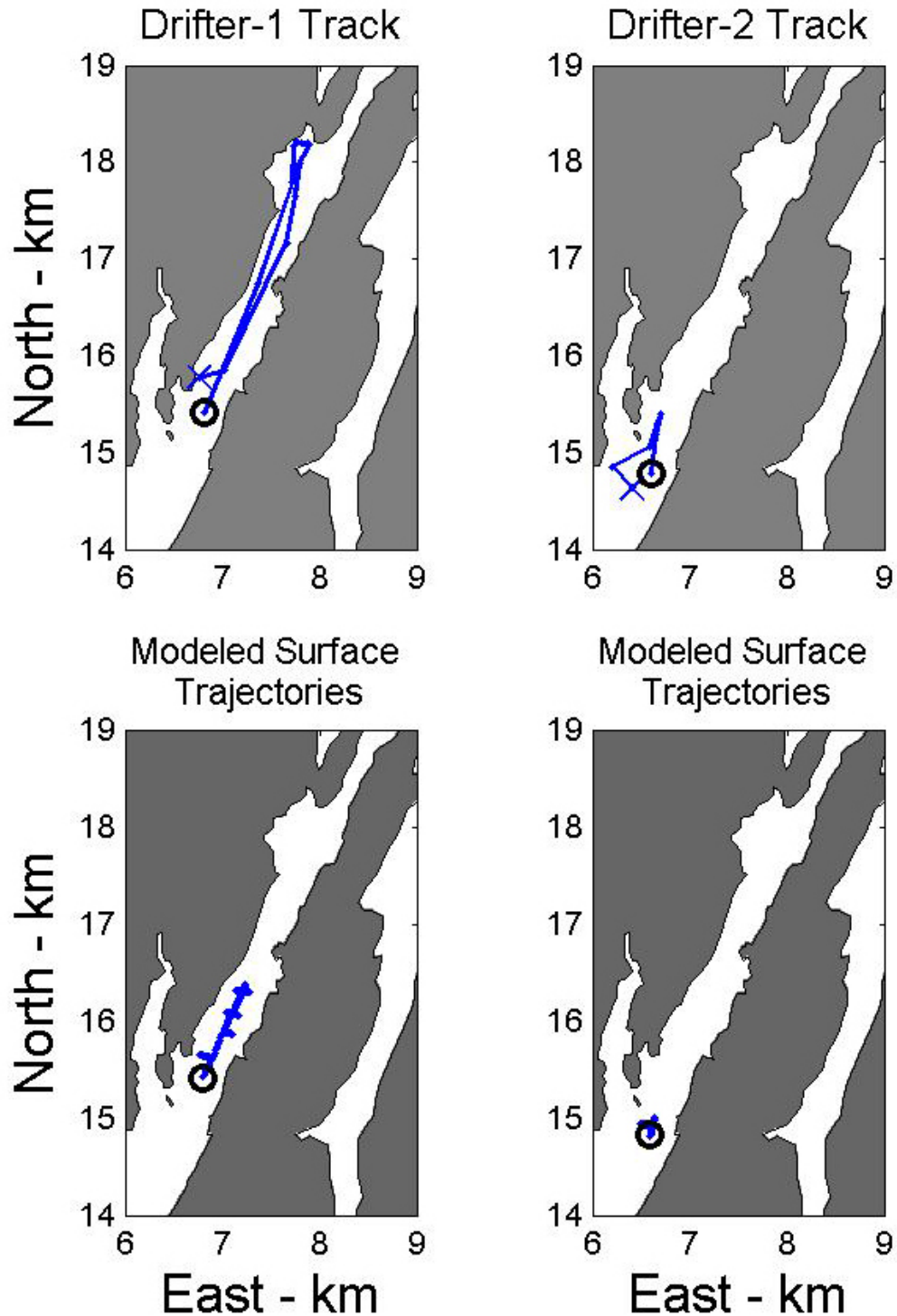


Figure 4-12. The top panels show the positions of drifter released during the ebb tide of July 8, 2004. The bottom panels show the positions of particles released into the model flow field at the same time and location as the first drifter position in the panel above. The particle positions encompass the same time period as the drifter tracks shown above.

On first consideration, this may seem to be an indictment of the model's ability to accurately represent flows in the vicinity of the diffuser. However, further reflection puts this result in a more favorable light. A principal difference between the modeled and the actual estuary is that the model assumes a vertically uniform velocity, whereas flow in the actual estuary will clearly vary with depth. Consider, for example, the situation in which the estuarine flow is dominated by changes in tidal elevation (i.e., with winds and fresh water inflow having negligible impact on the flows). Because of the effect of bottom friction, we may expect the velocity magnitude in such a system to increase going from the bottom towards the surface. The depth-averaged velocity, which is essentially the velocity estimated by the model, would then be less than the near-surface velocity. For the case in which the velocity increases linearly going upward from a value of zero at the bottom, it is easily shown that the depth-averaged velocity is exactly half the surface velocity. That the modeled velocities are substantially smaller than measured near-surface velocities is thus consistent with expectations. The conservatively low velocities of the model may be well suited for estimating the transport of radionuclides that are absorbed by the bottom sediments. This is because these radionuclides should be carried predominately in near-bottom waters where velocities tend to be the lowest.

To address the second question listed above, of whether or not the tide in Bailey Cove is significantly asymmetric, we deployed a device in Bailey Cove that measured temperature, salinity and water level. The device, a conductivity, temperature and depth (CTD) sensor package manufactured by Seabird Instrument Systems, was set out in the channel within the northern portion of Bailey Cove (see Figure 4-8 for location). Its deployment occurred during low water on the morning of July 7, 2004. The CTD was enclosed in a stainless steel cage to which lead weights were attached. Recovery of the CTD was done during low water, and in a steady shower, on the afternoon of July 8. An important observation of the recovery crew was that the CTD and its cage were covered with thick mat of seaweed and other debris.

This debris almost certainly compromised the conductivity measurements of the CTD, as it likely deprived the conductivity cell of the necessary continuous flow of water. As a consequence, we have little confidence in the salinity record derived from the CTD measurements, which are computed from temperature and conductivity. Our lack of confidence does not, however, extend to the CTD's pressure record, as the pressure measurement does not require a continuous flow of water.

The record of pressure sensor depth (Figure 4-13) shows two full tidal cycles and remarkably little difference between the two high water levels. A simple analysis of the depth record does indeed reveal a tidal asymmetry of the form predicted by the model (with a longer period of falling, as opposed to rising, water levels). As a measure of this, we have taken the times between the maximum sensor depth (high water) and a sensor depth of 0.5 m. For the first tidal cycle, the flood tide increases the sensor depth from 0.5 m to the maximum value over 4.2 hr, whereas the ebb tide decreases the sensor depth from its maximum level to 0.5 m over a longer period of 4.8 hr. A similar disparity between the rates of the rising and falling water level is observed over the second tidal cycle (Figure 4-13).

How well do these measured differences between the rates of falling and rising water in Bailey Cove compare with model predictions? To address this question, we have examined the modeled Bailey Cove water levels determined from the July 6-9 simulation mentioned above. Specifically, we have focused on the modeled water levels of channel 281, which encompasses the CTD location (Figure 4-8), over the period of the CTD data record (12:00 July 7 – 12:00 July 8).

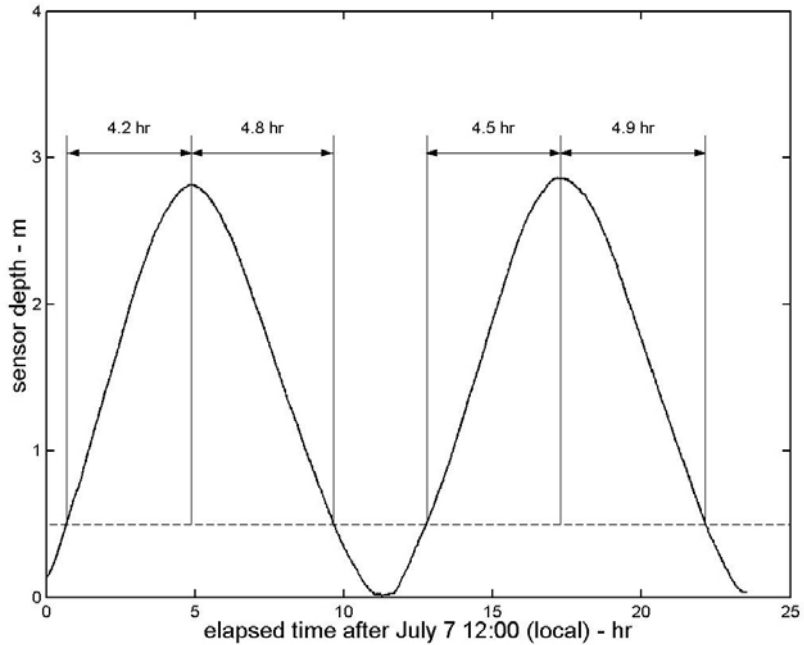


Figure 4-13. The sensor depth (i.e., water level) of the CTD deployed in Bailey Cove (at the location indicated in Figure 4-8). Indicated are the times of rising and falling water between the highest water level and a water level 0.5 m above the minimum sensor depth. These show a tidal asymmetry in which the rate of rising water of the flood tide exceeds the rate of falling water on the ebb tide.

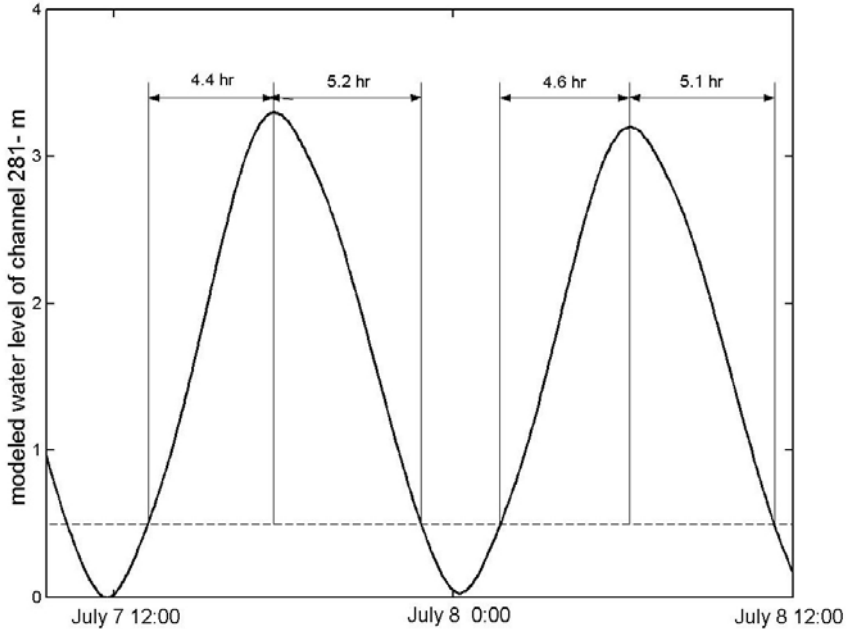


Figure 4-14. The modeled water level of channel 281 in Bailey Cove (Figure 4-8) during the time of the CTD measurements of water level shown in Figure 4-13. As in Figure 4-13, the times of rising and falling water between the highest water level and a water level 0.5 m above the minimum level are indicated. These show a tidal asymmetry of a degree nearly matching that indicated by the measurement of Figure 4-13.

Over this time, the simulated water levels of channel 281 nicely match the CTD measurements in that they show two full tidal cycles with little difference in the levels of high water (Figure 4-14). To quantify the difference in the rates of falling and rising modeled water levels, we have used a measure similar to that applied to the CTD measurements. It is the time difference between the occurrences of high water and a water level 0.5 m above the level of low tide. By this measure, the rising tide of the first modeled tidal cycle is 0.8 hr shorter than the falling tide (Figure 4-14). By the similar measure applied to the CTD measurements, the rising tide of the first tidal cycle is 0.6 hr longer than the falling tide (Figure 4-13). The comparison for the second tidal cycle is similarly favorable. For this cycle, the times of rising and falling water between the two chosen benchmarks differs by 0.5 hr in the simulated results and by 0.4 hr in the CTD measurements (Figures 4-13 and 4-14).

It thus appears that tidal asymmetry in Bailey Cove, as indicated by the model results, is an actual phenomenon. For the intermediate tidal ranges encountered during our field effort, the model seems to be capable of accurately reproducing this tidal asymmetry. It remains to be seen, however, if the extreme degree of tidal asymmetry predicted by the model during spring tide conditions actually occurs.

4.3 MODELING OF RADIONUCLIDE TRANSPORT

4.3.1 Model History and Description

The transport of radionuclides discharged from the Maine Yankee facility and the uptake of these radionuclides into bottom sediment have been modeled in previous studies described by Churchill *et al.* (1980) and Hess *et al.* (1983).

Churchill *et al.* (1980) considered the sediment uptake of radionuclides released from the Bailey Cove discharge in the early 1970's. Their approach was to simulate the movement of radionuclides entering Bailey Cove using the velocities derived from DYNHYD. Sorption of radionuclides into the bottom sediment was modeled according to

$$C_k(t) = C_{k0}[1 - E_{ek}(1 - e^{-\alpha_k t})]$$

where $C_k(t)$ and C_{k0} are the water borne concentrations of the radionuclide, k , at times t and 0, respectively. The sorption of the radionuclide onto the bottom sediment is parameterized by the equilibrium constant, E_{ek} and the sorption constant α_k .

For the radionuclides considered by Churchill *et al.* (^{134}Cs , ^{137}Cs , ^{58}Co and ^{60}Co), the transfer parameters, E_{ek} and α_k , were specified based on the results of laboratory experiments in which a tank of estuarine water and suspended estuarine sediments was spiked with a known amount of the radionuclides. Samples of the suspension were extracted at regular times and measured for radionuclide absorption. The rate of this absorption was used in determining the transfer parameters.

A correlation analysis presented by Churchill *et al.* showed a strong statistical relationship between modeled sediment-bound radionuclide concentrations and radionuclide concentrations measured in surficial sediment samples from Bailey Cove. For ^{134}Cs and ^{137}Cs , the correlation coefficients relating the measured and modeled concentrations all exceeded 0.8. For ^{58}Co and ^{60}Co , the correlation coefficients were all in excess of 0.62.

Hess *et al.* (1983) used the same numerical programs as employed by Churchill *et al.* to model the sediment uptake of radionuclides released through the diffuser. They noted an excellent qualitative agreement between the modeled and measured patterns of the short-lived ^{58}Co (half life of 70.8 days) in bottom sediments. The comparison between modeled and measured patterns of the longer-lived ^{137}Cs (30.17 yr half life) in the bottom sediments was also good, but somewhat inferior to that for ^{58}Co . Hess *et al.* attributed this difference to the impact of ^{137}Cs from fallout and from plant discharges of previous years. They noted that such sources of ^{137}Cs were not accounted for in the model, which simulated the initial sorption of the radionuclide onto bottom sediment from a single release or a small number of recent releases.

In modeling the transport of radionuclides, Churchill *et al.* (1980) and Hess *et al.* (1983) used the program DYNQUA. This is a Fortran-based companion program to DYNHYD (Feigner and Harris, 1970). In the modeling for this project, we decided against the use of DYNQUA for the principal reason that a working version of the program was not readily available. Instead, the same equations and numerical approach used by DYNQUA were implemented by MATLAB routines. In our experience, implementing numerical schemes is much easier in the MATLAB, as opposed to the Fortran, working environment. In addition, our analysis of the model results and the graphical presentation of these results were done entirely within MATLAB.

In our modeling, the basic procedure was to first upload files of time varying velocity fields produced by DYNHYD and use these to simulate the movement of discharged radionuclides through the model domain. The principal equation invoked was the diffusion-advection equation with a constant coefficient of turbulent diffusion. Sorption of radionuclides into the bottom sediments was modeled with the equation given above. The model was executed with a time step of 250 s.

The model produced averaged concentrations of sediment-bound radionuclides distributed over the top 1-cm of the sediment, a depth roughly corresponding to the average sampling depth of the surface sediment samples of our survey and the previous surveys described by Churchill *et al.* (1980) and Hess *et al.* (1983). The model-produced concentrations of sediment-bound radionuclides were thus volume concentrations. These are expressed here (Figures 4-16 to 4-20) in units of pCi l^{-1} . To convert these to mass concentrations (in units of pCi kg^{-1} , for example), one should note that a 1-liter sample of surface sediment from our study area typically has a mass of 1.8 kg.

4.3.2 Model Results

Our modeling effort needs to be viewed in the context of the history of radionuclide discharge from the Maine Yankee facility. Over the course of the power plant's operation and decommissioning, the discharge location and mode of discharge have undergone a number of changes. From the time of the plant's initial operation until July 1975, cooling water and radionuclides were discharged into Bailey Cove over a weir a short distance to the north of Foxbird Island (Figure 4-2b). On July 16, 1975, discharge was switched to the subsurface diffuser system. The diffuser was 305 m (1000 ft) in length and supported 42 discharge nozzles spaced 7.6 m (25 ft) apart. It was located off the southern tip of Foxbird Island (Figure 4-2b) at a depth range (relative to mean water) of 9 to 14 m. The diffuser system was used for the discharge of cooling water and radionuclides throughout the remainder of the plant's operation. The mode of discharge was altered in the late 1990's as a consequence of the plant's decommissioning. In October 1998, Maine Yankee approved a change in the discharge procedure that allowed for effluent releases with low or no dilution flow from the service water system. Later, in February 1999, this method of release was augmented, to maximize tidal dilution of effluents, by requiring that the release of liquid radioactive

effluents be carried out under low tide conditions just after the tide had turned. The final major alteration in the mode of discharge occurred in July 2002 when the discharge path for liquid effluent was switched from the forebay-diffuser route to a hose which ran through the intake channel and discharged effluents a short distance north of Little Oak Island (Figure 4-2b).

Of the long-lived radionuclides discharged by the plant, ^{60}Co and ^{137}Cs were released in, by far, the greatest volumes. As revealed by the time series of their quarterly mass releases (Figure 4-15), most of the total mass of ^{60}Co and ^{137}Cs released was discharged during the time of the plant's operation. For both nuclides, only a small amount of mass was released, relative to the total mass discharged, over the period of tide specific discharge from February 1999 through July 2002. When

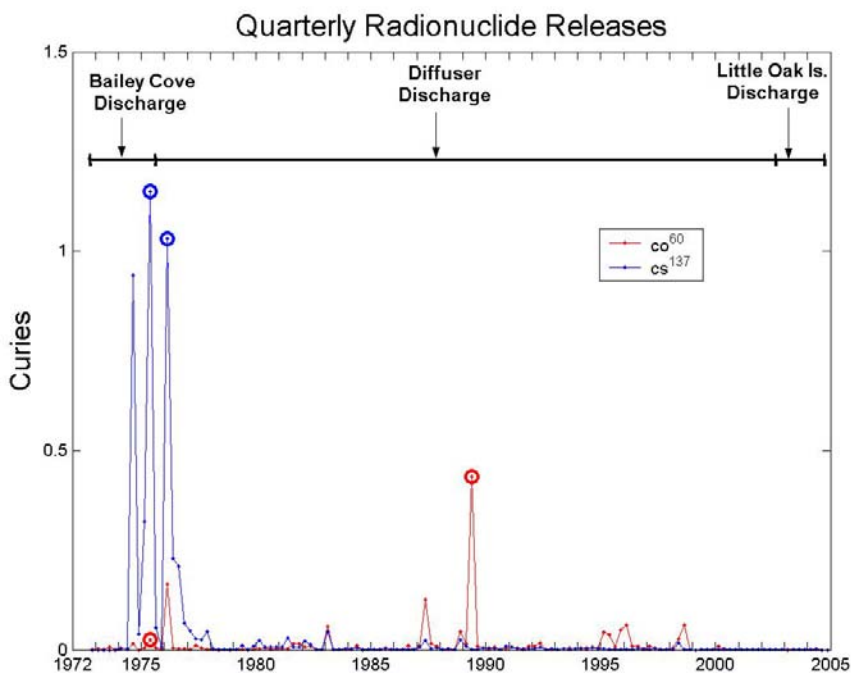


Figure 4-15. Time series of the quarterly amounts of ^{60}Co and ^{137}Cs released from the Maine Yankee facility. Time periods of the Bailey Cove, diffuser and Little Oak Island discharges are indicated on the bar above time series lines. The circled values show the amounts of radionuclides released in the simulations of discharges from the Bailey Cove outflow and the diffuser.

considering the input of these radionuclides into the estuarine system, three modes of discharge stand out as most important. One is the discharge into Bailey Cove and another is the “non-tidal specific” discharge from the diffuser. These account for most of the total discharged mass of these radionuclides. The third is the discharge into the Back River near Little Oak Island. This is deemed important because it is the most recent source of radionuclides in the sediments of Back River and Montsweag Bay. Our modeling has focused on these three modes of discharge and considered only the release of ^{137}Cs and ^{60}Co . In modeling releases of these elements from the diffuser or the Bailey Cove outflow, we simulated episodic discharges in which a specified quantity of ^{137}Cs or ^{60}Co was set out at a steady rate over a 24-hr period. This mimicked actual discharges during the period of the power plant's operation. During this time, most of the material set out during a quarterly period was discharged in one or two releases of roughly one day duration (Michael Whitney, Maine Yankee, personal communication). The simulations of the transport and sediment uptake of these releases

were carried out over the discharge period and the subsequent 4 days. The velocity fields used for these simulations were determined from DYNHYD runs with a steady intake of water ($20 \text{ m}^3 \text{ s}^{-1}$) imposed at the plant intake and a steady outflow ($20 \text{ m}^3 \text{ s}^{-1}$) at the location of either the Bailey Cove outflow or the diffuser. The total mass of ^{137}Cs or ^{60}Co set out was set equal to the largest quarterly amount of the radionuclide released from the diffuser (for the diffuser release simulations) or from the Bailey Cove outflow (these masses are displayed graphically in Figure 4-15). For each discharge location, these largest quarterly discharge amounts accounted for a large fraction of the total quantity of radionuclide set out from the location (Figure 4-15). For the period of diffuser discharge, for example, the largest quarterly release of ^{137}Cs accounted for 50% of the overall quantity of discharged ^{137}Cs .

The Little Oak Island releases differed from those from the diffuser and the Bailey Cove outflow in that they were not episodic but tended to be spread out over a number of days. In the simulations, these releases were represented by a steady discharge of ^{60}Co or ^{137}Cs extending over 4 days. The total amount released was set equal to the largest quarterly discharge amount from the Little Oak Island discharge. The simulations included this discharge period and the subsequent day.

For all discharge locations, simulations were carried out using DYNHYD velocity fields representative of spring and neap tide conditions. As would be expected, the distributions of sediment-bound radionuclides determined for spring tide conditions were a bit more expansive than the distributions computed for neap tide conditions. Nevertheless, overall patterns of radionuclide uptake determined for spring and neap tides were not dramatically different. Only those distributions resulting from spring tide simulations are displayed here (Figures 4-16 to 4-20).

The estimated distributions of sediment-bound of ^{60}Co and ^{137}Cs released from the Bailey Cove outflow (Figure 4-16) bear a close similarity in magnitude and structure to the modeled distributions determined from the study of Churchill *et al.* (1980). As would be expected, the concentrations within the sediments of Bailey Cove are the highest of the modeled distributions, exceeding 100 pCi l^{-1} for ^{60}Co and 12000 pCi l^{-1} for ^{137}Cs . Outside the cove, the model predicts substantial concentrations of ^{137}Cs extending broadly over the estuary. For example, modeled ^{137}Cs concentrations exceeding 500 pCi l^{-1} (an easily detectable level) stretch over more than 8 km of the estuary. These dwarf the modeled ^{60}Co concentrations outside the Cove which do not rise above 75 pCi l^{-1} . Both the ^{60}Co and ^{137}Cs concentrations exhibit a northward bias outside the cove, tending to be higher to the north of the cove mouth than to the south. This is a consequence of the tidal node that appears in the DYNHYD simulations roughly 1 km south of the mouth of Bailey Cove that was discussed at length in Section 4.2.3.

The concentrations of sediment-bound radionuclides released from the diffuser (Figure 4-17) also exhibit a northward bias, tending to be higher to the north of the diffuser than to the south. Perhaps one of the most significant indications of the modeled concentrations is the extent to which radionuclides released from the diffuser are incorporated into the sediments of Bailey Cove. In fact, the simulations indicate that the diffuser may be the principal source of ^{60}Co found within Bailey Cove sediments. The concentrations of ^{60}Co in Bailey Cove sediment that originate from the modeled diffuser release are no less than 200 pCi l^{-1} , whereas the modeled concentrations in the cove's sediment that stem from the modeled Bailey cove discharge are not greater than 200 pCi l^{-1} . When comparing the modeled sediment-bound radionuclide distributions from historical releases with the recent measured distribution determined as part of this project, it is necessary to consider the effect of radioactive decay on the modeled concentrations. Clearly, there are other factors, such as desorption,

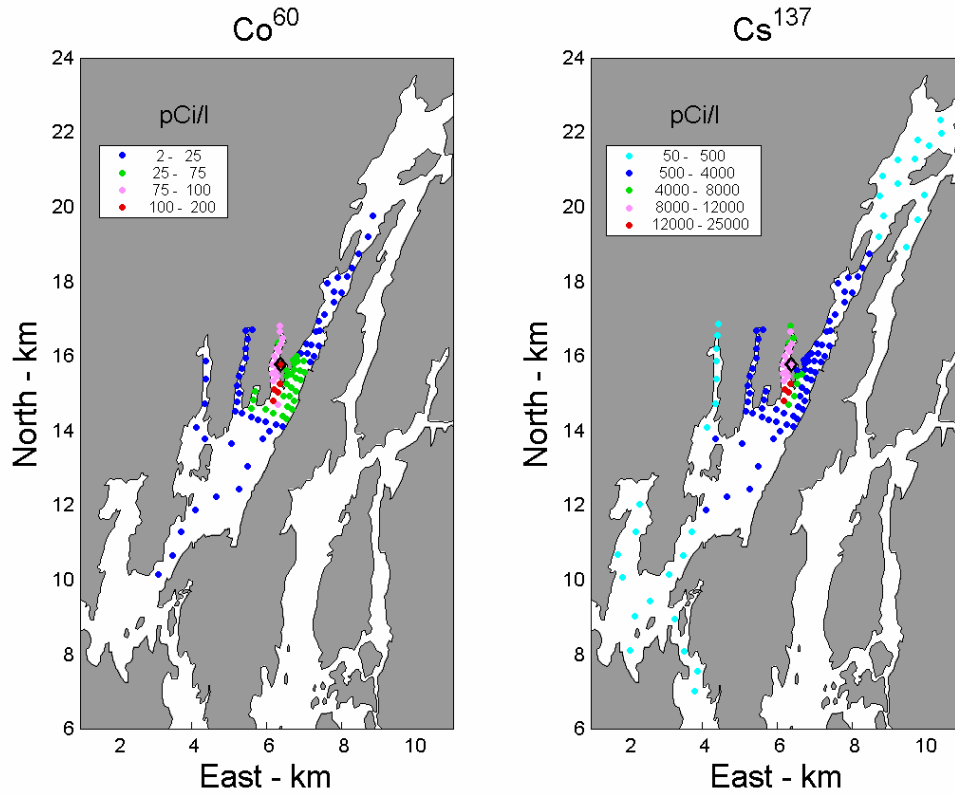


Figure 4-16a. Modeled concentrations of ^{137}Cs and ^{60}Co in bottom sediments. These were derived from simulations of radionuclide release from the Bailey Cove discharge (depicted by the black diamond) during flood tide conditions. Note that these are volume concentrations in units of pCi l^{-1} . They may be converted to mass concentrations in units of pCi kg^{-1} by dividing by the density of surficial sediment, typically 1.8 kg l^{-1} .

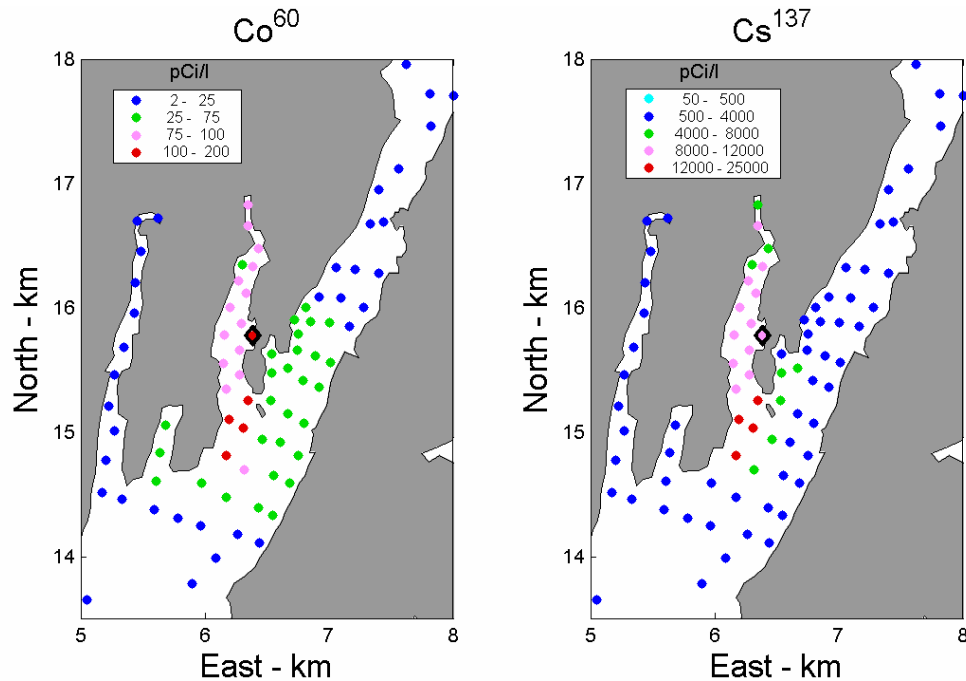


Figure 4-16b. A smaller scale view of the modeled concentrations of ^{137}Cs and ^{60}Co of Figure 4-16a.

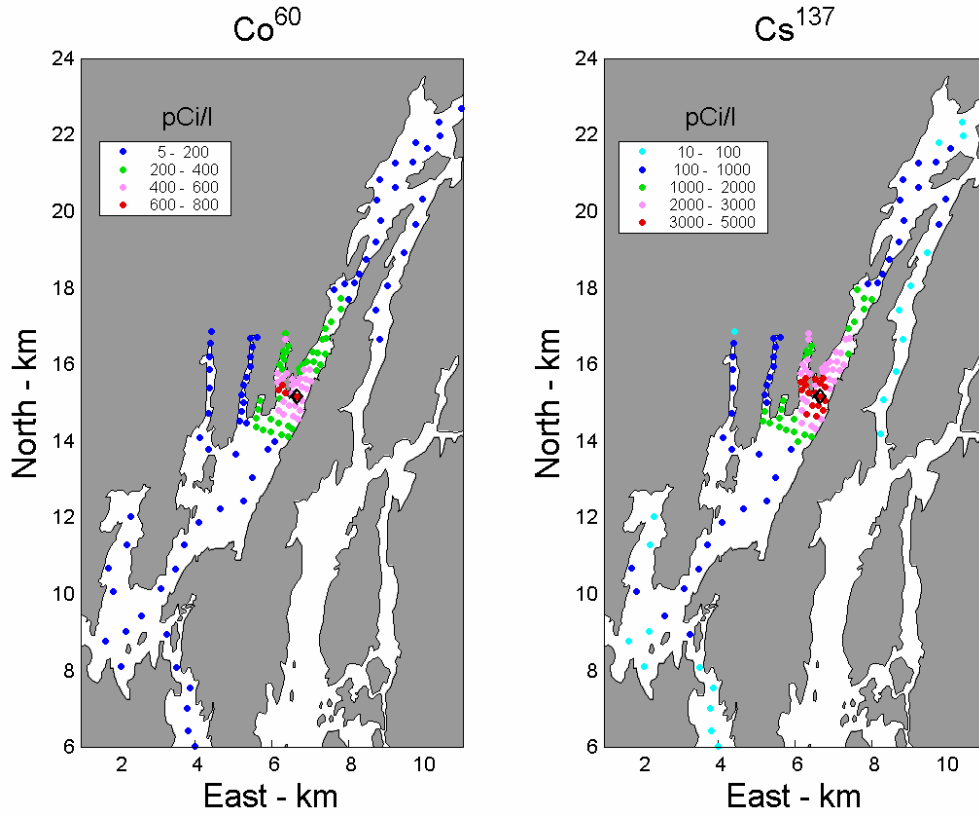


Figure 4-17a. Modeled concentrations of ^{137}Cs and ^{60}Co in bottom sediments. These were derived from simulations of radionuclide release from the diffuser (depicted by the black diamond) during flood tide conditions.

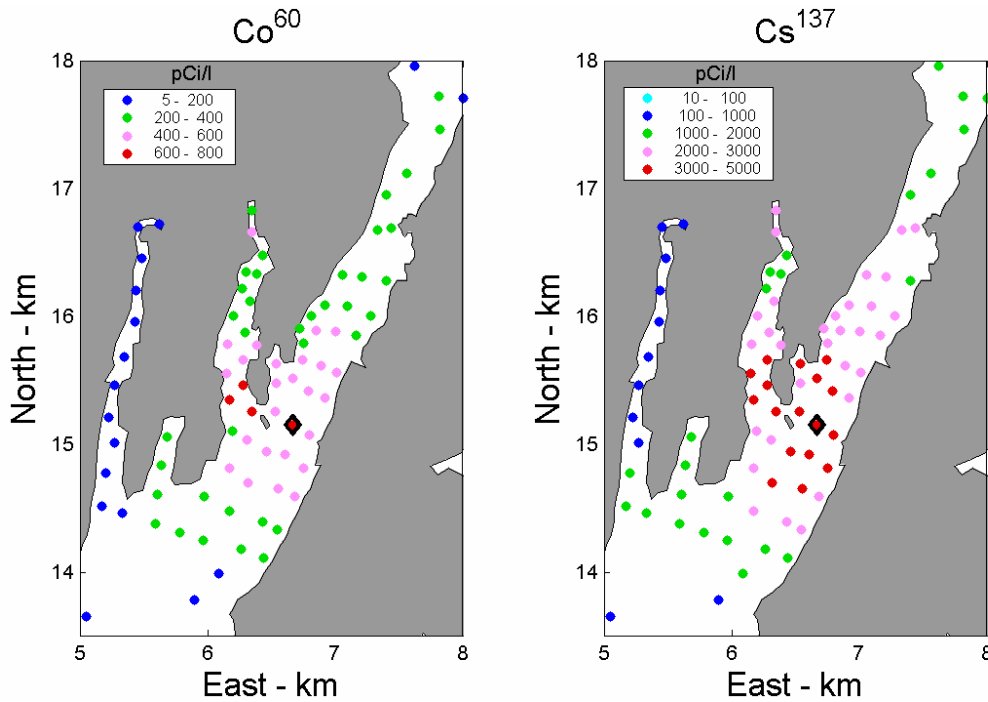


Figure 4-17b. A smaller scale view of the modeled concentrations of ^{137}Cs and ^{60}Co of Figure 4-17a.

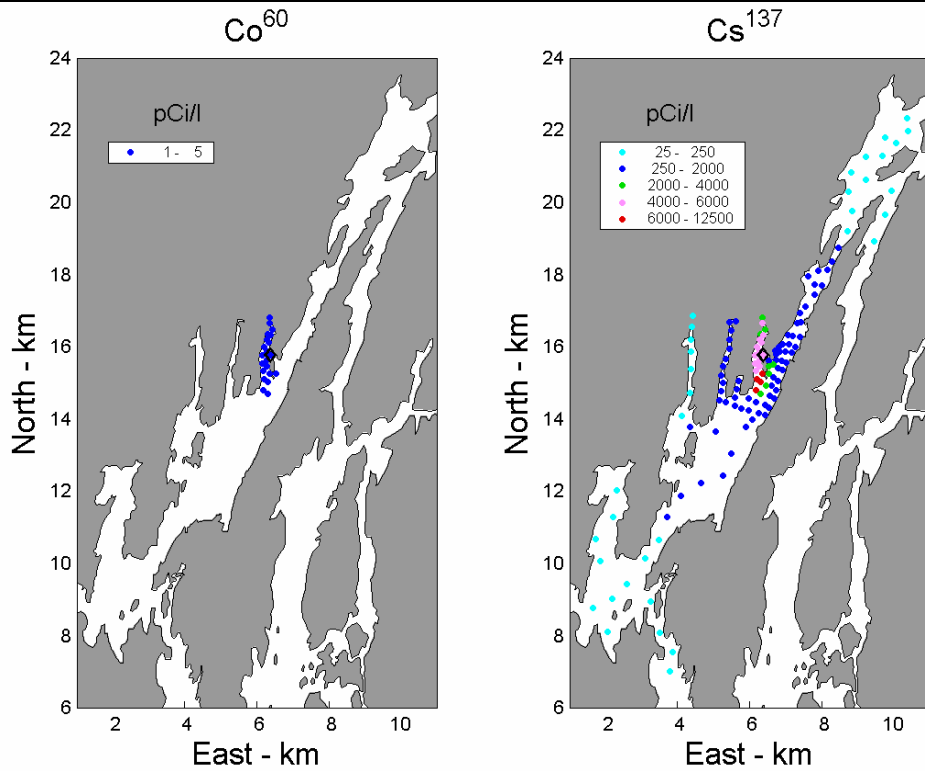


Figure 4-18a. Modeled concentrations of ^{137}Cs and ^{60}Co in bottom sediments as derived from simulations of radionuclide release from the Bailey Cove discharge (depicted by the black diamond) during flood tide conditions. These are the same concentration fields shown in Figure 4-16, except with the effects of radioactive decay accounted for.

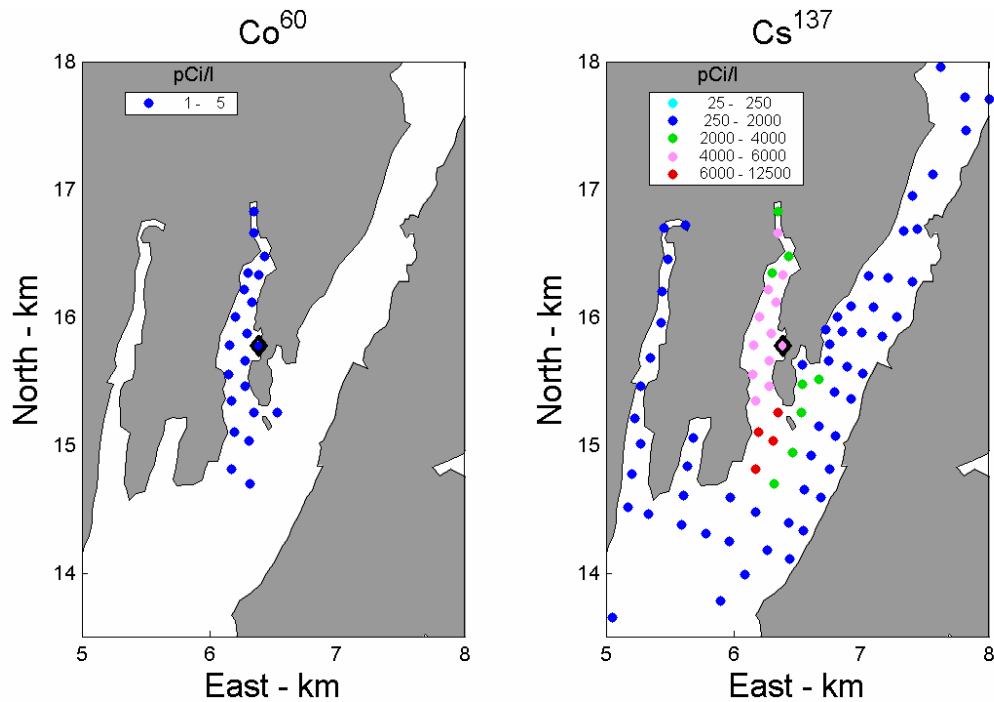


Figure 4-18b. A smaller scale view of the modeled concentrations of ^{137}Cs and ^{60}Co of Figure 4-18a.

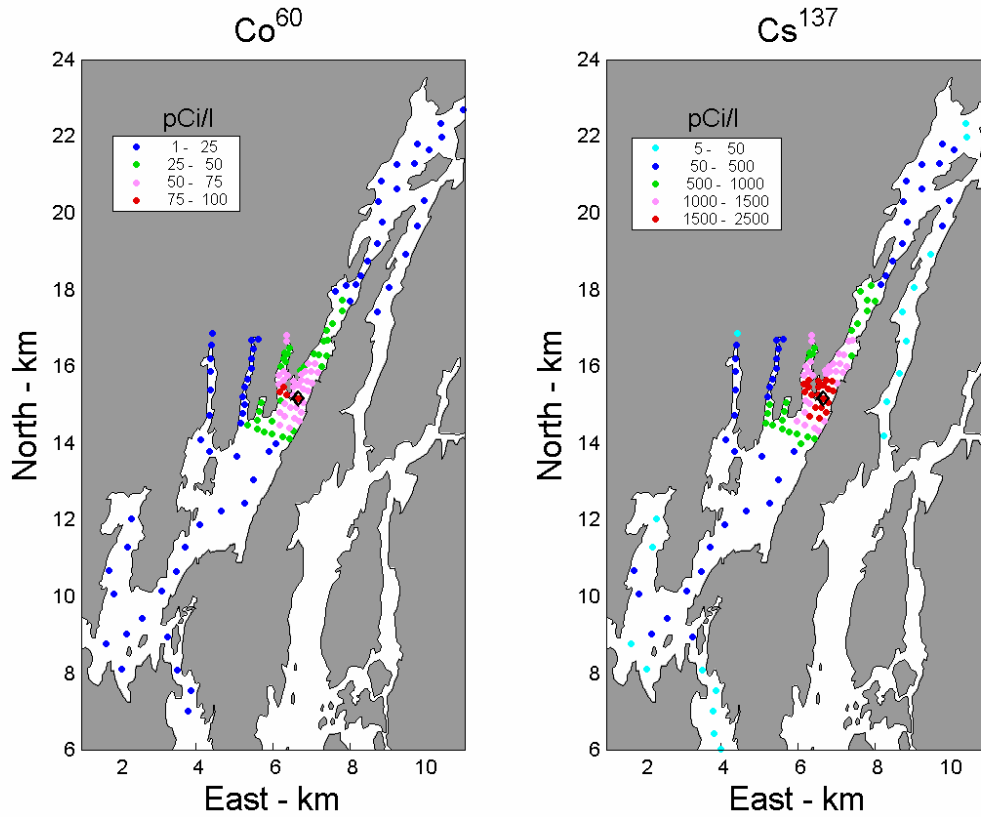


Figure 4-19a. Modeled concentrations of ^{137}Cs and ^{60}Co in bottom sediments as derived from simulations of radionuclide release from diffuser (depicted by the black diamond) during flood tide conditions. These are the same concentration fields shown in Figure 4-17, except with the effects of radioactive decay accounted for.

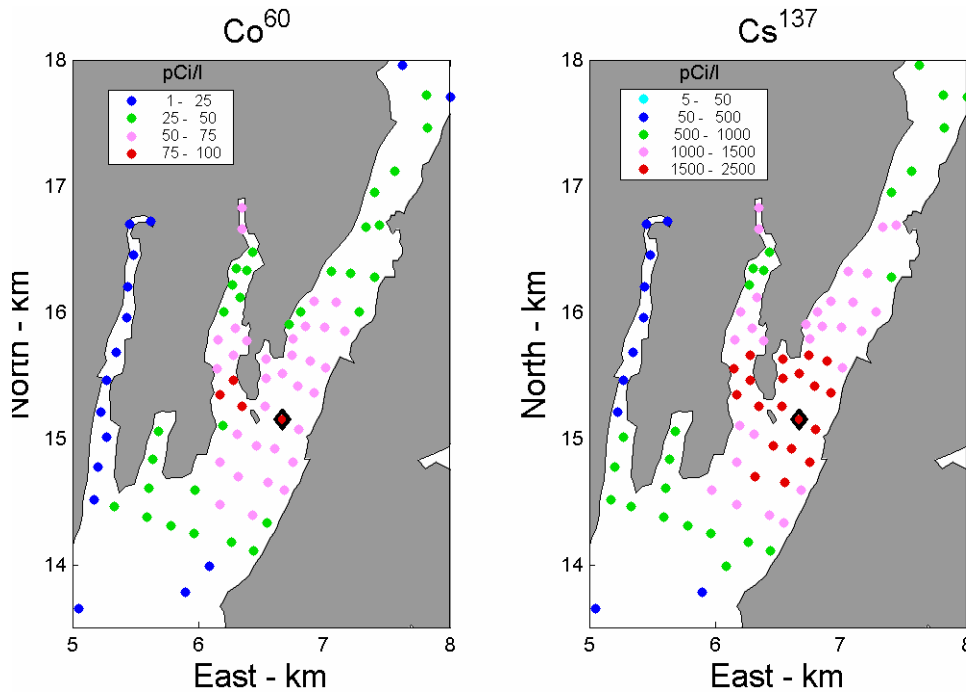


Figure 4-19b. A smaller scale view of the modeled concentrations of ^{137}Cs and ^{60}Co of Figure 4-19a.

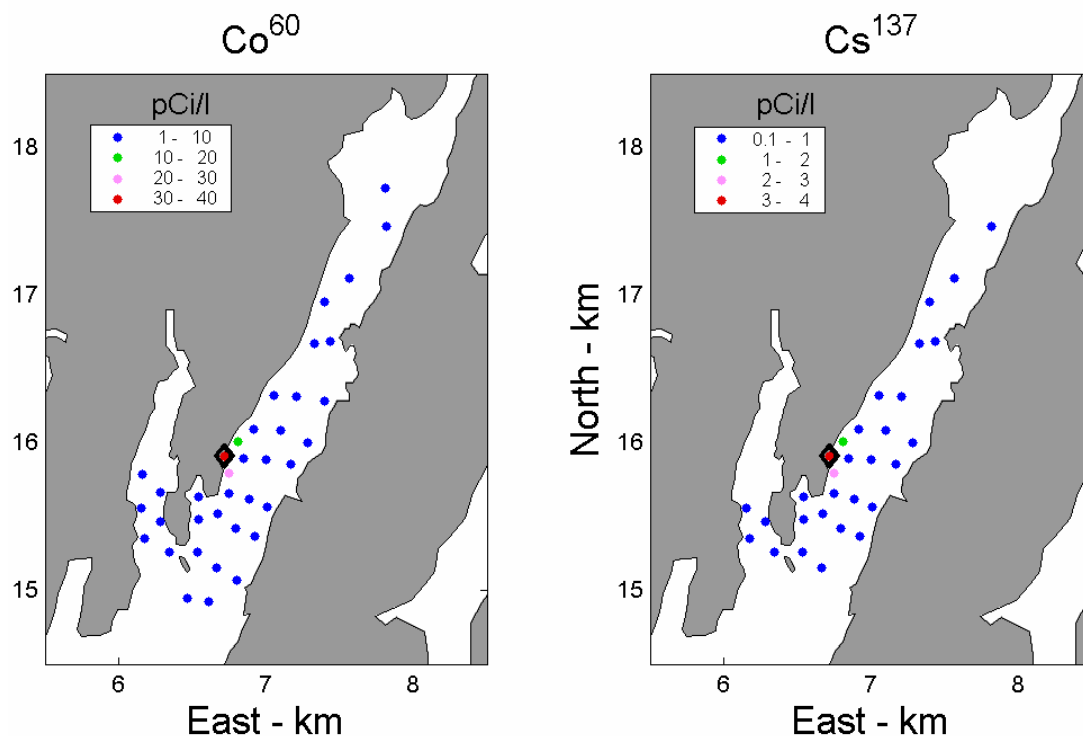


Figure 4-20. Modeled concentrations of ^{137}Cs and ^{60}Co in bottom sediments. These were derived from simulations of radionuclide release from the Little Oak Island Outfall (depicted by the black diamond) during flood tide conditions.

that may lead to a decline in sediment-bound radionuclide concentrations; but radioactive decay is one that will unquestionably occur and the only one that can easily be accounted for through calculations.

We have done this “accounting” by applying a radioactive decay factor to the model results. This took the form of:

$$C_k = C_{k0} 2^{-t/t_{k1/2}}$$

Where C_{k0} is the modeled concentration of radionuclide k due to an historical release, C_k is the current concentration with the effects of radioactive decay taken into account, t is the time since the release and $t_{k1/2}$ is the half life of the radionuclide (30.17 yr for ^{137}Cs and 5.26 yr for ^{60}Co).

With this decay formula applied, the sediment-bound radionuclide concentrations derived from the simulations of large historical releases still rise above a detectable level over broad areas of the estuary (Figures 4-18 and 4-19). For ^{60}Co , the “decayed” concentrations resulting from the simulated diffuser discharge are above 50 pCi l^{-1} (a conservatively low level of detection) over a band in Back River and Montsweag Bay of roughly 1.5 km in length (Figure 4-19b). Of particular significance are the relatively high decayed concentrations of ^{60}Co in the upper reaches of Bailey Cove, where model results and observations reveal tidal conditions conducive to sediment accumulation (Sections 4.2.3 and 4.2.4). For ^{137}Cs , the decayed concentrations are much higher and extend more broadly. The range of detectable ^{137}Cs concentrations, determined from both simulated diffuser and Bailey Cove discharges, extend over a region encompassing Bailey Cove and all of the Back River and Montsweag Bay. Within Bailey Cove and in the southern portion of the Back River,

Maine Yankee Marine Sampling Study

the decayed ^{137}Cs concentrations are particularly high, well in excess of 2000 pCi l⁻¹ in many locations.

In the absence of significant desorption and sediment movement, it thus appears very likely that remnants of large historical discharges of ^{137}Cs may be found, at relatively high concentration, in the sediments of Bailey Cove and the Back River. By far, the largest of these historical discharges occurred in the mid-1970's (Figure 4-15). If buried, the sediment-bound ^{137}Cs from these discharges may very likely be found in a single depth band. Our results also indicate a likelihood of finding ^{60}Co remnants from historical discharges, but that these remnants may be near the level of detection.

The most recent releases of radionuclides, from the Little Oak Island discharge, have contained much higher concentrations ^{60}Co than ^{137}Cs . This is reflected in the results of simulations of sediment uptake of these releases. The modeled concentrations of ^{137}Cs in the sediment are everywhere well below the level of detection (Figure 4-20); whereas modest ^{60}Co concentrations of 20-40 pCi l⁻¹ are predicted near Little Oak Island. It should be noted that the simulation that produced these ^{60}Co concentrations accounted for roughly 1/3 of the total mass of ^{60}Co released from the Little Oak Island discharge. The model simulations thus indicate the possibility of sediment-bound ^{60}Co concentrations of order 100-200 pCi l⁻¹ resulting from the Little Oak Island releases.

An important property that is easily calculated with the model is the fraction of released radionuclides that are absorbed by bottom sediments. Here we refer to this as the fraction retained, as the remainder is presumably flushed from the estuarine system. The close agreement between modeled and measured sediment-bound radionuclide concentrations near the Maine Yankee facility reported by Churchill *et al.* (1980) and Hess *et al.* (1983) offer a good degree of confidence in the model's estimates of such a fraction. Here we present fraction retained values of ^{137}Cs and ^{60}Co computed for all three release sites from simulations using spring tide velocities (Table 4-1). Taken together, these indicate that only a small fraction of the radionuclides released are retained in the system through absorption in the sediments. The fraction retained is of order 5% for ^{60}Co and 10% for ^{137}Cs .

Table 4-1. According to model simulations, the percent of the total radionuclide released from the indicated location that is absorbed in the bottom sediment. The values were computed from simulations using velocities representative of spring tide conditions.

	^{137}Cs	^{60}Co
Bailey Cove Outflow	12.6	4.9
Diffuser	8.7	3.4
Little Oak Island	5.2	2.0

4.3 MODELING SUMMARY

The modeling component of our project has yielded new insights into the workings of the Sheepscot estuarine system and the manner in which these affect the transport of radionuclides introduced to the system. Of particular importance is the indication of a tidal node to the south of the Maine Yankee diffuser. This corresponds to a minimum of tidal energy and is the product of the merging of two tidal waves which travel in opposite directions around Westport Island. Although the presence of this node was not recognized in previous studies of the region (e.g., Churchill *et al.*, 1980 and Hess *et al.*, 1983), its effect on the transport of material released from the Maine Yankee facility

is likely to have been significant. Our simulated particle tracks indicate that the node acted as something of a barrier to the southward movement of material released from the Back River discharge and from the Bailey Cove outflow. On the basis of this result, we biased our sample collection in the Back River-Montsweag Bay region to the north of the diffuser location.

We should note, however, that there is some question as to the exact location of the node. In the model simulations, it appears roughly 1 km south of the diffuser. As discussed earlier, however, this location is sensitive to the depths of the model channels ringing Westport Island. In addition, the model does not include the Kennebec River, which connects with the Sheepscot estuary through the Sasanoa River (Figures 3-2, 4-2a). The addition of the tidal wave from the Kennebec River mouth, which undoubtedly enters the Sheepscot estuary through the Sasanoa, will likely impact the tidal node's location and complicate its dynamics.

Another important dynamical feature revealed by the modeling, and by the observations meant to test the model, is a tidal asymmetry within Bailey Cove. This is a flood dominated asymmetry, characterized by a flood tide flow that is shorter and stronger than the ebb tide flow. Such an asymmetry favors particle retention. A tendency for particles to be retained in Bailey Cove is confirmed by the measurements of this project. As will be shown in an ensuing section, the radionuclide concentrations within core samples from Bailey Cove indicate a substantial rate of sediment accumulation.

Modeling of radionuclide uptake by bottom sediments has indicated that easily detectable remnants of historical discharges of ^{137}Cs are likely found over a broad area of the estuary. For ^{60}Co , the model results indicate that marginally detectable remnants of historical releases may be found in bottom sediments. According to the model, sediment uptake of the recent releases near Little Oak Island is expected to produce marginally detectable levels of ^{60}Co , but no detectable levels of ^{137}Cs .

5 GAMMA SCAN RESULTS

5.1 SEDIMENT CORES

There are four sources of the radionuclides in the vicinity of the Maine Yankee nuclear reactor. The first was global fallout from the United States and Russian weapons testing which started in 1945 and became a maximum in 1957 through 1969. There were smaller additions in 1983 due to the Chernobyl reactor accident and from French and Chinese atmospheric weapons testing. This activity included radionuclides such as ^{137}Cs , ^{134}Cs , ^{60}Co , ^{95}Nb and ^{95}Zr and ^{239}Pu , and ^{240}Pu to mention just a few. In the early 1970's, Maine Yankee nuclear reactor discharged nuclides into Bailey cove on monthly basis using the cooling water. Their intake water came from near Oak Island on the other side of Bailey point.

Over the course of the power plant's operation and decommissioning, the discharge location and mode of discharge have undergone a number of changes. From the time of the plant's initial operation until July 1975, cooling water and radionuclides were discharged into Bailey Cove over a weir a short distance to the north of Foxbird Island. On July 16, 1975, discharge was switched to the subsurface diffuser system. The diffuser was 305 m (1000 ft) in length and supported 42 discharge nozzles spaced 7.6 m (25 ft) apart. It was located off the southern tip of Foxbird Island at a depth range (relative to mean water) of 9 to 14 m. The diffuser system was used for the discharge of cooling water and radionuclides throughout the remainder of the plant's operation. The mode of discharge was altered in the late 1990's as a consequence of the plant's decommissioning. In October 1998, Maine Yankee approved a change in the discharge procedure that allowed for effluent releases with low or no dilution flow from the service water system. Later, in February 1999, this method of release was augmented, to maximize tidal dilution of effluents, by requiring that the release of liquid radioactive effluents be carried out under low tide conditions just after the tide had turned. The final major alteration in the mode of discharge occurred in July 2002 when the discharge path for liquid effluent was switched from the forebay-diffuser route to a hose which ran through the intake channel and discharged effluents a short distance north of Little Oak Island. The pattern of radionuclides in Bailey Cove and Montsweag Bay area depends upon these different types of releases as well as the sedimentation in the Montsweag Bay, Bailey Cove area.

As we look at the radionuclides taken in cores from 40 points in Tables 5-1, 5-2, 5-3, and Figures 5-1 to 5-52 in the Montsweag Bay, Bailey Cove area, we note that the ^{137}Cs and ^{60}Co are the strongest nuclides observed. Prior to 1982, the sediments in Bailey Cove were closed for clam digging allowing only worm digging. This was due to presence of sewage contamination in the Bay. After the cleanup of discharge waters in the area, the Cove was opened by the Department of Marine Resources for clam digging after radionuclides were measured in the clams sampled from Bailey Cove. The harvesting of worms and clams from this area has resulted in mixing of the sediments down to a depth of 2 feet. Cores taken in this area reflect this plowing and mixing of the sediments by human digging. At the same time the sediments in the Bay may be slowly increasing in depth even though the overall depth has not changed sufficiently to change the low tide area. Some of the change in sediments may be due to gradual compaction of the sediments near the bottom of the mixed zone. The four-inch cores that were taken in the zones which are exposed at low tide show sediments' radioactivity from ^{137}Cs down to the bottom of the 2 foot level. The less disturbed three-inch cores that were taken by boat from areas that are not exposed at low tide show activity down to 10 inches. The highest activity observed from ^{137}Cs was observed in a core from the north end of Bailey Cove

Maine Yankee Marine Sampling Study

near where the road crosses the small stream that enters in the north end of Bailey Cove. The sediments in this area are dominated by the freshwater input and have no value for clam or worm digging and are thus not disturbed. The core at station Long Creek shows its maximum of 913 pCi/kg at about 4 inches depth. Another core that has 250 pCi/kg of ^{137}Cs at 6 inches was collected at station 68 near Long Ledge, close to the location of the diffuser. We would expect higher levels due to this discharge from diffuser starting in 1980. Finally the highest Co-60 sediments at 158 pCi/kg is found at station 109 in surface sediments just north of the diffuser. This location reflects releases during the final decommissioning phases of the reactor, which involved liquids from the spent fuel pool and from parts with high activity from the reactor vessel.

The general trend of radioactivity is higher close to the discharge points and lower as distance increases from them.

The distant cores included samples from distant locations such as the north end of Back River, Barry Cove, Chewonki, Robin Hood Cove and Sasanoa (Station 149) stations as well as samples from the Damariscotta River. We notice peak values of ^{137}Cs between 100 and 127 pCi/kg at the distant Wiscasset, Eddy, Pottle Cove and 147 (Westport Island) stations. The Sasanoa station peaked at 5 inches with 330 pCi/kg, while control stations 148 and 149 had peaks of 36 and 73 pCi/kg, respectively. These levels represent fallout accumulation in the sediments along the coast. The circulation of water in the other direction toward the southwest, only Sasanoa is west. These values are lower than the Long Creek station in Upper Bailey Cove value of 913 pCi/kg at 4 inches. The ^{60}Co concentrations observed at these locations are very near the average error value of 25 -30 pCi/kg.

Cores taken from Bailey Cove with high values of ^{137}Cs include Long Creek station, station 74 in Bailey Cove, station 77 in Upper Bailey Cove, station 85 in South Bailey Cove, station 99 in North Bailey Cove, Station 101 in Eaton Farm of Bailey Cove, and Station 105 at the top of Bailey Cove. The highest of these is the Long Creek station with 913 pCi/kg. Upper Bailey Cove station 77 has 222 pCi/kg, South Bailey Cove station 85 has 70 pCi/kg, North Bailey Cove station 99 has 155 pCi/kg and Eaton Farm Bailey Cove shows 213 pCi/kg. The top of Bailey Cove station 105 shows 100 pCi/kg. All of these values are lower than values in Bailey Cove that were observed in the 1970s. Small amounts of ^{60}Co about 20 to 30 pCi/kg also show up in the samples. The level of cesium decreases after 10 inches' depth in the sediments of Bailey Cove and decreases after 6 inches at the top of Bailey Cove and for the Long Creek station.

Cores from Montsweag Bay shoreline had generally lower ^{137}Cs concentrations, including station 113 and station 117, Little Oak Island; station 118; station 134, the Westport Island ferry landing; stations 143; station 144, Oak Island or Murphy Corner; and station 145 or Murphy Corner. The ^{137}Cs levels range as much as 120 pCi/kg but generally are less than a hundred pCi/kg for the Stations. The ^{137}Cs concentration with depth goes as deep as nine to 14 inches deep and in some instances we even see two peaks. Station 118 shows two peaks for the ^{137}Cs . ^{60}Co values in the stations range around 20 to 30 pCi/kg. Oak Island Murphy Corner shows 40 pCi/kg.

The cores from the mid-channel, Stations 38, 44, 50, 59, 60; South Oak Island 61, 62, 63; Long Ledge 64, 65 and 67 were three-inch cores that show decrease in ^{137}Cs from around 52 to as high as a 100 pCi/kg down to low values in six to 8 inches depth. They contained small amounts of ^{60}Co of the order of 20 pCi/kg.

Maine Yankee Marine Sampling Study

The cores have a structure of two ^{137}Cs peaks for many instances. Low sedimentation rate will give one broad peak instead. Long Creek station shows this one broad peak, which represents dates from 1953-1983 as a single broad peak from 1" to 6" deep. Double peaks can be seen in Bailey Cove station 2 with a peak from 1" to 11" deep. This is 10" in 30 years. Two weak peaks are seen for Wiscasset station from 3" to 9" (6" for 30 years). Station 8 has a peak at 6" to 13" with 7" in 30 years. Station 34 shows two peaks from 1" up to 7" or 6" in 30 years.

A summary of these peaks are given below in Table 5-2.

The results in table 5-3 show a total activity contained in the cores. It was calculated by summing the activity found in each slice of the core to yield a grand total activity (in pCi) for the whole core. This number gives the measure of activity still contained in the deep sediments of the bay. This number can be useful in determining the remaining total activity in the bay after 30 years of decay and loss by sediment dispersal and dilution due to off shore ocean sediment. Long Creek's total activity is the highest ^{137}Cs activity at 1297 pCi. The highest ^{60}Co activity of 73 pCi was found at station 118 near Little Oak Island.

5.2 LEAD-210 CORE RESULTS

The station 144 core was analyzed for ^{210}Pb and found to have a sedimentation rate dating to 4" = 20 years, or one inch for each 5 years. The graph of the data can be seen in Figure 5-48. This core is consistent with the double peak time of 30 years from 1957-87, or 30 years between the two peaks.

5.3 SURFICIAL SEDIMENTS

The University of Maine received 136 surface samples collected from around Maine Yankee Nuclear Power Plant. All samples were gamma counted on one of three systems, one being a very low background system. Each system is an intrinsic germanium detector and was calibrated using U.S. EPA Quality Assurance liquid gamma standards under the RADQA program. A cross calibration was then accomplished to ensure that each system provide the same result for a given sample. Thus, unless the very low background system was needed, the germanium system used was transparent to the results. The results were compared with a pre- and post-operational study of the area completed in 1976 (Technical Note 76.3).

The gamma spectrum was analyzed for 14 radionuclides with results presented in tabular fashion included with the table of core results. Surficial samples are marked with "S" in the depth column. However, this discussion concentrates on the results for ^{60}Co (1332.51 eV peak) and ^{137}Cs . To begin, the values were examined without regard to location to see the range of values. For sediment samples, the ^{137}Cs values ranged from a high of 287.2 pCi/kg to a low of 2.9 pCi/kg with one sample below detection limits while ^{60}Co ranged from 168.7 pCi/kg to a low of 0.5 pCi/kg with four samples below detection limits. These results are summarized in Table 5-5 along with the pre- and post-operational values.

The results indicate that currently, the values of ^{137}Cs sediment samples around the Maine Yankee site are lower than before the power plant was brought on line. There are two possible explanations for this result. First, the ^{137}Cs seen pre-operation has decayed. Second, a mixing is occurring within the tidal flat, lowering the radioactivity seen at the surface. The first explanation is certainly plausible since approximately one half life of ^{137}Cs has occurred since inception of the

power plant, but the second explanation is more tenable. As people dig clams or worms in the tidal flat area, they are turning over the tidal flat area, mixing any Cesium into the soil. Also, the area is washed by tides. In general, we feel that the ^{137}Cs values are low predominately due to a mixing in the tidal flat. For the ^{60}Co sediment samples, the values, while still generally low, are higher than the pre-operational study which found all samples below detectable limits. However, the new ^{60}Co values are well below the post-operational study values. Again, these results are probably due to decay of the ^{60}Co and due to mixing within the tidal flat.

Additionally, six soil samples from dry ground were taken around power plant. The ^{137}Cs values ranged from 46.3 pCi/kg to 120.8 pCi/kg while the ^{60}Co values ranged from 3.1 pCi/kg to 26.5 pCi/kg. The ^{137}Cs values are orders of magnitude less than soil samples taken in the pre-operational study, which found values from 1110 pCi/kg to 4960 pCi/kg. The pre-operational study values are also significantly higher than anything seen in the tidal marsh sediment during this study. Thus, no accumulation of radionuclides on dry ground was found.

It is now necessary to discuss the distribution of ^{60}Co and ^{137}Cs around the power plant (Figures 5-53 to 5-56 with corresponding station numbers in Figures 5-1 to 5-4). Although a quick perusal of the results shows no significant accumulation and no "hot areas" by the 3x background definition, the distribution of ^{60}Co and ^{137}Cs is not random. In particular, ^{60}Co has its most significant values near the diffuser along the Back River while ^{137}Cs has its most significant values near the outfall in Bailey Cove. Figure 5-53 shows the distribution of ^{60}Co values while Figure 5-54 shows the distribution of ^{137}Cs . The difference in distribution is related to a variety of factors. First, as shown in Figure 4-15, early Maine Yankee's discharges into Bailey Cove before the diffuser installation were characterized by predominantly ^{137}Cs effluents. Later Maine Yankee discharges through the diffuser into the Back River were characterized by predominantly ^{60}Co effluents. Second, the shorter decay period of ^{60}Co versus ^{137}Cs makes the difference between the more recent Back River ^{60}Co dominated effluents and the earlier Bailey Cove ^{137}Cs dominated effluents more pronounced. Comparison with the modeling for ^{137}Cs shows that particles released from the diffuser also migrate to Bailey Cove as well.

5.4 BIOTA GAMMA SCAN

The biota gamma scan results are shown in Table 5-4. The biota included clamshells, mussels, rockweed, fish tissue, control mussels, clam tissue and lobster. The majority of the samples have less nuclide content than their errors in measurement. Some of the nuclides found above their two-sigma error are 16.8 pCi/kg of ^{137}Cs in fish tissue, 97.2 pCi/kg of ^{65}Zn in rockweed, 46.5 pCi/kg of ^{65}Zn in lobster, 13.8 pCi/kg of ^{22}Na in clam shells, and 8.4 pCi/kg of ^{54}Mn in clam tissue.

Control biota samples were taken from South Portland and near the Darling Center in the Damariscotta Bay. The results of the control biota samples are shown in the lower half of Table 5-4. The control sea scallops and rockweed each show a ^{60}Co concentration above their 2 sigma level, but only from one of the two ^{60}Co gamma ray energies. The control horse mussels have 14.4 pCi/kg of ^{137}Cs . Other nuclides with a value greater than their 2-sigma error are ^{65}Zn found in the control sea scallops, oysters and blue mussels while ^{54}Mn was found in the control sea scallops. These control results are similar to those found near the plant.

5.5 HARD TO DETECT NUCLIDES

The marine samples of clams, clam shells, muscles, mussel shells, fish, lobsters, seaweed, and sediments were measured by Framatome for hard to detect nuclides. The samples were collected from the vicinity of the diffuser, near Oak Island, and in Bailey Cove. Sites were selected where the sediments were highest. The samples were delivered to Framatome on October 22, 2004, measurements of ^{55}Fe , ^{63}Ni , ^{90}Sr , ^{239}Pu , ^{238}Pu . Results were obtained on December 9-13, 2004. These results are shown in Table 5-6.

The results of the hard to detect measurements show very low concentrations for 35 out of the 40 measured. The five with a measured concentration greater than their 1-sigma uncertainty are: 1.5 pCi/g of ^{63}Ni in mussel shells, 1.25 of ^{90}Sr in lobster, 3.9 pCi/g of ^{63}Ni in sediment, while 9.3×10^{-1} of ^{90}Sr in fish, and 9.3×10^{-3} pCi/g of ^{239}Pu in sediment are above their 2-sigma uncertainty. All of the values measured are well below the required minimum detectable activity.

5.6 ERROR DISCUSSION OF GAMMA SCANS

The results of our gamma-ray measurements are stated with the value entered in a column labeled by a nuclide, ^{60}Co for example, and the one-sigma statistical error in the measurement is given in the next column to the right. The average error for our ^{60}Co and ^{137}Cs columns is 10-15 pCi/kg and 20-25 pCi/kg, respectively. Measurements which are lower or equal to this error are so low that they represent a mixture of signal and noise. Our ability to determine the signal is hampered by the presence of counting noise. Thus, our certainty of the value or existence of low readings is doubtful for the smaller than error readings. A repeated counting of the same sample value may yield a positive value for one count and a reading of zero for another. When the sample shows values twice as large as the error, we can be more confident of the presence of the nuclide in the sample.

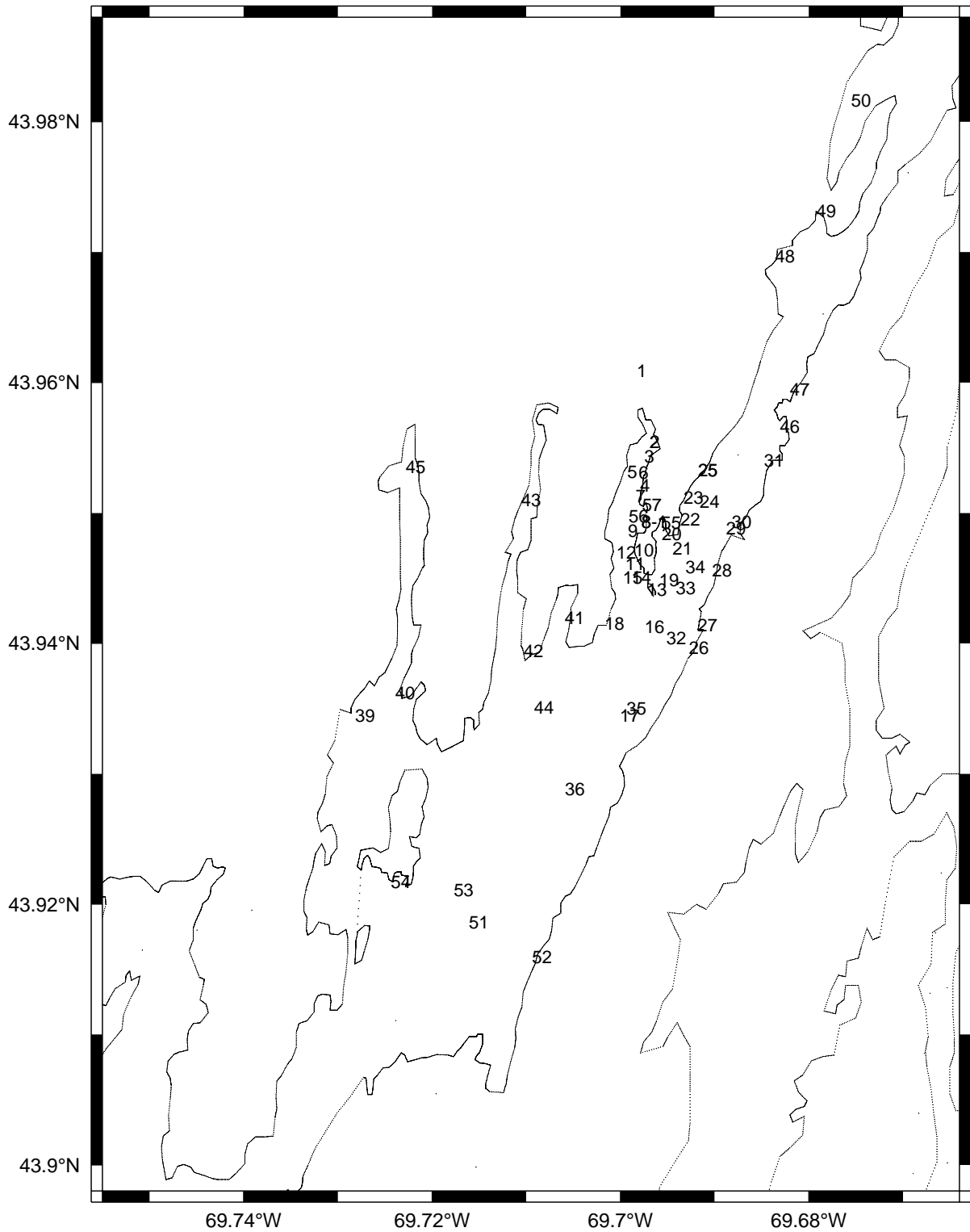


Figure 5-1. 6-9 July 2004 Station Locations

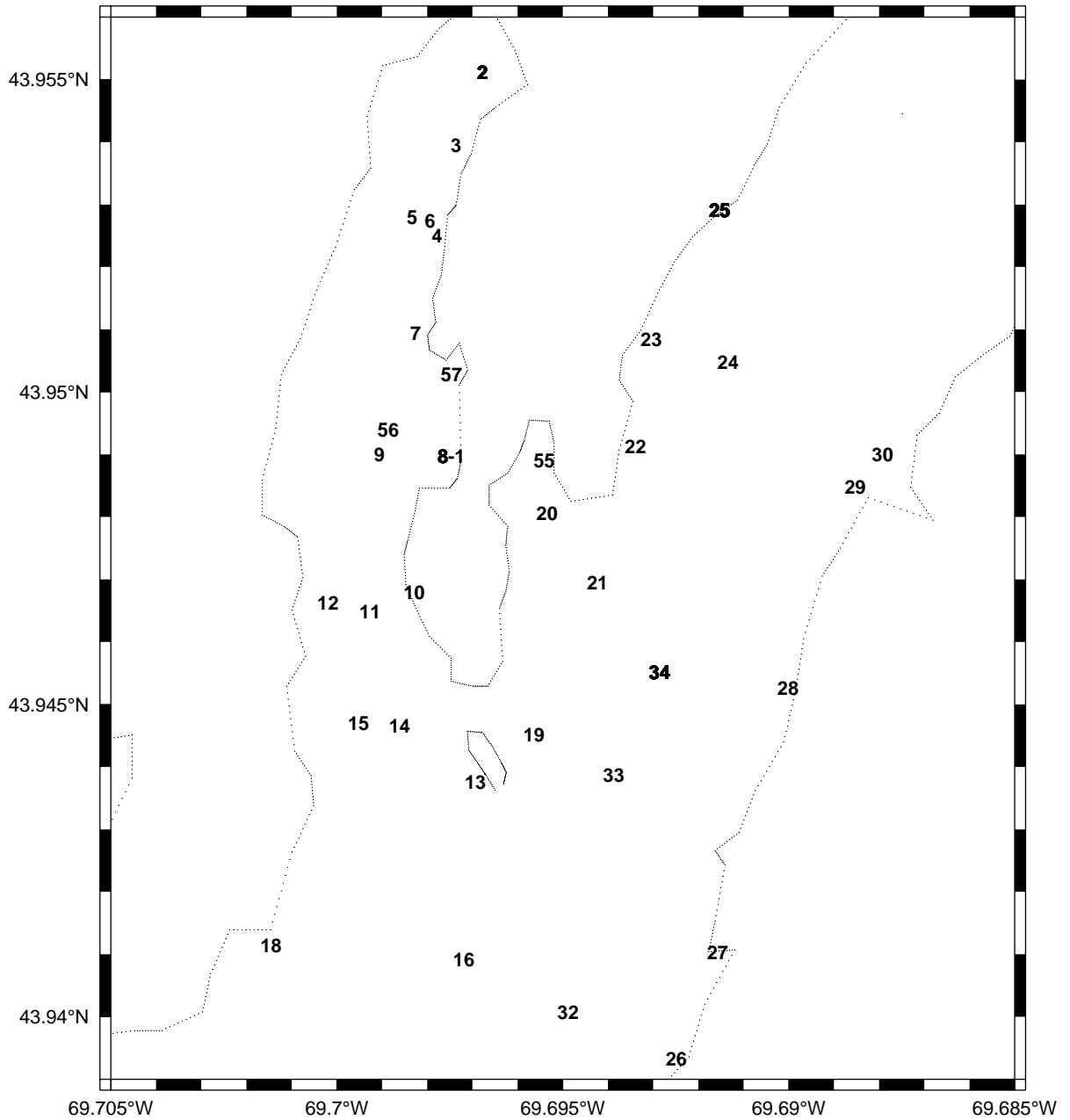


Figure 5-2. 6-9 July 2004 Station Locations - Close to Plant

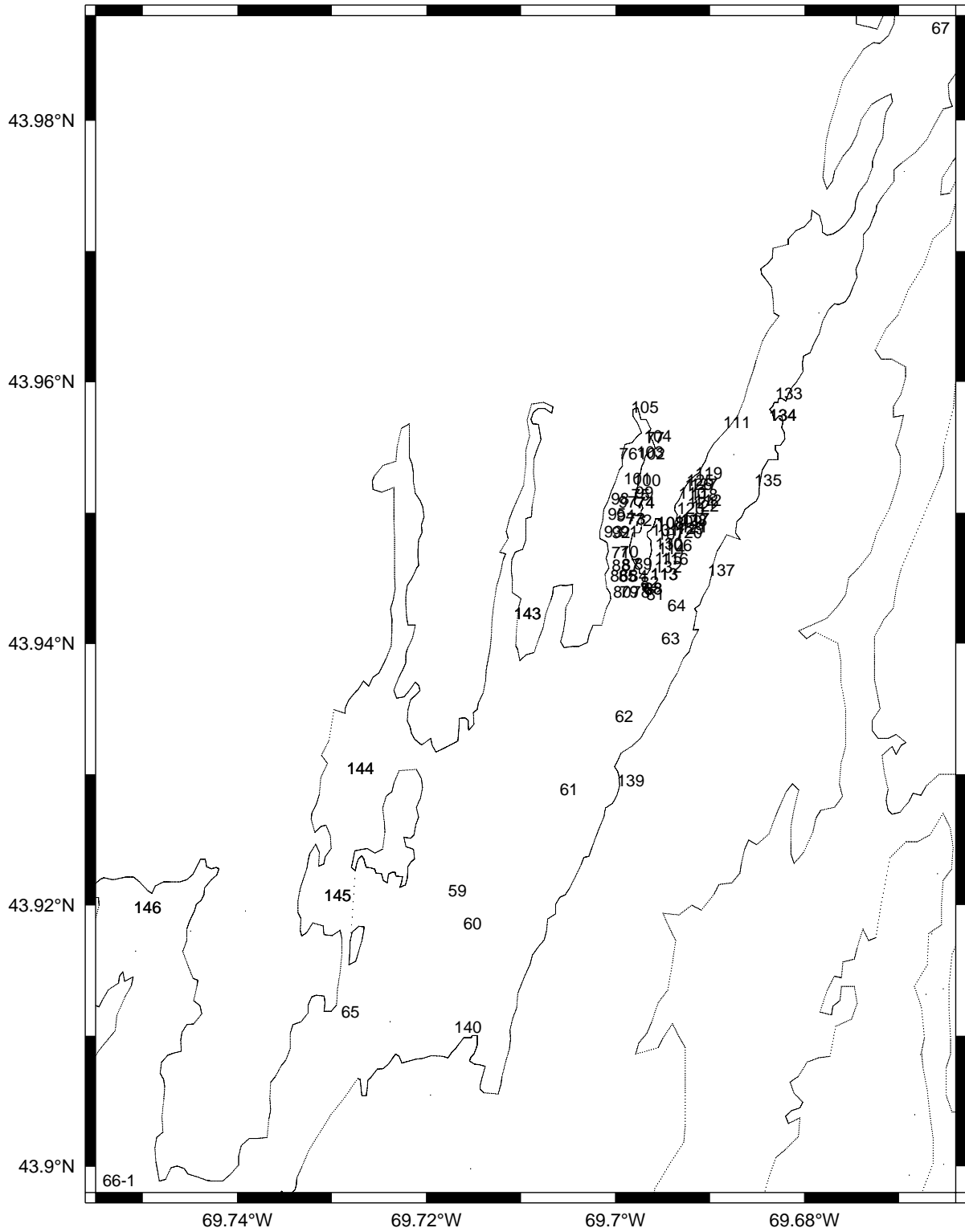


Figure 5-3. 2-5 Aug 2004 Station Locations

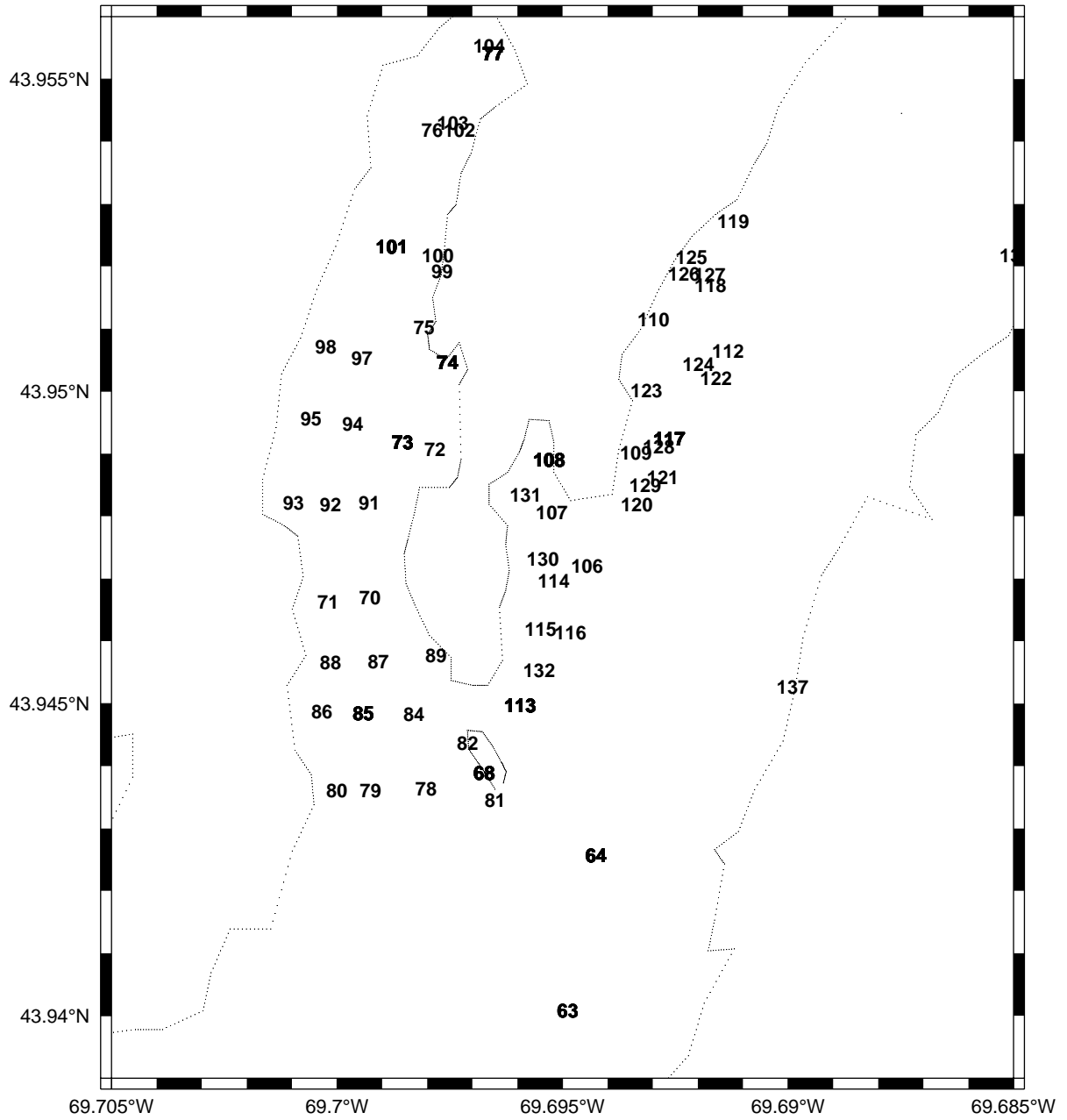


Figure 5-4. 2-5 Aug 2004 Station Locations - Close to Plant

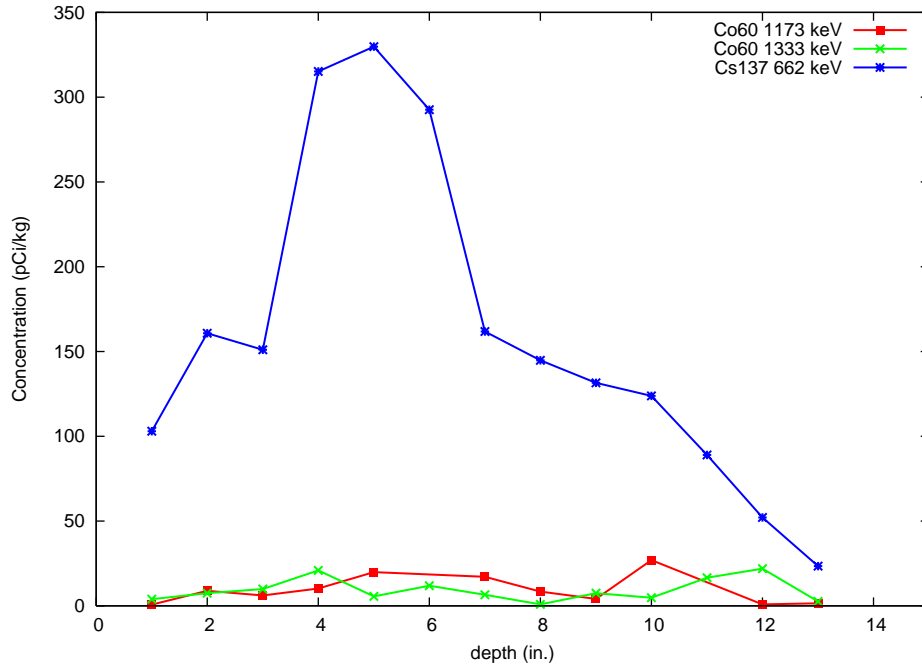


Figure 5-5. Station Sasanoa core: ^{60}Co and ^{137}Cs vs. depth

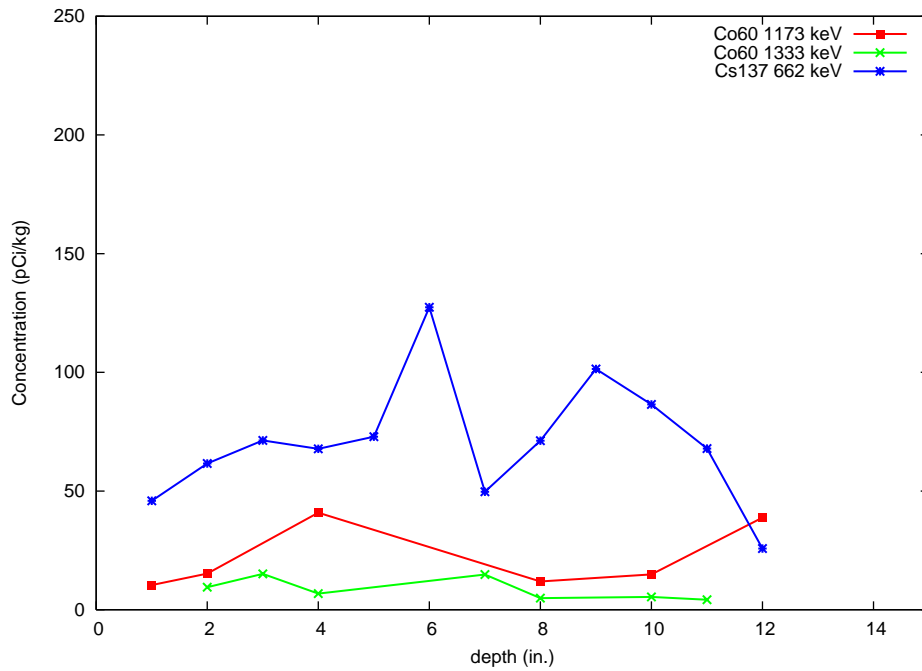


Figure 5-6. Station Pottle Cove core: ^{60}Co and ^{137}Cs vs. depth

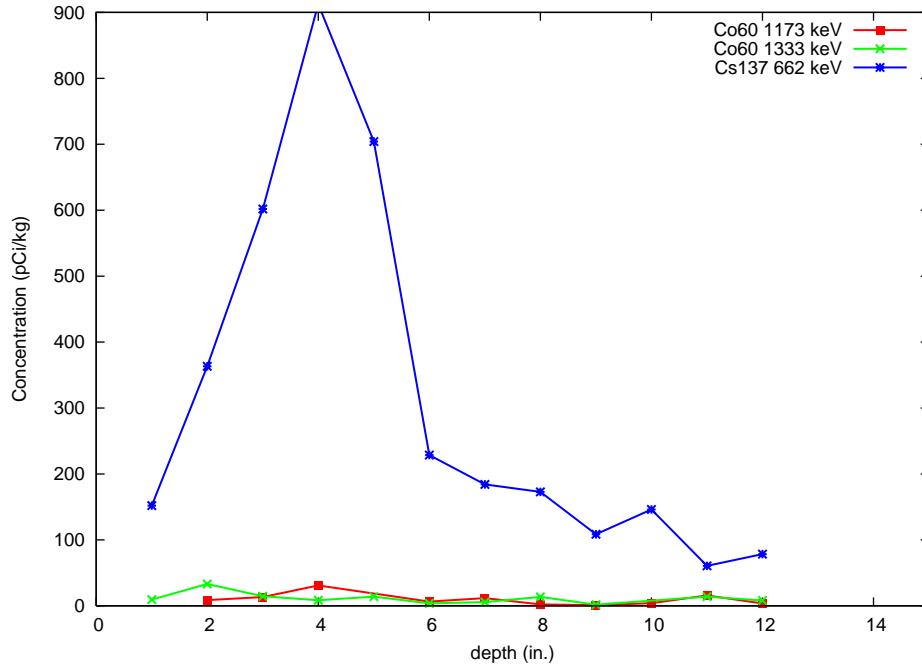


Figure 5-7. Station Long Creek core: ⁶⁰Co and ¹³⁷Cs vs. depth

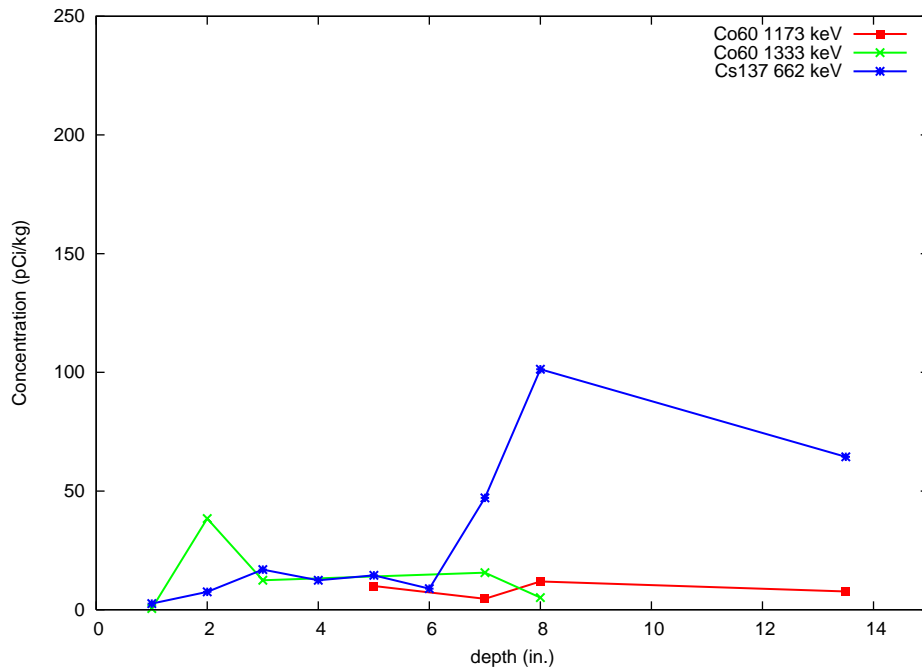


Figure 5-8. Station Barry Cove core: ⁶⁰Co and ¹³⁷Cs vs. depth

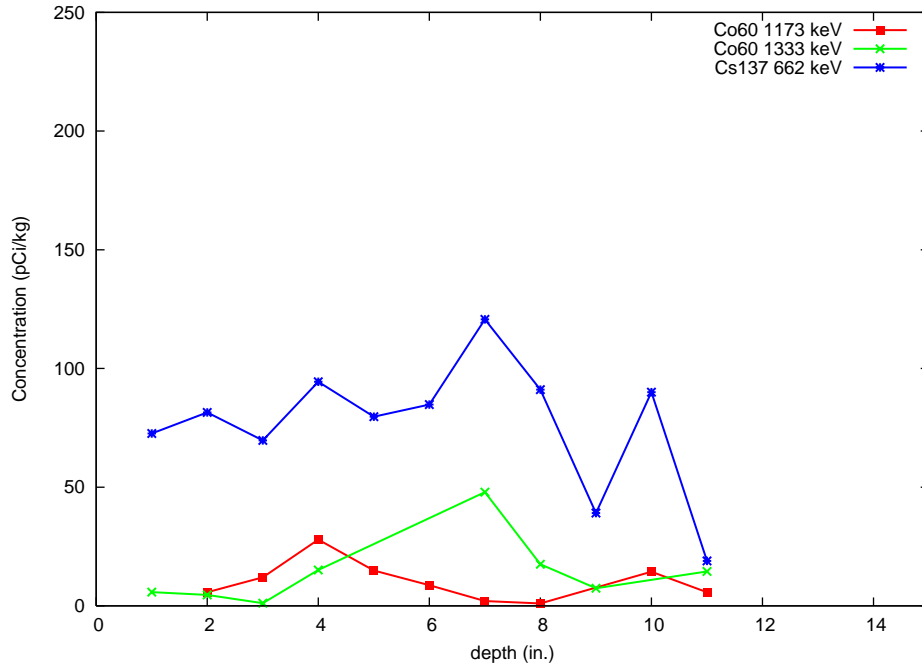


Figure 5-9. Station Wiscasset core: ^{60}Co and ^{137}Cs vs. depth

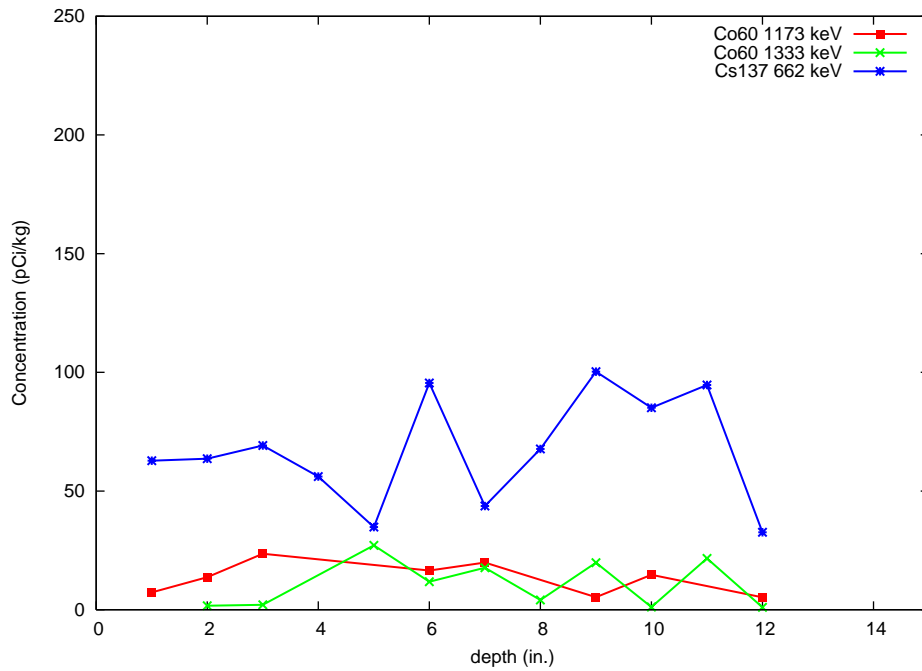


Figure 5-10. Station Eddy core: ^{60}Co and ^{137}Cs vs. depth

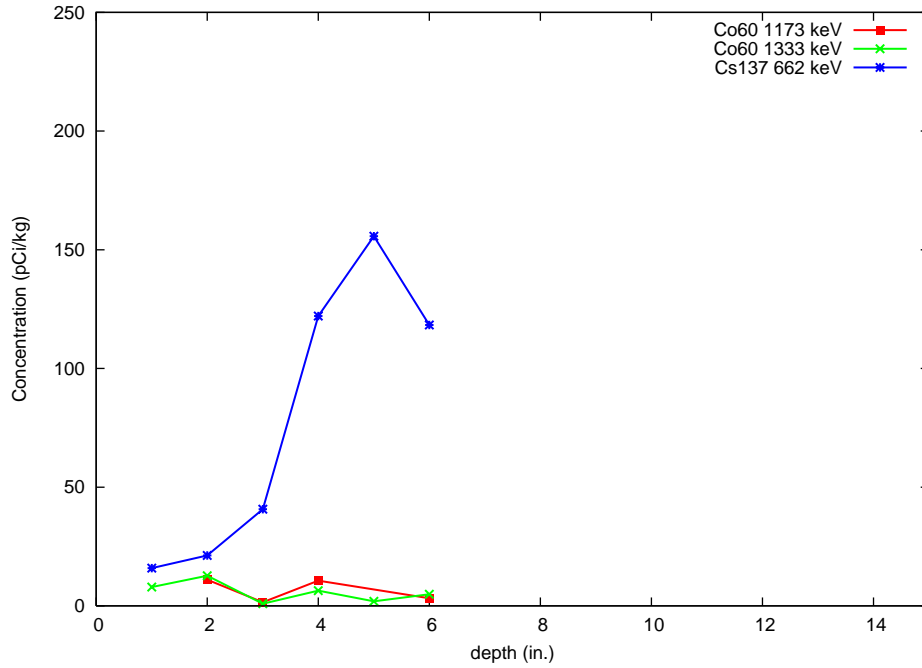


Figure 5-11. Station Chewonki Camp core: ^{60}Co and ^{137}Cs vs. depth

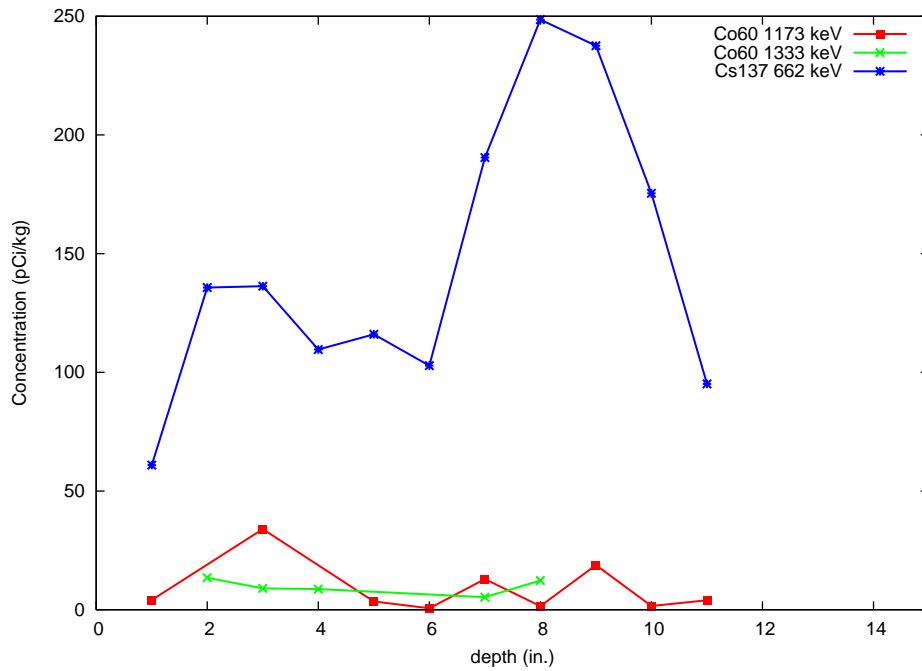


Figure 5-12. Station 2 core: ^{60}Co and ^{137}Cs vs. depth

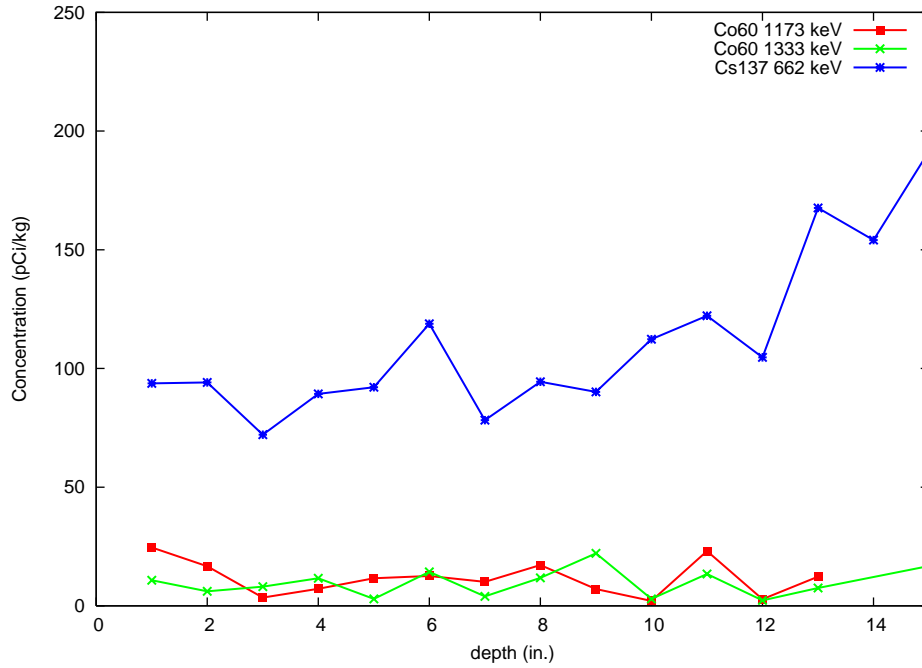


Figure 5-13. Station 8-1 core: ^{60}Co and ^{137}Cs vs. depth

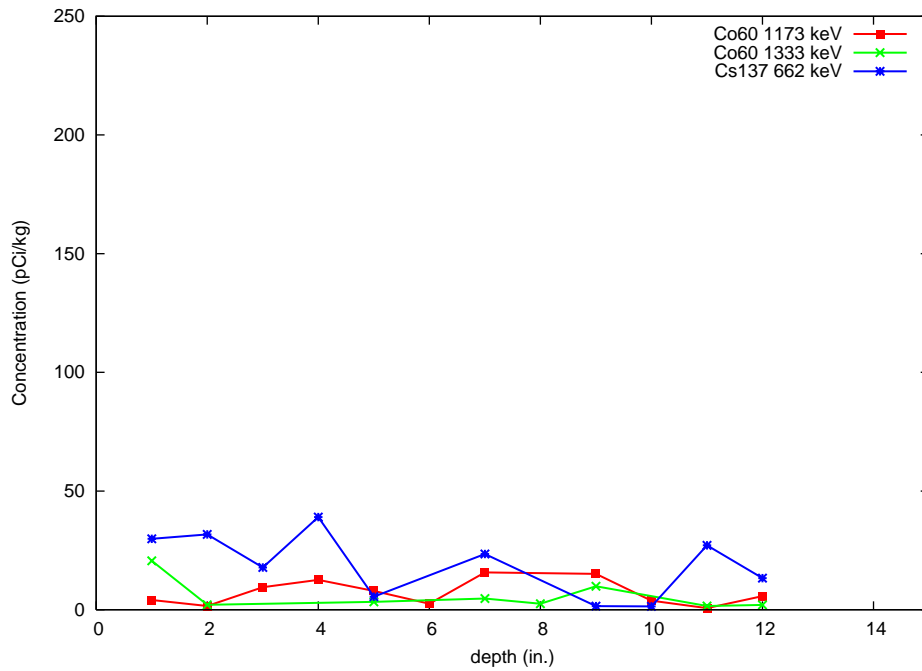


Figure 5-14. Station 25 core: ^{60}Co and ^{137}Cs vs. depth

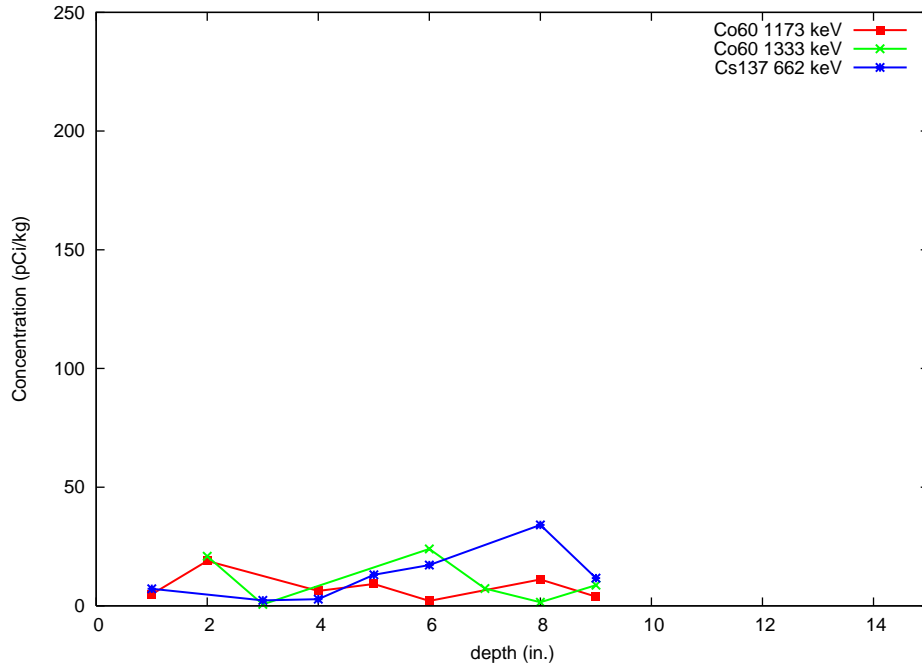


Figure 5-15. Station 34, Diffuser, core: ^{60}Co and ^{137}Cs vs. depth

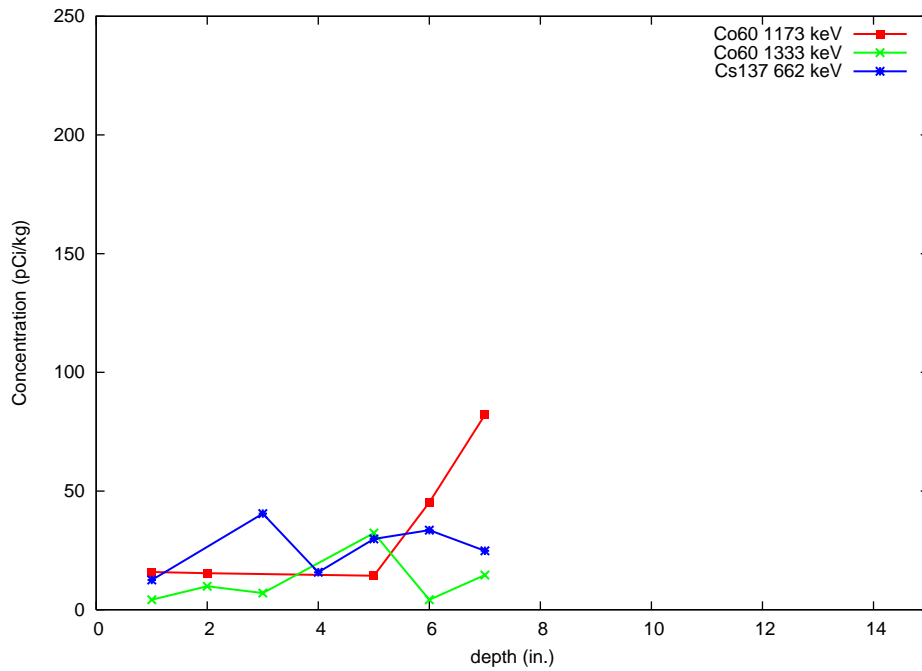


Figure 5-16. Station 38, Westport Island, core: ^{60}Co and ^{137}Cs vs. depth

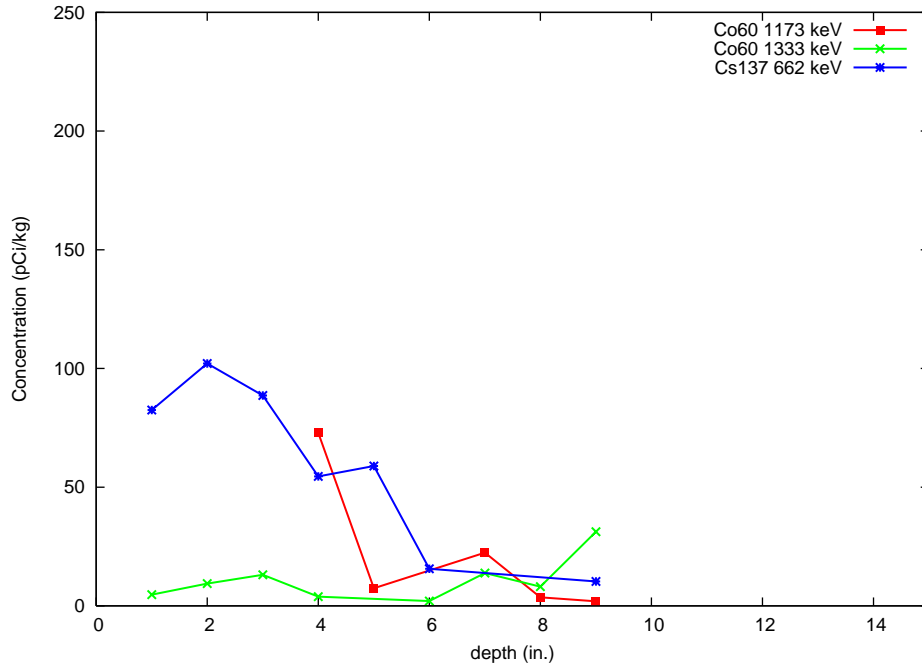


Figure 5-17. Station 44, Eaton Farm Point, core: ^{60}Co and ^{137}Cs vs. depth

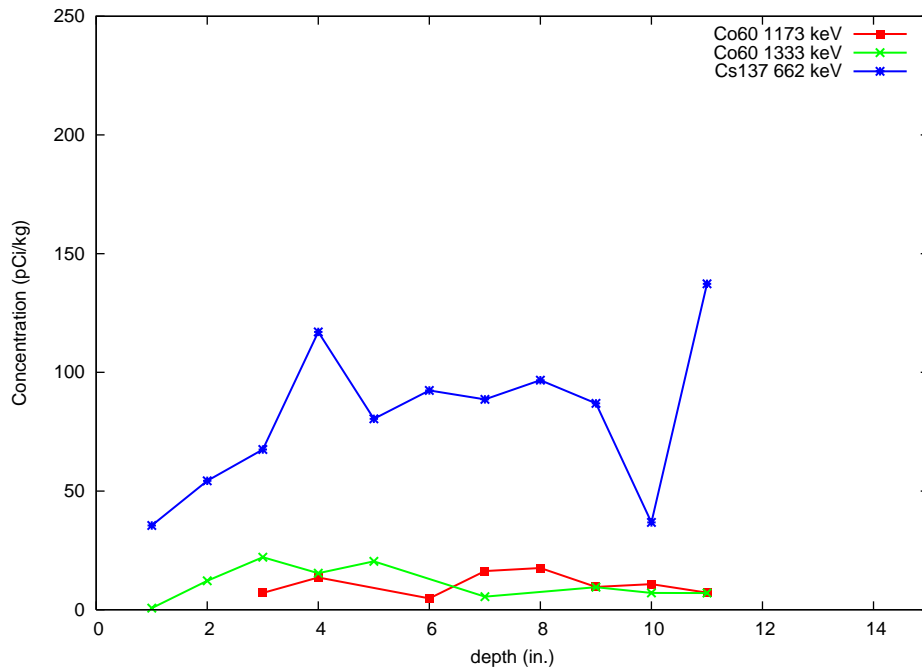


Figure 5-18. Station 50, Pottle Cove, core: ^{60}Co and ^{137}Cs vs. depth

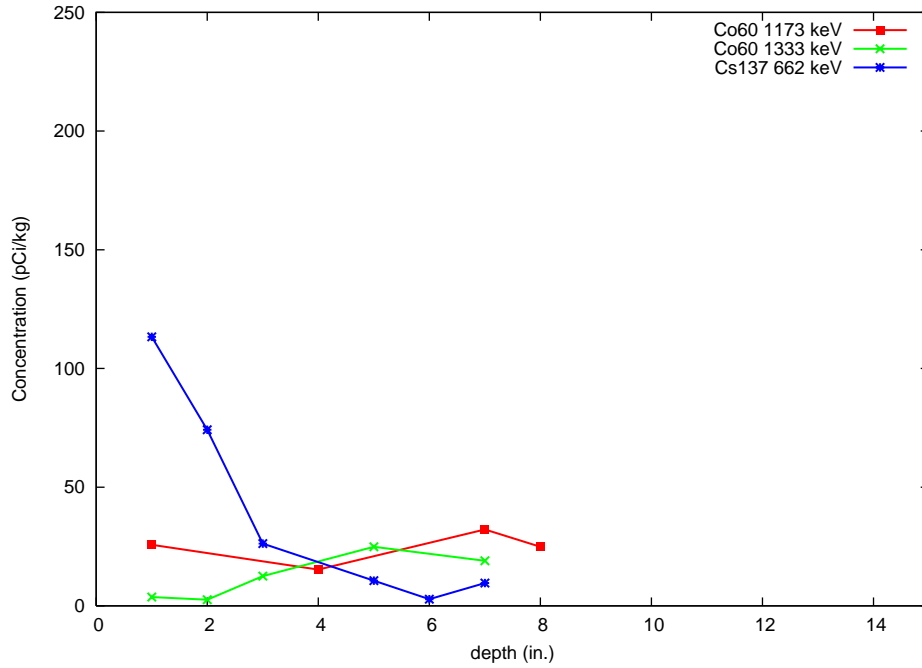


Figure 5-19. Station 59, South Oak Island, core: ⁶⁰Co and ¹³⁷Cs vs. depth

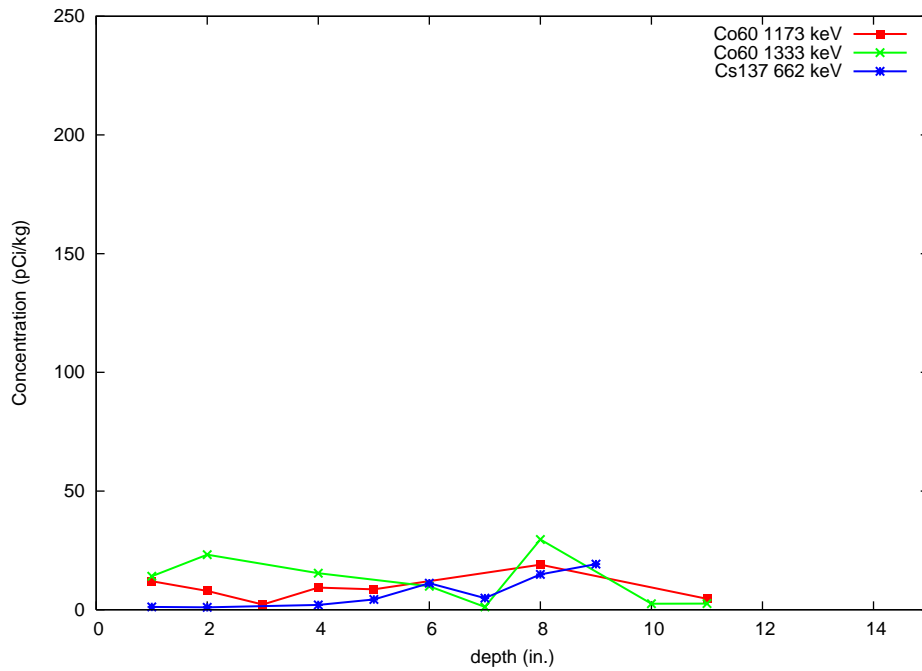


Figure 5-20. Station 60, South Oak Island, core: ⁶⁰Co and ¹³⁷Cs vs. depth

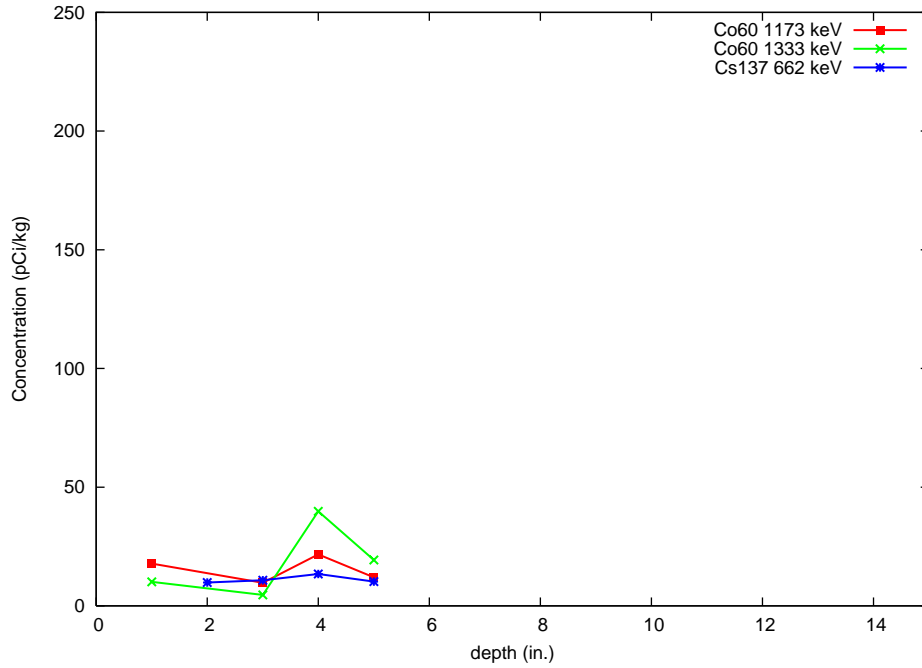


Figure 5-21. Station 61, Westport Island, core: ^{60}Co and ^{137}Cs vs. depth

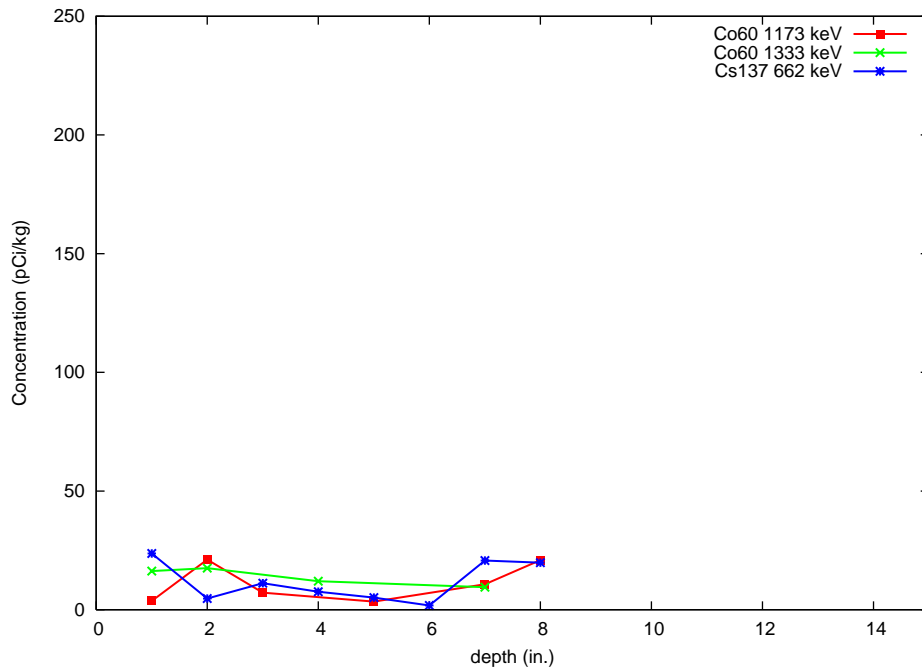


Figure 5-22. Station 62, Westport Island, core: ^{60}Co and ^{137}Cs vs. depth

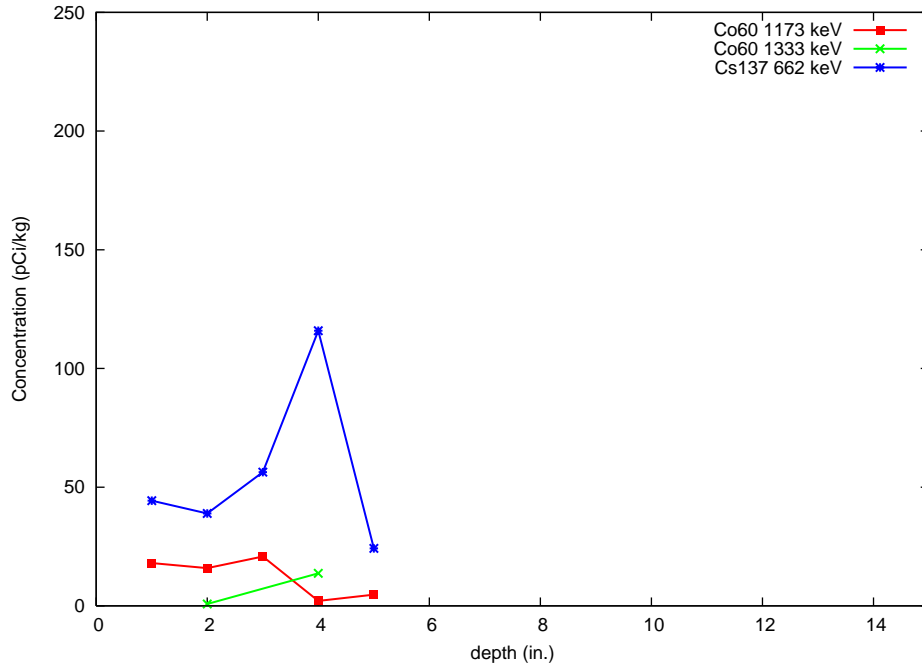


Figure 5-23. Station 63, Long Ledge, core: ⁶⁰Co and ¹³⁷Cs vs. depth

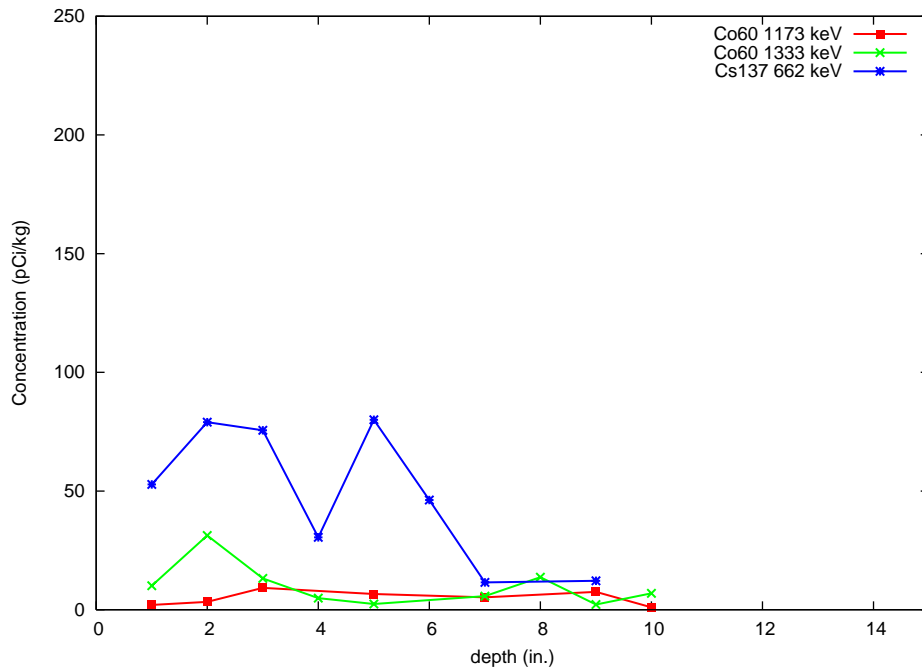


Figure 5-24. Station 64, Long Ledge, core: ⁶⁰Co and ¹³⁷Cs vs. depth

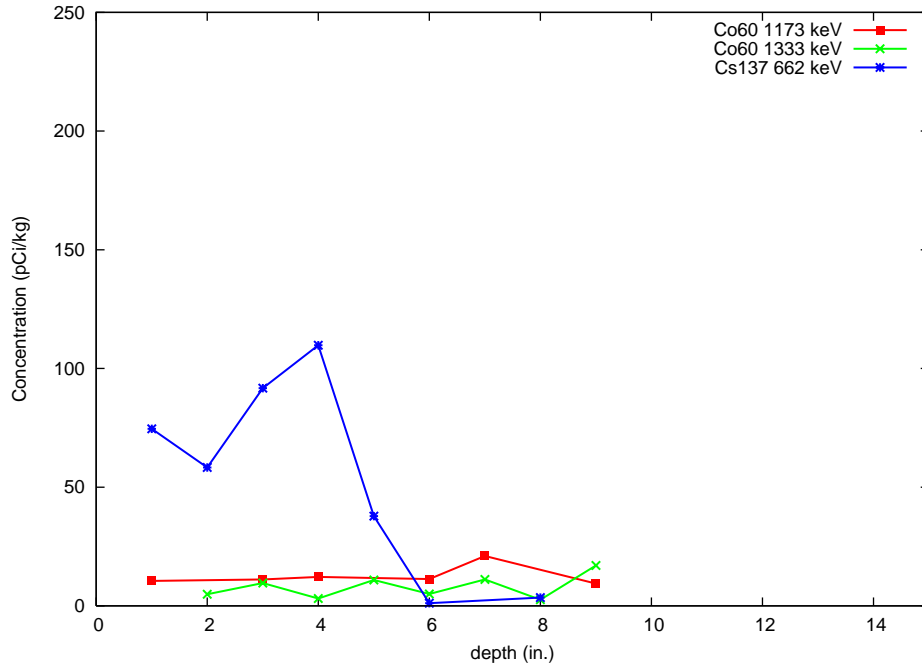


Figure 5-25. Station 65, Bluff Head, core: ⁶⁰Co and ¹³⁷Cs vs. depth

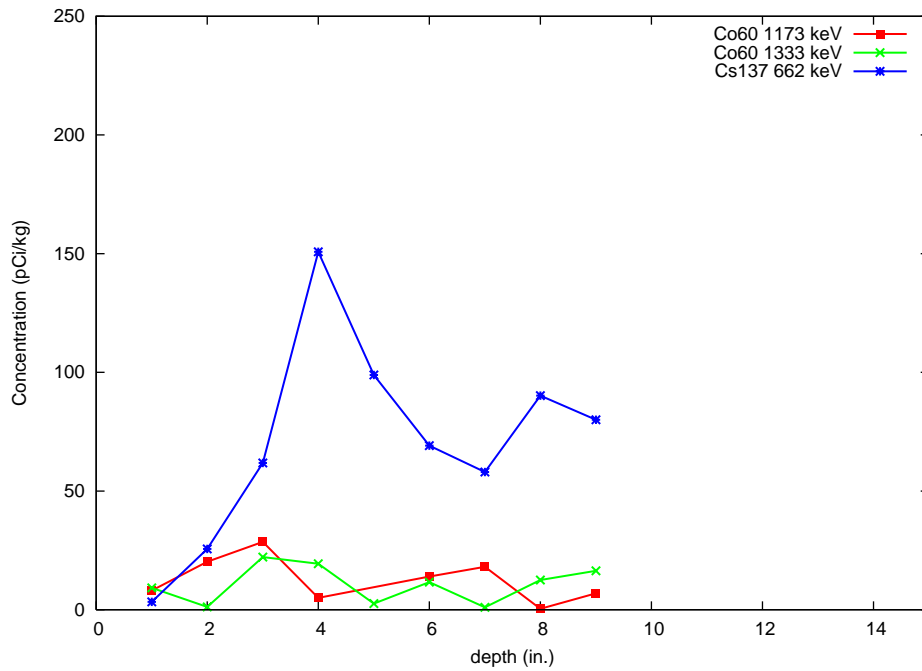


Figure 5-26. Station 66-1 core: ⁶⁰Co and ¹³⁷Cs vs. depth

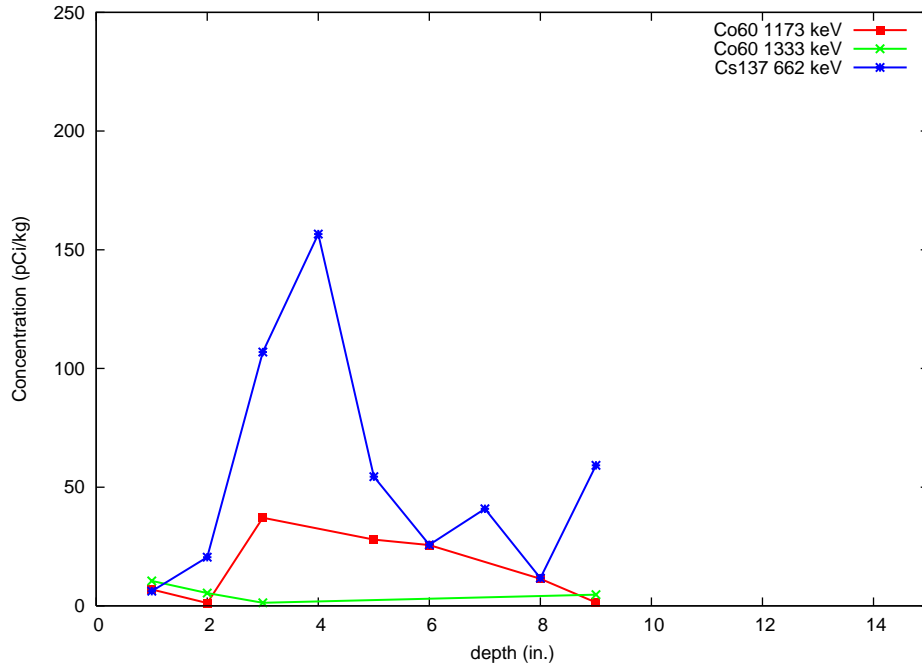


Figure 5-27. Station 67, Cushman Cove, core: ^{60}Co and ^{137}Cs vs. depth

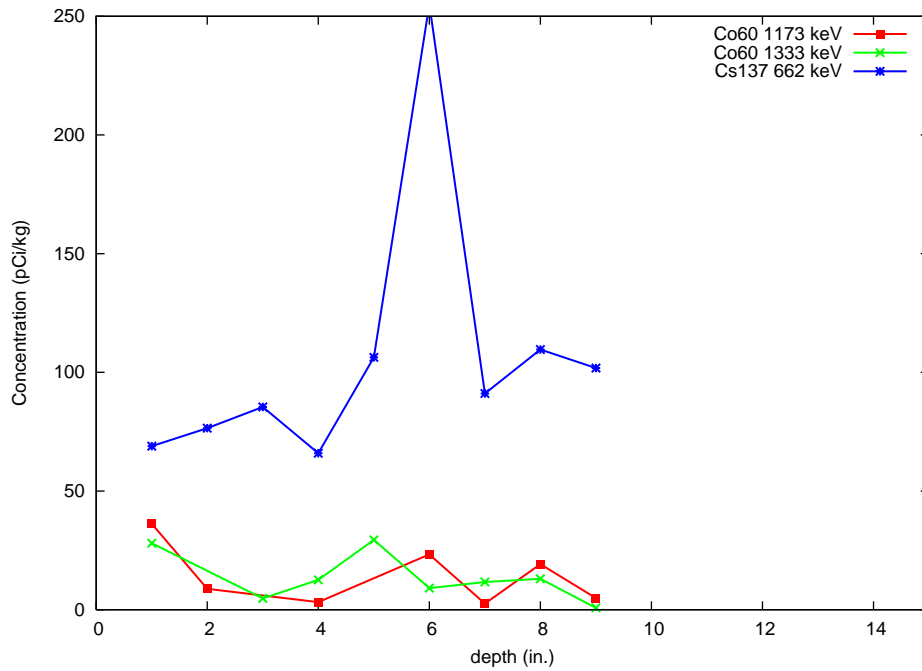


Figure 5-28. Station 68, Foxbird Island, core: ^{60}Co and ^{137}Cs vs. depth

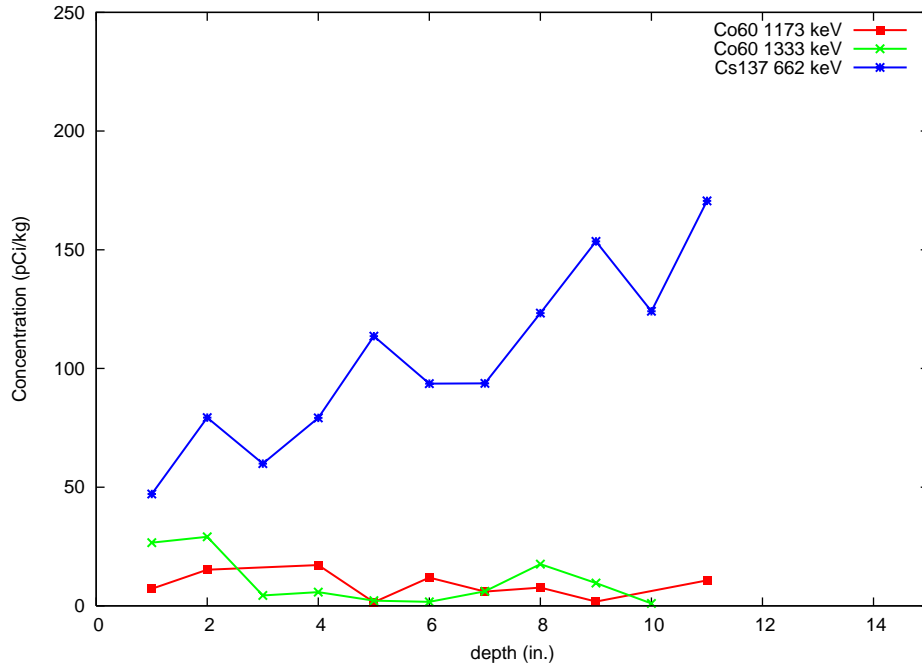


Figure 5-29. Station 73, Bailey Cove Outfall, core: ⁶⁰Co and ¹³⁷Cs vs. depth

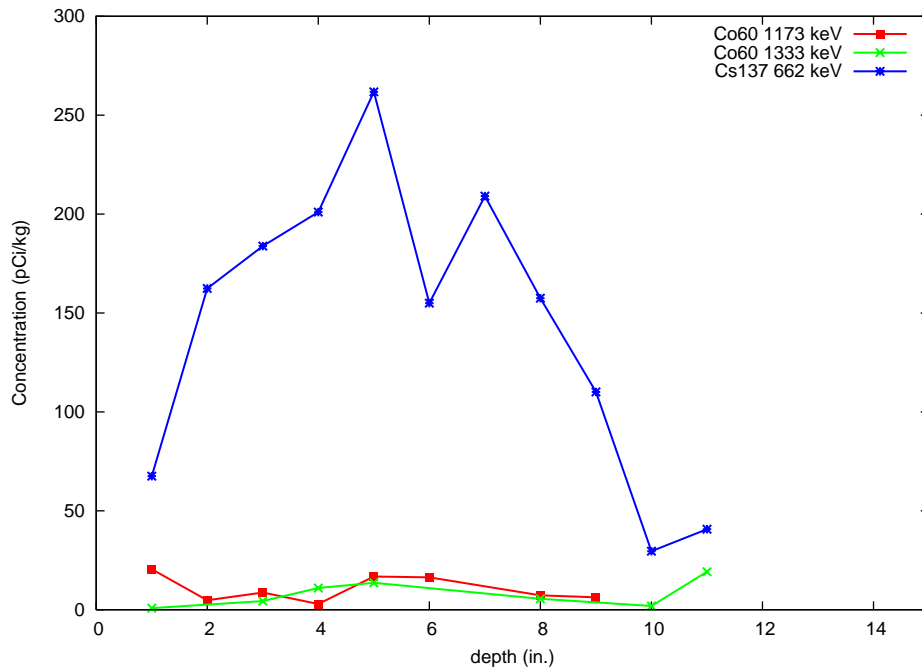


Figure 5-30. Station 74, Bailey Cove Outfall, core: ⁶⁰Co and ¹³⁷Cs vs. depth

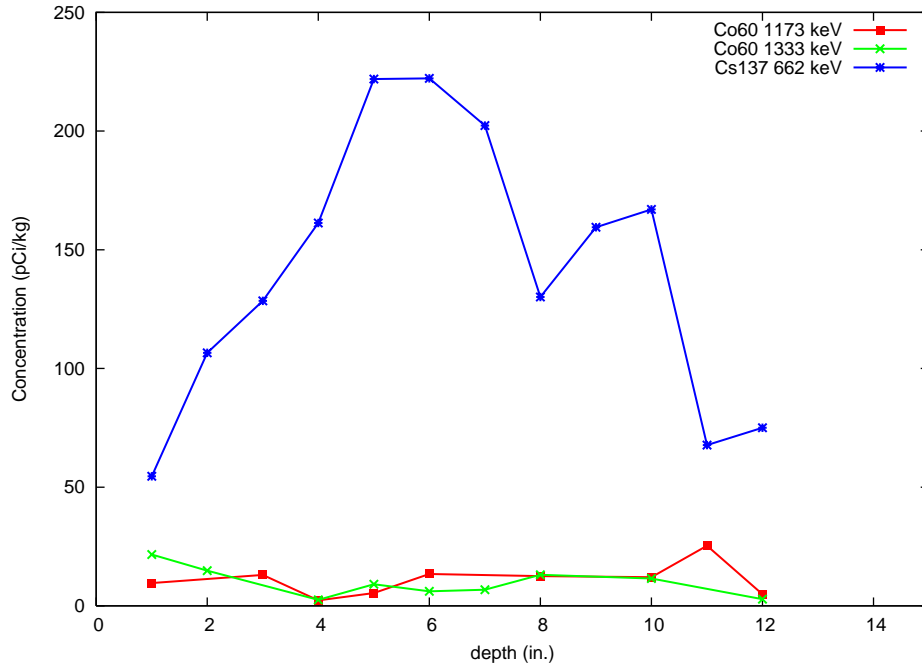


Figure 5-31. Station 77, Upper Bailey Cove, core: ⁶⁰Co and ¹³⁷Cs vs. depth

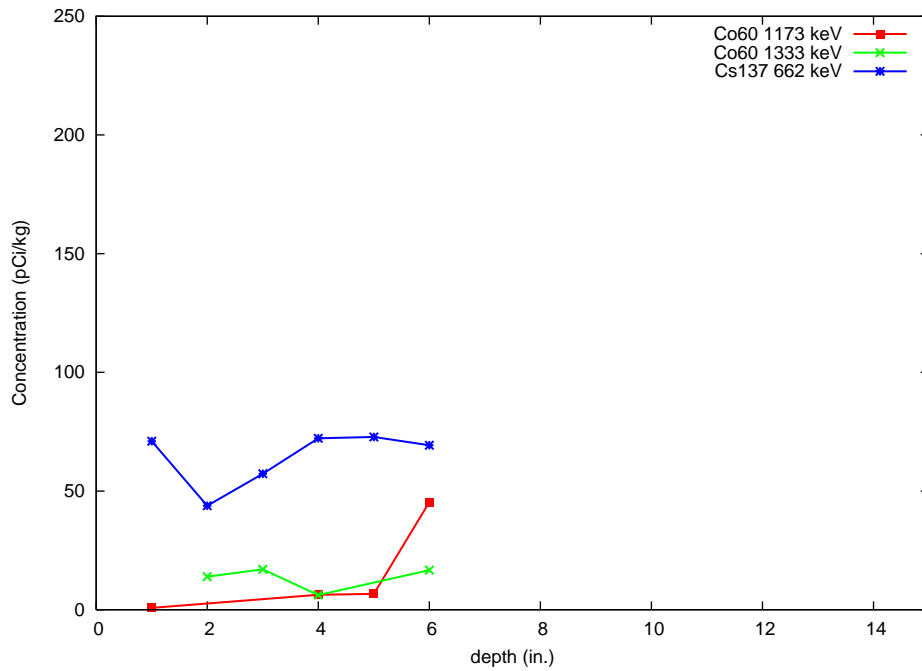


Figure 5-32. Station 85, South Bailey Cove, core: ⁶⁰Co and ¹³⁷Cs vs. depth

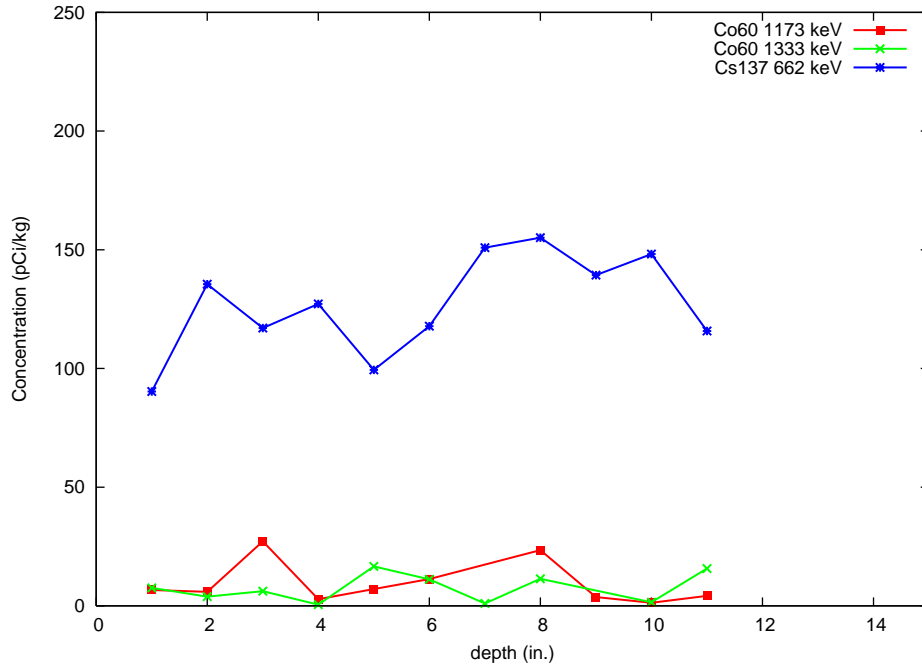


Figure 5-33. Station 99, North Bailey Cove, core: ⁶⁰Co and ¹³⁷Cs vs. depth

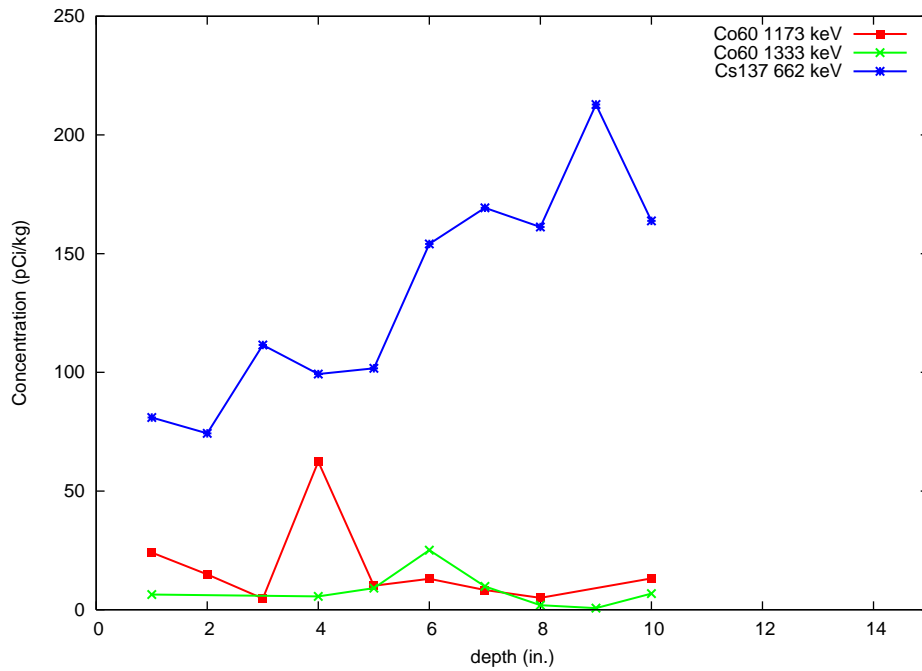


Figure 5-34. Station 101, Eaton Farm Bailey Cove, core: ⁶⁰Co and ¹³⁷Cs vs. depth

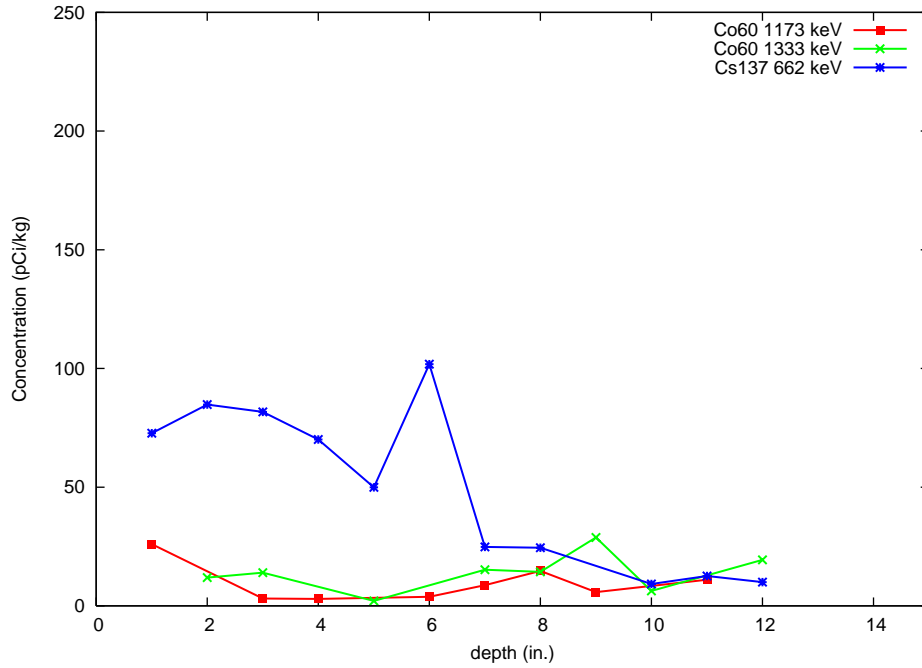


Figure 5-35. Station 105, Top of Bailey Cove, core: ^{60}Co and ^{137}Cs vs. depth

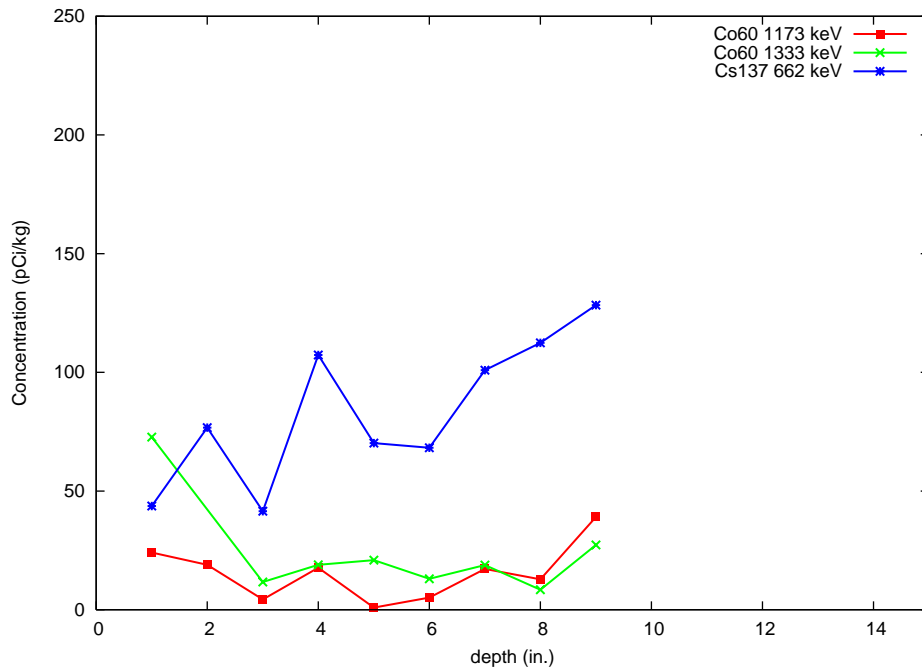


Figure 5-36. Station 108, Bailey Point West, core: ^{60}Co and ^{137}Cs vs. depth

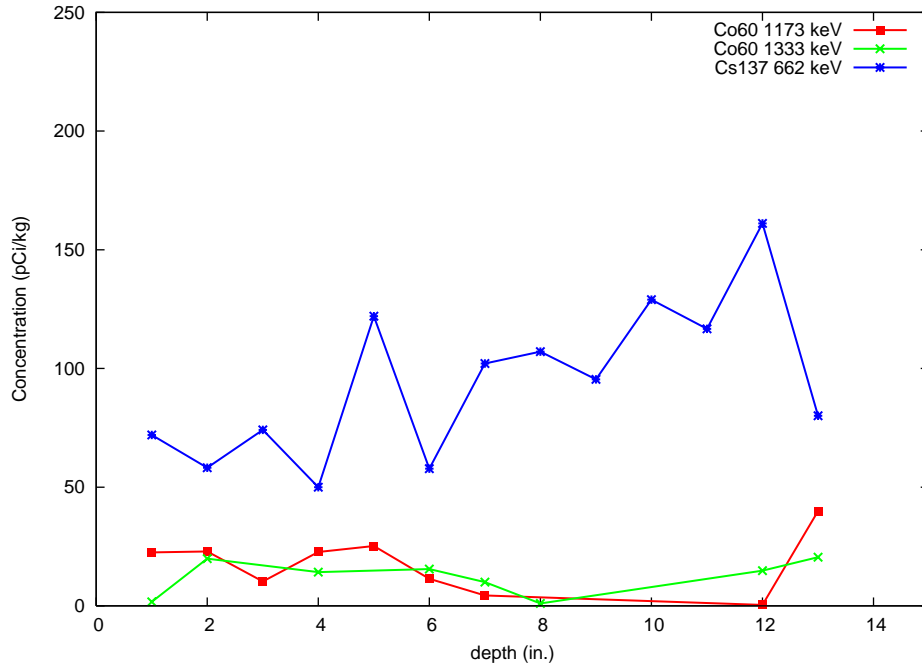


Figure 5-37. Station 113, South Foxbird Island, core: ⁶⁰Co and ¹³⁷Cs vs. depth

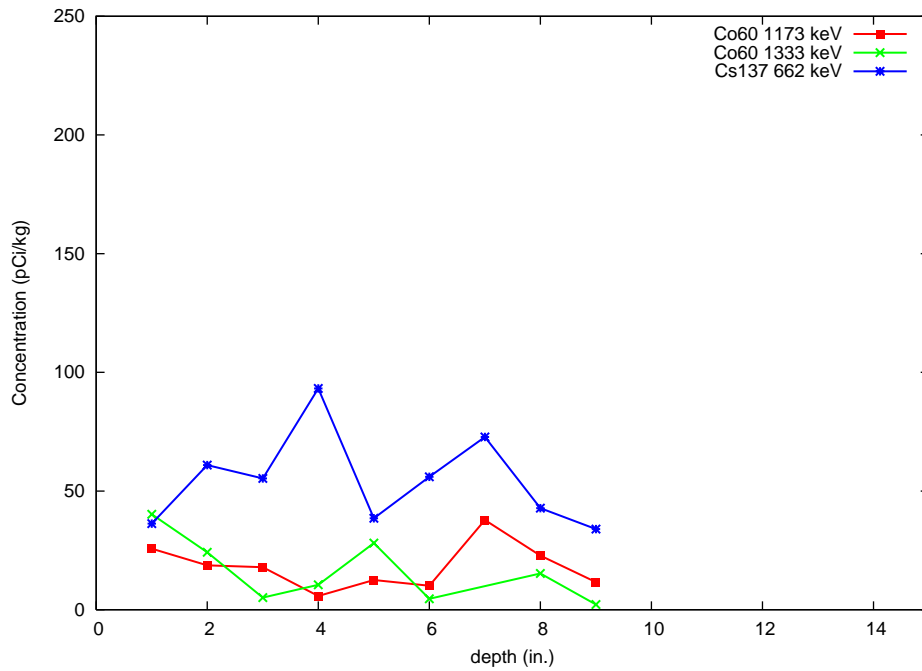


Figure 5-38. Station 117 core: ⁶⁰Co and ¹³⁷Cs vs. depth

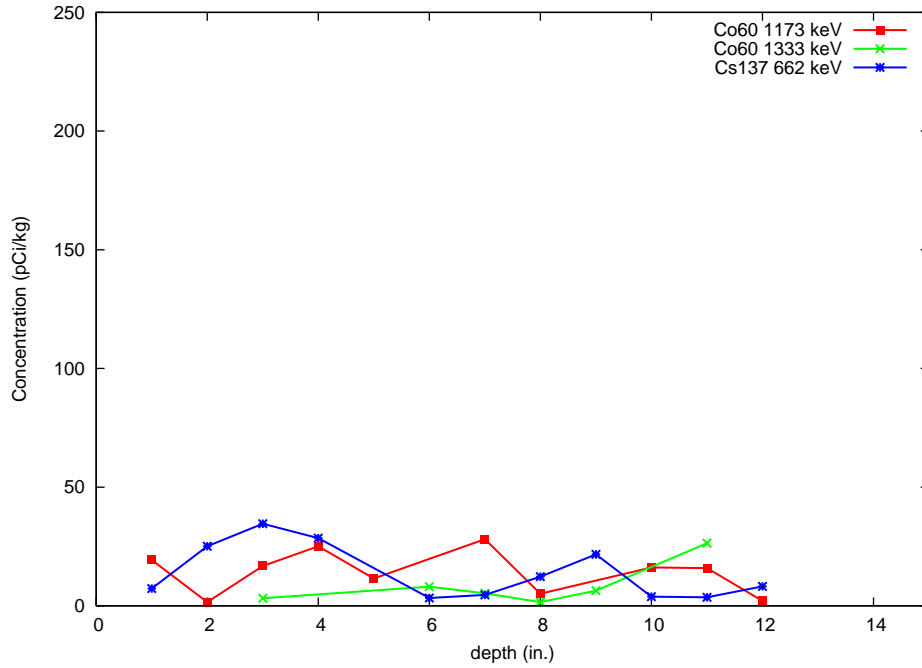


Figure 5-39. Station 118, Little Oak Island, core: ⁶⁰Co and ¹³⁷Cs vs. depth

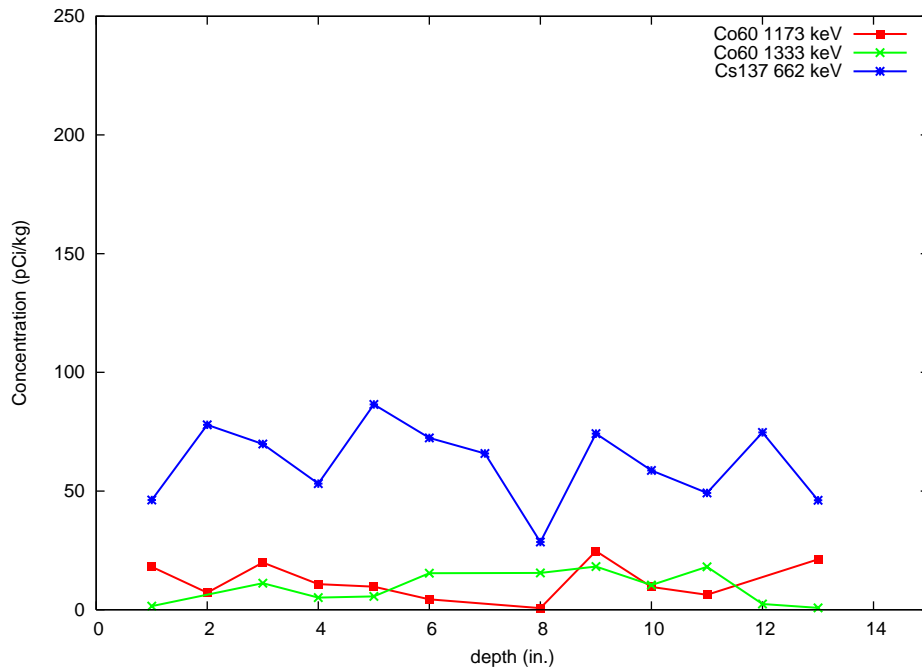


Figure 5-40. Station 134 core: ⁶⁰Co and ¹³⁷Cs vs. depth

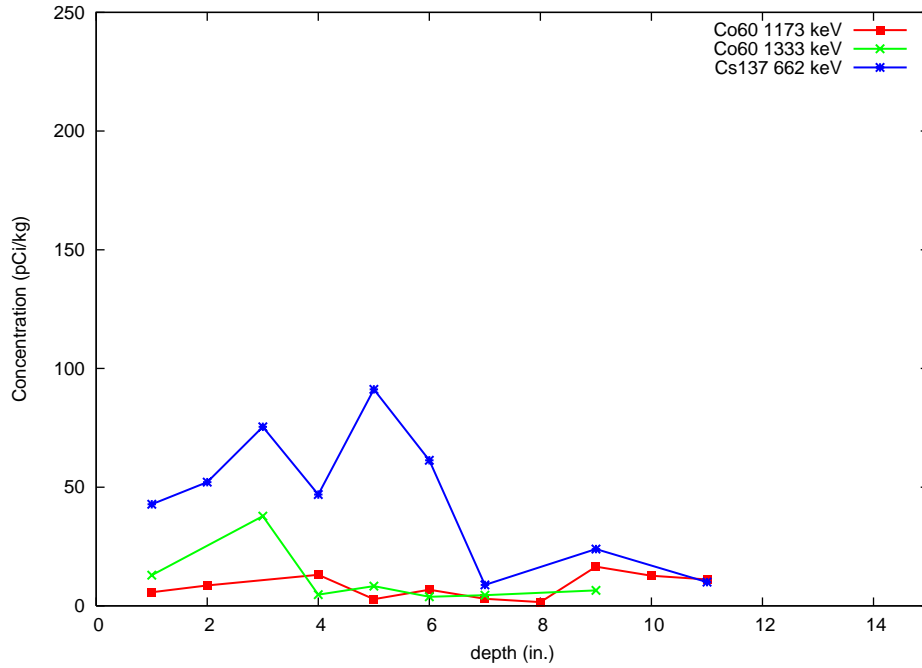


Figure 5-41. Station 143, Youngs Point, core: ^{60}Co and ^{137}Cs vs. depth

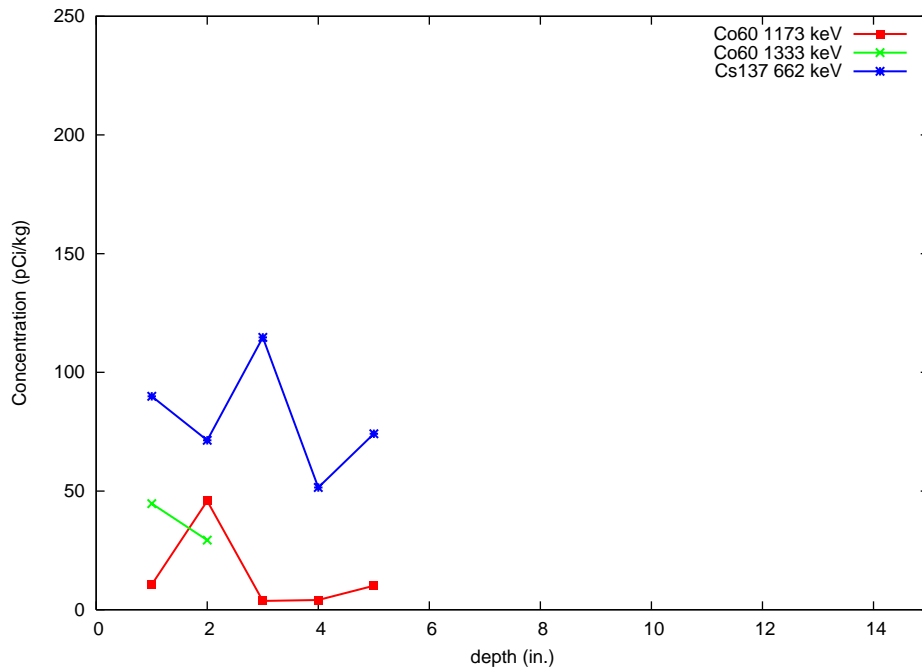


Figure 5-42. Station 144, Oak Island Murphy Corner, core: ^{60}Co and ^{137}Cs vs. depth

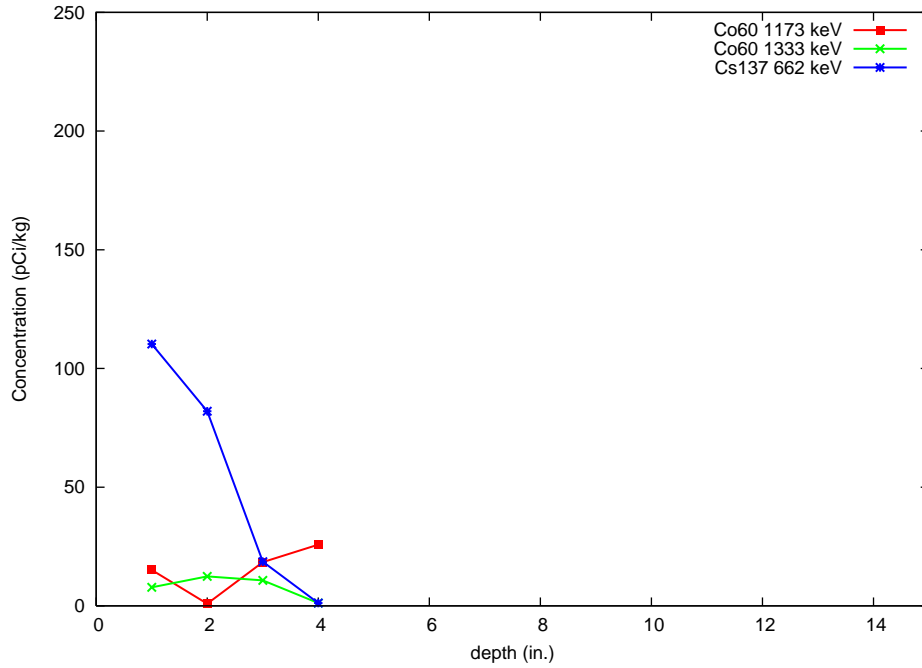


Figure 5-43. Station 145, Oak Island Murphy Corner, core: ^{60}Co and ^{137}Cs vs. depth

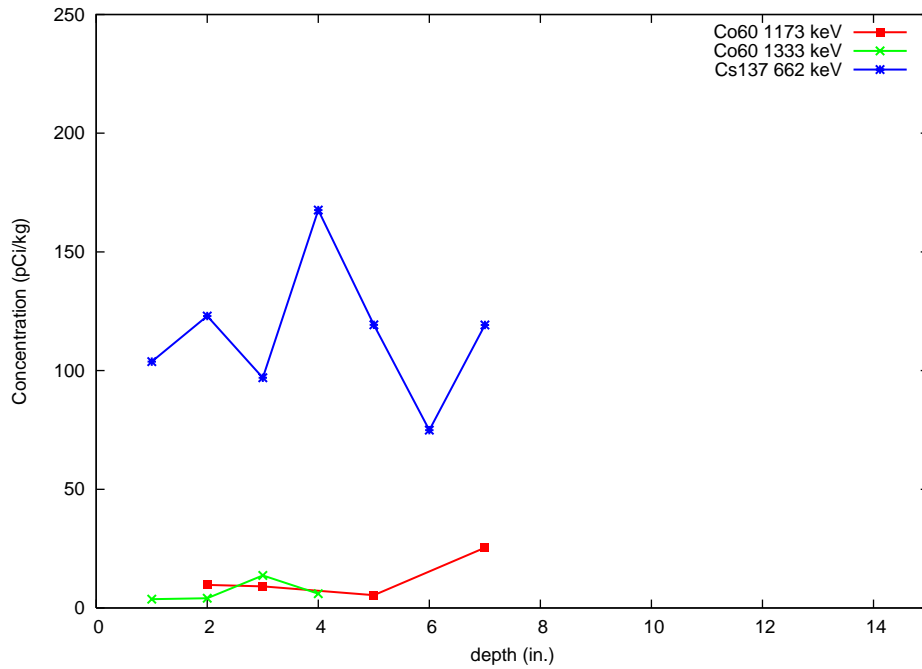


Figure 5-44. Station 146, Darling Center, core: ^{60}Co and ^{137}Cs vs. depth

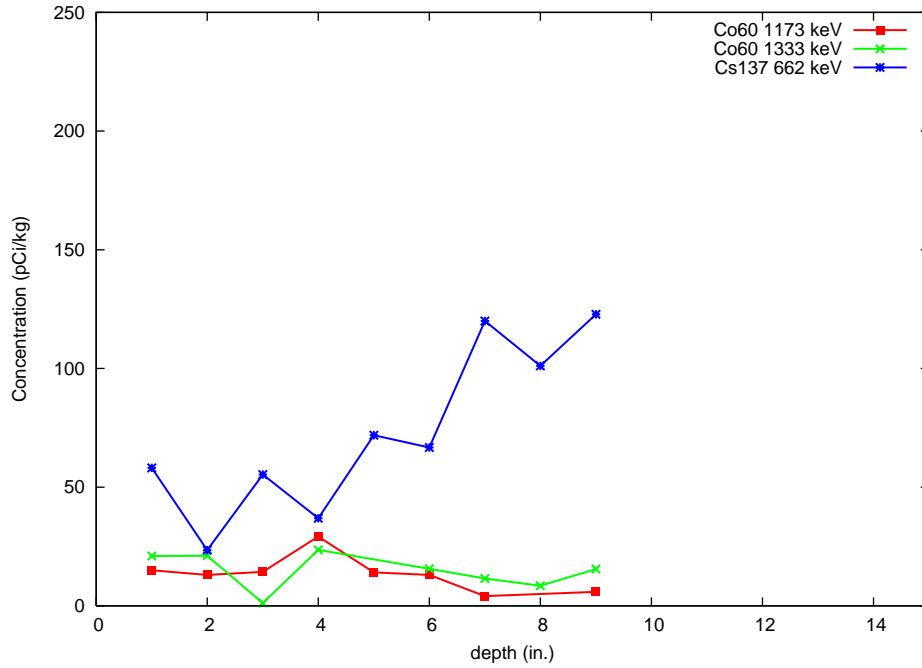


Figure 5-45. Station 147 core: ^{60}Co and ^{137}Cs vs. depth

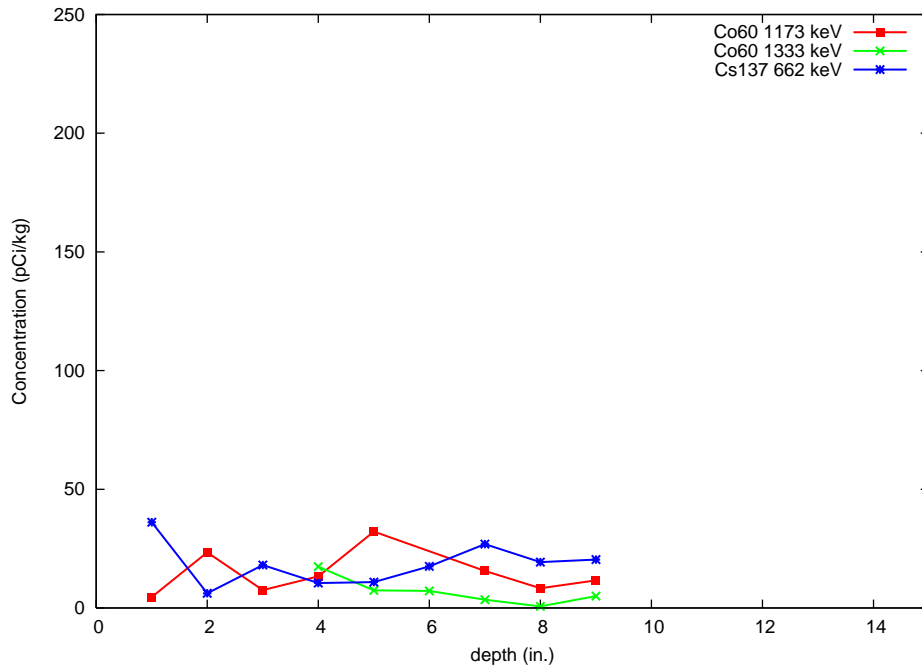


Figure 5-46. Station 148 (Darling Center) core: ^{60}Co and ^{137}Cs vs. depth

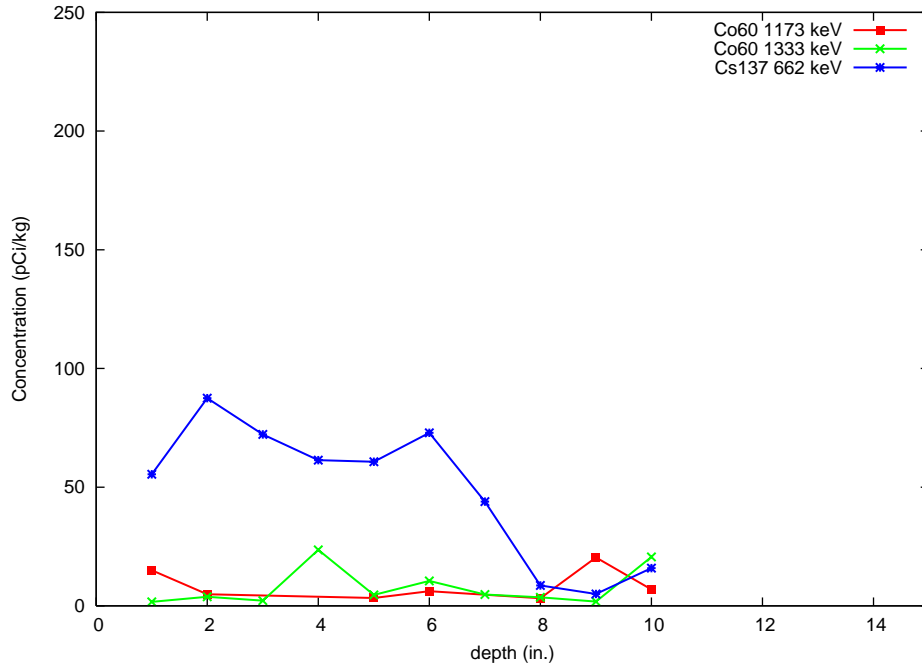


Figure 5-47. Station 149 (Sasanoa) core: ^{60}Co and ^{137}Cs vs. depth

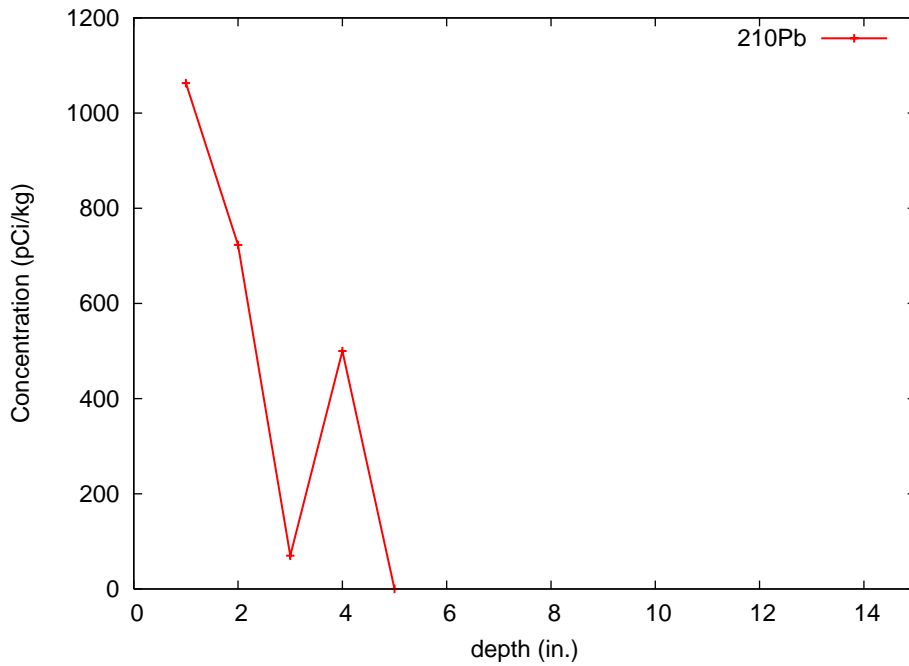


Figure 5-48. Station 144 core: ^{210}Pb vs. depth

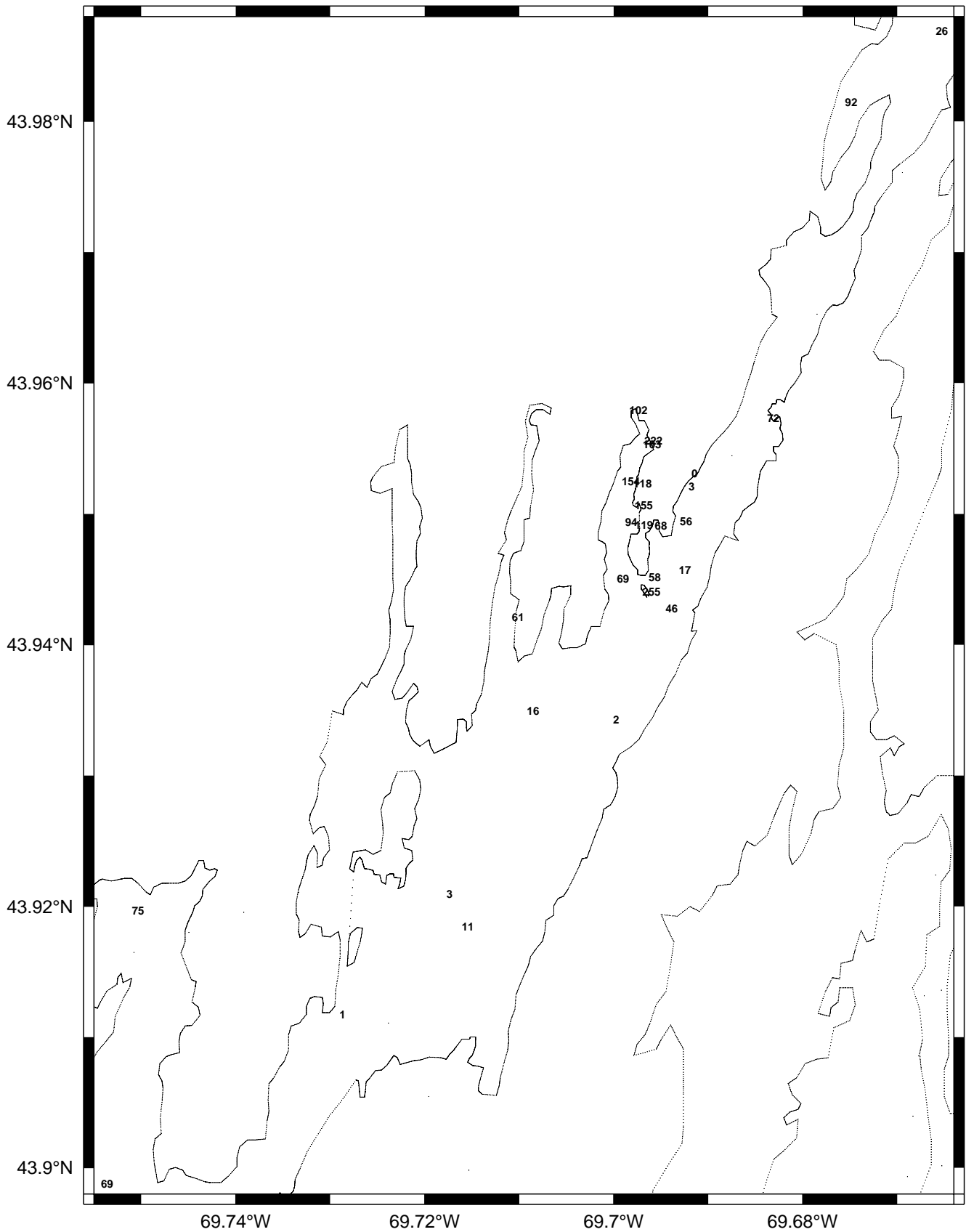


Figure 5-50. ¹³⁷Cs Concentrations at 6 in. (pCi/kg)

Maine Yankee Marine Sampling Study

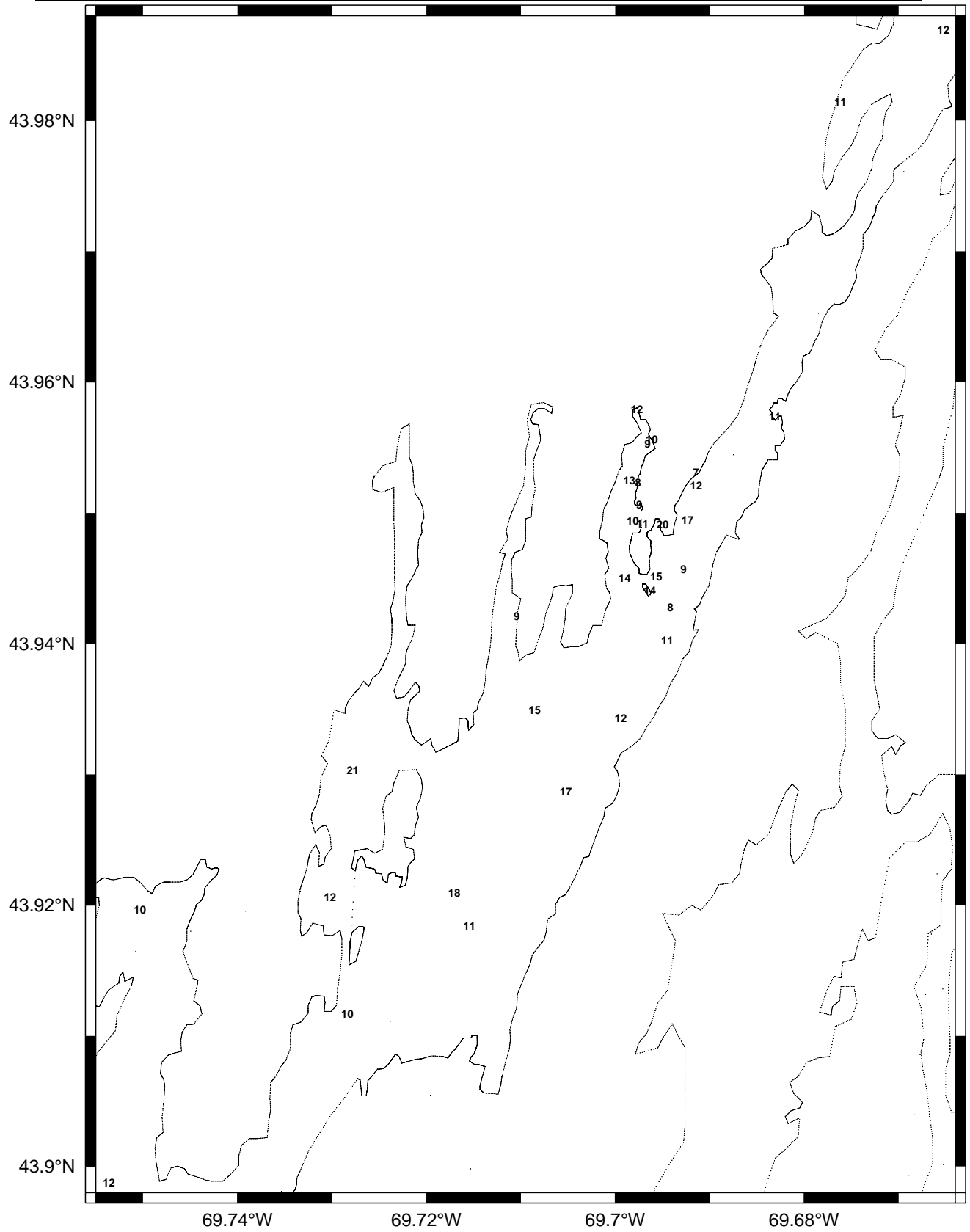


Figure 5-51. ⁶⁰Co Average Core Concentrations (pCi/kg)

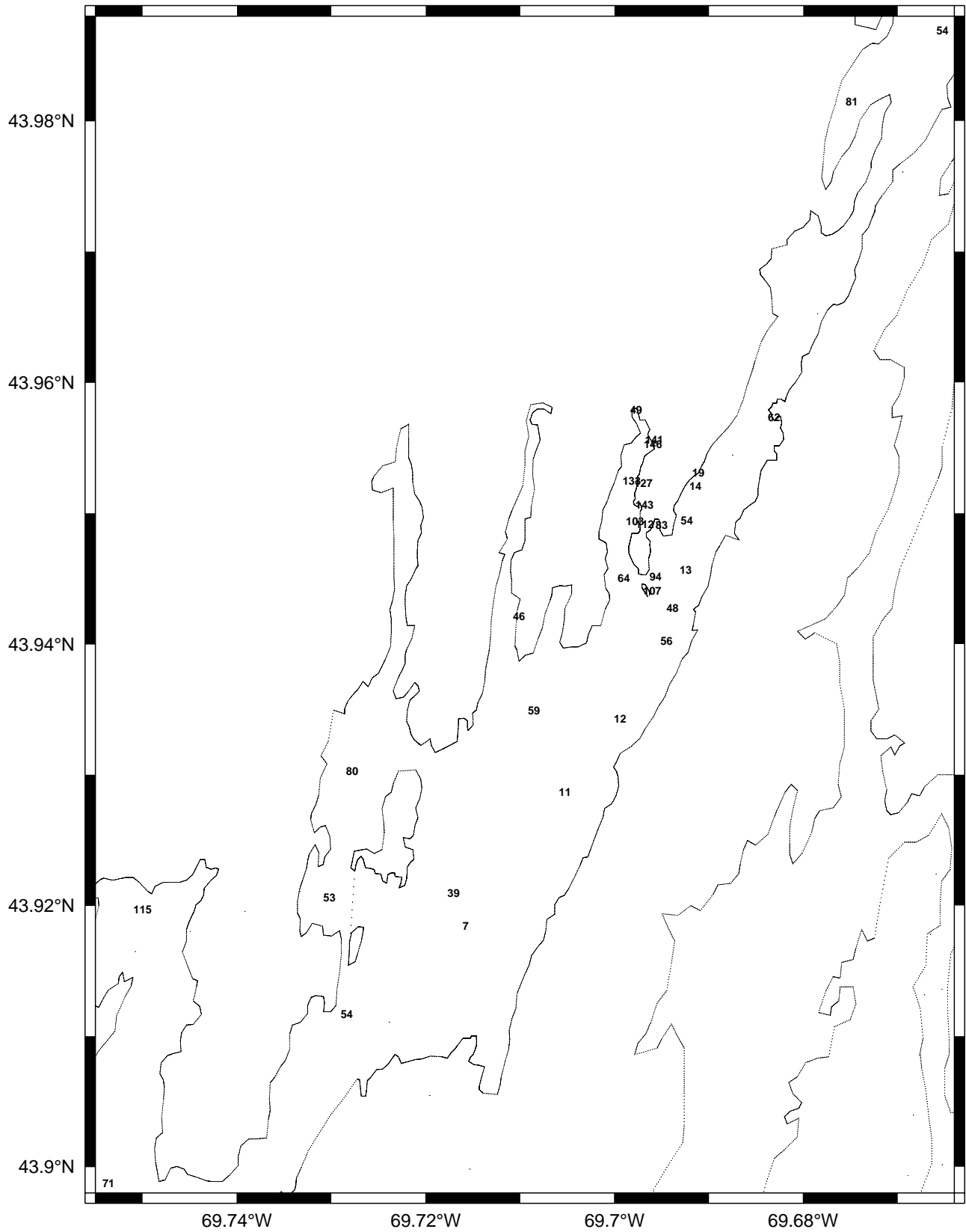


Figure 5-52. ¹³⁷Cs Average Core Concentrations (pCi/kg)

Maine Yankee Marine Sampling Study

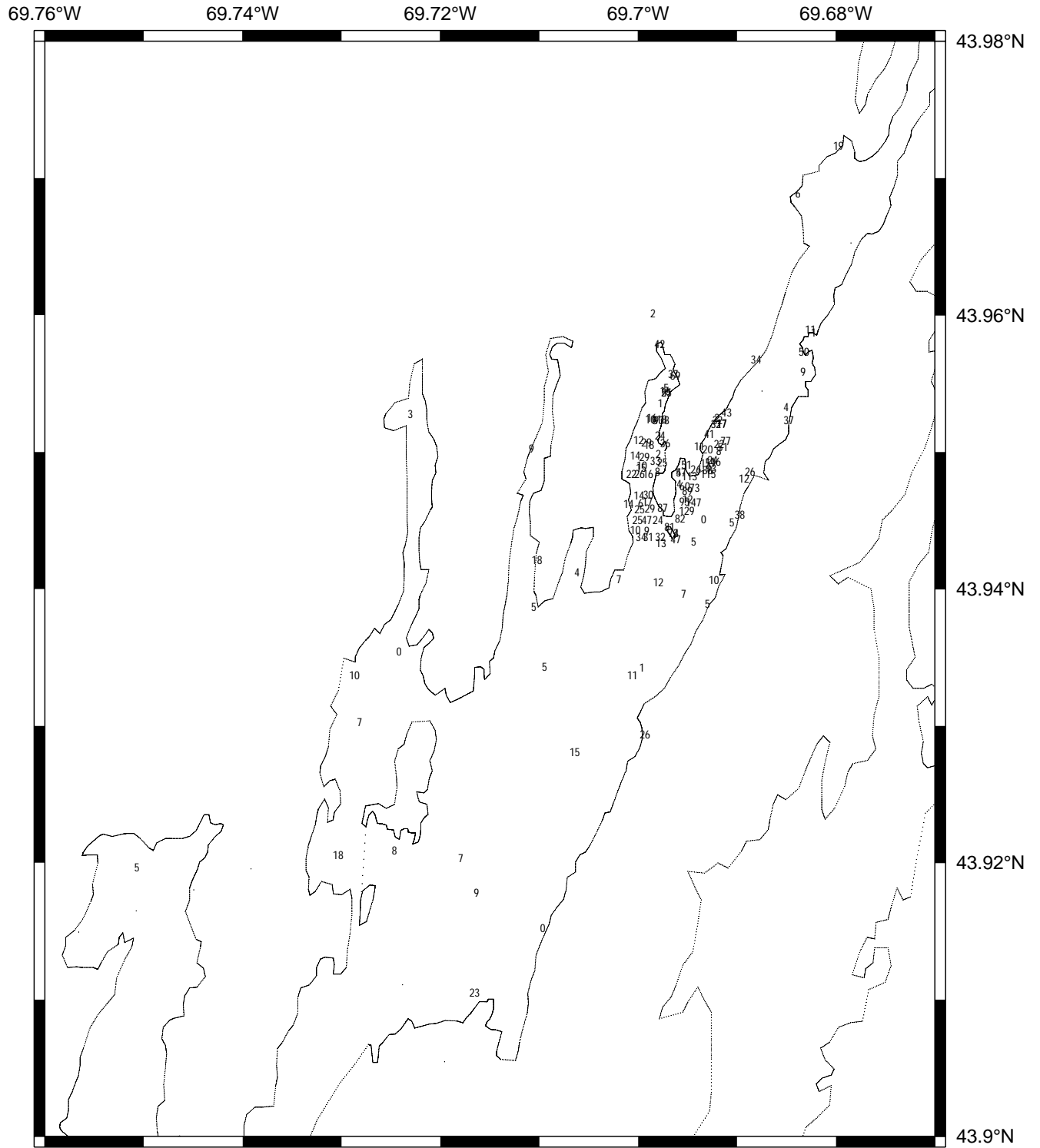


Figure 5-53. ⁶⁰Co Surficial Concentrations (pCi/kg)

Maine Yankee Marine Sampling Study

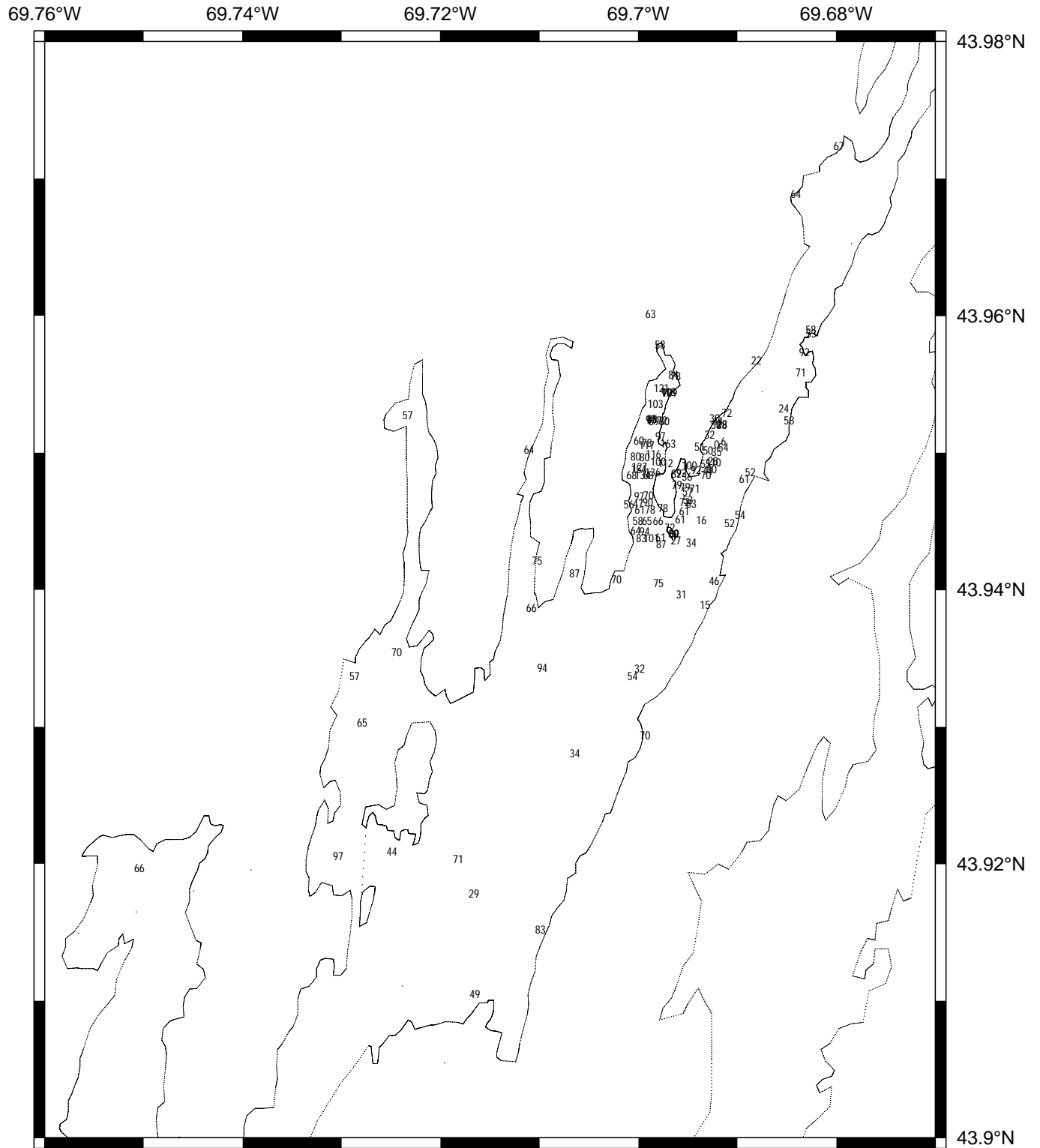


Figure 5-54. ¹³⁷Cs Surficial Concentrations (pCi/kg)

Maine Yankee Marine Sampling Study

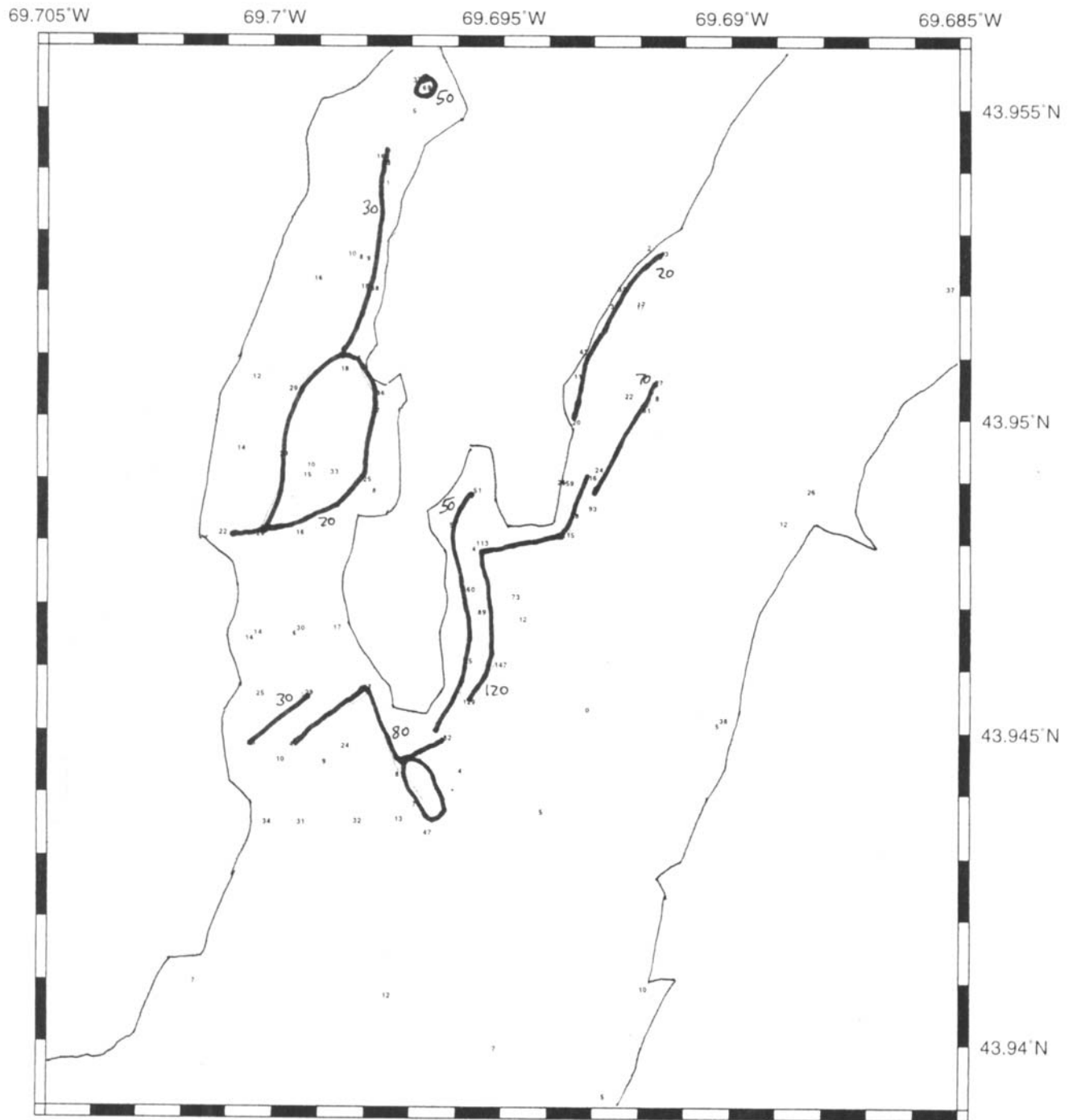


Figure 5-55. ⁶⁰Co Surficial Isocoric Concentrations (pCi/kg) - Close to Plant

Maine Yankee Marine Sampling Study

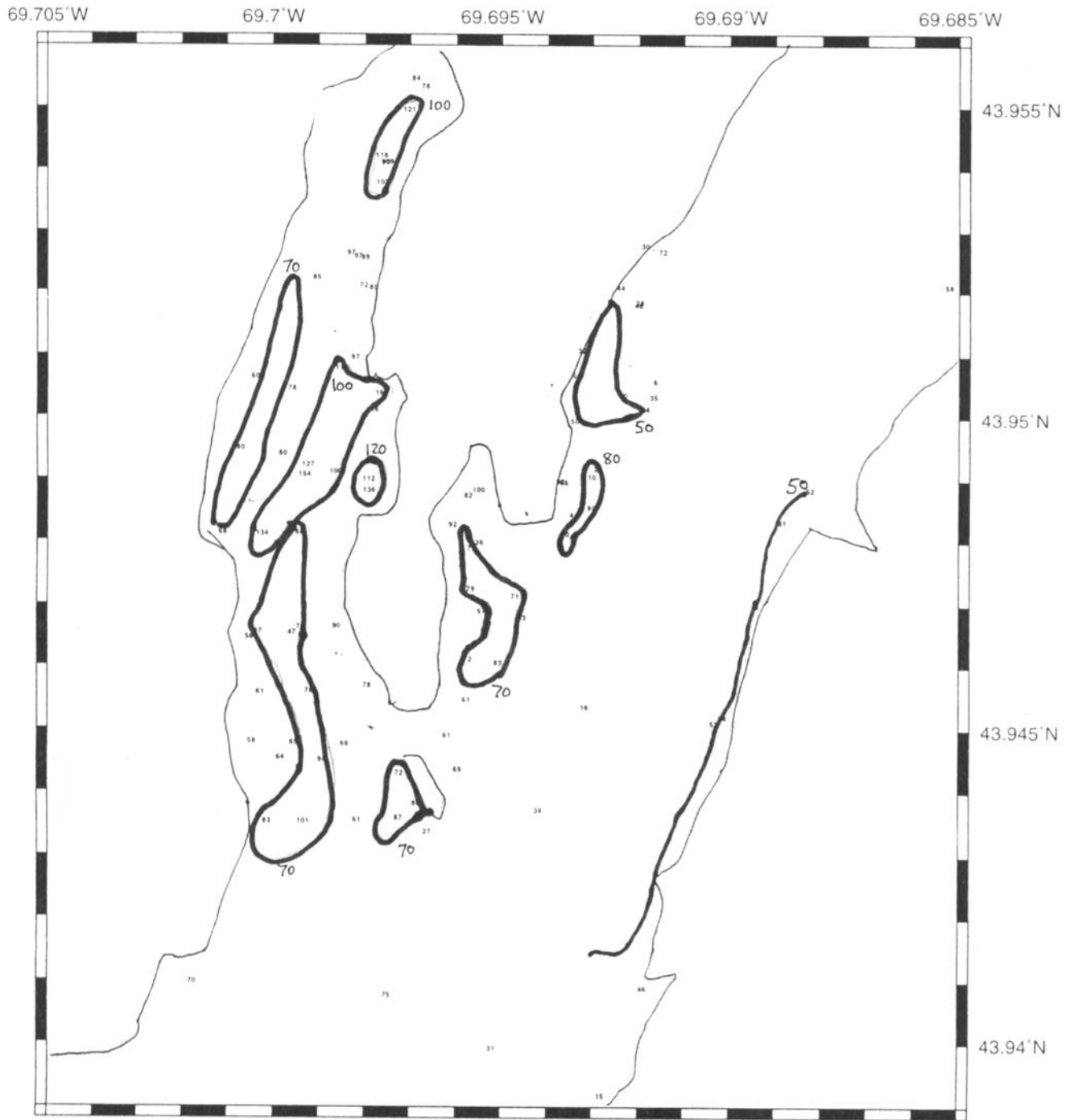


Figure 5-56. ¹³⁷Cs Surficial Isocuric Concentrations (pCi/kg) - Close to Plant

Maine Yankee Marine Sampling Study

Table 5-1. Sediment gamma scan results

sample	mass(g)	depth(in)	station	lat.	long.	60Co		137Cs		65Zn		22Na		54Mn		58Co		133Ba		7Be		210Pb		40K		214Bi		214Pb		212Pb		208Tl					
						pCi/kg	+/-	pCi/kg	+/-	pCi/kg	+/-	pCi/kg	+/-	pCi/kg	+/-	pCi/kg	+/-	pCi/kg	+/-	pCi/kg	+/-	pCi/kg	+/-	pCi/kg	+/-	pCi/kg	+/-	pCi/kg	+/-	pCi/kg	+/-	pCi/kg	+/-	pCi/kg	+/-	pCi/kg	+/-
						Gamma energy (keV)		Branching Ratio		1173.23		1332.51		661.62		1115.52		1274.54		834.81		810.75		383.7		477.56		46.52		1460.75		609.32		351.99		238.63	
Samples collected on 19 April 2004 (preliminary and distant samples):																																					
2-C4-439-23	736	1	Barry Cove	43.9727	69.6797	--	--	0.5	5.8	2.6	7.2	--	--	2.7	7.1	4.7	7.1	1.9	5.9	--	--	28.9	48.4	--	--	11796.3	347.6	419.7	31.8	489.5	29	775.7	26.8	210.9	15		
2-C4-439-24	272.7	2	Barry Cove	43.9727	69.6797	--	--	38.4	17.6	7.5	16.1	12.4	33.6	--	--	7.9	11	--	--	--	--	--	--	--	340.8	651.6	16627.4	679.4	628.4	62.3	665.2	59.7	1088.6	52.7	314.3	30.7	
2-C4-439-25	339.6	3	Barry Cove	43.9727	69.6797	--	--	12.4	13.3	16.9	11.4	--	--	16.3	11.3	33.1	10.9	--	--	--	--	--	--	280.9	532.8	14183.8	563	363.6	46.7	534.2	47.7	811.4	41.6	242.9	24.7		
2-C4-439-26	379.1	4	Barry Cove	43.9727	69.6797	--	--	--	--	12.4	9.2	--	--	8.6	10	18.4	11.9	5.6	9	79.4	70.8	3.2	58.1	77.4	388.5	13628.6	509.3	527.9	46.5	491.9	44.5	787.5	38.7	189.5	22.2		
2-C4-440-27	329.9	5	Barry Cove	43.9727	69.6797	10	12.5	--	--	14.5	12.6	--	--	3	9.9	5.2	8.9	1.9	8.5	35.1	74.6	118.9	92.1	--	--	12662.1	536.3	432.1	46	543.7	47.6	668.7	40.1	199.4	23.6		
2-C4-440-28	446.7	6	Barry Cove	43.9727	69.6797	--	--	--	--	8.9	8.3	30.3	21.4	6.7	7.7	6.5	5.8	7.9	8.4	114.9	92.3	8.2	54.8	--	--	13153.9	470.5	432.5	42	515.1	41.3	815.2	35	237.2	20.5		
2-C4-440-29	304.3	7	Barry Cove	43.9727	69.6797	4.6	17.3	15.6	15.8	47.1	13.8	174.8	49.9	1.1	12.3	--	--	2.8	9.2	15.2	106.6	--	--	241.1	481.9	17839.9	664.5	558.5	54.3	546.9	53.4	971.6	48.2	236.6	25.1		
2-C4-440-30	266.5	8	Barry Cove	43.9727	69.6797	11.9	13.9	5.1	9	101.3	25.9	12.7	27.3	--	--	--	--	3.2	11.4	76.7	133.6	--	--	426.7	518.2	15817.5	679.9	515.4	56.8	622.6	59.1	624.9	43.7	261.5	26.9		
440-32	11.5-13.5		Barry Cove	43.9727	69.6797	--	--	Not Counted	--	--	--	--	--	--	--	--	--	--	--	--	--	--	--	--	--	--	--	--	--	--	--	--	--	--	--	--	
2-C4-440-33	327.5	13.5-15	Barry Cove	43.9727	69.6797	7.7	16.4	--	--	64.4	23.8	--	--	21.9	14.5	5.7	11.5	2.3	7.9	--	--	--	--	28	467.1	11444.5	499.1	343.2	44.8	295.9	46.6	757	40.2	171.3	21.3		
440-31	9-11.5		Barry Cove	43.9727	69.6797	--	--	Not Counted	--	--	--	--	--	--	--	--	--	--	--	--	--	--	--	--	--	--	--	--	--	--	--	--	--	--	--	--	
2-NG-438-2a	748.9	S	Barry Cove	43.9727	69.6797	--	--	10.6	13.2	120.5	24.2	4.4	30.2	--	--	34.8	19.4	5.1	14.2	143.2	116.1	446.8	149.9	1172	1219.1	15816.7	692	452.2	62.7	675.5	66.8	999.3	61.9	236.7	33.3		
2-NG-438-2b	1215	S	Barry Cove	43.9727	69.6797	8.8	14.7	--	--	92.8	19.8	--	--	9.4	10.8	5.4	9.7	6.6	8.6	--	--	470.3	100.1	236.2	541.4	10470.9	433.8	355.4	40.5	472.1	46.8	684.4	39.9	168.5	21.6		
2-C4-438-4	343.8	1	Chewonki Camp	69.7111	69.7111	--	--	7.9	8.3	15.9	11.6	--	--	--	--	20.1	10.1	1.8	7.8	23.6	69.4	35.7	66.7	569.1	342.1	10264.6	481	316.8	42.4	318.1	42.2	943.4	40.5	230.1	23.6		
2-C4-438-5	492.5	2	Chewonki Camp	69.7111	69.7111	11	9.6	12.7	10.4	21.2	16.4	--	--	--	--	7	7.2	7.7	7.5	21.2	56.6	54.8	86.7	--	--	10339.9	397.7	326.8	33.6	354.9	35.7	857.7	33.5	227.8	19.8		
2-C4-438-6	395.3	3	Chewonki Camp	69.7111	69.7111	1.5	9.1	0.9	7.2	40.7	15.7	--	--	14.8	11.9	11.5	8.3	8.6	8.6	11.7	83.9	43.4	79.4	1030.2	578.4	10948.7	465.6	275.5	39.3	453.8	39.6	906.7	38.2	239.7	23		
2-C4-438-7	356.4	4	Chewonki Camp	69.7111	69.7111	10.6	11.9	6.4	9.4	122.1	21.6	6.3	20.6	--	--	15.4	12.8	--	--	376.8	130.4	133	83.5	--	--	11098.1	482.2	291.2	42.6	372.3	44.2	936.7	42	251.9	24		
2-C4-438-8	358.8	5	Chewonki Camp	69.7111	69.7111	--	--	1.9	7.4	155.7	23.3	110	36.8	--	--	--	--	7.1	9.1	109.7	103.1	--	--	184	396.3	12038.4	496.6	311.3	41.8	384.7	43	993.5	40.6	218	22.1		
2-C4-438-8	358.8	5	Chewonki Camp	69.7111	69.7111	--	--	1.9	7.4	155.7	23.3	110	36.8	--	--	--	--	7.1	9.1	109.7	103.1	--	--	184	396.3	12038.4	496.6	311.3	41.8	384.7	43	993.5	40.6	218	22.1		
2-C4-438-9	382.2	6	Chewonki Camp	69.7111	69.7111	3.2	9.3	4.9	8.4	118.3	20.4	--	--	4.3	8.7	--	--	5.3	7	153.5	79.7	62.6	59.9	566.3	366.6	10339.9	452.6	285	39.7	326.6	40.5	803.5	36.5	214	20.6		
2-NG-441-46a	1274.9	S	Chewonki Creek	69.7111	69.7111	7	9.1	3.1	6.1	92.4	16.7	0.9	14.4	11.9	9.4	6.1	7.1	--	--	--	--	623.8	132.8	198.6	494.8	9121	400.9	329.5	36.9	372.5	39.3	572.9	36.2	152	18.5		
2-NG-441-46b	973.3	S	Chewonki Creek	69.7111	69.7111	16.4	10	7.1	8.6	46.3	12.8	81	25.9	18.5	9.8	14.1	8	0.4	5	30.4	94.3	380.8	118.7	147.4	792.7	7996	430.1	229.6	37	305.8	45	506.3	39.1	127.8	18.3		
2-C4-440-34	397.7	1	Long Creek	43.9597	69.6983	--	--	9.6	7.5	152.1	20.4	14.2	25.5	--	--	10.5	10.4	11.7	8.3	99	96.9	--	--	392	470.2	15724.7	542.8	435.2	47	573.5	47.3	1195.4	43.7	321	25.4		
2-C4-440-35	313.8	2	Long Creek	43.9597	69.6983	8.6	13	33.1	14.7	363.2	32.3	--	--	20.8	14.7	4.8	10.8	3.6	11.1	--	--	7.8	66.8	39	369.9	7213.8	524.1	540.9	49.8	632.3	57.4	1312.1	52.1	356.4	30		
2-C4-440-36	373.3	3	Long Creek	43.9597	69.6983	13.4	13.4	14.6	11.8	601.8	32.6	--	--	1.5	15.8	1.2	8.5	2.3	7.6	--	--	65.7	75.3	956.6	481.2	14068.8	532.2	516.6	44.4	473	49.8	1000	43.7	263.4	25.2		
2-C4-440-37	322.1	4	Long Creek	43.9597	69.6983	30.9	17.3	8.4	8.4	912.5	41.2	17.5	21.1	--	--	8.7	8.8	5.7	9.8	--	--	--	--	--	--	12699.7	548.8	422.1	50.4	430.1	51.8	994.9	46.7	226.1	27.7		
2-C4-440-38	332.7	5	Long Creek	43.9597	69.6983	--	--	14	13.2	704.2	37.2	--	--	10.8	11.6	8.5	10	--	--	--	--	--	--	--	--	13920.5	553.5	417	49.3	482.7	50.9	991.6	45.7	298.7	26		
2-C4-440-39	421.8	6	Long Creek	43.9597	69.6983	6.4	9.3	3.8	6.3	228.6	25.3	--	--	6.7	10.4	6.8	9.8	6.5	7.7	--	--	29.1	62.6	243.5	355.4	10355.4	438.8	333.9	38.8	356.1	40.4	834.8	36.8	225.5	21.7		
2-C4-441-40	324.1	7	Long Creek	43.9597	69.6983	11.8	13.7	5.6	10.5	184.1	24	7	21.9	2	8.8	8	7.3	--	--	42.9	93	93.3	81.8	886.7	522.2	9925.9	482.6	295.4	43.6	344.4	45	808.5	40.3	262	23.2		
2-C4-441-41	365.6	8	Long Creek	43.9597	69.6983	2.2	8.2	13.5	9.2	172.8	22.1	--	--	19.6	9.8	--	--	6.2	11	8.4	87.9	13.4	66.9	--	--	10610.2	473.4	332.1	42.3	402.5	44.2	786.5	38.2	207.7	22.9		
2-C4-441-42	378.5	9	Long Creek	43.9597	69.6983	1.1	13.4	1.8	12.6	108.5	18.5	121.6	30.3	5.2	10.4	5.7	5.7	3.4	6.1	67.3	67.6	38.9	61	--	--	10582.9	454	394.5	38.1	403.5	41.4	783.1	35.6	160.7	20.7		
2-C4-441-43	299.8	10	Long Creek	43.9597	69.6983	4	11.9	--	--	146.1	25.2	--	--	5.1	16.9	3.8	11	9.5	9.7	85	134.4	49.1	75.6	--	--	12314.6	557.5	458.2	51.3	314.8	46.5	828.4	43.7	181.5	25.5		
2-C4-441-44	485.1	11	Long Creek	43.9597	69.6983	15.7	11.9	14	8.5	60.7	13.9	35.4	16.1	9.9	10.9	4	6.9	8.7	6.1	46.9	77.7	48	51.7	329	412.8	9318.5	387.3	306									

Maine Yankee Marine Sampling Study

			nuclide		60Co		60Co		137Cs		65Zn		22Na		54Mn		58Co		133Ba		7Be		210Pb		40K		214Bi		214Pb		212Pb		208Tl				
			Gamma energy (keV)		1173.23		1332.51		661.62		1115.52		1274.54		834.81		810.75		383.7		477.56		46.52		1460.75		609.32		351.99		238.63		583.14				
			Branching Ratio		0.9986		0.9998		0.8462		0.5075		0.9994		0.9998		0.9945		0.0884		0.103		0.04		0.107		0.4609		0.371		0.431		0.861				
sample	mass(g)	depth(in)	station	lat.	long.	pCi/kg	+/-	pCi/kg	+/-	pCi/kg	+/-	pCi/kg	+/-	pCi/kg	+/-	pCi/kg	+/-	pCi/kg	+/-	pCi/kg	+/-	pCi/kg	+/-	pCi/kg	+/-	pCi/kg	+/-	pCi/kg	+/-	pCi/kg	+/-	pCi/kg	+/-				
2-C4-443-6A	402.6	6	eddy	43.9944	69.6494	16.5	9.4	11.8	9.1	95.5	18.8	--	--	--	--	11.8	9.1	11.6	6.9	9.6	78.7	59.1	154.9	491.5	9988.2	440.7	349.8	38.9	429.8	39.3	646	34.6	177.1	20.7			
2-C4-443-5	393.6	7	eddy	43.9944	69.6494	19.9	12.9	17.7	9.5	43.7	12.3	106	32.8	--	--	0.5	7.2	8.4	10.2	--	--	31.2	93	--	--	9181.7	421.4	322.5	39.9	423.5	39.5	628.9	38.3	192.9	21.3		
2-C4-443-4	374.6	8	eddy	43.9944	69.6494	--	--	4.1	13.5	67.7	15.9	64.7	24.1	3.5	6.8	--	--	6.8	7.9	63.9	85.5	--	--	--	--	10383.1	461.2	325	40.9	392.8	41.9	825.8	37.7	176.1	19.1		
2-C4-443-3	395.6	9	eddy	43.9944	69.6494	5.3	9.7	19.8	8.7	100.3	20.6	15.2	24.3	7.4	9.4	18.6	8.4	2.1	7.3	--	--	24.8	56.1	--	--	10760.8	452.5	383.2	40.9	404.7	41.1	875.7	38.3	250.8	21.3		
2-C4-443-2	430.6	10	eddy	43.9944	69.6494	14.7	9.1	1.1	8.6	85.1	19.6	154.9	31.3	2.3	8	--	--	--	--	26.9	67.4	11.4	90.8	140.6	469.4	9862	418.7	434.6	41.3	441.9	39.7	806.6	35.4	233.3	20.4		
2-C4-443-1	366.6	11	eddy	43.9944	69.6494	--	--	21.6	12.5	94.7	17.3	--	--	--	--	1.2	8	12.1	7.4	--	--	63.6	67.5	--	--	9607.3	456.9	410.6	42.7	433.9	42.8	819.6	39	175.6	23.5		
2-NG-444-1	1275.5	12	eddy	43.9944	69.6494	5.2	8.7	1	7.9	32.6	18.6	--	--	3	7.6	10.7	7.8	4	6.9	181.2	98.3	405.6	105.4	--	--	8602.2	387.1	394	39.5	424.8	40.4	686.7	37.6	167.5	19.8		
2-C4-442-12	445.6	1	pottle cove	43.9969	69.6708	10.4	13.8	--	--	45.9	16.9	--	--	3.4	8.5	--	--	7.8	6.1	229.9	79.3	316.5	82.8	407.5	264.9	7056.1	351.3	284.9	31.4	263.6	33.1	525.7	29.4	128.5	17.7		
2-C4-442-11	356.6	2	pottle cove	43.9969	69.6708	15.2	14.8	9.5	9.9	61.6	12.7	--	--	21.9	14.2	6.5	9.4	2.8	9.7	--	--	75.7	63.8	144	370.9	9896.2	454.5	420.6	40	345.1	41	591.8	39	133.1	21.6		
2-C4-442-10	314.6	3	pottle cove	43.9969	69.6708	--	--	15.1	12	71.3	18	--	--	--	--	--	--	8.7	8.7	83.4	86.8	10.4	83.9	151.6	573.7	10390.9	513.4	407.9	45.9	353.2	47.2	714.1	41	211.4	22.7		
2-C4-442-9	301.6	4	pottle cove	43.9969	69.6708	40.9	21.3	6.8	9.6	67.8	22.2	6.5	24.4	--	--	11.5	9.5	2.8	9.1	115.2	83.6	20.3	69.8	97.3	443.3	11091.7	537.3	312.4	43.9	493	52.6	794.6	42.5	192.8	25.5		
2-C4-442-8	308.6	5	pottle cove	43.9969	69.6708	--	--	--	--	72.9	18.4	--	--	--	--	8.4	10.8	--	--	--	--	173.5	126.1	59.4	429.8	12244.2	538.7	361.9	44.5	493.3	48.1	766.4	42.3	221.2	24.6		
2-C4-442-7	251.6	6	pottle cove	43.9969	69.6708	--	--	--	--	127.4	24.4	--	--	20.7	17.3	2.6	9.5	3.4	10.6	--	--	--	--	194.4	572.2	11670.1	614.1	339.1	56.7	452.8	54.8	833.2	49	225.3	29		
2-C4-442-6	245.6	7	pottle cove	43.9969	69.6708	--	--	14.8	14.2	49.7	18.9	43.6	24.2	--	--	11.2	13	5.2	10.6	--	--	89.9	96	--	--	10769.6	595.7	353.1	52.3	331.6	53.9	727	48.5	238.2	26.4		
2-C4-442-5	278.6	8	pottle cove	43.9969	69.6708	11.9	13	4.9	10.5	71.2	20.5	--	--	--	--	--	--	4.6	11.3	97	102	70.4	93.2	48.3	340.7	9730.3	532.9	274.9	52.7	427.1	49.3	736.8	45.7	153.6	25.4		
2-C4-442-4	306.6	9	pottle cove	43.9969	69.6708	--	--	--	--	101.4	19.8	34.9	33.4	--	--	28.9	13.3	--	--	45.3	84.3	12	110.1	--	--	13262.6	569.9	448	50.5	478.3	52.4	997.7	45.8	267.9	26.7		
2-C4-442-3	313.6	10	pottle cove	43.9969	69.6708	14.9	11	5.4	9.3	86.5	20.4	--	--	--	--	15.6	10	--	--	128	92	--	--	245.7	255.9	8898.6	481.2	383.4	41.2	409.4	45.8	706.8	40.7	231.3	23.9		
2-C4-442-2	323.6	11	pottle cove	43.9969	69.6708	--	--	4.2	9.4	67.9	18.3	12.2	20.4	12.1	16.4	4	13.4	--	--	--	--	--	--	389.2	310.9	9635.9	486.5	347.3	44.9	422.6	46.3	790.3	41.6	250.3	24.7		
2-NG-444-2	1179.5	12	pottle cove	43.9969	69.6708	--	--	5	10.5	61.3	18.2	28.2	22.6	6.4	8.3	19.9	11.9	--	--	--	--	--	--	316.4	85.2	--	--	9034	413.4	353.4	40.6	413.7	44	701.6	39.9	148.9	21
2-C4-442-1	174.6	12	pottle cove	43.9969	69.6708	38.8	21.5	--	--	25.8	27.6	6.5	32.3	3.7	16.3	5.6	13.5	1.2	12.9	53	147.7	--	--	1071.6	683.8	13401.7	804.7	472.8	72.1	473.7	75	866.9	65.1	270.9	37.1		
2-C4-445-13	459.6	1	sassanoa	43.8944	69.7661	0.7	7.3	3.9	8.9	103	13.3	13.5	24.4	7.1	8.4	1.4	5.5	--	--	52.9	50.3	159.2	90.9	--	--	6373.5	325.8	255.1	30.5	311.3	31.9	565.4	30.9	116.1	16.3		
2-C4-445-12	315.6	2	sassanoa	43.8944	69.7661	8.9	12.1	7.5	8.3	160.8	24.2	--	--	11.4	9.2	--	--	--	--	165.1	77.6	19.4	68.7	58.1	305.7	7315.4	431.3	286.9	42.5	336.8	45.4	599	37.9	159.4	23.4		
2-C4-445-11	246.6	3	sassanoa	43.8944	69.7661	6.1	10.4	9.9	10.7	151	23.8	45.7	26.7	--	--	--	--	9.4	9.2	450.7	115	102.8	93.4	1093.5	618.3	6227.5	468.6	306.6	46.3	297.3	46.4	505.4	43.4	109.1	23.1		
2-C4-445-10	309.6	4	sassanoa	43.8944	69.7661	10.2	10.2	20.9	8	315.2	28.6	5.5	18.1	20.4	13.9	--	--	8.2	7.9	127.1	117.3	59.4	99.8	521.4	406	7524.4	437.1	272.2	42.8	333.5	45.5	592.7	39.4	168.8	21.9		
2-C4-445-9	242.6	5	sassanoa	43.8944	69.7661	19.9	15.3	5.6	11.6	329.8	34.1	17	26.5	9.4	10.8	17.8	10.6	13.1	11.3	222.7	121.1	40.4	122.2	--	--	8259.2	533.9	224.2	47.1	346.2	53.9	791.7	48.6	189.1	27.3		
2-C4-445-8	284.6	6	sassanoa	43.8944	69.7661	--	--	11.9	12.5	292.6	29.6	23.8	30.7	5.2	10.1	6.8	9.4	5.5	9.7	203.4	127.9	--	--	769.1	487.4	6942.9	457.4	279.1	39.2	273.7	47.6	653.2	42.3	138.7	24.6		
2-C4-445-7	263.6	7	sassanoa	43.8944	69.7661	17.1	13	6.5	8.5	161.8	23.3	2.1	18.8	9.9	13.1	6.6	11.7	3.6	14.7	--	--	27.9	88.1	640.2	464.1	8479.7	479.6	228.5	40.9	315.7	48.6	779.9	44	193.4	24.1		
2-C4-445-6	251.6	8	sassanoa	43.8944	69.7661	8.4	11.7	0.9	11.5	144.8	30.5	--	--	--	--	10.3	17.5	25.2	11.1	36.8	89.9	--	--	--	--	7908.7	502.1	437	56.3	401.3	54	737.7	47.5	218.4	28.5		
2-C4-445-5	295.6	9	sassanoa	43.8944	69.7661	4.1	11.3	7.5	11	131.5	23.6	16.2	21.5	4.4	9.1	--	--	--	--	50.9	77.2	87.1	72.2	409.6	417	7294.4	442.5	318	44.3	299.5	43.5	750.3	41.5	158.6	21.4		
2-C4-445-4	211.6	10	sassanoa	43.8944	69.7661	27	15.1	4.8	12.1	123.8	26.8	--	--	9.2	12.5	11.2	12.1	--	--	142.2	139.7	69.5	90.9	69.4	577.1	10065.5	601.9	233.9	50.1	268.6	57.7	1014.1	55.8	312.6	29.4		
2-C4-445-3	266.6	11	sassanoa	43.8944	69.7661	--	--	16.6	9.7	89	18.2	--	--	14.7	17.5	19.1	9.8	6.6	12.4	130.3	139.2	--	--	431.2	357.7	8855	518	284.9	49.9	373.5	59.5	873	47.3	311.1	30.4		
2-NG-444-3	1280.5	12	sassanoa	43.8944	69.7661	--	--	8.2	8.9	103.2	17.3	37.3	19.4	--	--	5.8	8.2	--	--	34.7	62.1	340.7	136.2	678.8	714.1	6967.3	351.6	319.7	37.1	396.4	40.8	724.9	36.9	170	20.8		
2-C4-445-2	341.6	12	sassanoa	43.8944	69.7661	0.9	10.1	21.9	13.7	52.1	16.6	32.2	19.4	10.2	12.8	3.2	9.1	1.9	7.5	--	--	70.6	83.9	--	--	8849.1	452	277.2	42.2	324.2	40	764	38.2	202	21.7		
2-C4-445-1	262.6	13	sassanoa	43.8944	69.7661	1.5	15	2.6	9.3	23.4	12.7	--	--	11.2	11.6	25.9	14.2	3.2	8.7	130.8	117.7	3.1	103.4	253.8	530.4	9273.7	529.6	351.4	48.6	338.5	43.5	879.5	46.5	205.8	29.5		
Samples collected 6-9 July 2004 (phase 1)+A224:																																					
1-NG-171653	1519	S	1	43.960	69.698	--	--	3.6	4.3	62.8	12.3	95	21.6	--	--	--	--	9	5.3	51.9	79.6	299.9	73.7	610.6	178.7	8585.1	256.7	386.7	27	401.5	30.6	684.5	31.8	158.3	13.8		
1-C4-171731	425.9	1	2	43.955	69.697	4.1	5.5	--	--	60.9	9.9	5.1	9.3	5.5	5.7	1.6	4.2	5.3	4.6	--	--	64.3	65.5</														

Maine Yankee Marine Sampling Study

			nuclide		60Co		60Co		137Cs		65Zn		22Na		54Mn		58Co		133Ba		7Be		210Pb		40K		214Bi		214Pb		212Pb		208Tl				
			Gamma energy (keV)		1173.23		1332.51		661.62		1115.52		1274.54		834.81		810.75		383.7		477.56		46.52		1460.75		609.32		214.99		238.63		583.14				
			Branching Ratio		0.9986		0.9998		0.8462		0.5075		0.9994		0.9998		0.9945		0.0884		0.103		0.04		0.107		0.4609		0.371		0.431		0.861				
sample	mass(g)	depth(in)	station	lat.	long.	pCi/kg	+/-	pCi/kg	+/-	pCi/kg	+/-	pCi/kg	+/-	pCi/kg	+/-	pCi/kg	+/-	pCi/kg	+/-	pCi/kg	+/-	pCi/kg	+/-	pCi/kg	+/-	pCi/kg	+/-	pCi/kg	+/-	pCi/kg	+/-	pCi/kg	+/-				
1-C4-171763	326.4	10	8-1	43.949	69.698	2.1	6.8	2.9	8.5	112.3	15	--	--	2.8	5.5	16.4	7.3	2.4	5.3	--	--	--	--	662.1	365.4	8632.3	329.1	239.8	30.1	252.5	35.3	709.2	34.5	185	16.7		
2-C4-171764	390.6	11	8-1	43.949	69.698	23.1	17	13.4	10.5	122.2	19.7	32.5	21.3	6.7	10.6	--	--	--	--	4	118.6	54.4	77.5	175.3	445.8	9629.4	428.9	283.3	37	235.1	38.3	638.6	35.1	188.9	20.6		
1-C4-171765	249	12	8-1	43.949	69.698	2.8	10.4	2.3	6.6	104.7	21.5	145.5	32.9	1.5	7.8	3.8	7.2	--	--	61.1	115.5	115.4	74.1	715.8	540.5	9161	386.8	224	37.7	278.6	43.4	762.1	43.5	219.4	20.3		
1-C4-171766	336.5	13	8-1	43.949	69.698	12.3	7.2	7.5	6.1	167.6	18.3	--	--	2.2	6.3	5.3	8.1	--	--	52.8	54.9	147.5	53.7	401.8	403	8695.5	323.5	199.2	31.1	259	34.4	665.5	34.2	181.9	17.5		
2-C4-171767	330.6	14	8-1	43.949	69.698	--	--	--	--	154.1	23	--	--	3	9.8	6.5	12.9	--	--	--	--	155.8	81.6	271.9	259.2	9175	469.5	313.7	42.8	271.7	33.9	827.1	40.7	225.3	23.6		
2-C4-171768	283	15	8-1	43.949	69.698	--	--	16.8	11.3	191.6	27.5	25.9	27	--	--	4.6	9.5	3	8.8	12.3	80.5	69.3	77.5	--	--	9811.8	549.4	397.1	47.7	300.3	48.1	780.5	44.4	222.1	24		
2-NG-171664	1383.6	S	9	43.949	69.699	18.8	18.7	11.9	9.7	154	20.4	210.5	33	--	--	1.9	5.4	4.9	8.2	10.7	90.4	704.5	154.1	2037.2	635	14353.5	476.1	429.1	40.5	346.8	39.2	521.6	42.4	176.3	19.9		
2-NG-171665	1402.1	S	10	43.947	69.699	5.1	9.1	29.1	10.4	90.3	19.6	--	--	7.7	9.7	4.6	8.4	--	--	92.3	111.9	170.7	99.3	--	--	9792.7	393.4	274.4	36.6	343.9	38	594.5	34.3	136.2	18.8		
2-NG-171666	1265.9	S	11	43.947	69.699	12.6	7.7	--	--	47.2	11.2	14	19.8	2	9.4	14.4	6.5	12.6	8	60.4	83.9	364.9	83.3	133.3	336.4	6040.3	319	215	29.4	234.9	30.3	251.1	27.5	132.9	16.8		
1-NG-171667	1454.3	S	12	43.947	69.700	25	11.5	3	4.5	55.6	8.1	--	--	--	--	0.5	4.6	--	--	97.6	74	364.9	79.8	291.8	219.8	7604.6	244.9	295.1	25.3	295.8	29.6	513.2	28.8	148.2	13.1		
2-NG-171668	1349.5	S	13	43.944	69.697	12.5	9.5	13.2	11.2	86.8	18	91.8	32.3	23	10	6.4	8.4	--	--	--	--	473	131	--	--	9487.1	404.4	286.7	34.1	425.1	37.7	608.5	34.8	193.8	18.8		
2-NG-171669	1302.1	S	14	43.945	69.699	17.7	13.8	--	--	93.5	16.4	21.7	21.2	15.3	8.1	0.7	7.9	--	--	--	--	272.8	102.7	149.1	310.8	9716.3	409.3	348.1	37.4	448.1	40.2	663.1	35.9	142.2	22		
1-NG-171673	1321.8	S	15	43.945	69.700	9	5.7	10.6	5.8	63.5	12.3	18.5	11.1	--	--	11.9	5.8	1.8	5.2	--	--	1.3	53.8	290.2	154.1	8059.4	265.7	288.3	27.3	318.3	31.8	631.9	31.1	225.2	14.1		
2-NG-171674	1450.1	S	16	43.941	69.697	23.7	14.1	0.7	7	74.9	12.8	13	15.1	9.2	7.5	3.6	8.2	--	--	149.6	75.2	181.9	111.8	721.6	493.8	9266.9	385.3	363.6	36.4	407.4	40.1	723.6	35.7	213.3	19.6		
1-NG-171675	1312.6	S	17	43.934	69.700	14.3	5.9	8.2	5	53.5	12	--	--	0.8	5	--	--	--	--	--	--	295.2	81.8	608.2	330.7	7904	269.9	363.2	28.7	324.6	38.3	691	33.1	179.7	15.6		
2-NG-171676	1449.1	S	18	43.941	69.702	3.7	9	10.9	8.4	69.8	14.5	--	--	16.4	7.3	5.8	6.5	5.9	7.5	117.4	97.3	110.1	113.4	151.4	466	8668.1	367.6	262.9	29	320.4	35.4	603.1	32.1	129.5	17.7		
2-NG-171677	1347.6	S	19	43.944	69.696	3.3	9	4.4	7.4	69.3	15.2	--	--	0.7	7.3	1	6.7	--	--	52.2	63.7	389.6	102.8	150.3	366.3	9186.3	390.6	326	36	328.2	38.1	609.7	34.8	201.4	19.6		
1-NG-171678	1190.7	S	20	43.948	69.696	7.1	7.1	0.5	5.2	78.8	13	--	--	7.3	6.6	4.9	5.7	--	--	75	90.6	105.5	57.5	671.6	274.5	9445.3	304	346	30.9	342	34.2	667.3	34.3	151.6	15.3		
2-NG-171679	1351.6	S	21	43.947	69.694	8.5	11.4	16.1	8.6	52.8	14.6	--	--	11.2	9.7	1	8.3	8.5	6.6	5.5	62.4	463.7	91.6	--	--	9718.5	393.4	398	39	379.7	45.8	663	38.6	176.1	17.3		
2-NG-171680	1421.5	S	22	43.949	69.694	36	13.1	16.7	10	91.7	16.6	10.5	16.4	10.2	9.4	--	--	26	11.7	98.9	92	370.3	112.6	130.6	434.7	9644.8	385.8	369.4	36.4	433.4	39.5	776.7	36.7	179.3	19.8		
2-NG-171681	1546.1	S	23	43.951	69.693	22.9	14.8	--	--	51.1	13.9	--	--	0.8	10.2	3.7	8.8	3.7	9.7	--	--	273	76.9	447.6	567.6	12460.2	414.8	560.3	41.9	541.5	41.3	824.7	35.7	185.1	20		
2-NG-171685	1690	S	24	43.950	69.692	8	11.2	9	8.3	34.8	16.3	--	--	2.2	8.4	--	--	10.8	12.3	0.7	85.1	269.6	128.1	--	--	15026	442.5	421.7	36.6	428.3	40.5	713.5	35.2	178.2	19.4		
2-C4-171742	437.5	1	25	43.953	69.692	4.1	8.8	20.6	6.9	29.9	12.2	9	17.2	6	8.3	--	--	--	--	--	--	224.2	90	--	--	9781.7	400.7	282.2	34.9	352.6	34.7	555.3	30.5	151.2	17.2		
2-C4-171743	494.6	2	25	43.953	69.692	1.6	10.6	2.1	6.8	31.7	11.6	--	--	--	--	--	--	0.9	6.3	106.1	65.9	185.1	64.4	222.5	310.5	11978.1	424.8	408.2	34.3	406.3	36.4	631.2	31.9	170.8	17.8		
2-C4-171744	349.1	3	25	43.953	69.692	9.5	11.4	--	--	17.8	14.2	155	41.4	20.5	12.8	19.2	9.2	4.2	8.9	88.4	107.7	65.6	84.2	134.9	361.7	12869.4	534	447.1	46.8	421.5	50	732.1	41.7	179.8	23.8		
2-C4-171745	493.4	4	25	43.953	69.692	12.6	10.8	--	--	39	10.7	--	--	7.9	9	9.6	9.4	6.4	6.2	--	--	72.1	54.8	--	--	11866.8	432.1	450.6	37.2	449.9	37.8	545.1	29	201.8	17.8		
2-C4-171746	406.1	5	25	43.953	69.692	7.9	11.8	3.3	7.5	5.5	9	--	--	8	9	3.2	7.6	9.9	7.2	59.9	69.7	106.7	74.8	1355.1	511.8	10683.2	458.4	471.5	42.7	492.9	43.2	778	36.8	222.9	20.7		
1-C4-171747	412.3	6	25	43.953	69.692	2.5	6.3	--	--	--	--	--	--	2.1	6.7	15.2	5.3	--	--	--	--	60.2	43.5	357.7	318	7590.6	273.6	305.1	26.7	385.2	30.8	578.2	30.9	152.5	14.5		
2-C4-171748	435	7	25	43.953	69.692	15.7	12.8	4.7	7.4	23.5	13.1	--	--	8.5	10.7	12.6	9.9	--	--	--	--	54.5	71.7	75.9	220.6	13228.8	487.4	431	43.1	500.4	40.9	724.2	36.2	229.3	20.5		
2-C4-171749	413.1	8	25	43.953	69.692	--	--	2.5	7.4	--	--	30	25.5	3.2	9.7	--	--	--	--	8.7	7.5	28	69.4	53.4	71.7	290.1	469	11689.5	474	423.2	42.3	450.2	42.9	761.2	38.1	248.8	21.3
2-C4-171750	413.3	9	25	43.953	69.692	15.1	12.9	9.9	7.8	1.5	8.1	--	--	11.8	14.2	13.1	8.4	21	12	--	--	29.7	63.5	204.2	365.7	12698.8	481.7	432.7	41.3	445.7	41	741.9	37.5	178.1	20.8		
2-C4-171751	582.1	10	25	43.953	69.692	3.8	9.6	--	--	1.4	6.3	--	--	--	--	1.7	7.2	6.8	8	--	--	--	--	--	--	11076.9	377.6	323.6	32.1	363.9	31.8	607	28	229.5	17.5		
2-C4-171752	438.3	11	25	43.953	69.692	0.7	9.9	1.6	8.2	27.1	12.8	--	--	13	10.5	4.9	7.8	3.9	6.8	--	--	--	--	661.2	490.3	13833.1	490.3	435.9	41.5	419.1	41.2	755.8	36.5	226	21.5		
2-C4-171753	850.6	12	25	43.953	69.692	5.7	5.5	2	4.6	13.3	6	--	--	8.4	6.3	--	--	1.2	4	62.6	45.8	43.2	36.2	--	--	9870.8	289.7	325.4	24.4	280.1	23.9	386.8	18.7	142.7	11.5		
1-NG-171686	1681.4	S	25	43.953	69.692	--	--	3.6	6.2	30.2	8.9	--	--	5.8	5.8	10.3	9.3	2.1	4	3.1	78.1	275.6	92.4	412.5	291.7	10868.1	274	373.1	27.1	447.8	30.5	732.5	31.1	187.9	14.1		
1-NG-171687	1547.6	S	26	43.939	69.693	0.2	7.1	10.5	5.9	14.8	11.8	--	--	9.4	5.1	10.2	5.1	2.8	5.4	99	70.7	513.7	88.6	756.7	341.6	9748.2	269.4	422.7	29.6	486.5	33.1	801.4	32.4	198.1	15.1		
2-NG-171688	144																																				

Maine Yankee Marine Sampling Study

			nuclide		60Co		60Co		137Cs		65Zn		22Na		54Mn		58Co		133Ba		7Be		210Pb		40K		214Bi		214Pb		212Pb		208Tl			
			Gamma energy (keV)		1173.23		1332.51		661.62		1115.52		1274.54		834.81		810.75		383.7		477.56		46.52		1460.75		609.32		214Pb		212Pb		208Tl			
			Branching Ratio		0.9986		0.9998		0.8462		0.5075		0.9994		0.9998		0.9945		0.0884		0.103		0.04		0.107		0.4609		0.371		0.431		0.861			
sample	mass(g)	depth(in)	station	lat.	long.	pCi/kg	+/-	pCi/kg	+/-	pCi/kg	+/-	pCi/kg	+/-	pCi/kg	+/-	pCi/kg	+/-	pCi/kg	+/-	pCi/kg	+/-	pCi/kg	+/-	pCi/kg	+/-	pCi/kg	+/-	pCi/kg	+/-	pCi/kg	+/-	pCi/kg	+/-			
1-NG-171700	1438.5	S	39	43.934	69.728	10.7	5.8	10.3	6.1	57	11.1	12.1	2.9	4.5	10.4	7.2	--	--	--	--	136.5	90.5	618.3	301.4	7989.2	252.5	361.5	26.2	355.4	30	598.1	29.3	192	13.6		
2-NG-171701	1403.6	S	40	43.936	69.724	--	--	--	--	69.6	14.2	--	--	10.8	9.4	3.3	9.3	14.1	6.6	--	--	271.4	86.1	721.5	476.5	8133.9	365.3	346.6	36	434.8	42.5	657.8	33.2	138.1	17.4	
1-NG-171702	1463.3	S	41	43.941	69.706	3	5.6	5.2	5.8	87.2	12.7	93.2	19.4	--	--	5.6	4	--	--	--	--	48.3	41.2	479.6	300.2	7799	248.6	303.2	25.2	290	29.5	494	28	155.3	13.3	
2-NG-171703	1418.9	S	42	43.939	69.710	10.7	11	--	--	65.9	14.7	1.9	15.9	--	--	0.9	8.4	6	7.3	26.1	75.9	229.9	90.4	41.6	543.7	8318.3	354	365.5	37.1	388.7	37.3	670	34.7	175	18.6	
1-NG-171704	1422.1	S	43	43.951	69.711	15.3	6.8	2.7	4.3	64.5	10.4	18	15	4.4	4.4	4.6	4.9	2.2	3.9	192.2	73.9	266.9	72.8	810	253	7014.1	237.6	193	24.4	256.4	27.9	478.3	27.5	124.4	11.9	
2-C3-171973	199.5	1	44	43.935	69.709	--	--	4.7	10.1	82.5	18	--	--	6.4	16	2.2	8.7	--	--	--	--	68.3	64.7	421.1	438.9	6881	431.1	308.1	41.9	223.1	39.6	349.6	31.1	81.6	17.2	
2-C3-171974	99.8	2	44	43.935	69.709	--	--	9.4	18.4	102.1	29.7	40.9	32.2	12	20.9	3	25.2	8.8	14.3	462.4	174.9	68.3	113.8	928.4	1096	9265.6	749.9	283.9	76.2	403.5	65.8	739.8	68.8	180.4	31.7	
2-C3-171975	134.1	3	44	43.935	69.709	--	--	13.1	12.5	88.6	25.1	--	--	10	18.6	14.9	14.5	1.1	11.6	--	--	194.7	122.5	635.7	544.1	8104.2	579.2	281.1	60.4	316.1	62.5	606.1	55.9	169.2	30.3	
2-C3-171976	119.3	4	44	43.935	69.709	72.9	18	3.9	14.9	54.5	27.1	--	--	15	19.2	18.8	19.1	18	18.4	20.2	118.6	--	--	683.5	762.3	9728.9	691.7	387.1	59	473.8	69.4	790.4	62.7	114.7	36.2	
2-C3-171977	112.1	5	44	43.935	69.709	7.4	23	--	--	58.9	28.2	20.8	31.8	6	14.3	--	--	6.1	15.8	143.6	194.8	--	--	661.3	1011.5	9252.5	682.9	362	70.2	324.6	67.4	701.7	64.6	234.8	35.2	
2-C3-171978	117.7	6	44	43.935	69.709	--	--	2	12.7	15.6	15.8	19.8	41.6	23.8	16.2	17.8	13.8	14.9	19.4	266.7	173.8	130.2	146.8	--	--	9456.2	715.6	281.5	54	238.1	60.2	789.5	61.2	204.3	33.9	
2-C3-171979	101.5	7	44	43.935	69.709	22.4	19.5	13.8	20.1	--	--	--	--	--	--	8.8	17.8	12	18.7	296	174.4	75.5	118.9	1058.9	1211.9	10284.5	739.9	260.2	62.2	275	76.6	529.1	78	138.5	39.1	
2-C3-171980	114.9	8	44	43.935	69.709	3.6	28.1	8.1	22.1	--	--	--	23.7	39.6	17.6	15.5	12.1	17.2	--	--	171.6	130.7	--	--	967.7	1402.3	10454.1	714.9	252.9	57.5	82.4	69.7	680	61.9	163.1	38.2
2-C3-171981	109.8	9	44	43.935	69.709	1.9	15.2	31.2	22.8	10.3	15	35.4	35	--	--	22.3	15	13.3	13.2	77	131.2	98.2	150.5	702.1	1102.2	9967.2	713.2	317.8	64	331.4	76.7	720.2	62.6	260.5	35.6	
2-NG-171708	1425.1	S	44	43.935	69.709	1.2	7.7	9	6.3	94.1	15.2	--	--	--	--	7.8	6.5	0.9	9.3	41.5	58.7	29.8	56	47.4	518.3	8460.4	358.8	258.7	34.4	329.8	35.9	514.3	32.5	159.5	17.1	
2-NG-171712	1372.1	S	45	43.953	69.723	--	--	5.8	6.5	57.1	16.6	--	--	--	--	--	--	1.9	6.1	62	62	626.5	107.4	166.1	278	7241.3	340.9	283.5	32.8	297.9	35.4	516.7	32.2	138.8	17	
1-NG-171713	1425.1	S	46	43.956	69.683	6.9	5.4	10.8	6.2	70.6	10.5	78.1	21.1	2.6	4.6	3.6	4	10.6	5.8	20.3	45.7	489.6	85.6	607	233.9	7494	247.2	342.2	27.4	277.9	30.2	527.3	28.9	137.7	13.5	
2-NG-171714	1362.1	S	47	43.959	69.682	2	8.4	--	--	53.4	12.3	1.2	14	3.5	7.1	10	6.4	--	--	62.5	59.6	430.8	120.2	532.8	532.7	7867.3	355.1	316.3	34.1	363.6	34.2	451.8	32.5	114	15	
2-NG-171715	1387.6	S	48	43.969	69.684	10.2	8.6	0.9	9.4	64	12.7	--	--	--	--	--	--	0.5	6.4	50.6	59.1	637.1	126.4	407.5	637.3	8180.4	362.7	288.8	34.3	271.7	36.6	584.6	32.7	157.5	17.2	
2-NG-171719	1374.4	S	49	43.973	69.679	--	--	37.1	12.4	67.3	14.7	31.5	21	3.5	7.2	9	6.9	3.2	5.7	70	60.7	469.1	126.5	1326.3	646.4	8442.4	370.9	332.9	33.1	276.7	36.2	564.1	33	155	18.4	
2-C4-171953	496.1	1	50	43.981	69.676	--	--	0.7	5.3	35.5	9.5	--	--	9.2	10.2	6.5	5.7	--	--	14	55.8	44.5	44.1	60.4	228.4	6652.3	321.3	198.6	22.3	168.6	24.9	382.6	23.9	95.3	14.1	
2-C4-171954	297.8	2	50	43.981	69.676	--	--	12.2	11	54.3	16.5	--	--	5.5	9.4	--	--	9.7	11	70	73.1	38.4	81.1	250.5	467.6	9481.3	498.5	235.3	36.8	214.7	44.2	530.5	37.6	118.2	15.4	
2-C4-171955	339.3	3	50	43.981	69.676	7.1	10.8	22.1	10	67.5	13.7	--	--	4.5	10.5	4.5	7.6	1.2	7.4	3.4	66.8	115.7	82.4	551.4	527.9	9343.3	460.8	262.7	41	201.9	35.9	516	34.5	131	20.8	
2-C4-171956	310	4	50	43.981	69.676	13.6	11.3	15.4	10.7	117	19.9	55.8	30.4	3.2	17	3.5	8.6	31.4	12.9	--	--	83.1	67.5	710.1	313.9	10019.5	489	327.8	43.4	320.8	43	611.8	39	148	23.1	
2-C4-171957	316.6	5	50	43.981	69.676	--	--	20.4	7.8	80.4	17.9	10.7	19	--	--	10.2	9.7	15.8	13.7	12.2	87.7	3.9	67.6	--	--	9547.9	484	309	42.8	258	41.3	565.4	37.3	144.5	21.7	
2-C4-171958	315.6	6	50	43.981	69.676	4.8	10.5	--	--	92.4	22	40.5	25	55.8	19.3	2.4	8.9	1.3	8.5	178.5	91.5	11.7	64.9	--	--	9512.2	480.3	189	33.5	274.9	42.6	650.9	39.4	208.5	21.5	
1-C4-171959	276.3	7	50	43.981	69.676	16.3	10.4	5.5	8.5	88.6	17	--	--	1.3	7.2	8.7	7.7	2.1	6.1	--	--	--	--	506	226.6	8903	361.1	285.2	32.1	388	40.9	590.9	37.6	180.7	20	
2-C4-171960	296.2	8	50	43.981	69.676	17.6	13	--	--	96.7	19.8	--	--	15.4	9.6	--	--	14.3	7.7	--	--	45.5	72.5	330.3	548.6	10322.5	508	278.7	48.4	400.9	47.2	738.6	43.7	187.6	22.6	
1-C4-171961	360.3	9	50	43.981	69.676	9.6	6.6	9.5	5.6	86.9	13.3	44.6	15.6	10.2	6.6	6.4	8	3.7	8.7	9.4	84.5	--	--	520.2	408	8588.4	315.7	242.1	28.8	348.9	31.7	543.2	31.9	145.8	15.5	
2-C4-171962	333.2	10	50	43.981	69.676	10.8	10.8	7.1	8.2	36.8	23.1	2.3	16.5	15.7	10.3	5.2	9.8	--	--	13.9	75.3	36.8	86.2	205.5	309	11003.2	487.5	488.2	47.3	434.8	45.6	703	41	204.9	22.6	
2-C4-171963	252.6	11	50	43.981	69.676	7.2	14	7	10.8	137.3	29.3	42.4	25	11.6	10.8	6.8	10.6	3.4	10.1	36.7	91.7	--	--	--	--	11925.8	598.7	403.7	56.1	497.2	58.3	918.5	49.1	246.4	29.7	
2-NG-171720	1400.6	S	50	43.981	69.676	12.2	10.7	0.7	6.7	60.4	14.8	--	--	9.5	7	--	--	3.2	6	--	--	374.9	98.3	329.4	580.5	8536.4	367.9	211.2	33.9	302.4	36	530.8	33	154.9	17.9	
2-NG-171721	1490.4	S	51	43.918	69.716	17.3	9.5	--	--	28.6	12.2	--	--	--	--	10.1	6.9	6	6.8	23.2	125.8	252.6	87.9	194.4	425.5	10240.6	388.4	366	36.6	409	37	624.5	33.9	179.1	18.5	
2-NG-171725	1312.6	S	52	43.915	69.709	--	--	--	--	83.2	13.5	14.4	14.5	--	--	4	7.7	7.1	7.2	--	--	382.4	95.4	424.3	541.4	7910.6	370.7	296.5	38.3	281.6	38.2	567.5	33.6	153.9	18.4	
2-NG-171726	1347.3	S	53	43.921	69.718	5.5	11	8.8	6.7	71.2	13.4	17.3	15.2	1.4	7.7	--	--	--	--	--	--	160.5	62.1	--	--	7108.2	348.6	182.9	37.2	269.5	34.3	461.9	31.6	111.1	16.5	
2-NG-171727	1585.9	S	54	43.921	69.724	14.5	11.9	2.5	6.4	43.5	12.8	--	--	--	--	5.5	7.3	2.8	6	119.7	70.9	38.9	83.5	--	--	8810.3	348.9	404.8	35.8	440.9	35.7	575.9	30.1			

Maine Yankee Marine Sampling Study

			nuclide		60Co		60Co		137Cs		65Zn		22Na		54Mn		58Co		133Ba		7Be		210Pb		40K		214Bi		214Pb		212Pb		208Tl		
			Gamma energy (keV)		1173.23		1332.51		661.62		1115.52		1274.54		834.81		810.75		383.7		477.56		46.52		1460.75		609.32		351.99		238.63		583.14		
			Branching Ratio		0.9986		0.9998		0.8462		0.5075		0.9994		0.9998		0.9945		0.0884		0.103		0.04		0.107		0.4609		0.371		0.431		0.861		
sample	mass(g)	depth(in)	station	lat.	long.	pCi/kg	+/-	pCi/kg	+/-	pCi/kg	+/-	pCi/kg	+/-	pCi/kg	+/-	pCi/kg	+/-	pCi/kg	+/-	pCi/kg	+/-	pCi/kg	+/-	pCi/kg	+/-	pCi/kg	+/-	pCi/kg	+/-	pCi/kg	+/-	pCi/kg	+/-		
1-C3-179262	119.6	5	61	43.928	69.706	12	11.1	19.3	10.8	10.2	13	--	--	5.8	10.8	--	--	--	--	--	--	187.1	108.4	--	--	8914.1	513.2	350.2	47.7	354	51.1	664	50.6	186	24.9
1-C3-179277	106.1	1	62	43.934	69.700	3.7	11.5	16.3	15.4	23.7	12.8	12.4	28.7	18.4	10.5	28	12	13.4	13.7	190.8	149.3	11.5	80.5	388.2	280.5	5264.1	448	253.8	41.7	213.2	55	367.2	48.5	108.7	22.9
1-C3-179278	123.9	2	62	43.934	69.700	21.1	13.3	17.5	10.5	4.7	9.4	31	24.7	--	--	10	10.6	12.5	10.4	--	--	24.6	71.5	346.3	211	7272.3	436.9	40.2	34.3	218.9	47.6	598.1	46.4	169.9	23
1-C3-179279	109.1	3	62	43.934	69.700	7.2	13.5	--	--	11.2	14.2	27.1	25.8	18.8	14.5	--	--	9.8	9.5	--	--	39.2	87.6	23.6	244.8	7785.6	494.9	227.9	41.2	276.5	51.4	694.4	53.4	162.8	29
1-C3-179280	120.8	4	62	43.934	69.700	--	--	12	8.6	7.6	10.8	--	--	--	--	--	--	11.3	9.2	19.7	120.2	80.8	76.6	135	206.5	7428.9	440.6	203.6	44.4	262.8	46.3	577.3	42.9	161.3	22.1
1-C3-179281	126.3	5	62	43.934	69.700	3.4	12	--	--	5.1	10.2	--	--	--	--	--	--	16.9	14	58.1	120.6	--	--	47.6	323.6	9316.4	482.2	215.8	42	199.7	46.5	592.6	46.6	148.4	22.5
1-C3-179282	108.7	6	62	43.934	69.700	--	--	--	--	1.8	10.4	53.5	27.9	--	--	--	--	4.5	9.8	323.2	168.2	183.4	108.9	31.6	243.3	8563.6	511.3	191.6	37.6	358.6	52.8	669.5	53.8	197.7	28.8
1-C3-179283	121.6	7	62	43.934	69.700	10.7	12.1	9.5	16.7	20.7	10.6	59.8	21.9	2.3	10	11.4	9.3	1.6	10.2	4.9	83.8	80.3	83.7	--	--	8360.8	477.4	319.8	46.5	276.3	49.6	625.1	48.3	172.9	26.2
1-C3-179284	107.6	8	62	43.934	69.700	20.9	15.4	--	--	19.8	18.3	20.6	26.6	--	--	11	10.6	1.8	8.7	110.7	156.5	--	--	--	--	9137.7	523.9	236.9	48.6	178.3	49.1	686.4	52.9	221.7	23.2
1-C3-179263	104.9	1	63	43.940	69.695	18	12.3	--	--	44.3	19.2	36	25.7	22.6	10.8	5.7	10.6	--	--	136.2	94.3	159	101.4	389.4	298.1	5157.9	414.6	192.3	41.5	208.5	45.8	514.8	46.4	85.6	24.6
1-C3-179264	180.6	2	63	43.940	69.695	15.9	9.3	0.8	7.3	38.9	11.3	13.7	15.2	10.8	9.9	2.4	9	9.7	7.1	--	--	13.5	54.5	465.6	264.6	6338.1	347.9	172.4	33	225.1	35.2	503.2	34.2	119.3	19.3
1-C3-179265	106.6	3	63	43.940	69.695	20.8	12.8	--	--	56.3	24.4	--	--	--	--	9.3	10.5	6.4	9.2	52.1	140.2	171.7	92	424	312.8	8677.7	525.3	261.9	49.9	393.4	47.4	628.1	54.5	153	27.4
1-C3-179266	126.9	4	63	43.940	69.695	2.1	9.6	13.7	11.1	115.9	22.9	85.5	35.2	--	--	15.6	11.2	9.2	10.4	18.8	88.5	81.8	72.8	635.6	268.3	7564.6	448.3	231.4	45.4	298.2	41.1	488.4	45.5	144.1	23.3
1-C3-179267	138.4	5	63	43.940	69.695	4.7	10.6	--	--	24.2	12.9	--	--	8.7	12.6	--	--	0.7	8.6	126.2	93	149.9	104.6	59.9	310.4	7976.5	446.2	335.1	47.5	376.2	44.5	686.7	46.5	197.2	23.4
1-C3-179350	128.4	1	64	43.942	69.694	2	10.5	10.1	10.1	52.8	17.1	10.2	23.7	--	--	5.4	9.6	3.3	9.4	207.1	124.8	23.8	68	80.2	355.7	9198	485.1	248.5	47	286.4	46.2	440	46.1	148.4	20
1-C3-179351	120.1	2	64	43.942	69.694	3.3	11.8	31.3	12.9	79	17	28.7	34.1	--	--	0.8	10.3	0.8	13.5	39.7	83.8	--	--	423	373.1	9724.7	522.4	279.6	39.2	293	44.2	545.1	48.2	160.1	23.9
1-C3-179352	120.3	3	64	43.942	69.694	9.2	14.8	13.2	16.4	75.6	20.3	13.3	20.7	2.9	11.3	10.1	13	10.1	9.4	145.2	128.1	106.5	83.8	--	--	7205.9	452.7	306.7	47.7	176.7	46.2	503.4	47.6	169.8	23
1-C3-179353	103.7	4	64	43.942	69.694	--	--	4.9	17.2	30.5	16.1	--	--	--	--	13.7	11.1	12.2	10.3	80.4	100.1	179.5	94	248.3	254	7587.9	520	249	45.8	236.4	54.7	598.4	55.4	161.4	27
1-C3-179354	118.6	5	64	43.942	69.694	6.6	10.8	2.4	8.8	80	19	5.5	18.4	8.2	9.5	10.8	12.6	--	--	100.4	94.2	--	--	--	--	7578.9	461.5	381.2	46.4	254.7	43.8	609.4	48.1	154.9	19.1
1-C3-179355	90.8	6	64	43.942	69.694	--	--	--	--	46.2	24.6	67	39.2	6.9	13.5	21.1	13.5	8.6	11.3	--	--	--	--	459.9	400.5	8153.4	525.6	265.4	55.1	246.2	61.2	718.7	61.9	103.3	22.6
1-C3-179356	101.1	7	64	43.942	69.694	5.2	13.2	5.7	11.2	11.5	12.6	--	--	--	--	8.8	18.6	19.8	12.9	55	119.9	48.3	90.7	198	292.7	7006.2	491.9	171	40.3	249.9	46.6	579.3	59.3	146	27.6
1-C3-179357	105.1	8	64	43.942	69.694	--	--	13.7	18	--	--	20.3	30.4	--	--	10.5	10.9	22.2	13.3	56.6	100.4	38.7	104.6	106.1	235.6	7459.2	493.8	226.1	46.7	271.4	51.6	695.6	53.5	143.7	23
1-C3-179358	132.5	9	64	43.942	69.694	7.5	11	2.2	8.7	12.2	12.5	27.9	22.1	23.2	11.3	13.4	9.1	1.7	10.2	38.9	97.9	23	73	--	--	9045.2	465.5	336.2	42.4	317.5	48.1	505.6	51	167.5	22.6
1-C3-179359	125.1	10	64	43.942	69.694	1	10.5	6.9	9.4	--	--	13.8	17.3	4.5	9.2	--	--	10.9	9	19	89	4.9	74.5	--	--	11045.1	506.8	323.3	43.1	407.7	54.7	561.8	48.4	120.3	22.1
1-C3-179268	111.5	1	65	43.911	69.729	10.5	15.8	--	--	74.6	20.6	--	--	12.5	9.9	--	--	2.2	10.2	165.5	138.2	35.6	90	415.6	319.3	6444	433.6	196.8	33.9	256.3	53.3	518.6	48.2	145.5	25.3
1-C3-179269	103.5	2	65	43.911	69.729	--	--	4.9	9.2	58.3	17.9	76.2	33	27	15.4	9.6	8.8	1.9	11	--	--	76.6	91.2	1376.3	488.3	7405.9	484.6	208.8	53.3	278.7	59.8	633.3	50.9	191.3	25.2
1-C3-179270	105.5	3	65	43.911	69.729	11.1	11.1	9.6	10.5	91.7	21.9	82.6	36.3	--	--	19.1	12.9	--	--	11.3	101.3	28.9	80.4	699.5	309.9	7541.2	500.7	288.3	55.7	170	54	554.3	54.4	97.6	27.1
1-C3-179271	93	4	65	43.911	69.729	12.2	15.1	3.1	18.9	109.8	28.1	5.3	21.9	16.5	13.3	14.2	14.9	5.6	13.5	--	--	150.9	160.9	--	--	6459.1	499.7	180.5	46.4	140	51.2	572.6	56.3	162.4	30.2
1-C3-179272	119.5	5	65	43.911	69.729	--	--	10.9	13.8	37.8	15.2	--	--	4.7	10.8	3	13.3	--	--	--	--	37.4	94.7	1508	520	9298.9	498.6	312.5	46.1	294.5	44.7	774.4	51.3	172.4	25.8
1-C3-179273	115.2	6	65	43.911	69.729	11.3	12.5	5	10.8	1.1	13.7	--	--	13.7	15.2	8.9	13.5	--	--	398	200.3	63.6	94.5	521.4	302.3	10555	538.9	373.7	53.5	395	58.4	808.7	60.6	273.4	28.8
1-C3-179274	130.4	7	65	43.911	69.729	21	11.6	11.1	9.1	--	--	64.3	22.8	16.4	12.3	13.7	12.8	12.2	12	4.6	83.6	49.9	90.3	1026.6	283.7	9698.3	484.3	372.2	49.6	299.3	52.5	712.9	50.3	171.1	23.8
1-C3-179275	111.4	8	65	43.911	69.729	--	--	2.6	8.2	3.5	12.1	8.9	21.4	13.8	17.1	14.2	10	5.2	9.8	85.5	125.6	98.6	90	518.7	319.2	10157.8	552.4	404.3	53.3	463.7	55.5	777.8	56.6	205.7	30.5
1-C3-179276	124.8	9	65	43.911	69.729	9.4	10.7	17	11.6	--	--	15.8	25.5	--	--	--	--	22.3	12.4	--	--	107.6	118.6	130.6	230.8	8985.5	485.7	221.1	47.4	400.2	47.9	796.1	51.8	187.7	26.3
1-C3-179325	118	1	66-1	43.898	69.754	8.1	13.9	9.2	10.4	3.3	10.9	14.6	26	49.7	10.8	16.2	11.7	--	--	280	188.8	--	--	705.4	337.6	7481.9	457.7	359.2	44.8	304.6	48.7	815.2	51.9	182.8	25.8
1-C3-179326	116.4	2	66-1	43.898	69.754	20.2	11.9	1.2	8.5	25.6	13.3	--	--	--	--	5.7	12.1	1.7	9.5	56.3	101.1	24.5	104.9	29.5	417	9071.7	509.4	312.7	55.9	376.2	58.3	852.1	55.1	220.2	26.6
1-C3-179327	120.6	3	66-1	43.898	69.754	28.6	14.3	22.2	9.5	61.8	21.7	--	--	8.8	11.6	8.2	9.7	4.8	12.3	24.7	126	30.4	90.3	94.9											

Maine Yankee Marine Sampling Study

			nuclide		60Co		60Co		137Cs		65Zn		22Na		54Mn		58Co		133Ba		7Be		210Pb		40K		214Bi		214Pb		212Pb		208Tl			
			Gamma energy (keV)		1173.23		1332.51		661.62		1115.52		1274.54		834.81		810.75		383.7		477.56		46.52		1460.75		609.32		351.99		238.63		583.14			
			Branching Ratio		0.9986		0.9998		0.8462		0.5075		0.9994		0.9998		0.9945		0.0884		0.103		0.04		0.107		0.4609		0.371		0.431		0.861			
sample	mass(g)	depth(in)	station	lat.	long.	pCi/kg	+/-	pCi/kg	+/-	pCi/kg	+/-	pCi/kg	+/-	pCi/kg	+/-	pCi/kg	+/-	pCi/kg	+/-	pCi/kg	+/-	pCi/kg	+/-	pCi/kg	+/-	pCi/kg	+/-	pCi/kg	+/-	pCi/kg	+/-	pCi/kg	+/-			
1-C4-179422	457.6	1	73	43.949	69.699	7.2	5.5	26.6	7.7	47.1	10	--	--	--	--	5.7	4.8	3.7	4.5	70.9	57.4	104.7	59.4	873	257.7	6082.5	232.3	258.8	22.4	223.9	24.1	350.2	26.3	127	12	
1-C4-179423	363.8	2	73	43.949	69.699	15.2	7.9	29.1	9.1	79.3	14.6	21.6	21.2	8.1	6	1.7	7.6	4	4.6	9.3	50.1	47	41.8	394.2	326.3	7509.5	295.9	239.8	28.7	245.8	30.9	478.2	30.5	129.7	15.5	
1-C4-179424	342.1	3	73	43.949	69.699	--	--	4.4	5.7	59.9	12	11.9	11.8	4.3	6	--	--	--	--	--	--	--	--	565.9	407.5	8347.4	324.6	234.2	25.7	278.5	33.4	521	31.8	151.5	15.1	
1-C4-179425	426.6	4	73	43.949	69.699	17.2	6.5	5.8	4.9	79.2	12.5	--	--	--	--	15.9	7	--	--	18.5	61.4	2	39.2	569	259.4	7411.9	262.9	222.8	25.1	261.1	30.6	481.3	26.4	141.5	13.7	
1-C4-179426	351.2	5	73	43.949	69.699	1.5	6.7	2.2	8.9	113.6	14.8	3.7	12.6	--	--	9.5	5.5	--	--	2.4	51	--	--	857.4	348.3	8060.6	305.4	284.5	32.3	362.8	33.1	516.1	30.2	113.7	15.8	
1-C4-179427	335.2	6	73	43.949	69.699	11.9	7.1	1.7	5.5	93.6	15.7	--	--	3.3	5.7	5.6	6.4	--	--	--	--	30.6	59.5	1049.6	432.5	7843.8	315.7	308.9	31.3	278	33.3	495.1	33	140.7	15.6	
1-C4-179428	343.3	7	73	43.949	69.699	6	7.3	6.1	6.1	93.7	14.9	9.6	12	--	--	7.8	7.3	0.4	5	103.5	71.6	19.9	58.1	--	--	7836	306.7	208.6	29.5	268.2	32.9	576.2	33.4	162.6	15.6	
1-C4-179429	335.4	8	73	43.949	69.699	7.7	7.6	17.6	11	123.3	17.1	--	--	6.6	6.1	0.8	5.3	7.9	5.1	--	--	--	--	616.1	407.4	8905.5	331.2	239.5	30.5	255.3	34.3	694.7	31.2	195.3	16.7	
1-C4-179430	315.3	9	73	43.949	69.699	1.8	7.3	9.6	6.6	153.5	17.6	11.4	12.8	17.8	8.1	0.3	7.2	4.6	5.6	10.7	60.3	12.7	61.1	687.1	377.4	9047.8	344.6	279.6	32.3	275.2	37	716.4	35.4	194.9	18.6	
1-C4-179431	388.9	10	73	43.949	69.699	--	--	1	4.9	124.1	15.7	5.1	13.5	7.6	5.5	6.9	5.3	0.9	5.2	28.3	48.2	92.4	45.7	409.6	326.5	8184.3	293.6	230.8	27.5	273.2	31.2	607.7	31.1	185.8	15.4	
1-C4-179432	355.5	11	73	43.949	69.699	10.7	8.2	--	--	170.6	18.3	--	--	--	--	--	--	2.6	5.6	176.9	98.6	1.6	57.2	289.6	333.9	8937.1	324.2	271.2	28.5	252.6	32.8	623.8	33.7	179.2	16.6	
2-NG-179009	1423	S	73	43.949	69.699	19.5	10.5	45.8	11.2	100.1	16.5	90.1	24.2	13.6	10.1	1.8	6.6	--	--	72.8	60.5	301.1	106	118.6	383.6	8359.5	363.3	309.5	34.7	376.2	40.2	537.1	32.8	147.8	17.3	
2-C4-179433	602.6	1	74	43.950	69.698	20.5	12.3	0.8	6.1	67.5	10.3	--	--	2.7	6	--	--	2.1	4.5	30.7	50.3	--	--	--	--	6719.2	288.6	230.2	25.5	203.4	25.9	378.6	22.6	99.4	13.1	
2-C4-179434	377.9	2	74	43.950	69.698	4.8	9.2	--	--	162.4	20.8	14.9	17.7	3.5	9.5	--	--	--	--	93.9	79	--	--	508.1	278.6	9099.9	435.5	309.9	32.7	304.8	38.4	493.5	35	180.9	21	
2-C4-179435	311.1	3	74	43.950	69.698	8.7	11.7	4.4	13.6	183.8	21.6	7.9	29.9	--	--	--	--	2.4	9.4	141.4	82.4	138	109.2	1043.6	569.4	10240.4	502.4	433.7	47.9	386.6	46.5	661.8	40.9	156.6	23.4	
2-C4-179436	310.2	4	74	43.950	69.698	2.9	10.2	11	11	201	23.9	--	--	--	--	16.7	14.8	24.1	10.8	92.1	96.4	--	--	130.1	454.2	9912.5	495.9	252	38.7	327.2	54.4	629.8	46.5	209.2	23.9	
2-C4-179437	375.9	5	74	43.950	69.698	16.8	11.2	13.6	8.7	261.8	24.5	17	17.5	10.4	11.5	8.6	7.8	--	--	70.8	74.7	62	65.3	--	--	10485.5	458.2	315	36.4	352.3	43.4	699.9	37.3	188.3	21.4	
2-C4-179438	330.5	6	74	43.950	69.698	16.4	12.2	--	--	155	22.7	11.9	22.3	1.3	11.6	10.5	13.1	--	--	3.5	77.1	76.7	99.1	--	--	8800.2	461.2	352.6	44.7	370	44.9	666.5	40.7	184.3	20.5	
2-C4-179439	338.6	7	74	43.950	69.698	--	--	--	--	209.1	25.9	--	--	--	--	--	--	23.7	12.6	88.9	132.8	94.2	73	--	--	9674.9	478.3	315.5	44.4	308	46.4	650.1	41.1	191.1	23.2	
2-C4-179440	331.2	8	74	43.950	69.698	7.3	12.9	5.5	12.4	157.5	24	--	--	37.4	18.2	30	13.2	--	--	--	--	--	--	596.3	497	10759.8	491.6	389.6	46.2	275.8	49.1	737.2	42.4	196.5	25	
2-C4-179441	332.8	9	74	43.950	69.698	6.3	15.4	--	--	110.1	24.2	28.8	23.9	--	--	3.2	8.9	9.5	8.3	20.9	75.3	18.4	67.6	716.5	552.3	9666.4	473.5	303.3	37.3	301.3	41.4	782.4	41.5	242.6	24	
2-C4-179442	352.4	10	74	43.950	69.698	--	--	1.9	11.8	29.6	11.3	3.2	24	--	--	5.5	8.8	13.2	10	56.9	90.8	--	--	--	--	9679.7	459.1	348.4	43.3	370.8	43.9	692.9	39.8	244.7	23.6	
2-C4-179443	342.2	11	74	43.950	69.698	--	--	19.2	13.1	40.7	11	--	--	9.5	12.3	7.6	13.3	6.8	8.6	142.1	120.5	78.8	113.1	396.7	419.8	9563	467.3	294	41.9	317.3	44.3	829.8	39.6	164.2	23	
2-NG-179010	1416	S	74	43.950	69.698	52.6	15.3	20.2	10.2	162.8	19.2	80	28.8	5.4	9.2	0.5	5.8	--	--	133.2	64.8	245.4	97.1	--	--	8877.8	369.2	330.7	34.3	313.5	37.5	535.2	33.5	97.8	19	
1-NG-179011	1421.5	S	75	43.951	69.698	20.2	7.8	28.8	8.2	96.8	11.8	--	--	2.6	4.8	0.8	4.3	6.3	4.5	--	--	103.1	74.4	916.2	332.3	8043.4	258.6	316.5	27.5	322.6	31.1	509.7	32.7	132.1	12.1	
2-NG-179012	1278.3	S	76	43.954	69.698	59.9	17.7	50.8	13.9	109.1	18.6	--	--	0.7	7.7	9.2	11.8	8.7	7	46.3	82.8	324.2	123.9	--	--	9439.8	401.3	246.9	36.7	360.6	38.3	598.7	35.7	169.7	19.2	
2-C4-179213	472.6	1	77	43.955	69.697	9.6	8	21.6	8.1	54.6	11.8	--	--	3.1	6.8	2.7	5.6	2.7	5.7	127.4	62.5	44.1	50.9	282	327.1	6476.9	332.2	160.7	28.2	168.6	28.6	371.1	25.7	85	14.9	
2-C4-179214	368.6	2	77	43.955	69.697	--	--	14.8	9.2	106.6	20.8	--	--	2.7	9.1	4.1	7.6	17.8	7.6	52.3	104.3	153	98	806.2	509.1	8812.2	446	241.7	35.7	295.3	40.1	491.3	35.2	149.5	21.7	
2-C4-179215	324.9	3	77	43.955	69.697	13	11.3	--	--	128.5	24	23.1	20.6	--	--	4.3	9.8	--	--	71.3	77.9	218.9	110.7	1174.3	430.9	11315.2	514.6	245.5	33.3	443.5	46.6	625.8	40.2	177.3	23.4	
2-C4-179216	267.7	4	77	43.955	69.697	2.3	12.2	2.5	11.1	161.3	29.5	59	38.1	7.3	11.2	40.4	15.2	17.4	9.9	34.6	141.6	100.8	133.1	--	--	10515	559.1	296.1	47.8	254.9	51.5	626.6	45.7	132.8	18	
2-C4-179217	335.6	5	77	43.955	69.697	5.4	11.8	9.1	8.4	221.9	25.7	2.2	18.5	13	12.6	12	10.8	4	8.9	110.4	80.5	--	--	573.9	481.6	12209.5	521	332.8	42.3	379.9	49.3	630.9	39.5	152.1	24	
2-C4-179218	314	6	77	43.955	69.697	13.4	13.6	6.1	13.2	222.2	29.3	--	--	44.1	15	--	--	--	--	--	--	--	--	--	--	13888.4	576.4	327	47.2	315.9	47.4	889.5	45.4	230.5	27.7	
2-C4-179219	331.7	7	77	43.955	69.697	--	--	6.8	12.6	202.3	23.6	--	--	--	--	10.4	10.2	11.5	9.5	--	--	--	--	--	--	12823.3	531.8	459.1	49.3	369.8	46.6	856.2	46.4	233.7	24.8	
2-C4-179220	337.6	8	77	43.955	69.697	12.5	14.4	13.1	10.4	130.1	23.5	--	--	25.1	11.5	17.2	8.9	4.4	8.4	--	--	--	--	--	--	13903.3	551.8	374	40.1	326.2	42.4	988.2	44.4	238.1	25.8	
2-C4-179221	316.5	9	77	43.955	69.697	--	--	--	--	159.5	24.9	109.2	33.7	5.2	11.6	23.2	10.5	4.7	9.1	6.1	125.1	69.7	82.2	173.9	478.1	14074.4	575.9	400	42.3	355.1	50.8	1053.7	47.1	264.6	27.5	
2-C4-179222	324.7	10	77	43.955	69.697	12.1	12.8	11.5	14.3	167	25.9	11.6	20.5	2	11.2	6.7	16.6	1.3	9.1	--	--	--	11.3	73.1	--	--	14413	581.8	385.6	45.9	352.4	49.8	924.9	47.3	274.3	26.8</

Maine Yankee Marine Sampling Study

			nuclide		60Co		60Co		137Cs		65Zn		22Na		54Mn		58Co		133Ba		7Be		210Pb		40K		214Bi		214Pb		212Pb		208Tl		
			Gamma energy (keV)		1173.23		1332.51		661.62		1115.52		1274.54		834.81		810.75		383.7		477.56		46.52		1460.75		609.32		351.99		238.63		583.14		
			Branching Ratio		0.9986		0.9998		0.8462		0.5075		0.9994		0.9998		0.9945		0.0884		0.103		0.04		0.107		0.4609		0.371		0.431		0.861		
sample	mass(g)	depth(in)	station	lat.	long.	pCi/kg	+/-	pCi/kg	+/-	pCi/kg	+/-	pCi/kg	+/-	pCi/kg	+/-	pCi/kg	+/-	pCi/kg	+/-	pCi/kg	+/-	pCi/kg	+/-	pCi/kg	+/-	pCi/kg	+/-	pCi/kg	+/-	pCi/kg	+/-	pCi/kg	+/-		
2-C4-179105	308.1	2	99	43.952	69.698	5.9	11.7	3.9	8.9	135.5	24.6	7.3	19.6	9.2	11.4	2.8	8.7	5.5	7.6	132.8	98	221.6	101.9	--	--	9496.3	490.2	313	46	358.2	45.2	567.8	40.5	151.2	22.9
2-C4-179106	287.4	3	99	43.952	69.698	27.2	20.5	6.2	9.5	117	21.7	3.9	21.8	6.8	12.4	6.3	12.6	--	--	319.6	107.7	--	--	191.5	285.3	10228.5	542.9	222.1	39.5	269.2	47.8	643.2	41.3	161.5	21.9
2-C4-179107	291.1	4	99	43.952	69.698	2.8	15.9	0.5	9.8	127.2	24.2	54.2	43.8	19.7	10.1	5.2	9.4	3.6	8.6	79.5	80.7	250.6	122.8	926.3	514.6	9538.8	513.2	319.9	47.1	386.1	46	617.6	44.1	144.1	24.8
2-C4-179108	341.7	5	99	43.952	69.698	7.1	13	16.6	10.2	99.4	19.1	20.9	25.7	18.1	10.9	7.6	8.3	2.1	9.6	71.1	124.3	--	--	1224	568.8	10297.3	478.5	251.7	38.3	237.3	36.4	493.9	41.5	133.5	19.9
2-C4-179109	294.1	6	99	43.952	69.698	11.3	13.5	11.2	16.2	148.2	21.6	15.3	19.3	--	--	12.5	9.2	13.7	9.1	--	--	27.8	93	262	463.2	9983.7	520.4	297.2	39.7	333	47.4	655.6	42.8	218.9	24.6
2-C4-179110	324.3	7	99	43.952	69.698	--	--	1	9.6	150.9	24.1	17.4	27.3	--	--	7.1	10.9	0.7	8.3	3.6	81.9	--	--	543	607.4	11416.3	521	242.8	46.4	372.4	45.7	789.9	43.3	205.1	24.2
2-C4-179111	358.8	8	99	43.952	69.698	23.5	16.5	11.4	9.3	155.1	23.8	--	--	--	--	--	--	10.6	8	103.2	76.5	--	--	--	--	11130.2	468.6	298.7	41.4	359.2	42.4	770.1	40.4	192.3	24
2-C4-179112	321.7	9	99	43.952	69.698	3.7	10.8	--	--	139.3	22.1	18.7	21.3	--	--	12.1	10.7	5.9	8.6	--	--	172.8	90.7	1282.9	625.8	11637.9	531.2	333.2	47.3	368.3	49.4	939.2	44.3	219.4	26.2
2-C4-179113	230.6	10	99	43.952	69.698	1.3	15.6	1.5	11.3	148.2	31.7	24.4	37.3	26.9	14.9	72.7	21.4	3.7	11.3	--	--	--	--	111.4	588.6	13274	665.7	388.1	59.5	447.8	62.5	1102.4	56.5	295.3	32.7
2-C4-179114	426.9	11	99	43.952	69.698	4.2	7.9	15.7	9.5	115.8	17.9	1.3	16.8	--	--	8.1	8.1	--	--	--	--	97.7	89.9	--	--	9890.6	417.7	277.9	31.1	337.6	37.4	681	35.5	187.4	21.2
1-NG-179041	1428	S	99	43.952	69.698	44.8	13.1	31.2	8.5	80.2	12.4	--	--	1.5	4.1	8.4	5.2	3.5	4.3	--	--	261.6	78.7	551.5	141.7	7066.8	241.2	235.1	24.8	244.2	29	473.3	28	152.2	13.4
1-NG-179042	1338.3	S	100	43.952	69.698	14.2	8.1	21	7.3	71.6	11.2	--	--	--	--	5	4.6	2.3	4.5	17.7	69.3	170.2	48.9	908.5	325	8563.4	272.8	303.3	26.9	386	30.7	590.5	32	151.7	14.5
2-C4-179225	399.2	1	101	43.952	69.699	24.1	14.3	6.4	9.1	81	18.1	124.3	39.9	5.7	7.7	11.6	11	6.4	6.5	46.4	63.7	--	--	358.4	486.2	8379.9	394.6	252	35.1	204.6	35.7	394.2	30.3	117.1	20.4
2-C4-179226	262.6	2	101	43.952	69.699	14.9	13.7	--	--	74.3	23.1	107.3	36.3	--	--	--	--	12.5	14.2	379.1	128.3	--	--	--	--	11141.6	578.7	295.9	53.1	335.3	52.6	585	46.5	118.5	27.5
2-C4-179227	256.9	3	101	43.952	69.699	4.7	14.2	--	--	111.5	22.1	10.2	22.3	6.8	17	--	--	14.8	9.9	108.2	115.9	28.6	81.8	1237.6	672.5	11672.2	610.2	351.1	43	350.6	46.9	600.9	47.7	150.4	26.7
2-C4-179228	243.1	4	101	43.952	69.699	62.4	25	5.6	14.8	99.3	24	--	--	10.7	12.1	7.1	13.9	--	--	114.3	101.7	3.4	104.9	870.3	701.5	11650.3	599.8	389.5	54.5	492.6	57	681.3	49.4	210.6	28.9
2-C4-179229	269.6	5	101	43.952	69.699	10.1	11.8	9.1	13.7	101.7	21.5	20.9	24.2	--	--	8	13.5	10.2	10.1	--	--	72.8	85.8	598.7	529.8	11361.5	567.6	464.5	51.6	335	54.3	537.9	45.9	177.4	25.9
2-C4-179230	262.3	6	101	43.952	69.699	13	18.8	25.1	13.9	154.1	31.1	1.4	19.8	13.1	17.1	3.3	11.6	--	--	151.5	171.8	--	--	517.5	540.8	11775.5	573.2	306.4	44.7	325	43.6	660.1	47.3	176.2	21.9
2-C4-179231	332.7	7	101	43.952	69.699	8.3	11.8	9.8	18.5	169.3	22.4	--	--	11.2	13.3	25.3	16	1.5	8.7	--	--	93	77.7	505.9	488.5	10551.7	529.2	298.1	36.4	365.6	46	631	44	201	24.6
2-C4-179232	364.4	8	101	43.952	69.699	5	8.6	1.9	8.8	161.2	23.7	12.4	30.5	3.6	12	11.3	9.2	1.9	9.5	22.2	82.6	20.2	105.8	--	11063.8	477.6	295.1	40.9	357.9	44.2	679.5	38.5	187.9	22.7	
2-C4-179233	315.4	9	101	43.952	69.699	--	--	0.7	10	212.8	24.1	--	--	4.7	11.3	15.5	11.1	--	--	51.4	89.3	--	--	286.9	360.4	11331.8	511.6	346.4	46.1	329	47.2	802.2	44.6	219.6	22.6
2-C4-179234	502.3	10	101	43.952	69.699	13.2	8.6	6.8	6.3	163.8	17.3	58.4	26.7	6.8	6.8	8.2	8.9	4.2	7.9	26.1	45.3	73.2	78.9	--	--	8040.2	348.8	213.4	30	216.2	31.2	391.3	27.9	131.7	15.8
1-NG-179043	1374	S	101	43.952	69.699	12.2	9	20.4	8.1	85.1	12.5	4.6	10	8.9	4.9	--	--	1.4	4.1	--	--	167.7	90.3	1021.5	234.1	8302	263.4	203.1	25.5	344.5	30.3	500.5	29.2	142.8	13.3
1-NG-179044	1354.3	S	102	43.954	69.698	30.7	9.2	11.2	5.2	89.9	12	--	--	--	--	5.8	5.2	1.3	4.9	19.4	79.1	451.1	68.7	433.8	232.6	7649.6	250.9	311.6	27.3	270.6	29.8	486.1	28.8	115.6	13.4
1-NG-179045	1350.2	S	103	43.954	69.698	16.5	6.3	16.5	6.2	118.5	12.7	16.7	17.9	--	--	1.4	5.2	2.3	4.3	15.6	73.9	235.3	87.7	474.4	305.2	7232.4	249	231.3	25.2	225	28.5	505.8	27.7	130.5	13.4
1-NG-179049	1329.5	S	104	43.955	69.697	50.6	10.6	23.5	8.9	84	13.6	--	--	0.4	4.5	8.9	4.7	8.1	5.3	--	--	488.4	98.6	718.1	319.2	7908.1	259.8	232.3	25.7	296.5	29.8	515.5	28.8	137.1	13.7
2-C4-179201	416.8	1	105	43.958	69.698	26	11	--	--	72.7	12.4	28.4	17.4	--	--	--	--	--	--	69.4	92.4	153	92.7	466.5	351.3	8525.1	399.3	317.9	36	320.8	37.4	613.5	33	135.2	18.9
2-C4-179202	342.7	2	105	43.958	69.698	--	--	11.9	7.8	84.8	17.1	35.1	28.1	4.8	9.1	20.2	11	--	--	--	--	35.8	66.4	219.5	452.5	10378.5	487.4	297.6	43.9	442	52.6	636.2	38	143.5	17.4
2-C4-179203	360.6	3	105	43.958	69.698	3.1	13.4	14	8	81.7	19.9	9.4	17	--	--	1.2	7.6	--	--	--	--	64.6	88.7	--	--	8873.1	437.5	321.3	39.5	304.6	40.8	486.8	35.7	162.7	21.1
2-C4-179204	315.3	4	105	43.958	69.698	2.9	12	--	--	70.1	23.4	--	--	--	--	8.9	8.9	--	--	216.6	135.6	18.1	86.4	--	--	11258.4	525.9	301.4	46.4	371.8	47.2	667.7	41.9	183.3	23.1
2-C4-179205	329.1	5	105	43.958	69.698	--	--	2.1	7.9	49.9	16.2	--	--	18.3	15.7	19.7	11.6	--	--	165.3	106.6	5	102.8	468.2	592.4	10744.2	506.3	361.5	44.5	375.4	47.2	809.4	41.1	212.3	21
2-C4-179206	317.7	6	105	43.958	69.698	3.8	11.9	--	--	101.8	23.5	5.3	19.7	--	--	7.7	11.5	--	--	--	--	54	75.4	--	--	11457.1	527.8	323.9	39.4	396.1	46.1	698.1	42	221.6	24.5
2-C4-179207	313.2	7	105	43.958	69.698	8.7	11.4	15.2	10.2	24.8	17.5	43.2	24.5	--	--	3.5	8.7	0.2	12.4	66.5	81.5	53.5	102.2	--	--	10736.2	520.3	297.9	45.2	352.4	51	665.9	41.1	230.5	21.8
2-C4-179208	369.8	8	105	43.958	69.698	14.7	11.1	14.3	13	24.5	13.6	10.7	20.1	--	--	4.1	8.1	--	--	73	93	--	--	178.6	489	13405.1	519.4	245.8	44.9	474.8	46	897.8	41.2	243.3	24.5
2-C4-179209	361.6	9	105	43.958	69.698	5.8	11.9	28.8	10.5	--	--	60.8	27.4	1.8	13.9	23.5	11.5	6.4	8	80	78.7	--	--	--	--	13891.3	543.4	441.3	47.2	475	46.5	1083.9	44.2	256.7	25.2
2-C4-179210	380.5	10	105	43.958	69.698	--	--	6.3	7.8	9.2	15.7	--	--	11.1	10.2	--	--	11.5	10.2	48.7	93.9	5.4	95.5	298.9	421.7										

Maine Yankee Marine Sampling Study

			nuclide		60Co		60Co		137Cs		65Zn		22Na		54Mn		58Co		133Ba		7Be		210Pb		40K		214Bi		214Pb		212Pb		208Tl		
			Gamma energy (keV)		1173.23		1332.51		661.62		1115.52		1274.54		834.81		810.75		383.7		477.56		46.52		1460.75		609.32		351.99		238.63		583.14		
			Branching Ratio		0.9986		0.9998		0.8462		0.5075		0.9994		0.9998		0.9945		0.0884		0.103		0.04		0.107		0.4609		0.371		0.431		0.861		
sample	mass(g)	depth(in)	station	lat.	long.	pCi/kg	+/-	pCi/kg	+/-	pCi/kg	+/-	pCi/kg	+/-	pCi/kg	+/-	pCi/kg	+/-	pCi/kg	+/-	pCi/kg	+/-	pCi/kg	+/-	pCi/kg	+/-	pCi/kg	+/-	pCi/kg	+/-	pCi/kg	+/-	pCi/kg	+/-		
2-C4-179311	342.5	10	113	43.945	69.696	--	--	--	--	129	19.8	10.7	22.5	8.9	13.1	4.4	9.6	4.9	10	83.4	142.9	34.6	102.5	--	--	10986.8	499.4	318	43.3	360	46	752.3	41.3	271.5	24.2
2-C4-179312	344.1	11	113	43.945	69.696	--	--	--	--	116.7	19.8	3.3	25.3	10.9	10.5	0.6	9.1	--	--	3.4	73.2	110.5	78	80	623.2	10144.9	489.3	291.3	44.8	474.8	47.3	631.9	41.8	196.4	24.2
2-C4-179313	237.5	12	113	43.945	69.696	0.4	22	14.8	16.7	161.1	25.7	--	--	23.3	11.7	25.5	17.8	--	--	--	--	194.5	132.2	584.4	690.3	14202	675.4	390.7	60.8	319.4	60.4	834.6	54.1	202.1	34.3
2-C4-179314	166.1	13	113	43.945	69.696	39.9	20.5	20.5	23	80.1	28	40.7	44	14.4	26.8	9.1	14.6	3.8	15.4	148.7	160.7	--	--	876.1	605.6	13983.2	805.6	350.8	70.9	426.2	77.2	883.3	68.4	234.4	38.5
1-NG-179061	1350.3	S	113	43.945	69.696	73.5	13.1	90.3	13	61.2	9.5	93.1	19.4	3.1	4.8	--	--	--	--	110.3	70.1	364.5	98.8	1112	321.8	7897.2	258.4	254.2	26.3	294.1	29.8	487.2	29.1	134.2	13.8
1-NG-179062	1302.6	S	114	43.947	69.696	71.8	15.2	106.4	13.2	57.2	11.9	--	--	--	--	3.1	6.3	6.5	6.2	34.3	50.9	379.9	108.5	484.5	265.9	7685.5	260.1	268.3	27.9	255	31.9	576.8	32.8	154.5	14.6
1-NG-179063	1361.5	S	115	43.946	69.696	103.5	14.3	87.4	11.5	71.6	10.7	--	--	4.8	4.8	5.5	4.7	1.4	4.7	--	--	386.5	108	553.4	208	7743.9	254.7	273.8	26.8	288.2	31	524.4	29.1	129.4	13
2-NG-179064	1307.5	S	116	43.946	69.695	124.8	18.8	168.7	20.1	82.7	17.1	4.2	16.5	3.6	8.2	4.7	8.2	15.6	9	--	--	225.6	112.9	--	--	8735.6	389.4	278.3	36.4	386.9	39.8	592.2	36.6	149.9	15.8
2-C4-179293	304.8	1	117	43.949	69.693	25.7	13.4	40.2	14.3	36.3	14.4	6.2	17.9	--	--	0.7	8.1	4.9	8.8	--	--	--	--	529.6	433	8939.4	492.4	217.4	42.4	326.3	36	471	38.4	148.2	23.9
2-C4-179294	182.6	2	117	43.949	69.693	18.7	22	24.2	15	60.9	28.4	15.4	33.1	2.4	23.5	48.6	20.8	--	--	--	--	98.5	147.4	--	--	12074.2	736.7	438.8	67.3	453.4	61.8	745.9	61.9	185	30.6
2-C4-179295	269.1	3	117	43.949	69.693	17.9	14.3	5.1	14.3	55.3	15	11.2	21.8	19.4	15.3	1.6	9.6	6.8	11.7	30.1	86.1	63.8	89.8	377.2	360.7	10267.1	553.9	289.6	47.1	270.6	49.7	354.9	37.9	122.9	21.4
2-C4-179296	259.1	4	117	43.949	69.693	5.8	12.8	10.5	11.7	93.2	24.7	32.6	29.4	3.8	10	5.8	10.6	--	--	--	--	118.3	83.5	--	--	10476	558.3	301.2	49.5	331.9	52	645	45.6	123.8	26.5
2-C4-179297	338.4	5	117	43.949	69.693	12.5	13	28.1	13	38.5	14.3	15.5	27.9	5.8	11.1	--	--	0.6	7.8	88.9	74.3	137.7	68	1087.7	492.8	9696	469.2	236.8	43.1	361.4	42.5	481.9	37.8	144.5	21.5
2-C4-179298	297.8	6	117	43.949	69.693	10.1	12.5	4.6	9	56	16.5	45.4	29.1	7.7	10.2	3.4	12.9	14.2	8.5	27.2	81.3	157.8	103.6	209.4	443.3	9354.4	492.3	291.2	39.7	356.1	46.2	591.5	41.5	117	19.9
2-C4-179299	191.1	7	117	43.949	69.693	37.8	29.5	--	--	72.8	28.1	--	--	14.8	18.3	40.7	17.5	8.9	12	96.9	198.3	25.7	107	--	--	10684.5	649.8	403	66.9	446.1	82.6	634.9	59	171.8	29.7
2-C4-179300	501.6	8	117	43.949	69.693	22.8	10.4	15.3	8.8	42.8	13.1	--	--	5.2	8.6	6	9	--	--	20.8	91.2	24.4	58.9	469.9	277	7678.2	346	192.2	31.8	259	30.5	394.9	27.7	100	15
2-C4-179301	519.3	9	117	43.949	69.693	11.6	7.5	2.2	6.8	34	12.9	--	--	--	--	0.8	5.6	6.9	6.2	--	--	26	60.8	438	293.8	7556.7	330	250.3	29.6	245.3	30.7	479.1	26.5	110.6	15.8
2-NG-179065	1531.5	S	117	43.949	69.693	14.3	11.2	33.1	11.4	27.8	12.1	--	--	--	--	1.1	8.2	--	--	--	--	302.5	111.5	988.2	601.3	10327.8	385.1	395.3	35.4	447.5	39.7	710.2	34.1	183.3	18.7
2-C4-179235	613	1	118	43.952	69.692	19.3	13.1	--	--	7.3	7.6	63.5	17.8	7.8	8.1	--	--	7.9	5.5	--	--	--	--	--	--	8889.8	331.9	284.6	28.6	229.3	27.5	414	23.9	99.2	11.9
2-C4-179235	613	1	118	43.952	69.692	19.3	13.1	--	--	7.3	7.6	63.5	17.8	7.8	8.1	--	--	7.9	5.5	--	--	--	--	--	--	8889.8	331.9	284.6	28.6	229.3	27.5	414	23.9	99.2	11.9
2-C4-179236	369.1	2	118	43.952	69.692	1.6	18.4	--	--	25.1	11.4	8.1	25.8	22.1	10.6	11.1	9.2	--	--	43.9	115.5	99.7	78.2	329.7	345.5	12303.5	494.3	448.3	43.9	459.2	44.6	668.5	38.1	165.2	20
2-C4-179237	431.4	3	118	43.952	69.692	16.8	14.6	3.2	8.9	34.6	17.7	--	--	--	--	4.5	7.6	--	--	56.4	64.6	8.5	80.1	148.8	387.2	12093.7	459.2	385.9	37.8	334.6	39.9	605.5	33.9	139.9	18.8
2-C4-179238	351.8	4	118	43.952	69.692	25.1	15.7	--	--	28.5	10.7	--	--	--	--	--	--	--	--	120.7	88.2	53.4	82.5	432.8	570.5	12612.9	524.2	367.8	46.9	397.4	45.3	500.7	34.9	200.1	22.4
2-C4-179239	497.1	5	118	43.952	69.692	11.5	10.2	--	--	--	--	--	--	--	--	4.2	13.3	1.7	6.6	218.9	119.9	63.2	58.3	--	--	13696.2	456.7	405.4	37.3	369.5	36	780.9	34.9	205	19.9
2-C4-179240	376.6	6	118	43.952	69.692	--	--	8.1	8.7	3.3	9.1	--	--	6.9	10.3	1.5	7	10.5	9.9	21.5	73.7	--	--	70.6	392.6	13715.4	529.6	471.1	38.8	437.2	42.7	729.7	39.6	241.7	18.8
2-C4-179241	386	7	118	43.952	69.692	28.1	11.1	5.3	8.9	4.6	12.8	--	--	10.1	21.1	3.4	8	1.1	9.2	--	--	19.1	105.4	--	--	12025.3	486.4	422.7	41.9	364.8	43	715.8	37.7	179.6	22.1
2-C4-179242	415.6	8	118	43.952	69.692	5.1	10.5	1.6	10.5	12.3	9.8	1.8	18	--	--	11.4	12	21.4	10.4	--	--	--	--	--	--	11052	452.5	354.7	44	340	40.8	699.5	35.1	162.6	20.1
2-C4-179243	283.3	9	118	43.952	69.692	--	--	6.4	13.5	21.7	13.6	--	--	--	--	3.1	10	19.4	14.3	65.4	113	82.2	109.8	1282	607.3	14390	630.1	423.6	53.3	537.3	54.8	764.9	47.3	231	28.1
2-C4-179244	414.8	10	118	43.952	69.692	16.2	15.5	--	--	3.9	8.9	12.2	21.4	5.2	10.9	3.1	7.6	7.7	7.2	--	--	121.2	62.7	632.4	518.9	12347.8	482.6	400.4	43.5	467.9	42	733.4	36.4	211.8	21
2-C4-179245	340.9	11	118	43.952	69.692	15.9	14.3	26.4	11.5	3.6	15.5	3.3	17.8	14.3	11.1	10.2	8.7	--	--	--	--	39.6	100.1	--	--	12258.6	537.2	369.4	40.8	321.9	50.4	710.5	40.7	206.5	22.9
2-C4-179246	850.6	12	118	43.952	69.692	2.1	4.7	--	--	8.2	5.4	1.8	9.6	1.7	5.2	--	--	7.1	5	27.2	57.6	2.9	30.7	152.4	147.9	6296.6	236.8	227.5	21.9	265.2	21.7	401.3	19.3	125.6	11.5
2-NG-179066	1776.3	S	118	43.952	69.692	9	8.6	24.5	8.5	28.2	11	11.3	14.6	1.1	7.2	7.3	6.3	2.4	7	--	--	172.4	64.3	353.2	480	11095.2	368.9	385.5	32.6	406.1	33.4	566.9	29.7	130.8	16.3
2-NG-179067	1443	S	119	43.953	69.692	34.4	15	51.1	14.9	71.7	15.6	--	--	1.3	7.3	5	6.9	6.7	10.1	--	--	192.6	120	908.4	532.1	8760.6	364.2	264.4	35.6	336.5	36.4	593.2	35.1	122.1	18.7
2-NG-179068	1370.9	S	120	43.948	69.694	103.8	16.7	125.4	18.8	69.6	11.9	12.2	17.4	--	--	1.3	8.3	--	--	9.9	86.5	191.5	76.4	455.5	488.9	7860.9	359.7	300.2	35.7	330.9	38.2	559.3	33.2	155	16.5
2-NG-179069	1389	S	121	43.949	69.693	104.9	21.4	81.8	18.3	80.3	17.3	22.8	18.3	1.4	8.1	12.7	7.4	15.6	7.3	95.9	104.4	315	81	595.4	681.6	8819.6	369.5	266.9	36.1	287.3	37.7	641.4	34.9	161.7	17.9
2-NG-179073	1370.9	S	122	43.950	69.692	80.2	16.3	21.1	12.5	53.9	15.9	--	--	16.3	8.7	24.2	13	--	--	64.8	89.9	242.2	86.4	--	--	9552.3	396.9								

Maine Yankee Marine Sampling Study

			nuclide		60Co		60Co		137Cs		65Zn		22Na		54Mn		58Co		133Ba		7Be		210Pb		40K		214Bi		214Pb		212Pb		208Tl		
			Gamma energy (keV)		1173.23		1332.51		661.62		1115.52		1274.54		834.81		810.75		383.7		477.56		46.52		1460.75		609.32		351.99		238.63		583.14		
			Branching Ratio		0.9986		0.9998		0.8462		0.5075		0.9994		0.9998		0.9945		0.0884		0.103		0.04		0.107		0.4609		0.371		0.431		0.861		
sample	mass(g)	depth(in)	station	lat.	long.	pCi/kg	+/-	pCi/kg	+/-	pCi/kg	+/-	pCi/kg	+/-	pCi/kg	+/-	pCi/kg	+/-	pCi/kg	+/-	pCi/kg	+/-	pCi/kg	+/-	pCi/kg	+/-	pCi/kg	+/-	pCi/kg	+/-	pCi/kg	+/-	pCi/kg	+/-		
1-NG-179097	1387.1	S	140	43.910	69.717	29.2	10.5	16.3	6.6	48.9	10.7	--	--	0.8	4.3	12.2	6.7	3.9	4	--	--	45.3	68.8	--	--	7067	243.3	321.3	26.6	344.3	30.1	497.2	28.8	144.8	13.3
2-C4-179477	315.3	1	143	43.942	69.711	5.7	13.5	12.9	8.8	42.8	11.7	34	22.7	1	9.8	--	--	--	--	3.7	75.7	215.2	135	494.5	558.5	8300.9	461.9	79.6	36.2	354.9	43.8	502	39	57.5	18
2-C4-179478	314.1	2	143	43.942	69.711	8.6	10.1	--	--	52.1	22.1	21.5	24.9	5.7	8.6	7.1	11.6	--	--	51.6	90.4	23.4	69.6	373.8	417.9	8167.1	457.7	288.2	44	324.7	44.2	618.1	38.7	223	22.5
2-C4-179479	333.1	3	143	43.942	69.711	--	--	37.8	12.5	75.4	18.4	6.8	19.6	--	--	3.9	8.1	18.2	9.7	222.4	124.3	3.7	66.2	214.8	261.4	8929.2	449.6	219	37	361.8	43.4	597.8	39.1	189	23.1
2-C4-179480	288	4	143	43.942	69.711	13.1	12.2	4.7	8.8	46.9	19	36.5	31.3	2.3	13.3	--	--	4.4	9.2	--	--	--	--	343.9	278.2	8726.6	510	132.5	38.5	137.4	38.1	594.4	43.8	114.8	21.4
2-C4-179481	327.5	5	143	43.942	69.711	2.8	9.9	8.3	10.9	91.2	17	43	22.1	18.6	13.9	0.9	17.3	6.5	8.9	63.6	75	86.1	71.7	22.4	252.7	9166.6	466.5	283.8	43	298.3	43.3	625.9	39.2	185.7	23
2-C4-179482	354.1	6	143	43.942	69.711	6.8	11.5	3.8	9.7	61.3	16.2	6.4	23	29.5	12.5	7.3	8.7	--	--	189.6	119.3	216.4	132	--	--	11659.7	499.9	233.1	35	483.8	43.2	751	39.4	140.4	24.4
2-C4-179483	303.7	7	143	43.942	69.711	3	11.8	4.5	8.8	8.8	10.5	--	--	23.6	13.2	9.3	9.8	13	10.8	38.1	84.2	115.7	103.4	--	--	11682.7	534.6	344.9	48.1	252.3	47.4	845	45	231.8	27.1
2-C4-179484	378.3	8	143	43.942	69.711	1.6	9.9	--	--	--	--	--	--	3.4	9.3	7.4	8.1	--	--	246.4	83.6	--	--	--	--	9484.3	433.2	306.2	38.3	334	39.2	676.4	37.5	181.4	21.2
2-C4-179485	365.7	9	143	43.942	69.711	16.5	13.1	6.5	7.6	23.9	11.7	12.3	21.2	--	--	13.5	8.4	2.9	7.4	158.3	102.7	33.5	58.3	558.4	499.2	10280.3	473.1	271.3	38.9	265	41	793.7	39	228	23
2-C4-179486	308	10	143	43.942	69.711	12.7	11.4	--	--	--	--	--	--	--	--	22.1	12.1	10.3	8.2	48.9	80.7	47.8	73.6	717.6	441.5	11975.5	544.2	321	46.4	297.4	48.5	896.6	44.5	181.6	29.4
2-C4-179487	367.3	11	143	43.942	69.711	11.1	9.2	--	--	10	9.1	13.3	26.1	10.7	13.3	4.7	10.1	12.7	9	--	--	--	--	659.2	393.7	9872.2	449.9	282.4	42.8	357.1	40.2	720.4	38.2	172.8	22.4
2-NG-179100	1409.6	S	143	43.942	69.711	36.5	13.3	0.5	9.8	75.1	17.2	141.8	25.5	6.7	9	--	--	4.5	5.7	--	--	178.9	79.9	556.8	562.6	8796.5	369.5	417.4	37.6	359.5	37.4	641.5	34.7	162.7	20.2
1-C3-179457	122.7	1	144	43.930	69.728	10.6	13.2	44.7	15.4	89.9	21.1	--	--	--	--	--	--	--	--	58.2	119.9	265.3	97.2	1063	475.6	8653.3	470.7	209.5	34.1	295.4	41.5	459	45.9	117.5	19.1
1-C3-179458	108.4	2	144	43.930	69.728	45.8	13.4	29.3	16.6	71.4	19.7	--	--	9.4	11.3	15.2	12.4	9	11.7	--	--	16.9	79.8	723	437.5	8372.6	501.7	272.9	48.3	233.5	47.2	601.6	51.4	142	27.8
1-C3-179459	118.7	3	144	43.930	69.728	3.7	13.4	--	--	114.7	19.8	35.3	25	21.2	13.2	24.7	10.8	9	9.2	45.1	93	257.1	110.3	69.9	334.4	9079.7	498.9	297.8	47.7	397.5	51.8	638.3	45.8	128.7	21.7
1-C3-179460	127	4	144	43.930	69.728	4.1	10.8	--	--	51.5	26	51.8	26.8	--	--	6.2	11.4	3.1	8.4	--	--	--	--	500	363.9	8486.3	477.3	272.2	48.5	266.7	34.3	689.4	49.4	166.2	24.7
1-C3-179461	103.6	5	144	43.930	69.728	10.1	11.8	--	--	74.1	20.1	52.4	29.3	17.2	13.9	23.9	11.4	14.1	11.1	--	--	110	112	--	--	9027.3	556.5	387.5	48.8	341	58.6	869.2	59.1	213.7	30.5
1-NG-179101	1396	S	144	43.930	69.728	3.7	8.2	10	7	64.7	11.3	23.2	14	--	--	2.8	7.1	0.6	5.2	57.7	57.5	155	82.7	5962.4	436.7	7539.1	247.6	293.2	25.9	279.4	29.8	512.5	29.4	132.6	13
1-C3-179418	123.7	1	145	43.920	69.731	15.1	14.2	7.8	12.3	110.3	25.3	--	--	7.9	10.3	--	--	25.9	11.7	--	--	84.9	101.8	404.7	326.3	8301.2	482.2	245.9	44.5	334.7	50.5	570.2	47.5	111	20.6
1-C3-179419	139.2	2	145	43.920	69.731	0.9	10.7	12.4	10.6	82	17.9	46.1	28.1	--	--	5.7	11.7	2.1	7.9	25.7	99.9	207.5	93	478.8	301.1	8459.3	443.4	222.1	36.8	373.5	50.4	709.6	46.3	237.7	25.7
1-C3-179420	135	3	145	43.920	69.731	18.4	10.2	10.7	11.5	18.6	10.8	--	--	14.5	15	10.3	10	6.5	9.1	67.6	153	--	--	563.6	407	8629.9	468.9	261	49.6	331.2	50.5	739	47.6	174.2	26.3
1-C3-179421	121.3	4	145	43.920	69.731	25.8	20.1	1.2	9.1	1.2	11.5	19	22.9	23	11.7	--	--	4	8.8	402.5	119.8	--	--	198.1	381.8	9820.4	500.6	395.1	45.7	344.6	46.1	808.4	54.4	194.6	28.7
2-NG-179102	1425.3	S	145	43.920	69.731	11.8	8.5	23.6	8.7	96.7	16.9	--	--	4	8.4	19.9	9.3	10.7	7.8	55.4	78.6	211.3	90.5	--	--	8211.6	359	264.7	35.8	381.3	37.7	681.7	33.6	144.1	18.8
1-C4-179360	203.6	1	146	43.919	69.751	--	--	3.7	8	103.8	15.9	8.1	20.2	16.2	11.8	1.3	10	9.1	12.5	74.8	78.2	--	--	480.4	363.6	7559.5	404.4	270.6	42.3	290.6	45.3	655	45.6	131	18.6
2-C3-179361	114.2	2	146	43.919	69.751	9.7	20.4	4.1	15.6	123	32.7	25.5	29	21.6	17.4	7.9	12.8	20.5	19.8	133.9	136.8	134.2	145.3	2109.5	800.9	8447.9	643.5	367.9	52.6	301.9	62.1	505.7	55.9	247.2	37.7
2-C3-179362	102.1	3	146	43.919	69.751	9.1	32.6	13.7	13.7	97	25	93.9	62.7	43.9	19.3	45.9	26.4	1.4	12.6	480.9	192.2	41.7	121.1	943.8	845.6	6769.3	668.4	202.2	48.5	284.9	63.3	289.7	45	82.1	24.6
2-C3-179363	117.3	4	146	43.919	69.751	--	--	6	13.4	167.6	36.6	--	--	19.1	15	5.1	15.8	--	--	247	125.8	225	126.5	1200.7	988.1	8797.6	691.6	167.8	61.8	304.2	54.1	381.6	47.6	248.1	32.9
2-C3-179364	114.6	5	146	43.919	69.751	5.4	14.3	--	--	119.3	31.7	98.3	51.7	20.5	13.4	13	14.8	8.7	12.1	21.1	119.8	--	--	468.9	881.7	9982.3	682.5	278.7	58.9	391.5	71.6	755	62.1	203.3	35.9
2-C3-179365	122.2	6	146	43.919	69.751	--	--	--	--	74.9	24.1	--	--	29.3	18.7	--	--	44.2	16.3	39.5	150	34.8	116	1678.3	1163.2	9907.6	666	361.5	67.8	318	59.1	748.4	58	158.7	31
2-C3-179366	103.2	7	146	43.919	69.751	25.4	24.5	--	--	119.2	29	--	--	10.9	17.8	7.7	17.9	8.5	14.3	--	--	185.6	133.1	--	--	9690.1	700.4	330.4	60.8	354.3	67.1	691.1	71.6	192.4	37.3
1-NG-179103	1411.5	S	146	43.919	69.751	7.7	7.1	1.9	4.2	66.2	12.8	--	--	5.9	4.6	6.7	4.5	0.5	4.7	--	--	330.2	93	942.4	228.4	7020.6	238.5	285.1	26.5	322.8	30	600.8	30.8	129.4	13.3
Samples collected 16-17 September 2004																																			
2-C4-171841	420.5	1	147 Westport Is	43.9494	69.688	15	10	21	11.8	58.1	15.4	53.6	20.1	9.3	9.3	6.2	6.3	8.4	7.3	--	--	163.3	60	366.4	383.9	7271.2	360.7	235.9	33.8	333.1	34.2	494.6	30.1	109.9	17.1
2-C4-171842	209.2	2	147 Westport Is	43.9494	69.688	13	14.3	21.1	13.1	23.5	18.4	35	29.4	4.7	14	17.9	13.2	--	--	--	--	87.9	96.8	920.7	520	9544.7	562.4	324.2	50	321.4	56	642.4	54.2	190.9	28.3
2-C4-171843	273.6	3	147 Westport Is	43.9494	69.688	14.3	12	1.2	9	55.3	22.3	--	--	34.6	16.6	12.6	9.4	1.5	9.4	56.4	99.7	636.4	177.2	643.6	641.9	10161.5	525.6	401.9	47.4	322.7	41.2	614.2	43.4	165.1	26.7
2-C4-171844	327.1	4	147 Westport Is	43.9494	69.688	29.2	16.3	23.6	11.9	36.9	11.9	144.1	34																						

Maine Yankee Marine Sampling Study

			nuclide		60Co		60Co		137Cs		65Zn		22Na		54Mn		58Co		133Ba		7Be		210Pb		40K		214Bi		214Pb		212Pb		208Tl		
			Gamma energy (keV)		1173.23		1332.51		661.62		1115.52		1274.54		834.81		810.75		383.7		477.56		46.52		1460.75		609.32		351.99		238.63		583.14		
			Branching Ratio		0.9986		0.9998		0.8462		0.5075		0.9994		0.9998		0.9945		0.0884		0.103		0.04		0.107		0.4609		0.371		0.431		0.861		
sample	mass(g)	depth(in)	station	lat.	long.	pCi/kg	+/-	pCi/kg	+/-	pCi/kg	+/-	pCi/kg	+/-	pCi/kg	+/-	pCi/kg	+/-	pCi/kg	+/-	pCi/kg	+/-	pCi/kg	+/-	pCi/kg	+/-	pCi/kg	+/-	pCi/kg	+/-	pCi/kg	+/-	pCi/kg	+/-		
2-C4-171840	347.4	10	149 Robin Hood Cv	43.8222	69.7486	6.9	9.9	20.6	12.2	15.9	10.2	129.8	39.5	--	--	12.5	13.1	3	11.4	13.3	76.7	84.7	68.1	454.1	532.7	11315.8	502.7	468.3	44.7	520.7	46.5	820.4	42.1	237.5	24.1
2-NG-179493	1405.4	S	149 Robin Hood Cv	43.8222	69.7486	13.9	9	--	--	51.7	15.7	14.2	19.3	4.5	8.3	--	--	7.3	7.2	152.7	80	166.7	65.3	--	--	6972.2	332.9	305	32.5	266.5	34.1	433.8	33	109.7	15.7
average of control samples:						12.3	12.5	9.9	10.2	72.4	17.0	61.5	28.7	10.5	11.1	12.3	10.5	6.9	9.2	97.7	94.0	99.9	81.8	355.6	448.5	10179.1	481.2	354.8	43.1	389.0	44.5	681.5	39.2	183.0	22.5
average of samples near plant:						19.2	12.4	17.8	10.4	73.2	16.5	36.1	24.3	10.4	10.6	9.2	9.7	7.6	8.8	87.8	95.7	154.9	89.3	551.3	421.6	9441.5	440.4	301.2	40.2	330.8	43.1	623.7	40.8	166.1	21.4

Maine Yankee Marine Sampling Study

Table 5-2. Summary of ¹³⁷Cs peaks observed in cores.

Location	Station No.	Bottom Of Peak 1	Top of Peak 2	30 y Separation of Peaks	pCi/Kg Max
Long Creek		1"	6"	5"	950
Bailey Cove	2	1"	11"	10"	250
Wiscasset		3"	9"	6"	92
Chewonki Camp		3"	6"	3"	135
Bailey Cove Outfall	8	6"	13"	7"	175
Diffuser	34	1"	7"	6"	17
Westport Island	38	2"	7"	5"	41
Eaton farm Point	44	1"	5"	4"	100
	50	2"	10"	8"	120
South Oak Is	59	1"	3"	2"	115
South Oak Is	60	5"	9"	4"	20
	61	Flat			10
	62	1"	8"	7"	24
Long Ledge	63	1"	5"	4"	60
Long Ledge	64	1"	7"	6"	80
	65	1"	6"	5"	110
	67	2"	9"	7"	155
Foxbird Is	68	2"	7"	5"	252
	73	1"	12"	11"	175
Bailey Cove	74	1"	10"	9"	250
Upper Bailey Cove	77	1"	12"	11"	225
South Bailey Cove	85	2"	6"	4"	70
North Bailey Cove	99	1"	11"	10"	155
Eaton Farm Bailey Cove	101	2"	10"	8"	150
Top of Bailey Cove	105	1"	7"	6"	100
	108	1"	11"	8"	130
	113	2"	13"	11"	160
	118	2"	11"	9"	35
	143	2"	11"	6"	90
Oak Island Murphy Corner	144	2"	5"	3"	110
Oak Island Murphy Corner	145	1"	3'	2"	110
	146	1"	7"	6"	165
Taunton Bay	Vc14	1cm	30cm	29cm	60
Taunton Bay	Vc15	1cm	25cm	24cm	100
	Vc23	1cm	25cm	24cm	250

Maine Yankee Marine Sampling Study

Table 5-3. Total ^{60}Co and ^{137}Cs activity contained in cores

Station	Diameter. in.	Depth in.	^{60}Co , 1173 keV pCi	^{60}Co , 1332 keV pCi	^{137}Cs pCi
9apr04 batch:					
Chewonki Camp	4	6	11	15	232
Wiscasset	4	11	33	38	294
Long Creek	4	12	36	47	1297
Barry Cove	4	15	10	21	86
1jun04 batch					
Pottle cove	4	12	37	24	329
Sasanoa	4	13	27	46	720
Eddy	4	12	46	45	349
5-9july04 batch					
2	4	11	26	14	519
8-1	4	15	50	43	538
25	4	12	37	21	91
34	3	9	7	7	11
38	3	7	19	8	18
44	3	9	12	10	55
50	4	11	27	32	279
2-5aug04 batch					
59	3	8	10	8	24
60	3	11	8	13	7
61	3	5	7	9	5
62	3	8	8	7	11
63	3	5	8	2	36
64	3	10	4	11	45
65	3	9	9	8	39
66-1	3	9	12	10	69
67	3	9	12	3	51
68	4	9	36	37	307
73	4	11	30	39	407
74	4	11	34	19	555
77	4	12	35	33	579
85	3	6	7	6	46
99	4	11	31	27	460
101	4	10	47	21	437
105	4	12	27	39	187
108	4	9	41	58	225
113	4	13	48	28	390
117	4	9	49	40	144
118	4	12	73	18	67
134	4	13	44	34	263
143	4	11	27	26	135
144	3	5	8	9	47
145	3	4	8	4	28
146	4	7	5	3	100
6-17sep04 batch					
147	4	9	36	39	225
148	4	9	49	18	74
149	4	10	28	26	182

Table 5-4. Biota gamma scan results

				nucl.		60Co		137Cs		65Zn		22Na		54Mn		58Co		133Ba		7Be		210Pb		40K		214Bi		214Pb		212Pb		208Tl			
				E(keV)		1173.23		1332.51		661.62		1115.52		1274.54		834.81		810.75		383.7		477.56		46.52		1460.75		609.32		351.99		238.63		583.14	
				%		0.9986		0.9998		0.8462		0.5075		0.9994		0.9998		0.9945		0.0884		0.103		0.04		0.107		0.4609		0.371		0.431		0.861	
sample	mass(g)	species	Location	pCi/kg	+/-	pCi/kg	+/-	pCi/kg	+/-	pCi/kg	+/-	pCi/kg	+/-	pCi/kg	+/-	pCi/kg	+/-	pCi/kg	+/-	pCi/kg	+/-	pCi/kg	+/-	pCi/kg	+/-	pCi/kg	+/-	pCi/kg	+/-	pCi/kg	+/-	pCi/kg	+/-		
2-NG-171993	343.5	clam shells	Little Oak Is.	6	7	--	--	11.7	10	31.8	16.8	13.8	6.4	--	--	8	6.7	3.6	62.9	83.7	66	364	676	2196.2	190	98.6	20.4	72.8	25.5	204	27.2	63.6	13.8		
2-NG-172000	829.8	mussels	Little Oak Is.	8.5	4.7	5	3.4	5.7	4.3	4.7	5.8	--	--	1.3	2.7	--	--	--	--	18.6	28.8	375	288	1243.2	89.4	14.3	7.9	9.5	10.3	30.1	5.9	5.7	3.6		
2-NG-171998	280.9	rock weed	Little Oak Is.	13.7	11.8	12.3	14.5	7.4	12.2	97.2	30.8	18	15.7	--	--	2.6	9	--	--	44.3	146	1282	884	15091	455	112	30.3	66.8	32.6	25.4	26.1	37.2	15.5		
2-NG-171997	472.3	fish tissue	Back River	5.6	7	2.4	5	16.8	7.6	8.8	16	10.4	8.1	0.2	4.9	5.7	6.8	--	--	--	--	609	324	5325.4	215	10.3	12.9	57	24.6	53.3	20.1	28	10.7		
2-NG-171989	999.2	clam tissue	Little Oak Is.	7.1	4.1	--	--	--	--	6.1	5.3	3.1	2.9	8.4	3.3	3.9	4.4	--	--	72.1	32	146	237	1543.6	84	10.1	8.9	3.7	5.4	42.4	9.9	12.5	5.5		
2-NG-45201	636.2	lobster		1.9	3.9	6.1	5	1	4.1	46.5	15.3	3.2	3.7	7.3	3.8	--	--	9.7	34	18.9	38	--	--	3236.7	143	31.4	12.5	40.6	14.1	17.5	11	8.8	5.2		
		average		7.1	6.4	6.5	7.0	8.5	7.6	32.5	15.0	9.7	7.4	4.3	3.7	5.1	6.7	6.7	48.5	47.5	62.2	555.2	481.8	4772.7	196.0	46.1	15.5	41.7	18.8	62.2	16.7	26.0	9.1		
2-NG-179200	736.3	control mussels	Darling Center	3.4	3.3	--	--	2.5	4.3	1.5	8.2	3.9	3.8	--	--	2.1	4	--	--	49.5	36.8	--	--	1804.5	108	51	11.8	32.9	16	48.5	13.4	15.1	3.9		
2-NG-0100	237.6	control sea scallops	Darling Center	5.4	11.9	30.1	10	--	--	26.9	18.8	--	--	13.3	9.6	14	12.5	25.9	104	121	117	2528	1103	3889.3	292	85.7	31.1	63.5	47.6	108	27.9	49.4	17.1		
2-NG-0101	797.1	control oysters	Darling Center	1.7	2.9	2.3	3.2	0.6	3.6	20.4	8.3	3.6	2.7	--	--	--	--	29.4	43.6	44.7	29.9	--	--	1178.3	83.9	17	9.5	21.6	12.9	22.7	5.5	7.8	4		
2-NG-0102	883.5	control ocean quahogs	Darling Center	--	--	--	--	5.5	3.7	5.2	7	3.6	2.6	1.8	2.9	2.4	3.6	14.2	35.4	46.6	34.8	358	264	1523.7	90.6	25.5	8.9	22.3	13	44.8	10.5	18	4.8		
2-NG-0103	669.2	control horse mussels	Darling Center	4.3	4.4	4.8	4.3	14.4	5.5	3.9	5.9	1.1	2.5	4.5	4.2	--	--	--	--	83.7	40.9	526	356	1328.2	104	64.2	13.7	63.4	18.1	27.5	10.8	9.2	6		
2-NG-045402	673	control blue mussels	South Portland	2.9	3.6	3.8	4	8.1	6.2	21.9	10.7	3.3	3.6	--	--	1.3	3.4	15.6	73	1.9	49.5	393	257	2427.9	122	53.6	16.5	83.7	15.3	58.6	12.3	14	4.9		
2-NG-045401	459.6	control Rockweed	South Portland	30.6	12.5	12.4	6.3	10.1	10.8	2.4	19.6	0.2	8.2	5.5	6.3	--	--	2.7	76.4	122	66	563	375	6075.8	235	60.8	16.6	32.5	19.2	69	20.6	5.1	9.7		
		control average		8.1	6.4	10.7	5.6	6.9	5.7	11.7	11.2	2.6	3.9	6.3	5.0	5.9	17.6	66.5	67.0	53.5	873.5	470.9	2604.0	147.8	51.1	15.4	45.7	20.3	54.2	14.4	16.9	7.2			

Maine Yankee Marine Sampling Study

Table 5-5. Comparison with Pre- and Post-operational study

	Cs- ¹³⁷ Low	Cs- ¹³⁷ High	Co- ⁶⁰ Low	Co- ⁶⁰ High
2004	2.9	287.2	0.5	168.7
Pre	350	800	<30	<30
Post	500	1000	<30	2,420

Table 5-6. Results of the Hard to Detect Nuclides

Sample	⁶³ Ni (pCi/g)	⁵⁵ Fe (pCi/g)	⁹⁰ Sr (pCi/g)	²³⁸ Pu (pCi/g)	²³⁹ Pu (pCi/g)
Clams	-1.2 x 10 ⁻¹ ± 3.2 x 10 ⁻¹	-1.7 x 10 ⁻¹ ± 2.0 x 10 ⁻¹	-1 x 10 ⁰ ± 1.1 x 10 ⁰	0 ± 1.5 x 10 ⁻⁵	8.2 x 10 ⁻⁴ ± 8.2 x 10 ⁻⁴
Clamshell	-1.6 x 10 ⁰ ± 2 x 10 ⁰	-2.6 x 10 ⁰ ± 1.2 x 10 ⁰	-5 x 10 ⁻¹ ± 1.2 x 10 ⁰	-3.2 x 10 ⁻⁴ ± 1.9 x 10 ⁻⁴	5.1 x 10 ⁻⁴ ± 8.5 x 10 ⁻⁴
Mussels	9.2 x 10 ⁻¹ ± 9.3 x 10 ⁻¹	-5.2 x 10 ⁻¹ 5.5 x 10 ⁻¹	5.0 x 10 ⁻¹ ± 1.2 x 10 ⁰	-6.1 x 10 ⁻⁴ ± 2.5 x 10 ⁻⁴	5.0 x 10 ⁻⁵ ± 8.3 x 10 ⁻⁴
Mussel shell	1.5 x 10 ⁰ ± 1.2 x 10 ⁰	-6.0 x 10 ⁻² ± 8.1 x 10 ⁻¹	-1.2 x 10 ⁰ ± 1.2 x 10 ⁰	0 ± 1.1 x 10 ⁻⁵	-3.3 x 10 ⁻⁴ ± 1.7 x 10 ⁻⁴
Lobster	2.0 x 10 ⁻¹ ± 1.2 x 10 ⁰	-6 x 10 ⁻² ± 8.2 x 10 ⁻¹	1.25 x 10 ⁰ ± 7.5 x 10 ⁻¹	0 ± 5.2 x 10 ⁻⁶	0 ± 5.2 x 10 ⁻⁶
Fish	9.0 x 10 ⁻² ± 3.8 x 10 ⁻¹	-2.3 x 10 ⁻¹ ± 2.6 x 10 ⁻¹	9.3 x 10 ⁻¹ ± 4.0 x 10 ⁻¹	-1.28 x 10 ⁻⁴ ± 5.7 x 10 ⁻⁵	0 ± 3.5 x 10 ⁻⁶
Rockweed	-6.0 x 10 ⁻¹ ± 2 x 10 ⁰	-1.1 x 10 ⁰ ± 1.2 x 10 ⁰	-1.0 x 10 ⁻¹ ± 1.3 x 10 ⁰	0 ± 1.6 x 10 ⁻⁵	-2.2 x 10 ⁻⁴ ± 1.6 x 10 ⁻⁴
Sediment	3.9 x 10 ⁰ ± 2.2 x 10 ⁰	-3 x 10 ⁻¹ ± 1.4 x 10 ⁰	5.0 x 10 ⁻¹ ± 1.1 x 10 ⁰	7.2 x 10 ⁻⁴ ± 7.2 x 10 ⁻⁴	9.3 x 10 ⁻³ ± 2.6 x 10 ⁻³

6. HOT PARTICLE SEARCH RESULTS

University of Maine researchers conducted a search for hot particles on three occasions, July 7, August 2, and August 18, around the site of the Maine Yankee Nuclear Power Plant. The goal of the search was to find any area on the tidal flat which measured three times normal background. The searches were conducted using a High Pressure Ion Chamber (HPIC) connected to a laptop computer. Each search was conducted at an extreme low tide so as to allow the investigators the ability to walk as far away from the shore into the tidal flat as possible. The HPIC records a dose in microrems/hour. At the same time, position was recorded using GPS. The HPIC was set to warn researchers if a measurement three times larger than background was detected by emitting a series of four beeps. Therefore, a background was initially established at a location well away from the power plant. In each case, the background was approximately 10 to 12 microrems/hour as expected. However, if a measurement over three times these values was noted, the researchers would mark the site with a flag, record the GPS location, notify Maine Yankee personnel, and return with a sodium iodide detector to perform a gamma ray analysis of the location. Results from the sodium iodide detector would provide a spectrum allowing a determination of the particular radioisotopes involved. The HPIC was loaded onto a sled and dragged over the tidal flat during low tide. The HPIC would record results for 30 seconds, then rest for 30 seconds. After recording for 30 seconds, the HPIC emitted a single beep at which time the researchers would move the sled for 30 seconds to the next location.

Results are shown in Figures 6-1 through 6-3. No measurement over three times background was seen. However, some variation was noted. The variation, from approximately 11 microrems/hour to approximately 5 microrems/hour, is most likely due to low sediment concentrations of nuclides and some gamma ray shielding by the ocean. As the researchers dragged the sled out away from the shore, the HPIC would see gamma rays from the immediate tidal flat, but not from the shore or from the soil underneath water. As a result of the low sediment concentrations and water shielding the HPIC from a large section of area, the values measured were reduced to very low values. These results are in agreement with a pre- and post-operational study of the area completed in 1976. In this report, total dose rates ranging from 8.89 to 14.45 microrems/hour (Technical Note 76-3). Figure 6-4 shows the three tracks taken around the power plant with the HPIC results color coded to show the variation. As can be seen from the figure, the three tracks were chosen to bracket the plant and to pick up any hot particles remaining in the area of the outfall and the diffuser. As stated above, no "hot" areas were seen.

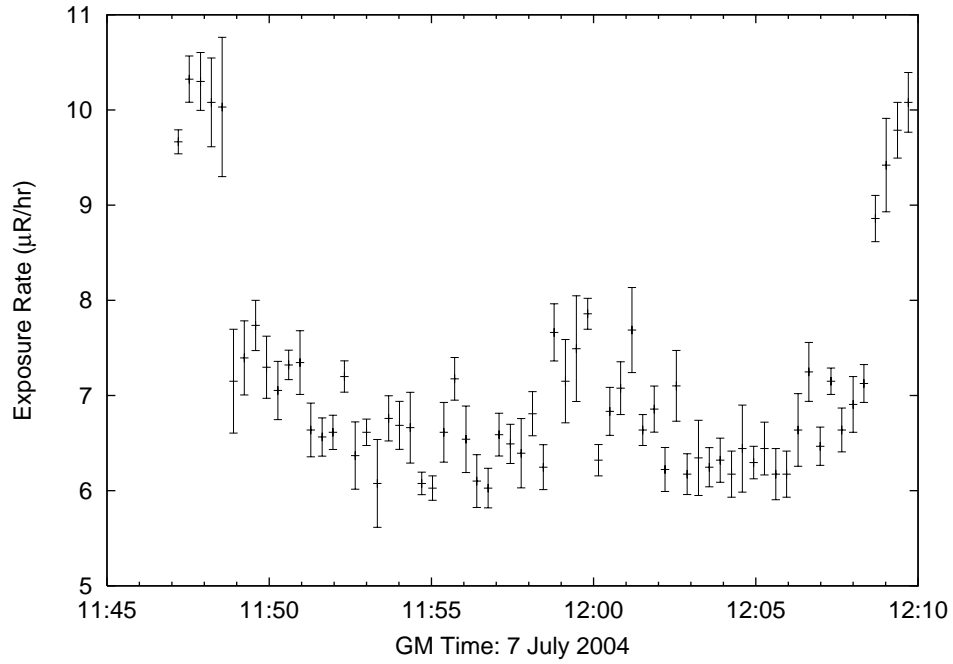


Figure 6-1. Hot Particle Scan, 7 July 2004

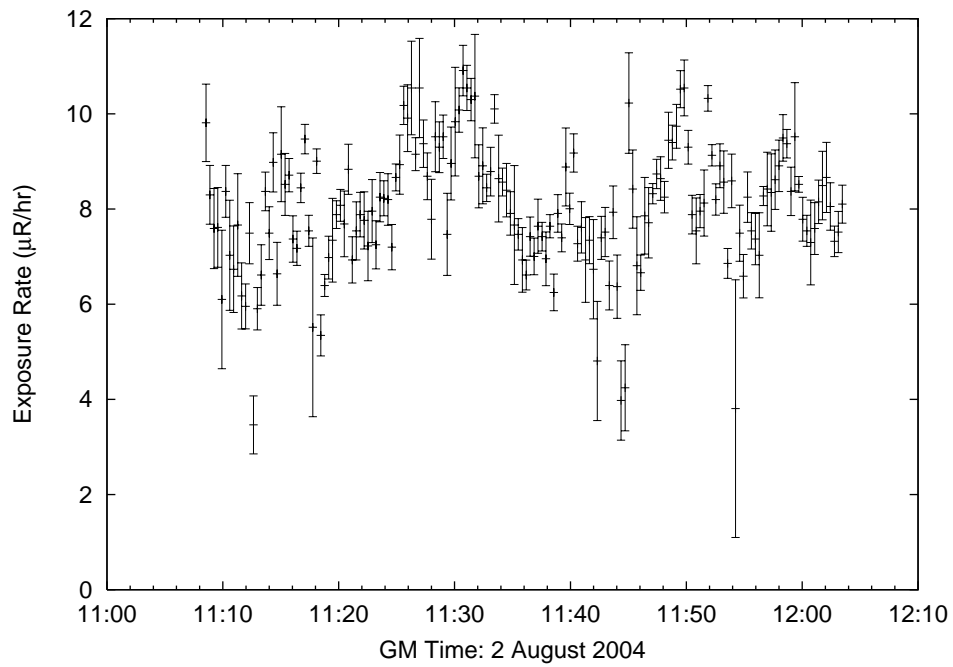


Figure 6-2. Hot Particle Scan, 2 August 2004

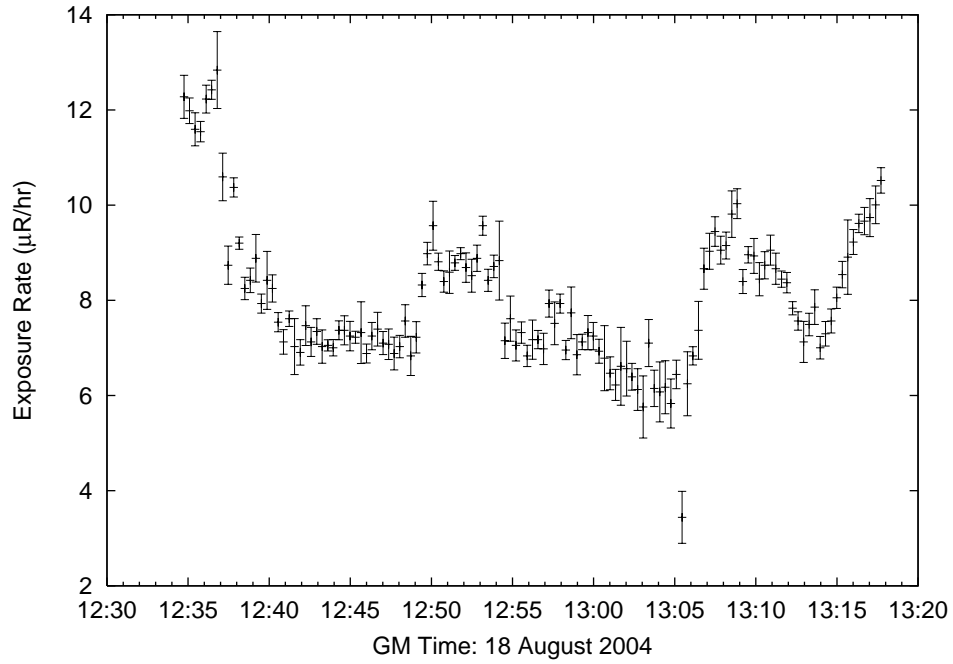


Figure 6-3. Hot Particle Scan, 18 August 2004

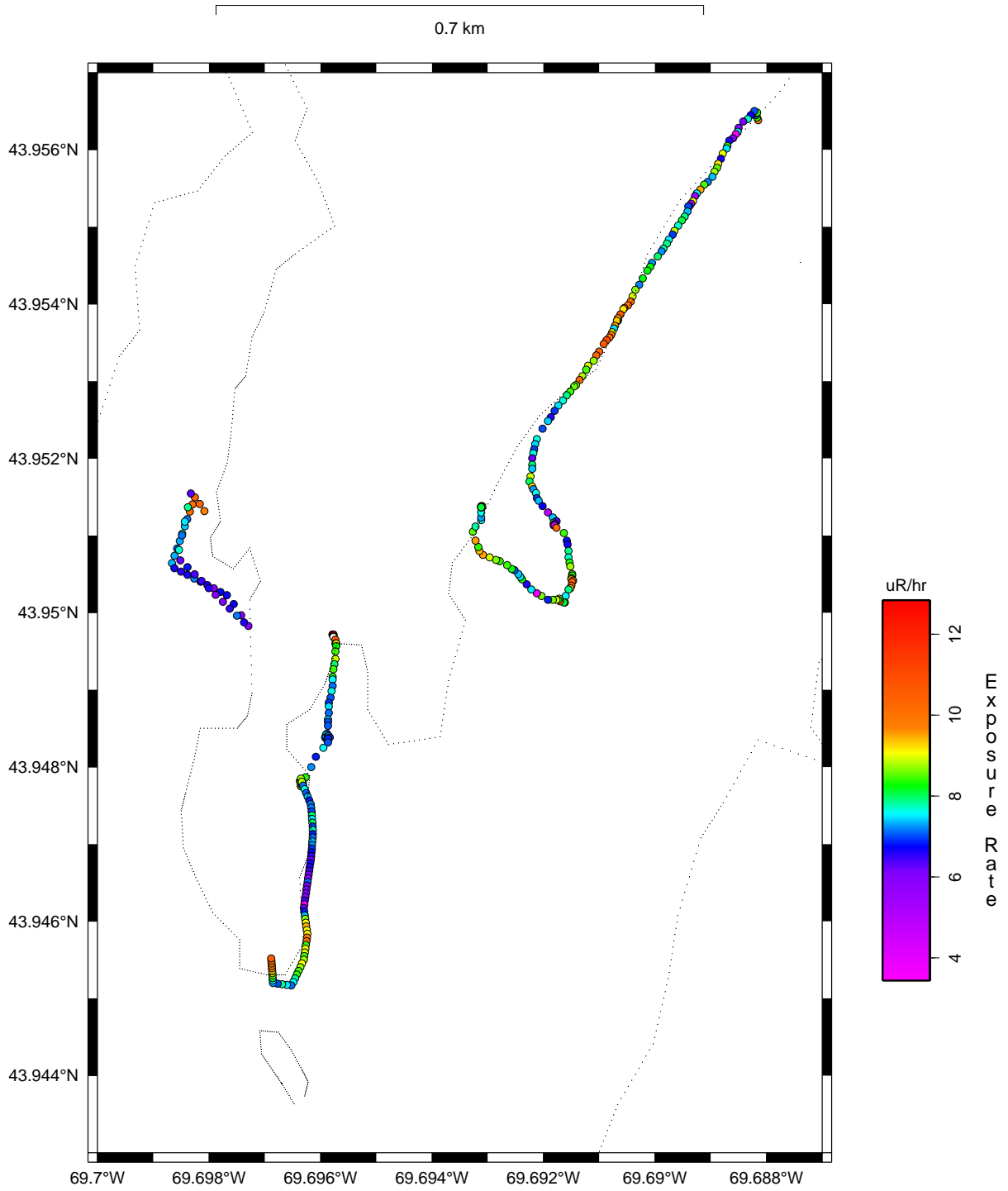


Figure 6-4. Hot Particle Scan Map

7 MARINE SAMPLE DOSIMETRY

7.1 MARINE SAMPLING DOSE ASSESSMENT

7.1.1 Purpose of the Dose Assessment Document

The purpose of this dose assessment is to support the study by identifying current and future uses of the marine environment around Maine Yankee and the associated dose pathways, by presenting the basis for the selection of marine biota for sampling and by establishing the framework to evaluate the results of the sediment and biota sample analysis. Specifically, the following objectives are accomplished in this dose assessment:

1. Identify the dose pathways associated with the intertidal zone considering both current and potential future uses. Maine Yankee will work with the Friends of the Coast to reach agreement on these dose pathways.
2. Develop a dose assessment framework to calculate an incremental intertidal zone dose from the sampling (characterization) results. Maine Yankee will use this framework to compare the incremental intertidal zone dose to the limiting “resident farmer” dose calculations in the License Termination Plan.
3. Present the dose basis for the identification of flora and fauna in the intertidal zone that may reasonably be considered contributors to an intertidal zone pathway dose (e.g., seaweed, shellfish, etc.). Priority in sampling and analysis should be given to both the highest bio-accumulator and the most significant dose pathways to human populations.

This dose assessment will be used by Maine Yankee in the Bid Specification to identify the current and future uses and associated dose pathways and by the Marine Sampling contractors to select flora and fauna for sampling and calculate the intertidal dose from the sampling results. The final report should include an assessment of the dose significance of the sampling results using this dose assessment basis.

7.1.2 Inputs and Data Sources

- Engineering Calculation EC-041-01 “Diffuser and Forebay Dose Assessment”
- NUREG -5512 “Residual Radioactive Contamination from Decommissioning”
- Federal Guidance Report No. 11 (FGR-11) “Limiting Values of Radionuclide Intake and Air Concentration and Dose Conversion Factors for Inhalation, Submersion, and Ingestion” (September 1988)
- Regulatory Guide 1.109 “Calculation of Annual Doses to Man from Routine Releases of Reactor Effluents for the Purposes of Evaluating Compliance with 10 CFR Part 50, Appendix I, October 1977
- Maine Yankee Offsite Dose Calculation Manual
- Maine’s Coastal Wetlands, by Alison E. Ward, for Maine Department of Environmental Protection dated September 1999

- Maine Aquaculture Review, by Normandeau Associates, Inc. and Battelle, for Maine Department of Marine Resources dated February 2003
- WWW.seaweed.ie, WWW.alcasoft.com, WWW.garden.org

7.1.3 Current Maine Yankee Intertidal Zone Uses

Currently the intertidal zone at Maine Yankee is used primarily for commercial baitworm digging and soft-shell clam harvesting. Other uses can, at times, include fishing, lobstering and even duck hunting. Recreational swimming has been known to occur historically in Young's (also known as Long) Creek which leads into Bailey Cove.

7.1.3.1 Offsite Dose Calculation Manual (ODCM)

Maine Yankee has been lawfully allowed to discharge low levels of radioactive effluents through its licensed discharges. These include both liquid and gaseous effluents. These effluents were monitored, evaluated for their dose consequences and reported on a semi-annual or annual basis, as required, throughout the operation and decommissioning of the plant. The resultant whole body and organ doses from these effluents were determined by summing the contributions from all pathways using the Offsite Dose Calculation Manual (ODCM). These whole body and organ doses to a theoretical member of the public were similarly reported on a semi-annual or annual basis. The estimated annual doses due to liquid effluents were consistently calculated to be below the 10 CFR Part 50, Appendix I dose criteria.

Exposure pathways that currently are assumed to exist in the ODCM as a result of liquid effluents are ingestion of fish and shellfish, and direct exposure from shoreline sedimentation. The potable water pathway and the irrigated foods pathway are not considered since the receiving water is not suitable for either drinking or irrigation. The direct exposure to worm diggers on tidal flats has been accounted for with an occupancy factor of 325 hours per year (0.037). It is expected that this same occupancy factor would apply to clam harvesters.

The dose analysis for the fish and shellfish pathways assumes a 10 to 1 dilution based on the discharge of effluents via a submerged multipart diffuser which extends approximately 1,000 feet into the tidal estuary. For shoreline direct exposure, a dilution ratio of 25 to 1 has been applied in order to calculate the radionuclide deposition on the exposed sediment.

7.1.3.2 Bailey Cove Mudflats Occupancy

The maximum personnel occupancy for the Bailey Cove was documented in the Maine Yankee Environmental Report and Off site Dose Calculation Manual (ODCM) to be 325 hours. Maine Yankee technical personnel re verified this occupancy factor through interviews with cognizant personnel. Interviews were conducted with Maine Yankee security force personnel, a Maine State Marine Patrol officer, a licensed clam digger, three licensed worm diggers, and one bait shop owner. Based on these interviews, the licensee determined that the occupancy factor of 325 hours per year, presented in the ODCM, was a conservative value. These verification activities were documented in the following records:

- Maine Yankee memorandum dated January 23, 1996 memorandum entitled, "1995 Density Characterization of Clam/Worm Digging Activities in Montsweag Bay;"

- Maine Yankee memorandum dated February 1, 1996, memorandum entitled, "Occupancy Factors for Bailey Cove;"
- Maine Yankee memorandum dated January 30, 1996, memorandum entitled "Information Gathered About Worm Digging Activity That May Impact Occupancy Factors in Bailey Cove;"
- NRC Inspection Report No. 50-309/96-06, dated July 25, 1996. In this inspection report, NRC documented the results of the NRC inspector's conduct of interviews of a Maine State Marine Patrol officer and a Maine State Radiation Control Inspector; reviews of the Maine Yankee ODCM; and walkdowns of the western perimeter of the site. None of the information reviewed by the inspector suggested that personnel occupancy, in areas affected by direct radiation in the Bailey Cove mudflats, exceeded the occupancy factor presented in the ODCM. Based on this review, the inspector concluded that the occupancy factor presented in the ODCM for the Bailey Cove mudflats was reasonable.

In order to derive an incremental dose to the individual clam/worm digger, the intertidal zone direct dose rate from the sediment must be compared to the direct dose rate from soil at background contamination levels. For instance, the hypothetical worm digger referred to in Maine Yankee's Environmental Report dated April 19, 1972 (pg. 5.2-6) would receive a total exposure of about the same magnitude if he did not dig worms. This was because background levels on the mud flats were found to be lower than the background levels on land.

7.1.3.3 Worm Digging

The two species of marine worms which form the basis for the commercial bait worm industry of Montsweag Bay and the Sheepscot River Estuary are the bloodworm, *Glycera dibranchiata*, and the sandworm, *Nereis virens*. Since these biota are not directly ingested by humans, the human dose pathways from commercial bait-worm digging is limited to direct exposure from standing on the mudflats and, to some degree, exposure to limited amounts of sediment which might be ingested and/or carried away on clothes or skin.

7.1.3.4 Clam Harvesting

Soft-shell clams are sometimes harvested in and around the Maine Yankee intertidal zone. The exposure pathways are similar to the worm digger with the exception that this biota is directly ingested by humans and is, therefore, subject to an internal dose pathway associated with this consumption.

7.1.3.5 Swimming

When swimming occurs the individual is subject to direct exposure pathways from the sediment which is subject to shielding by the water. Since the mudflats are not amenable to sunbathing, the occupancy time and exposure pathways associated with the worm/clam digger are expected to result in more dose.

7.1.3.6 Fishing

Fishing can be performed either from shore or a boat. Both forms of fishing subject the individual to internal dose pathways associated with the consumption of fish. When fishing from

shore, the individual is subject to direct exposure pathways from the sediment. However, the occupancy time is not expected to be any more than that estimated for the worm/clam digger.

7.1.4 Potential Future Uses of the Intertidal Zone

Potential future uses of the intertidal zone at Maine Yankee include sea weed production, flooding for lobster pound or fish farming and land reclamation gardening. Each of these possible future uses would involve disturbance of the mudflat environment which would probably require extensive environmental permitting. The consideration of these possible future uses is for potential dose assessment purposes only and does not presume that these uses will be found to be environmentally acceptable or commercially suitable for actual use.

7.1.4.1 Seaweed Growing and Harvesting

Seaweed is present in the shoreline surrounding Maine Yankee. It is used locally as garden fertilizer and by some people as a dietary supplement. Seaweed as a staple item of diet has been used in Japan and China for a very long time. It accounts for some 10% of the Japanese diet and seaweed consumption reached an average of 3.5 kg per Japanese household in 1973. In the western world, seaweed is largely regarded as a health food and, although there has been an upsurge of interest in seaweed as food in the last 20 years, it is unlikely that seaweed consumption there will every be more than a fraction of the Japanese.

When gardeners talk about using seaweed on their plants, they are usually referring to a brown algae, specifically the one know as knotweed or rockweed (*Ascophyllum nodosum*). It's common off the coast of Norway but also grows along the American coast from northern Maine to Canada and through out northern seas. Seaweed meals are best applied at the rate of 1 to 3 pounds per 100 square feet.

Seaweed cultivation takes many forms but there is a kind of evolutionary process through which it develops, the rate of which is market-driven. If demand is low and natural resources adequate, cultivation is unnecessary. As demand increases, natural populations frequently become inadequate and attempts are made to increase production by resource management techniques such as improving harvesting techniques, removing competing species, adding artificial habitats and seeding cleared areas. Such techniques are most highly developed in Japan, China and south-east Asia.

Should such management prove to be inadequate, the use of artificial structures to grow seaweeds becomes inevitable. Fragments of adult plants, juvenile plants, sporelings or spores are seeded onto ropes or other substrata and the plants grown to maturity in the sea. To do this, intimate knowledge of both the biology and life history of the plants is critical. For example, kelps cannot be grown from fragments as there is a high level of specialization and fragments of sporophytes do not regenerate. On the other hand, many red algae do not have this degree of specialization and can easily be grown from portions of the adult plant. Knowledge of the life history is critical in many cases and on-land cultivation of particular life history phases is often necessary for seeding. A considerable amount of technology has gone into the development of reliable methods for the cultivation of seed-stocks and their improvement.

The penultimate development in seaweed cultivation is the growing of plants in artificial impoundments on land. This involves the use of either tanks or ponds into which seawater is pumped and the seaweeds are grown detached and at very high densities. This necessitates the careful study of

the growth parameters of the seaweeds involved and the development of special strains, preferably with high growth rates, but more importantly, adapted to the artificial conditions.

The dose pathways from this potential future use would include direct ingestion of seaweed, indirect ingestion of vegetables fertilized with seaweed and any occupational dose associated with seaweed cultivation from direct exposure to sediment to the extent that impoundments are drained for seeding, harvesting or maintenance. The direct exposure occupancy time is not expected to be greater than that estimated for the worm/clam digger.

7.1.4.2 Flooding for Lobster Pound or Fish Farming

Mudflat areas could be used for fish farming or lobster storage. These uses could convert the intertidal zone into a subtidal area by changing the hydrologic system, by the installation of a dam structure that allows seawater to flood at high tide. This is similar to the creation of ponds as described above for cultivation of seaweed. The dose pathways from this potential future use would include ingestion of fish and shell fish and any occupational dose from direct exposure to sediment to the extent that the impoundment is drained for placement, retrieval or maintenance. The direct exposure occupancy time is not expected to be greater than that estimated for the worm/clam digger.

7.1.4.3 Land Reclamation Gardening

Although it is highly unlikely because of the amount of farmable land in Maine, it is possible that future generations may consider reclaiming underwater land areas for farming. If this were the case, the sediment would be farmed as soil. One could then apply all of the dose pathways associated with the residential farmer as described in the License Termination Plan. A simple relationship between dose and residual soil contamination could be made using the soil screening values.

7.1.5 Identification of Scenarios and Pathways/Dose Assessment Framework

As a result of the current and possible future uses described above for the intertidal zone around Maine Yankee, the following scenarios are evaluated for identification of dose pathways and calculation of an incremental intertidal zone dose.

7.1.5.1 Commercial Worm/Clam Digger and Fish/Shell Fish Ingestor

An individual harvests worms and/or clams in the intertidal zone surrounding Maine Yankee at a rate of no more than 325 hours per year. In the process of worm/clam digging, the individual directly ingests a trace amount of sediment and become smeared with a trace amount of sediment in contact with his clothes and exposed surfaces of his skin for a period of about twice as long as the occupational time in the intertidal zone. In addition, the individual consumes fish and seafood in quantities equal to that assumed in the Offsite Dose Calculation Manual. This scenario should produce a greater dose than the possible future use of the intertidal zone as a lobster pound or fish farm or the recreational shoreline fisherman.

Dose from Standing on the Sediment

Maine Yankee will calculate the dose from standing on three feet of sediment containing residual radioactivity in concentrations of 1 pCi/g of ^{137}Cs and the dose from a similar source of 1 pCi/g of ^{60}Co . The hard-to-detect nuclides will be assumed to be present for the ^{60}Co source in proportion to their nuclide fraction specified in the License Termination Plan for sediment, Table 2-

13. These relationships will be used to evaluate the average and maximum concentrations residual radioactivity found in the intertidal zone after the background concentrations have been subtracted.

Dose from Ingesting a Trace Amount of Sediment

The individual is assumed to ingest 0.05 g/day of sediment as a consequence of working in the mudflats. The exposure period is assumed to be 104 days per year, which is derived from two days per week for a year. The resulting dose is calculated by multiplying the dose factor from FGR-11 by the quantity of sediment ingested in a year for each nuclide.

Dose from Contact with a Trace Amount Sediment

The individual is assumed to have a source of sediment spread over a 100 cm² area of skin. The dose rate calculated from VARSKIN was extrapolated from a 1pCi/cm² to the actual 0.1 pCi/cm² for 104 occurrences per year and 12 hours contact hours per occurrence and converted to dose equivalent resulting in an annual dose of 0.0096 mrem/yr per pCi/g for ¹³⁷Cs and 0.0043 mrem/yr per pCi/g for ⁶⁰Co.

Dose from Fish Ingestion

The individual is assumed to consume 20.6 kg/y of fish as described in License Termination Plan section 6.6.7, 6.6.9 and NUREG-5512. This consumption rate is used, along with the dose factors from FGR-11, to establish a relationship between the dose received from this pathway and the average and maximum concentrations of residual radioactivity found in fish after the background concentrations have been subtracted

Dose from Shell Fish Ingestion

The individual is assumed to consume 1 kg/y of shell fish as described in License Termination Plan section 6.6.9 and NUREG-5512. This consumption rate is used, along with the dose factors from FGR-11, to establish a relationship between the dose received from this pathway and the average and maximum concentrations of residual radioactivity found in shell fish after the background concentrations have been subtracted.

7.1.5.2 Seaweed Cultivator, Eater and Fertilizer User

An individual cultivates seaweed for personal use as a dietary supplement and as a fertilizer for the garden. This individual receives no more dose from the sediment than that experienced by the commercial worm/clam digger. The individual consumes seaweed at a rate equal to that assumed in Engineering Calculation 041-01, specified below. The individual also cultivates the garden with seafood used as a fertilizer at a use rate and accumulation factor equal to that assumed in Engineering Calculation 041-01, specified below.

Dose from Standing on the Sediment

This dose will be calculated as described above.

Dose from Ingesting a Trace Amount of Sediment

This dose will be calculated as described above.

Maine Yankee Marine Sampling Study

Dose from Contact with a Trace Amount Sediment

This dose will be calculated as described above.

Dose from Seaweed Ingestion

The individual is assumed to consume 875 g/y of seaweed as described in Engineering Calculation EC-041-01. This consumption rate is used, along with the dose factors from FGR-11, to establish a relationship between the dose received from this pathway and the average and maximum concentrations of residual radioactivity found in seaweed after the background concentrations have been subtracted.

Dose from Ingestion of Vegetables Fertilized with Seaweed

The individual is assumed to consume 112 kg/y of vegetables fertilized with seaweed with a biotransfer factors from the seaweed to vegetables of 0.08 for ^{60}Co and 0.04 for ^{137}Cs as described in Engineering Calculation EC-041-01 and NUREG-5512. This consumption rate and these biotransfer factors are used, along with the dose factors from FGR-11, to establish a relationship between the dose received from this pathway and the average and maximum concentrations of residual radioactivity found in seaweed after the background concentrations have been subtracted.

7.1.5.3 Land Reclamation Farmer

This individual reclaims the submerged land and uses the sediment of the intertidal zone as a garden. All of the dose pathways described for the residential farmer apply to this individual. For ease of use, the soil screening values described in the License Termination Plan are used to establish a relationship between the sediment/soil concentration of residual radioactivity and the resulting dose.

7.1.6 Identification of Flora & Fauna Dose Contributors and Bioaccumulators

The intertidal zone surrounding Maine Yankee is almost entirely made up of mud flats. Mud flats are organically rich regions that support large populations of shellfish, shrimp, mussels, quahogs, baitworms, and small invertebrates. By slowing tidal and wave energy, mud flats buffer the upland against tidal erosion and lessen impacts from storm surge events. Eelgrass beds and macroalgae that add structure to the habitat cover many flats in Maine. Sediments contain high concentrations of benthic diatoms that form the base of the benthic food web, remove nutrients from the mud, and lessen erosion by binding sediments. Small fish like mummichogs and sticklebacks forage on invertebrates and algae during flood and ebb tide. Flats support high concentrations of bacteria, fungi, and other microorganisms that contribute to nutrient cycling and provide food for larger macrofauna like sand worms. They are limited resources that perform a vital function as sinks for contaminants.

Mud flats are critical feeding grounds for 25 species of migrating and resident shorebirds, six species of herons, two species of egrets, glossy ibis, Canada geese, commercial and non-commercial finfish, herring gulls and waterfowl. Flats are nursery grounds for winter flounder and other flatfish. They provide roosting and staging areas for migrating shorebirds. Mud flats are potential habitat for the rare plant pipewort (*Eriocaulon parkeri*).

Mud flats contribute to a multi-million dollar seafood industry in Maine by providing structure and foraging habitat for soft-shell clams, Atlantic herring, blood worms, blue mussels, sand worms, periwinkles, alewife, winter flounder, rainbow smelt, Atlantic mackerel and sand shrimp. The primary dose contributors to the human population are those which are directly ingested.

Therefore, the fauna that should be considered for sampling are soft-shell clams, blue mussels, periwinkles, if available, winter flounder, rainbow smelt, and Atlantic mackerel. Samples of seaweed should also be obtained to support the dose assessment for the seaweed eater and fertilizer user.

7.2 DOSIMETRY RESULTS

Applying these concentrations to the dose calculations, we calculate doses shown in Table 7-1 and 7-2. We calculate total doses of less than 0.1 mrem/year when using average values of ^{60}Co (6 pCi/kg) and ^{137}Cs (28 pCi/kg), and less than 3.3 mrem/year when the maximum values of ^{60}Co (180 pCi/kg) and ^{137}Cs (1000 pCi/kg) are used.

Most of the doses for clam diggers, fisherman, and worm digger are over wet sediment or standing in wet sediment. The correct dose rates are then necessarily for wet sediment. However, for the farmer who drains the tidal flat to form a dry farm using sediment as soil, the sediment should be dry for the dose estimate. We have done this for sediment cores and have calculated an average increase of activity per mass at a fraction of 1.9 times the wet sediment activity per unit mass in the core. The dose will be increased by the same factor and will closely resemble the dose measured on dry land by the high pressure ion chamber (HPIC), which was dragged over the mud flat and back onto dry land. Since the wet or dry sediment on the skin surface is thin, wet or dry activity will have less importance for the gamma dose. All shellfish, finfish and seaweed samples were measured and would be consumed as wet as food. Trace contaminants of sediment in food are also consumed wet. For this reason, the sediment measurements are presented as wet measurements conforming to realistic HPIC measurements for the exposed workers such as clam diggers, fisherman, worm diggers and swimmers.

Table 7-1. Calculated Doses Using Average Concentrations of Gamma Emitters

<i>Pathways</i>	Worm Digger (mrem/yr)	Clam Harvester (mrem/yr)	Lobster Eater (mrem/yr)	Recreation Fishing (mrem/yr)	Recreation Swimming (mrem/yr)	Seaweed Harvester (mrem/yr)	Lobster Pound (mrem/yr)	Land Reclamation (mrem/yr)
Direct Standing on Sediment	2.58E-03	2.58E-03	NA	2.58E-03	2.58E-03	2.58E-03	2.58E-03	NA
Contact with Trace Sediment	1.71E-02	1.71E-02	NA	NA	NA	1.71E-02	1.71E-02	NA
Ingestion of Trace Sediment	6.78E-05	6.78E-05	NA	NA	NA	6.78E-05	6.78E-05	NA
Ingestion of Clams/Mussels	NA	6.38E-03	NA	NA	NA	NA	NA	NA
Ingestion of Lobster	NA	NA	1.43E-02	NA	NA	NA	1.43E-02	NA
Ingestion of Fish	NA	NA	NA	2.34E-01	NA	NA	NA	NA
Ingestion of Seaweed	NA	NA	NA	NA	NA	6.31E-04	NA	NA
Ingest Veg. Fertilized w/Shells	NA	2.84E-03	2.84E-03	NA	NA	NA	2.84E-03	NA
Ingest Veg. Fertilized w/Seaweed	NA	NA	NA	NA	NA	4.80E-03	NA	NA
Integrated Res. Farmer Dose	NA	NA	NA	NA	NA	NA	NA	1.45E-01
Grand Total	1.97E-02	2.89E-02	1.71E-02	2.37E-01	2.58E-03	2.51E-02	3.68E-02	1.45E-01

Table 7-2. Calculated Doses Using Peak Concentrations of Gamma Emitters

<i>Pathways</i>	Worm Digger (mrem/yr)	Clam Harvester (mrem/yr)	Lobster Eater (mrem/yr)	Recreation Fishing (mrem/yr)	Recreation Swimming (mrem/yr)	Seaweed Harvester (mrem/yr)	Lobster Pound (mrem/yr)	Land Reclamation (mrem/yr)
Direct Standing on Sediment	8.48E-02	8.48E-02	NA	8.48E-02	8.48E-02	8.48E-02	8.48E-02	NA
Contact with Trace Sediment	2.67E-02	2.67E-02	NA	NA	NA	2.67E-02	2.67E-02	NA
Ingestion of Trace Sediment	3.31E-04	3.31E-04	NA	NA	NA	3.31E-04	3.31E-04	NA
Ingestion of Clams/Mussels	NA	6.38E-03	NA	NA	NA	NA	NA	NA
Ingestion of Lobster	NA	NA	1.43E-02	NA	NA	NA	1.43E-02	NA
Ingestion of Fish	NA	NA	NA	2.34E-01	NA	NA	NA	NA
Ingestion of Seaweed	NA	NA	NA	NA	NA	6.31E-04	NA	NA
Ingest Veg. Fertilized w/Shells	NA	2.84E-03	2.84E-03	NA	NA	NA	2.84E-03	NA
Ingest Veg. Fertilized w/Seaweed	NA	NA	NA	NA	NA	4.80E-03	NA	NA
Integrated Res. Farmer Dose	NA	NA	NA	NA	NA	NA	NA	3.31E+00
Grand Total	1.12E-01	1.21E-01	1.71E-02	3.19E-01	8.48E-02	1.17E-01	1.29E-01	3.31E+00

8 CONCLUSIONS

8.1 SUMMARY

This report characterizes radionuclides in the marine environment around Maine Yankee and describes the methodologies used in the study. Four sets of sampling were accomplished to complete this study. The results of each type of sampling were provided and are compared with a model of radionuclide distribution from licensed discharges. Additionally, the results are compared to previous work done in the area both pre and post plant operation. The results are also used to calculate an incremental intertidal zone dose, which is compared to the limiting “resident farmer dose calculations in the License Termination Plan for Bailey Point post-decommissioning. Maine Yankee operated from 1972-1996. Plant decommissioning is scheduled to be complete in late spring of 2005.

This sampling effort included a search for areas high in nuclear radiation (hot particle search), samples from the surface of the tidal region, core samples from the tidal region, and samples of biota including seaweed, lobsters, mussels, and fish. The results are discussed in this order. In all, about 600 samples from 147 locations were collected and analyzed. To ensure that the sampling effort was as comprehensive and efficient as possible, a model was used to determine the best locations.

8.2 KEY FINDINGS

- a. The nuclide ^{60}Co is stronger on the Oak Island side of Montsweag Bay, near the intake where recent discharges were released. This is reasonable since 5.2-year half-life of ^{60}Co will reduce levels when no additions are released in recent times.
- b. The nuclide ^{137}Cs is stronger on the Bailey Cove north of the outfall. This is the same area where the ^{137}Cs was high during the outfall discharge during 1972-76, before the diffuser was installed. Some of the ^{137}Cs is seen near the diffuser release area. The long half-life of ^{137}Cs makes this a reasonable result.
- c. Maximum nuclide levels are 10-30 times lower in the sediments of Montsweag Bay and Bailey Cove in comparison to the 1972 and 1974 surveys.
- d. Radionuclides in the biota are even lower by 10-30 than the concentration in sediments. This was seen in oysters 0.8pCi/kg (0.0008 pCi/g) versus sediment 4 pCi/kg (0.004 pCi/g) (1973-74).
- e. The modeled nuclides follow the same general pattern as the measured nuclides. Sediment from the shore and intertidal zones are higher than those from the main channel of Montsweag Bay, due to higher fluctuations in the main channel.
- f. Surficial samples were lower than deeper levels of core samples. This was due to burial of radionuclides in past releases in the lower ten inches of the cores.
- g. Cores showed double peaks, one from early 1957-69, and a second peak in 1983-85. We think that the first peak is mainly fallout, and second is the Maine Yankee power plant, Chernobyl, and Chinese and French fallout. ^{210}Pb dating of one core gives similar sedimentation rates (6 inches equals 30 years). This agrees with the sedimentation rate from Hess et al., (1976), for sediments in Bailey cove.

Maine Yankee Marine Sampling Study

- h. The total dose from marine biota and sediment ranges from 1.9×10^{-2} mrem/yr for worm diggers to 1.4×10^{-1} mrem/yr for land reclamation farming. This calculation was based on average values in the sediment for ^{60}Co and ^{137}Cs .
- i. The upper limit of doses from marine biota and sediment range from 1.1×10^{-1} mrem/yr for worm diggers to 3.3 mrem/yr for land reclamation farming.

9 QUALITY ASSURANCE

The report underwent peer review by all of the project's principal investigators. In addition, data collected during this study were compared to previous investigations.

10 PROJECT ORGANIZATION

At the outset of the project, the Project Manager Dr. Hess met with project staff to establish that the project would meet the highest standards of quality and safety. Copies of the Sample and Analysis Plan were distributed to all project staff. Prior to field collections, the field team leader met with field staff to review project protocol, safety, and operations. The core project staff (Dr. Hess, Mr. Churchill and Ms. Bowen) had weekly conference calls, along with electronic and telephone conversations as needed, to plan and implement the project SAP. Each core staff member met frequently with project staff to communicate project safety and quality objectives.

Acknowledgements

We are grateful to the staff of Camp Chewonki in Wiscasset for use of their facilities and for logistical support. Particular thanks go to Dr. Don Hudson, President of the Chewonki Foundation, and to Ryan Linnahan, a vessel operator a Camp Chewonki. For assistance in specifying the tidal boundary conditions of our model, we are grateful to Dr. Richard Luettich of the University of North Carolina at Moorhead City, NC. In our modeling effort, we benefited through discussions with James Manning of the National Marine Fisheries Service in Woods Hole, MA. We are grateful to Raymond Shadis of Friends of the Coast for his input and advice through all stages of our study. Thanks also go to Christopher Doherty, president of Friends of the Coast, for his involvement in the project and for participating (with Ray Shadis) in the drifter operations of July 2004. Friends of the Coast dedicates their involvement in this project to the late member, Edward Myers of Bristol, the man who inspired and instigated their settlement stipulation for a marine and intertidal zone radiological survey. We also would like to thank David Sutter, lobster fisherman, for specially setting traps for this project. Carol James, Chewonki Foundation, for helping us with site access, and Tim James, Wiscasset Shellfish Commission, for assisting us with shellfish procurement.

The project team also wishes to thank the staff at Maine Yankee, especially Mike Whitney, and Pat Dostie, State of Maine, for their assistance with this project.

11. REFERENCES CITED

- Aubrey, D. G., and Speer, P. E. (1985). "A study of non-linear tidal propagation in shallow inlet/estuarine systems, Part I: Observations," *Estuarine, Coastal and Shelf Science* 21, 185-205.
- Boon, J. D. and Byrne, R. J. (1981). "On basin hypsometry and the morphodynamic response of coastal inlets," *Marine Geology* 40, 27-48.
- Churchill J. H. 1976. Measurement and Computer Modeling of The Distribution of Reactor Discharged Radionuclides in the Estuarine Sediment near The Maine Yankee Power Plant in Wiscasset Maine. Master's Thesis, University of Maine, Orono Maine, 122 Pp.
- Churchill J. H, C. T. Hess, and C. W. Smith. 1980. Measurement and Computer Modeling of Radionuclide Uptake by Marine Sediments Near a Nuclear Power Reactor. *Health Physics* Vol. 38 March pp 327 to 340.
- Churchill J. H, C. W. Smith, C. T. Hess and A. Price. 1975. Measurement of radionuclides as a function of position in the estuary of the Maine Yankee atomic power plant. Presented at the American Physical Society Meeting New England section Apr. 19, 1975
- Davis, R.E. (1985) Drifter observations of coastal surface currents during CODE: The method and descriptive view. *Journal of Geophysical Research*, 90, 4741-4755.
- DiLorenzo, J. L. (1988). "The overtide and filtering response of small inlet/bay systems," *Hydrodynamics and sediment dynamics of tidal inlets*. D. G. Aubrey and L. Weishar, eds., 24-53, Springer Verlag, New York, NY.
- Feigner, K.D. and H.S. Harris (1970) Documentation Report FWQA Dynamic Estuary Model (Washington DC: FWQA Dept. of Interior).
- GPS Duratek "Characterization survey report of the Maine Yankee atomic power plant 1998 survey package numbers R 0400, R 1900, R 2000
- Hess, C. T., C. W. Smith, and A. H. Price, 1978, A Multiple Mechanism Description Of Radionuclide Loss from Marine Sediment, *Nature*, 807-809.
- Hess, C. T., C. W. Smith, J. H. Churchill, and G.F. Burke. 1976. Radioactive ISA Topic Characterization of The Environment near Wiscasset Maine Pre and Post Operational Surveys in The Vicinity of The Maine Yankee Nuclear Reactor. Technical Note ORP/EAD-76-3, U.S. Environmental Protection Agency, Washington D.C. 56 Pp.
- Hess, C.T., C. W. Smith, H. A. Kelly, and F. C. Rock. 1974. A Radioactive Isotopic Characterization of The Environment near Wiscasset Maine: a Pre-Operational Survey in The Vicinity of The Maine Yankee Atomic Power Plant. *Radiation Data and Reports*, 15 39-52.
- Hess, C.T., Smith, C.W. and Pearce, B.R. (1983) Radionuclide concentrations in the estuarine sediments: comparison of measured and calculated values. In: *Wastes in the Oceans*, Volume 3 of *Radioactive Wastes in the Oceans*, Eds: Park, Kester, Duedall, and Ketchum, Wiley pp. 270-284.
- Larson, P.F. 1975. Benthos study of the Sheepscot river Estuary. Annual report submitted to Maine Department of Marine Resources under project no. 3-205-R-1. 43 p.

Maine Yankee Marine Sampling Study

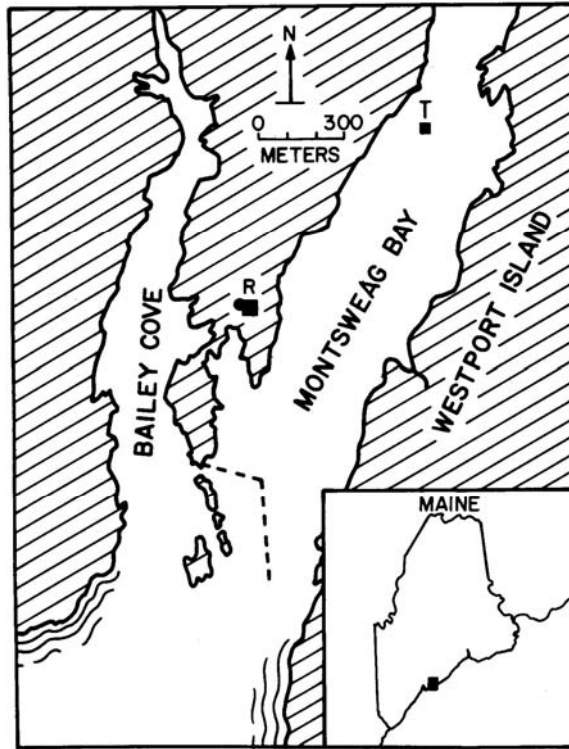
- Larson, P.F. and Doggett, L 1991. The macroinvertebrate fauna associated with the mud flats of the Gulf of Maine. *J. Coastal Res.* 7(2): 365-375.
- Larson, P.F., Doggett, L. and A.C. Johnson. 1983. The macroinvertebrate fauna associated with the five sand flats in the northern Gulf of Maine. *Proc. N.S. Inst. Sci.* 33: 57-63.
- Law, K.Y. (1979) Modeling of tidal flow and distribution of Radionuclides. Masters Thesis, University of Maine, Orono, Maine, 101 pp.
- Lincoln, J. M., and Fitzgerald, D. M. (1988). "Tidal distortions and flood dominance at five small tidal inlets in Southern Maine," *Marine Geology* 82, 133-148.
- Luettich, R.A., J.J. Westerink, and Scheffner, N.W. (1992) ADCIRC: an advanced three-dimensional circulation model for shelves, coasts and estuaries, Report 1: theory and methodology of ADCIRC-2DDI and ADCIRC-3DL. Technical Report DRP-92-6, U.S. Army Engineer, Waterways Experiment Station, Vicksburg, MS.
- Maine Yankee Atomic Power Company. 1978. Final Report. Environmental Surveillance and Studies at the Maine Yankee Nuclear Generating Station, 1969-1977. Maine Yankee Atomic Power Company.
- Maine Yankee Memorandum H.R. Cummings to PL Anderson dated June 24 1994. Results of May 1994 Clam and Sediment Sampling
- Maine Yankee Nuclear Power Station: Annual Radiological Environmental Operating Report, January-December 2002. Prepared by Framatome ANP.
- Mukai, A.Y, J.J. Westerink, and R.A. Luettich (2001) Guidelines for using the Eastcoast 2001 database of tidal constituents within the western North Atlantic, Gulf of Mexico and Caribbean Sea. U.S. Army Corp of Engineers, Coastal and Hydraulic Engineering Technical Note (IV-XX).
- Speer, P. E., and Aubrey, D. G. (1985). "A study of non-linear tidal propagation in shallow inlet/estuarine systems: Part II-theory," *Estuarine, Coastal and Shelf Science* 21, 207-224.
- U.S. Environmental Protection Agency, Environmental Analysis Division. 1976. Radioactive isotopic characterization of the environment near Wiscasset Maine using pre- and post-operational surveys in the vicinity of the Maine Yankee nuclear reactor.
- van de Kreeke, J. (1988). "Hydrodynamics of tidal inlets," *Hydrodynamics and sediment dynamics of tidal inlets*. D. G. Aubrey and L. Weishar, eds., 1-23, Springer, Berlin.
- Westerink, J.J., R.A. Luettich and J.C. Muccino (1994) Modeling tides in the western North Atlantic using unstructured graded grids, *Tellus*, 46A, 178-199.

APPENDIX A

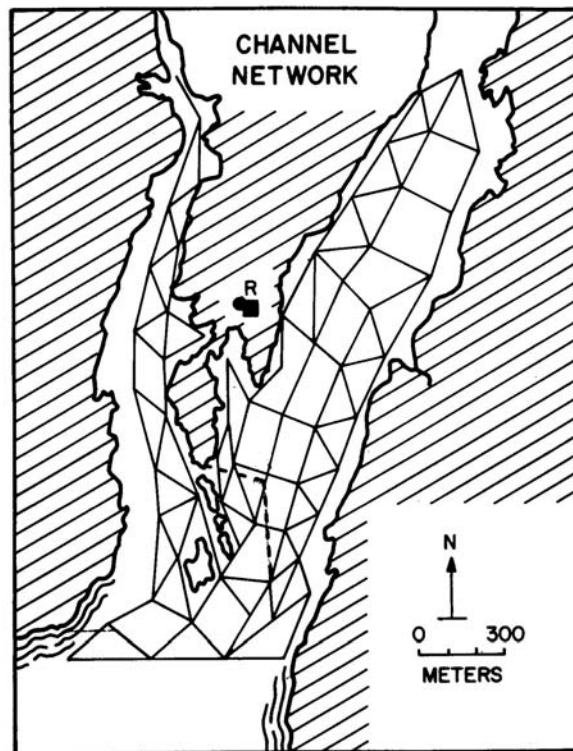
Introduction to Previous Work

This section shows the figures that were associated with two previous modeling projects in Bailey Cove and Montsweag Bay. The first study was done in 1972 modeling the area around Bailey Cove, and was done as a part of a Sea Grant Master's Thesis project by Churchill (1976), and Churchill et al. (1980). The second involved modeling the diffuser and changes in Montsweag Bay as well as Bailey Cove. This project was completed in 1983 by Hess et al. Thomas L. Cameron also helped with the modeling in his undergraduate thesis at the University of Maine. Sediment changes were modeled in 1978 by Hess et al. Appendix Figure A-1 shows the map of the State of Maine and Bailey Cove with Montsweag Bay. Appendix Figure A-2 shows the channel network used for the modeling of Montsweag Bay and Bailey Cove after the diffuser was put in. Two early isocuric plots for ^{60}Co in September 18, 1974 and June 12, 1975 are depicted in Appendix Figures, A-3 and A-4, and show concentrations of ^{60}Co when the plant was releasing at the outfall. Appendix Figure A-5 shows a construction sheet for isocuric plots for ^{137}Cs in a survey taken after the diffuser was in place and gives some higher values for ^{137}Cs along the shore of Westport Island and in a vicinity of the old outfall at Bailey Cove. Appendix Figure A-6 shows a sample of currents calculated at slack high tide. Appendix Figure A-6 shows concentrations estimated in the sediment for ^{137}Cs with releases at high tide of 4.38 hours. Appendix Figure A-8 shows sediment concentrations for ^{137}Cs for releases of 4.38 hours beginning and mid-ebb tide and Appendix Figure A-9 shows estimated sediment concentrations of ^{137}Cs for releases of 17.5 hours beginning at high tide. Appendix Figure A-10 shows sediment concentrations estimated for ^{58}Co for releases of 4.38 hours beginning and mid tide. Appendix Figure A-11 shows simulated pCi/ft contours after a 17.5 hour release on high tide. This shows a major concentration of the nuclides in the vicinity of the diffuser and to the south. Appendix Figure A-12 shows simulated contours for ^{58}Co for a 17.5 hour release on high tide, and also shows major concentrations around the diffuser and a smaller concentration at the head of Bailey Cove. Appendix Figure A-13 shows isocuric plots for the ^{58}Co actually measured in pCi/kg and shows maximum values around the diffuser and upper Bailey Cove.

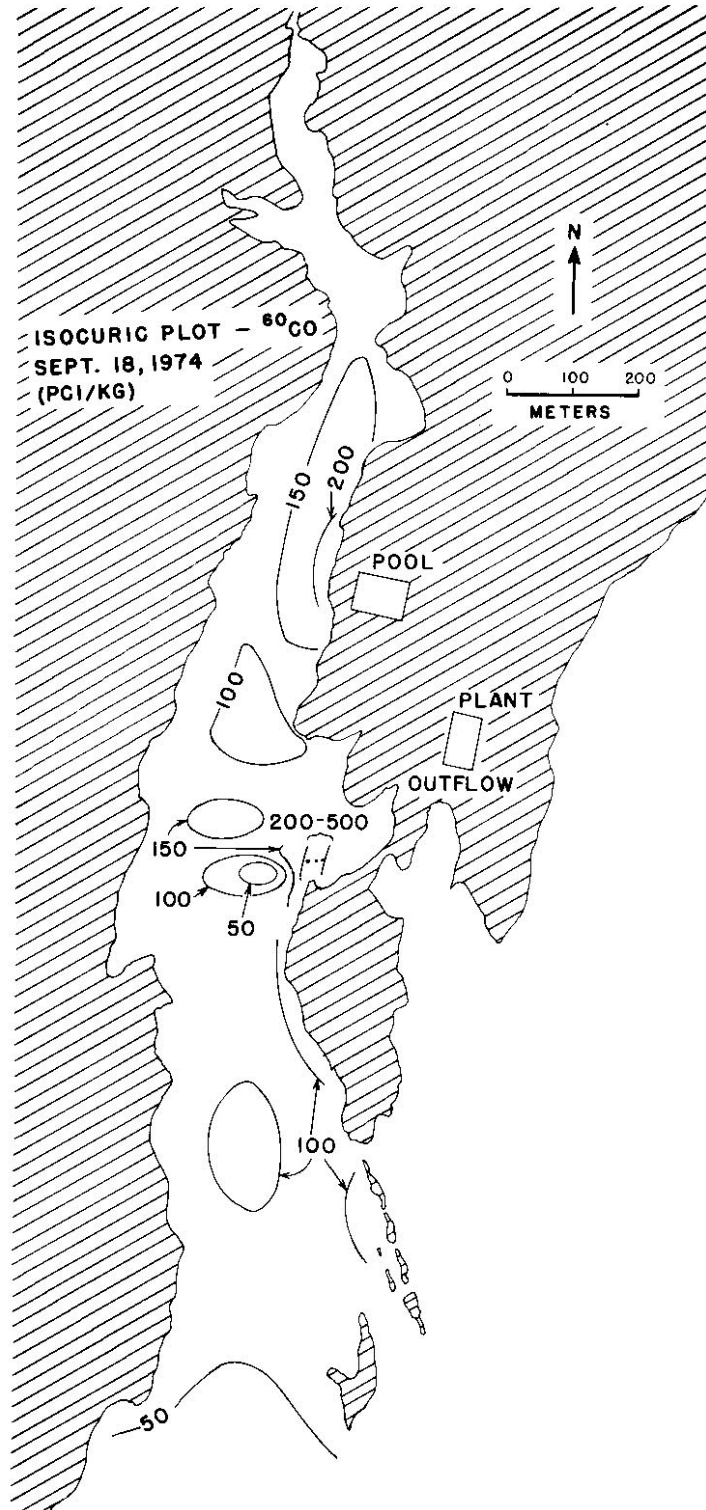
Fifty samples were taken in the first transect of Bailey Cove from south Long Ledge to the top of Bailey Cove, with one sample at the outfall. The maximum was 5620 pCi/kg of ^{58}Co and 500 pCi/kg of ^{60}Co at #28. A hot particle was found on the Eaton Farm side of Bailey Cove, near the shore (7700 pCi of ^{60}Co , 530 pCi of ^{58}Co , 670 pCi of ^{46}Sc , 120 pCi of ^{54}Mn) for a total of 9000 pCi in a sample weighing 20 micrograms. The average sediment was 1000 pCi/kg of ^{58}Co , and 120 pCi/kg of ^{60}Co , with ^{137}Cs at about 750 pCi/kg. The highest values were observed at the outfall and along the upper (north) half of Bailey Cove near the Eaton Farm side.



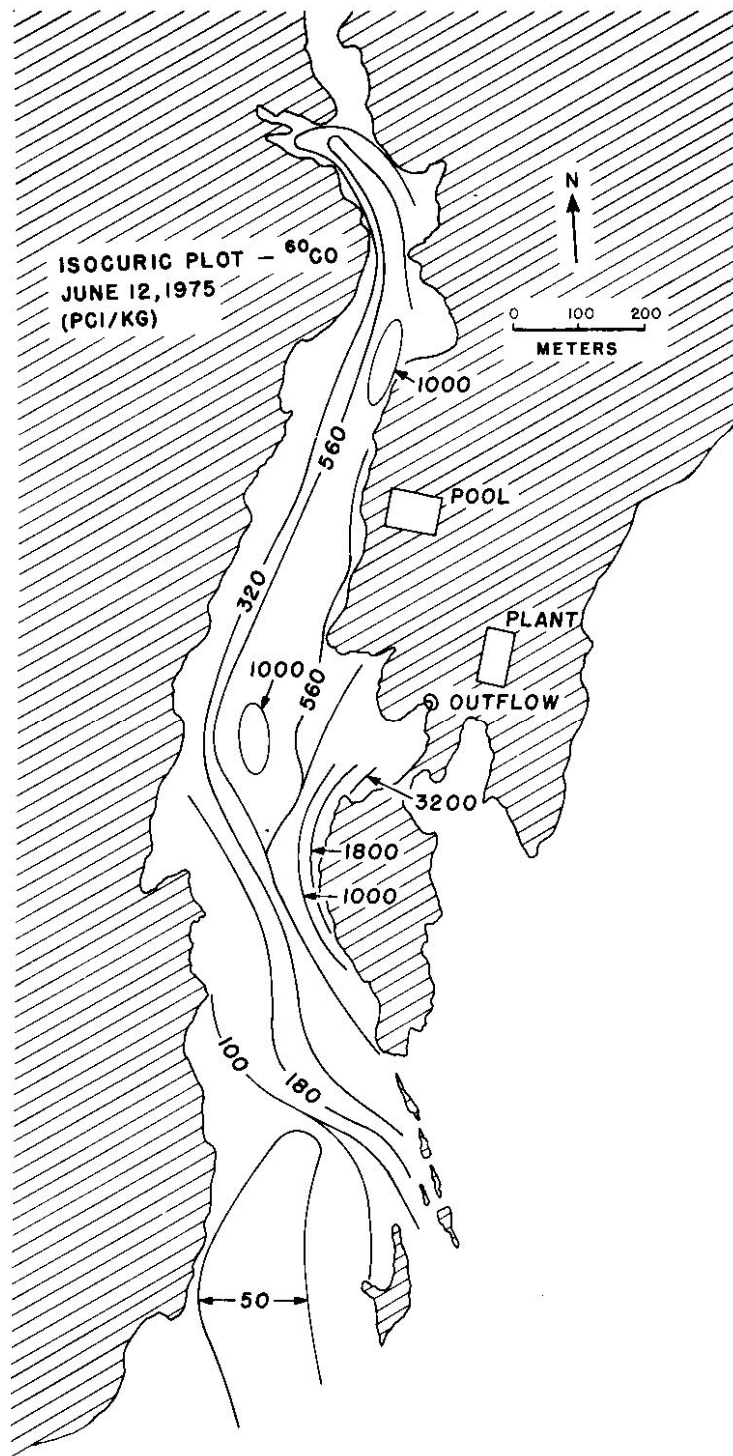
Appendix Figure A-1. Project locus map (1978).



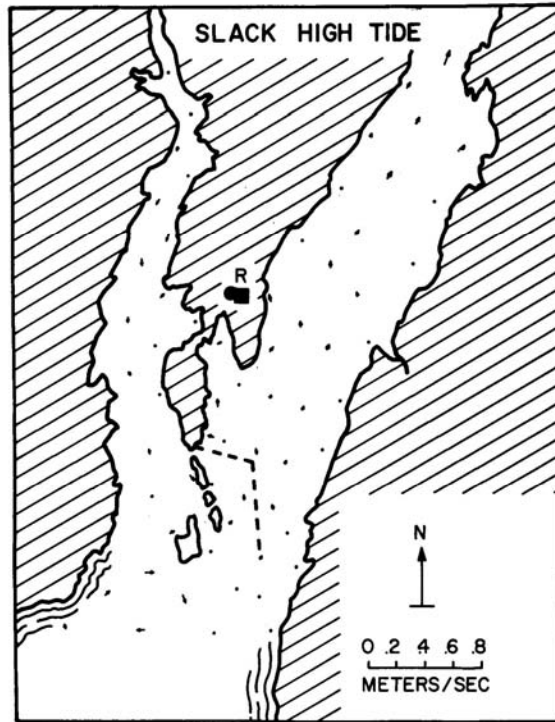
Appendix Figure A-2. Channel network used for Montsweag Bay and Bailey Cove modeling. (Source: Churchill et al. 1980; Hess et al. 1983)



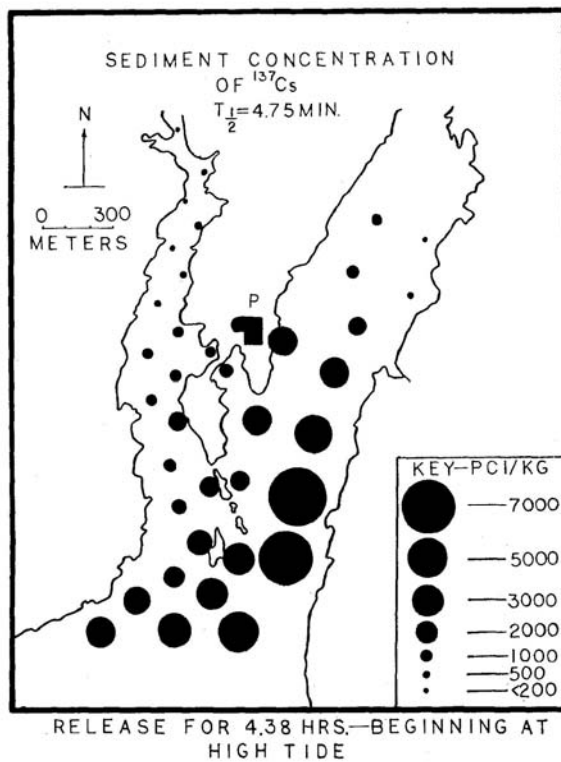
Appendix Figure A-3. Actual contours for ^{60}Co measured on September 18, 1974 during licensed releases.



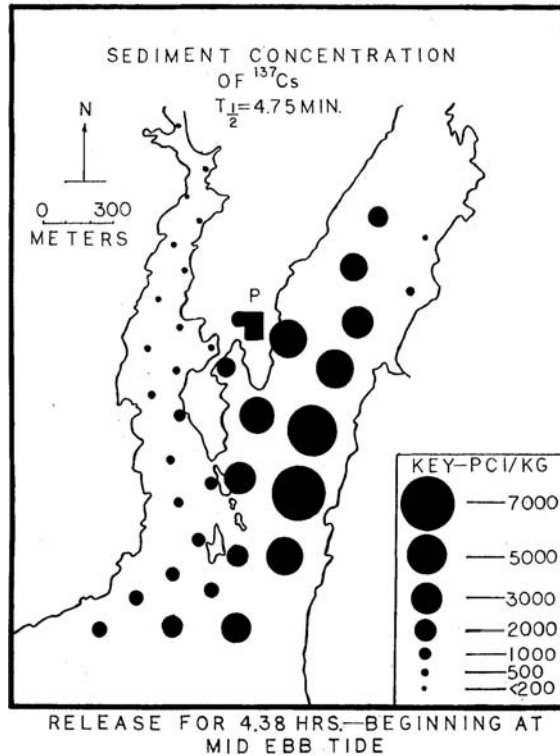
Appendix Figure A-4. Actual contours for ^{60}Co measured on June 12, 1975 during licensed releases.



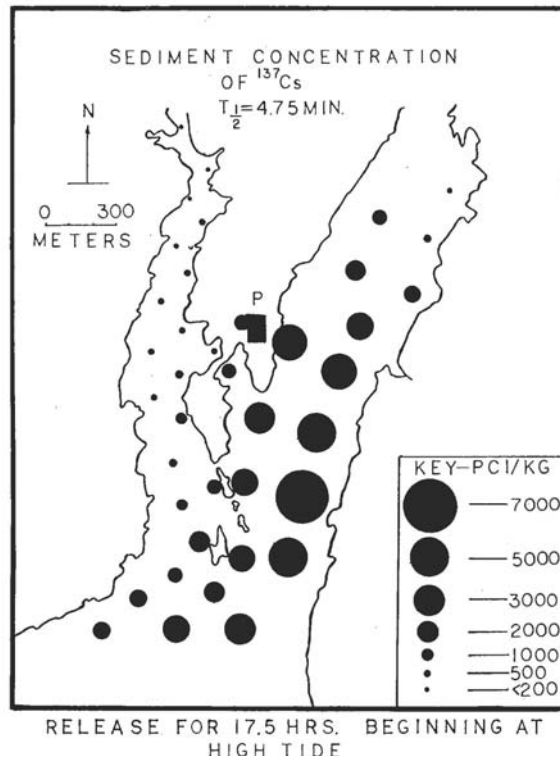
Appendix Figure A-6. Sample of currents at slack high tide (1978).



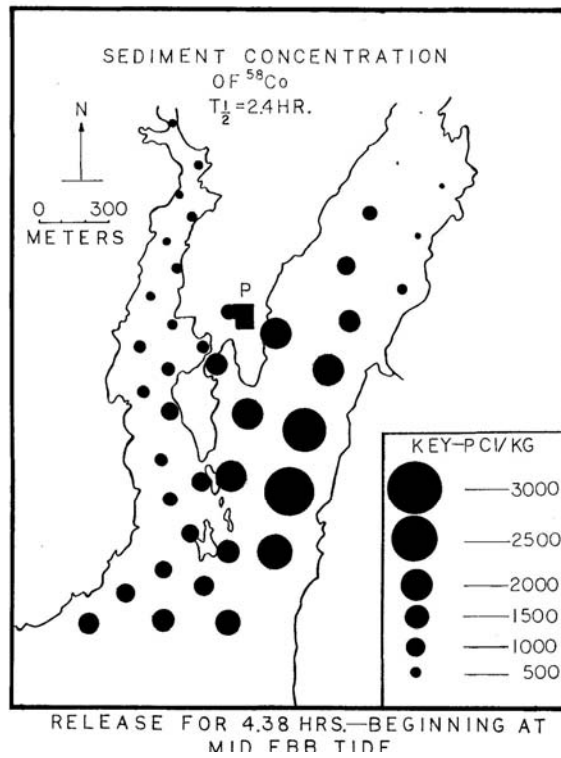
Appendix Figure A-7. Estimated ¹³⁷Cs concentrations 4.38 hours after a release beginning at high tide (1978).



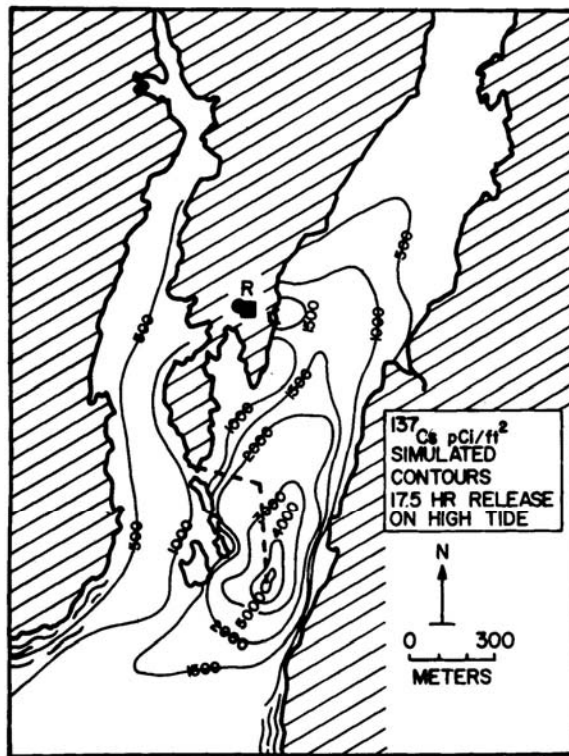
Appendix Figure A-8. Estimated ^{137}Cs concentrations 4.38 hours after a release beginning at mid-ebb tide (1978).



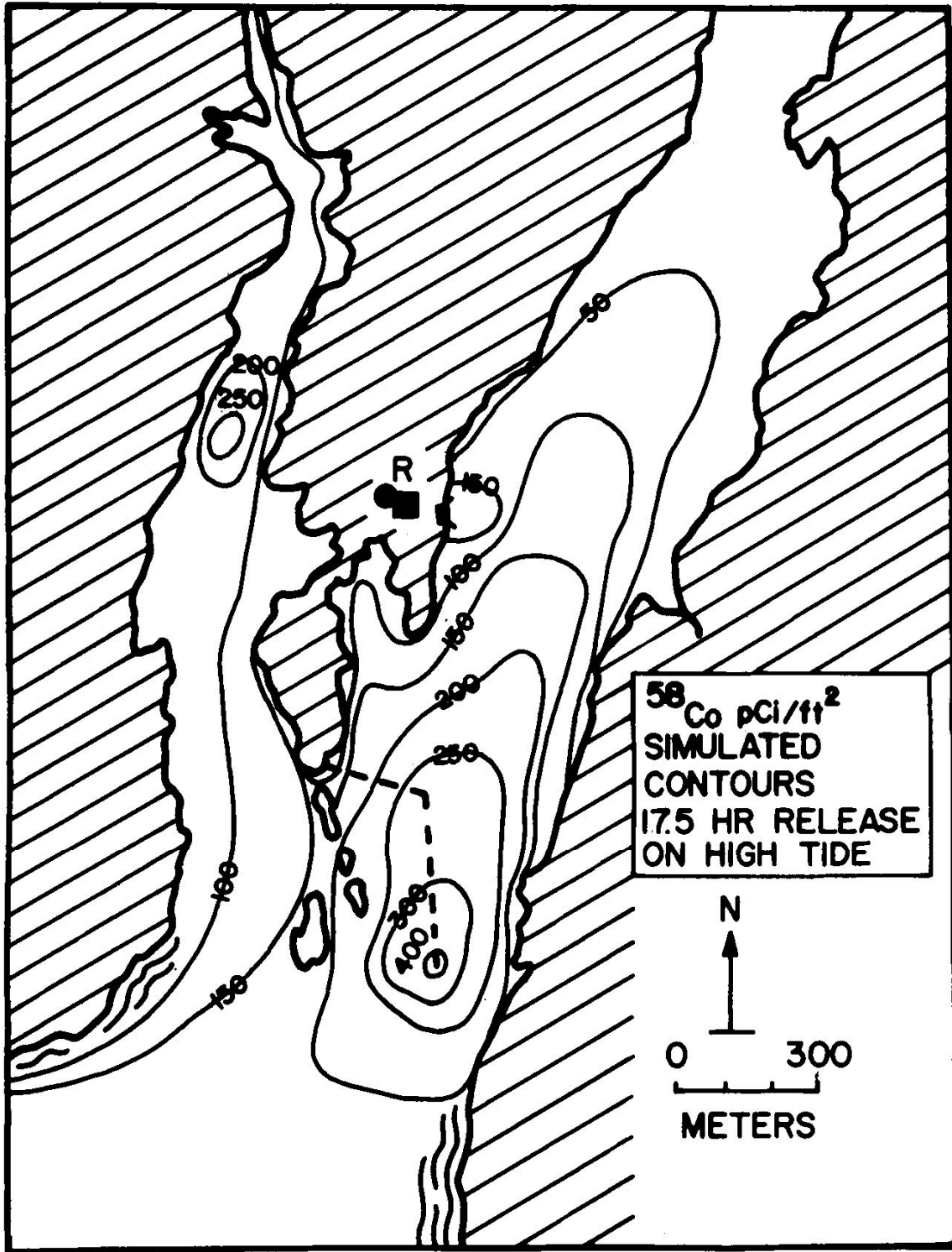
Appendix Figure A-9. Estimated ^{137}Cs concentrations 17.5 hours after a release beginning at high tide (1978).



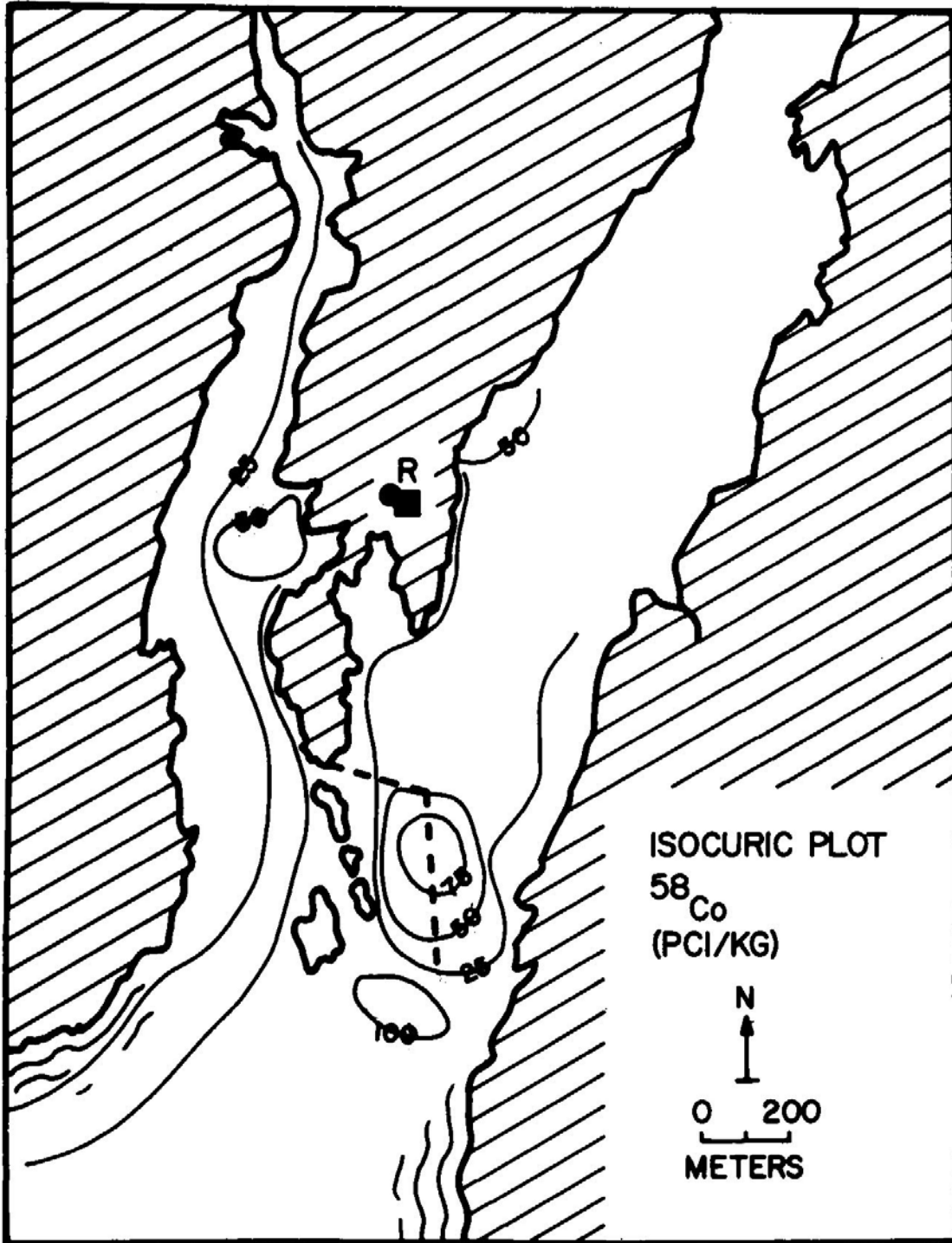
Appendix Figure A-10. Estimated ^{58}Co concentrations 17.5 hours after a release beginning at mid-ebb tide (1978).



Appendix Figure A-11. Simulated contours for ^{137}Cs concentrations 17.5 hours after a release beginning at high tide (Hess et al. 1978).



Appendix Figure A-12. Simulated contours for ^{58}Co 17.5 hours after a release beginning at high tide (1978).



Appendix Figure A-13. Actual contours for ^{58}Co measured after 17.5 hours beginning at high tide (1978).

The actual original data are shown in Appendix Tables A-1 and A-2.

Appendix Table A-1. Pre-operational Laboratory Soil & Sediment Gamma Ray Analysis

Location	Collection Date	Count Date	Type of Sample	Thorium Series pCi/kg	Uranium Series pCi/kg	Other Natural pCi/kg	¹³⁷Cs pCi/kg	¹³⁴Cs pCi/kg	⁵⁸Co pCi/kg	⁶⁰Co pCi/kg	⁵⁴Mn pCi/kg
Foxbird Island	6/29/72	7/28/72	Tidal marsh sediment	250 ± 130	500 ± 180	15000 ± 350	350 ± 32	< 15	< 12	< 15	< 10
Murphy's Corner	7/3/72	7/27/72	Tidal flat sediment	1660 ± 280	740 ± 120	15200 ± 1200	450 ± 80	< 30	< 25	< 30	< 20
Young's (or Long) Creek	6/12/72	7/14/72	Tidal marsh soil	880 ± 250	1075 ± 120	18200 ± 400	800 ± 80	< 30	< 25	< 30	< 20

Maine Yankee Marine Sampling Study

Appendix Table A-2. Post-operational Laboratory Soil & Sediment Gamma Ray Analysis

Location	Collection Date	Count Date	Type of Sample	Thorium Series pCi/kg	Uranium Series pCi/kg	Other Natural pCi/kg	¹³⁷ Cs pCi/kg	¹³⁴ Cs pCi/kg	⁵⁸ Co pCi/kg	⁶⁰ Co pCi/kg	⁵⁴ Mn pCi/kg
Young's (or Long) Creek	8/14/74	1/18/74	Tidal marsh soil	1100 ± 120	800 ± 70	19400 ± 780	700 ± 50	<35	<25	<30	<15
Foxbird Island	8/14/74	11/16/74	Soil	900 ± 90	700 ± 200	7300 ± 950	4600 ± 180	<35	<25	<30	<15
Murphy's Corner	8/14/74	11/20/74	Tidal flat sediment	900 ± 90	800 ± 72	18000 ± 500	500 ± 35	<35	<25	<30	<15